TRANSITION METAL CATALYZED SIMMONS–SMITH TYPE CYCLOPROPANATIONS

by

Jacob J. Werth

A Dissertation

Submitted to the Faculty of Purdue University

In Partial Fulfillment of the Requirements for the degree of

Doctor of Philosophy
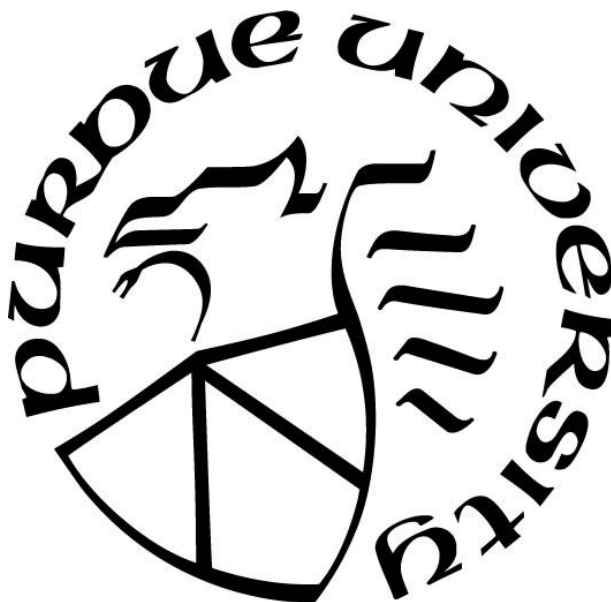
Department of Chemistry

West Lafayette, Indiana

August 2019

THE PURDUE UNIVERSITY GRADUATE SCHOOL
STATEMENT OF COMMITTEE APPROVAL

Prof. Christopher Uyeda, Chair
> Department of Chemistry

Prof. Suzanne Bart
> Department of Chemistry

Prof. Mark Lipton
> Department of Chemistry

Prof. Abram Axelrod
> Department of Chemistry

Approved by:
> Dr. Christine Hrycyna
>> Head of the Graduate Program

To Josie and Reggie

TABLE OF CONTENTS

LIST OF TABLES

LIST OF FIGURES

ABSTRACT

Author: Werth, Jacob, J. PhD
Institution: Purdue University
Degree Received: August 2019
Title: Transition Metal Catalyzed Simmons–Smith Type Cyclopropanations
Committee Chair: Christopher Uyeda

Cyclopropanes are commonly found throughout synthetic and natural biologically active compounds. The Simmons–Smith cyclopropanation reaction is one of the most useful methods for converting an alkene into a cyclopropane. Zinc carbenoids are the active intermediate in the reaction, capable of delivering the methylene unit to a broad variety of substrates. Significant advances have been made in the field to increase overall efficiency of the reaction including the use of diethyl zinc as a precursor and allylic alcohols as directing groups.

Despite the many notable contributions in zinc carbenoid chemistry, persistent limitations of the Simmons–Smith reaction still exist. Zinc carbenoids exhibit poor steric discrimination in the presence of a polyolefin with minimal electronic bias. Additionally, due to the electrophilic nature of zinc carbenoid intermediates, the reaction performs inefficiently with electron-deficient olefins. Finally, alkyl-substituted zinc carbenoids are known to be quite unstable, limiting the potential for substituted cyclopropanation reactions.

In this work, we demonstrate that cobalt catalysis can be utilized to access novel cyclopropane products through the activation of dihaloalkanes. The content of this thesis will focus on the limitations of Zn carbenoid chemistry and addressing them with cobalt catalyzed, reductive cyclopropanations. In addition to this reactivity, we also demonstrate the dimethylcyclopropanation of activated alkenes to furnish valuable products applicable to natural product synthesis and pharmaceutically relevant compounds. Finally, we will show the unique character of the cobalt catalyzed cyclopropanation reaction through mechanistic experiments and characterization of reaction intermediates. In whole, these studies offer a complementary method to zinc carbenoid chemistry in producing novel and diverse cyclopropane products.

CHAPTER 1.   REGIOSELECTIVE SIMMONS–SMITH TYPE CYCLOPROPANATIONS OF POLYALKENES ENABLED BY TRANSITION METAL CATALYSIS

1.1   Abstract

A $[^{i\text{-}Pr}PDI]CoBr_2$ complex (PDI = pyridine-diimine) catalyzes Simmons–Smith-type reductive cyclopropanation reactions using CH_2Br_2 in combination with Zn. In contrast to its non-catalytic variant, the cobalt-catalyzed cyclopropanation is capable of discriminating between alkenes of similar electronic properties based on their substitution patterns: monosubstituted > 1,1-disubstituted > (Z)-1,2- disubstituted > (E)-1,2-disubstituted > trisubstituted. This property enables synthetically useful yields to be achieved for the monocyclopropanation of polyalkene substrates, including terpene derivatives and conjugated 1,3-dienes. Mechanistic studies implicate a carbenoid species containing both Co and Zn as the catalytically relevant methylene transfer agent.

1.2   Introduction

Cyclopropanes are common structural elements in synthetic and natural biologically active compounds. The Simmons– Smith cyclopropanation reaction was first reported over half a century ago but remains today one of the most useful methods for converting an alkene into a cyclopropane. As compared to diazomethane, which is shock sensitive and must be prepared from complex precursors, CH_2I_2 is both stable and readily available, making it an attractive methylene source. Additionally, the stereospecificity of the Simmons–Smith reaction allows diastereomeric relationships in cyclopropanes to be established with a high degree of predictability. Several advances have addressed many of the limitations of the initial Simmons– Smith protocol. For example, Et_2Zn can be used in the place of Zn to more reliably and quantitatively generate the active carbenoid reagent. Acidic additives, such as $CF_3CO_2H_4$ and substituted phenols, have been found to accelerate the cyclopropanation of challenging substrates. Finally, Zn carbenoids bearing dialkylphosphate anions or bipyridine ligands are sufficiently stable to be stored in solution at low temperatures (Fig. 1).
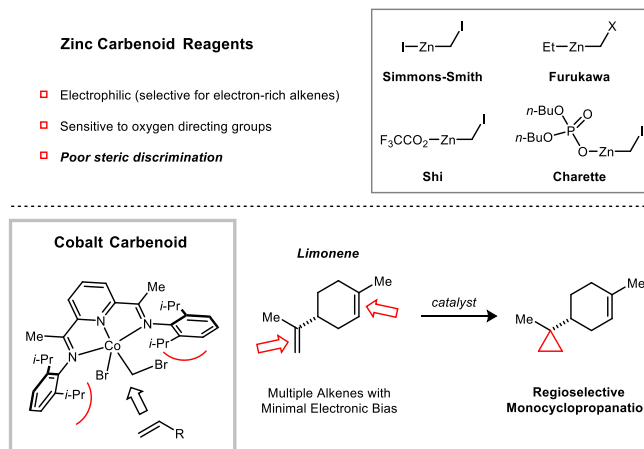
Figure 1.1 Factors governing alkene selectivity in Zn carbenoid-mediated cyclopropanation reactions. Cobalt-catalyzed reductive cyclopropanation exhibiting high regioselectivities in polyalkene substrates based on alkene substitution patterns.

Despite the many notable contributions in Zn carbenoid chemistry, a persistent limitation of Simmons–Smith-type cyclopropanations is their poor selectivity when attempting to discriminate between multiple alkenes of similar electronic properties. For example, the terpene natural product limonene possesses a 1,1-disubstituted and a trisubstituted alkene. Friedrich reported that, under a variety of Zn carbenoid conditions, the two alkenes are cyclopropanated with similar rates, resulting in mixtures of monocyclopropanated (up to a 5:1 ratio of regioisomers) and dicyclopropanated products. This issue is exacerbated by the challenge associated with separating the two monocyclopropane regioisomers, which only differ in the position of a non-polar CH_2 group. In general, synthetically useful regioselectivities in Simmons–Smith reactions are only observed for substrates containing directing groups.

In principle, catalysis may provide an avenue to address selectivity challenges in Simmons–Smith-type cyclopropanations; however, unlike diazoalkane transfer reactions, which are catalyzed by a broad range of transition metal complexes, there has been comparatively little progress toward the development of robust catalytic strategies for reductive cyclopropanations. Lewis acids in substoichiometric loadings have been observed to accelerate the Simmons–Smith

reaction, but in many cases, this rate effect is restricted to allylic alcohol substrates. Recently, our group described an alternative approach to catalyzing reductive cyclopropanation reactions using a transition metal complex that is capable of activating the dihaloalkane reagent by C–X oxidative addition. A dinickel catalyst was shown to promote methylene and vinylidene transfer using CH_2Cl_2 and 1,1-dichloroalkenes in combination with Zn as a stoichiometric reductant. Here, we describe a mononuclear [PDI]Co (PDI = pyridine-diimine) catalyst that imparts a high degree of steric selectivity in the cyclopropanation of polyalkene substrates. Mechanistic studies suggest that the key intermediate responsible for methylene transfer is a heterobimetallic conjugate of Co and Zn.

1.3   Regioselectivity Experiments Using Zn and Al Carbenoid Reagents

4-Vinyl-1-cyclohexene contains a terminal and an internal alkene of minimal electronic differentiation and thus provided a suitable model substrate to initiate our studies (Table 1). Under standard CH_2I_2/Et_2Zn conditions (entry 1), there is a modest preference for cyclopropanation of the more electron-rich disubstituted alkene (rr = 1:6.7) with increasing amounts of competing dicyclopropanation being observed at higher conversions (entries 2 and 3). Other modifications to the conditions, including the use of a Brønsted acid (entry 4) or a Lewis acid additive (entry 5), did not yield any improvements in selectivity. Likewise, an Al carbenoid generated using CH_2I_2 and $AlEt_3$ afforded a similar preference for cyclopropanation of the endocyclic alkene (entry 6).

Table 1.1 Comparison Studies. [a]Reaction conditions: 4-vinylcyclohexene (0.14 mmol), CH_2Cl_2 (1.0 mL), 24 h, 22 °C. Yields and ratios of regioisomers were determined by GC analysis against an internal standard.

entry	reaction conditions	yield (3 + 4)	rr (3:4)	yield 5
1	CH_2I_2 (1.0 equiv), Et_2Zn (0.5 equiv)	28%	1:6.7	3%
2	CH_2I_2 (1.0 equiv), Et_2Zn (1.0 equiv)	33%	1:4.6	5%
3	CH_2I_2 (2.0 equiv), Et_2Zn (2.0 equiv)	53%	1:6.5	16%
4	CH_2I_2 (1.0 equiv), Et_2Zn (1.0 equiv), 3,5-difluorobenzoic acid (2.0 equiv)	28%	1:3.5	19%
5	CH_2I_2 (2.0 equiv), Et_2Zn (2.0 equiv), $TiCl_4$ (0.2 equiv)	13%	1:4.6	1%
6	CH_2I_2 (1.2 equiv), $AlEt_3$ (1.2 equiv)	38%	1:3.1	9%

1.4   Catalyst Comparison Studies

In a survey of transition metal catalysts, the [$^{i\text{-Pr}}$PDI]CoBr$_2$ complex **1** was identified as a highly regioselective catalyst for the cyclopropanation of 4-vinyl-1-cyclohexene, targeting the less hindered terminal alkene (Table 2). CH_2Br_2 and Zn alone do not afford any background levels of cyclopropanation (entry 1); however, the addition of 6 mol% [$^{i\text{-Pr}}$PDI]CoBr$_2$ (**1**) provided monocyclopropane **3** (81% yield) with a >50:1 rr and <1% of the dicyclopropane product (entry 5). The steric profile of the catalyst appears to be critically important for yield. For example, the mesityl- (entry 6) and phenyl-substituted variants (entry 7) of the ligand provided only 58% and 4% yield respectively under the same reaction conditions. Related N-donor ligands similarly afforded low levels of conversion (entries 8–12) as did the use of other first-row transition metals, including Fe (entry 14) and Ni (entry 15), in the place of Co.

Table 1.2 Catalyst Comparison Studies. [a]Reaction conditions: 4-vinylcyclohexene (0.14 mmol), THF (1.0 mL), 24 h, 22 °C. Yields and ratios of regioisomers were determined by GC analysis against an internal standard.


entry	metal source	ligand	yield (3 + 4)	rr (3:4)	yield 5
1	–	–	<1%	–	<1%
2	CoBr$_2$	–	<1%	–	<1%
3	Co(DME)Br$_2$	–	<1%	–	<1%
4	–	$^{i\text{-}Pr}$PDI	<1%	–	<1%
5	CoBr$_2$	$^{i\text{-}Pr}$PDI	81%	>50:1	<1%
6	CoBr$_2$	^{Me}PDI	58%	>50:1	<1%
7	CoBr$_2$	^{Ph}PDI	4%	–	<1%
8	CoBr$_2$	$^{i\text{-}Pr}$DAD	<1%	–	<1%
9	CoBr$_2$	$^{i\text{-}Pr}$IP	2%	–	<1%
10	CoBr$_2$	terpy	4%	–	<1%
11	CoBr$_2$	$^{t\text{-}Bu}$PyBOX	<1%	–	<1%
12	CoBr$_2$	^{Ph}PyBOX	<1%	–	<1%
13	(PPh$_3$)$_2$CoBr$_2$	–	<1%	–	0%
14	FeBr$_2$	$^{i\text{-}Pr}$PDI	3%	–	<1%
15	NiBr$_2$	$^{i\text{-}Pr}$PDI	<1%	–	<1%

1.5   Competition Experiments

In order to define the selectivity properties of catalyst **1**, we next conducted competition experiments using alkenes bearing different patterns of substitution (Figure 2). Reactions were carried out using an equimolar amount of each alkene and run to full conversion of the limiting CH_2Br_2 reagent (1.0 equiv). Monosubstituted alkenes are the most reactive class of substrates using **1** but are not adequately differentiated from 1,1-disubstituted alkenes (3:1). By contrast, terminal alkenes are significantly more reactive than internal alkenes, providing synthetically useful selectivities (≥31:1). Furthermore, a model Z-alkene was cyclopropanated in preference to its E-alkene congener in a 33:1 ratio. Using catalyst **1**, trisubstituted alkenes are poorly reactive, and no conversion is observed for tetrasubstituted alkenes.


Figure 1.2 Intermolecular competition experiments probing selectivity based on alkene substitution patterns. Reactions were conducted using a 1:1:1 molar ratio of the two alkene starting materials and CH_2Br_2.

1.6   Substrate Scope for Regioselective Cyclopropanation

The synthetic applications of the catalytic regioselective cyclopropanation were examined using the terpene natural products and derivatives shown in Figure 3. In all cases, the selectivity properties follow the trends established in the competition experiments. Substrates containing ether or free alcohol functionalities (e.g., **7**, **10**, and **11**) exhibit a strong directing group effect under classical Simmons–Smith conditions; however, catalyst **1** overrides this preference and targets the less hindered alkene. Additionally, the presence of electron-deficient α,β-unsaturated carbonyl systems (e.g., **9**, **13**, and **14**) do not perturb the expected steric selectivity.
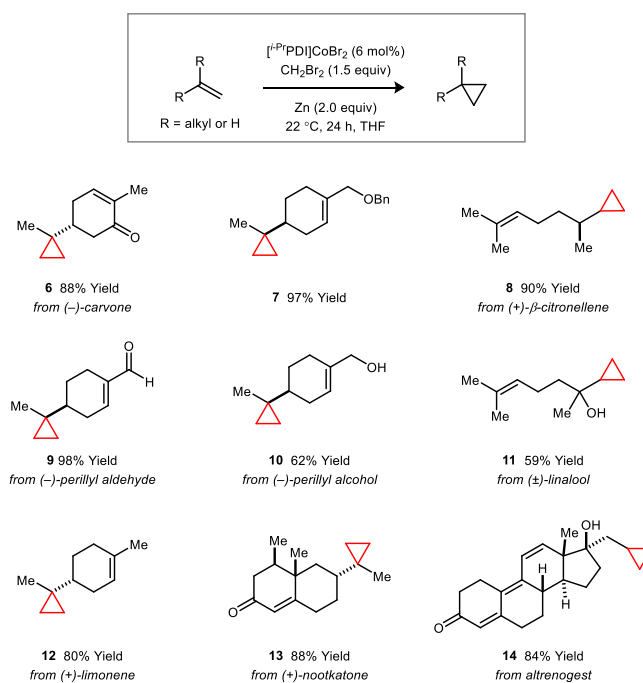
Figure 1.3 Catalytic regioselective monocyclopropanations of terpene natural products and derivatives. Isolated yields following purification are averaged over two runs.

Vinylcyclopropanes are a valuable class of synthetic intermediates that engage in catalytic strain-induced ring-opening reactions. The monocyclopropanation of a diene represents an attractive approach to their synthesis but would require a catalyst that is capable of imparting a high degree of regioselectivity and avoiding secondary additions to form dicyclopropane products. These challenges are addressed for a variety of diene classes using catalyst **1** (Figure 4). Over the substrates that we have examined, the selectivities for cyclopropanation of the terminal over the

internal double bond of the diene system are uniformly high. Additionally, the catalyst is tolerant of vinyl bromide (**15**) and vinyl boronate (**23**) functional groups, which are commonly used in cross-coupling reactions.
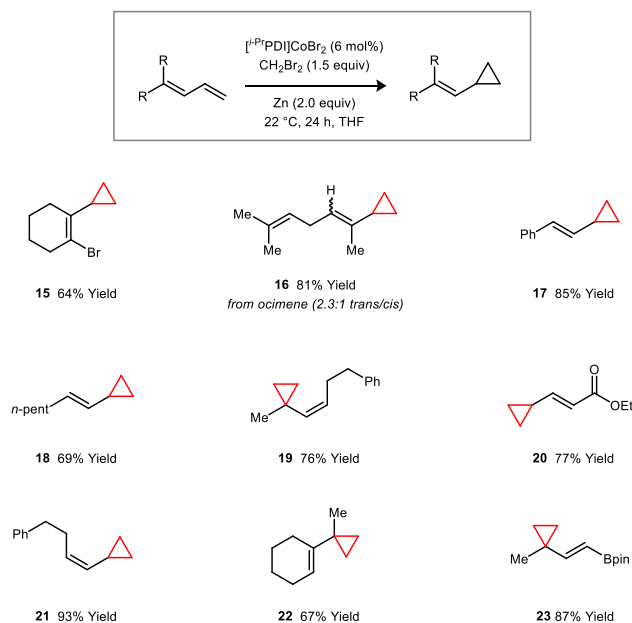

Figure 1.4 Catalytic regioselective monocyclopropanations of 1,3-dienes Isolated yields following purification are averaged over two runs.

1.7   Mechanistic Experiments

Like the non-catalytic Simmons–Smith reaction, the cyclopropanation using **1** is stereospecific within the limit of detection, implying a mechanism in which the two C–C σ-bonds are either formed in a concerted fashion or by a stepwise process that does not allow for single bond rotation. For example, cyclopropanation of the Z-alkene **24** affords the cis-disubstituted cyclopropane **25** in 95% yield as a single diastereomer (Figure 5a). Furthermore, the vinylcyclopropane substrates **26** and **28**, commonly used as tests for cyclopropylcarbinyl radical intermediates, react without ring-opening to afford products **27** and **29** (Figure 5b).

(a) Stereospecificity Experiment

(b) Radical Clock Experiments
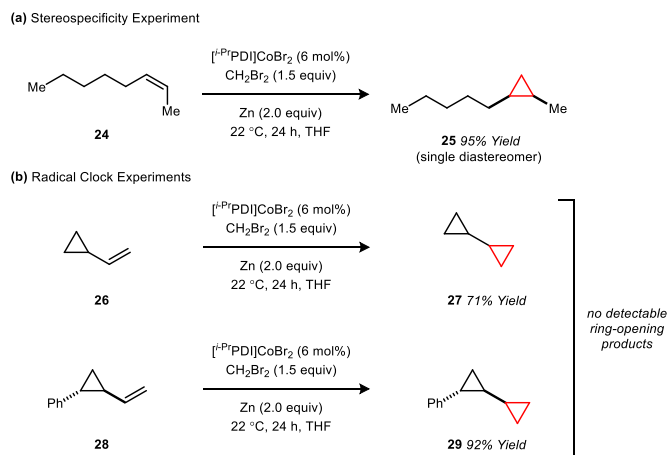
Figure 1.5 Mechanistic studies probing the concertedness of cyclopropane formation.

In order to decouple the cyclopropanation steps of the mechanism from catalyst turnover, we conducted stoichiometric reactions with the isolated [$^{i\text{-Pr}}$PDI]CoBr complex in the absence of Zn (Figure 6c). The reaction of 30 with 4-vinylcyclohexene and CH_2Br_2 generates the [$^{i\text{-Pr}}$PDI]CoBr$_2$ complex 1 within 24 h at room temperature but forms cyclopropanated products in a relatively low combined yield of 26%, which is not commensurate with the efficiency of the catalytic process. Furthermore, the regioselectivity is only 3:1, whereas the catalytic cyclopropanation achieves a >50:1 selectivity for this substrate. When the same stoichiometric reaction is conducted in the presence of $ZnBr_2$, the yield and selectivity of the catalytic process is fully restored.

The Co-containing product (**31**) of the stoichiometric reaction in the presence of $ZnBr_2$ is green, which is notably distinct from the tan color of the [$^{i\text{-Pr}}$PDI]CoBr$_2$ complex **1**. This green species is NMR silent but may be crystallized from saturated solutions in Et_2O to afford **31** (Figure 6f). The solid-state structure reveals the expected [$^{i\text{-Pr}}$PDI]CoBr$_2$ fragment in a distorted square pyramidal geometry ($\tau_5 = 0.36$) with a $Zn(THF/Et_2O)Br_2$ Lewis acid coordinated to one of the Br ligands. This interaction induces an asymmetry in the structure, causing the Co–Br1 distance (2.557(1) Å) to be elongated relative to the Co–Br2 distance (2.358(2) Å).

Collectively, these studies suggest that both Co and Zn are present in the reactive carbenoid intermediate, and that $ZnBr_2$ may interact with the [$^{i\text{-Pr}}$PDI]Co complex through Lewis acid-base interactions. There is a notable similarity between the observed Co/Zn effect and previous studies

of Lewis acid acceleration in the Simmons–Smith cyclopropanation. For example, Zn carbenoid reactions are known to be accelerated by the presence of ZnX_2,[12c] which is generated as a byproduct of the reaction. DFT calculations conducted by Nakamura have suggested that the origin of this rate acceleration may be due to the accessibility of a five-membered ring transition state, which requires the presence of an additional Zn equivalent to function as a halide shuttle.

Figure 1.6 Mechanistic studies probing the nature of the active carbenoid intermediate. (a) Identification of the catalyst resting state. (b) Cyclic voltammetry data for the [$^{i\text{-}Pr}$PDI]CoBr$_2$ complex. (c) Stoichiometric cyclopropanation reactions using the [$^{i\text{-}Pr}$PDI]CoBr$_2$ complex in the absence and presence of ZnBr$_2$. (d) A proposed Co/Zn carbenoid species. (e) Proposed dinuclear mechanism for the Lewis acid-accelerated Simmons–Smith reaction. (f) Solid-state structure for the [$^{i\text{-}Pr}$PDI]CoBr$_2$Zn(THF/Et$_2$O)Br$_2$ complex (**31**). The solvent molecule bound to Zn is disordered between Et$_2$O and THF. Only the THF-bound molecule is shown for clarity.

1.8   Conclusion

In summary, transition metal catalysis provides a pathway to accessing unique selectivity in reductive carbenoid transfer reactions. A [$^{i\text{-}Pr}$PDI]CoBr$_2$ complex functions as a robust catalyst for Simmons–Smith type cyclopropanation using a CH$_2$Br$_2$/Zn reagent mixture. This system exhibits the highest regioselectivities that have been observed in reductive cyclopropanations based solely on the steric properties of the alkene substrate. Accordingly, a range of terpenes and conjugated dienes may be converted to a single monocyclopropanated product. Ongoing studies are directed at exploring the applications of transition metal catalysts to other classes of carbenoid transfer reactions.

1.9   References

(1)   (a) J. Salaun and M. Baird, Curr. Med. Chem., 1995, 2, 511– 542; (b) W. A. Donaldson, Tetrahedron, 2001, 57, 8589– 8627; (c) L. A. Wessjohann, W. Brandt and T. Thiemann, Chem. Rev., 2003, 103, 1625–1648; (d) N. A. Meanwell, J. Med. Chem., 2011, 54, 2529– 2591; (e) D. Y. K. Chen, R. H. Pouwer and J.-A. Richard, Chem. Soc. Rev., 2012, 41, 4631–4642.

(2)   (a) H. E. Simmons and R. D. Smith, J. Am. Chem. Soc., 1958, 80, 5323–5324; (b) H. E. Simmons and R. D. Smith, J. Am. Chem. Soc., 1959, 81, 4256–4264; (c) A. B. Charette and A. Beauchemin, Org. React., 2001, 58, 1–415.

(3)   (a) J. Furukawa, N. Kawabata and J. Nishimura, Tetrahedron Lett., 1966, 7, 3353–3354; (b) J. Furukawa, N. Kawabata and J. Nishimura, Tetrahedron, 1968, 24, 53–58.

(4)   (a) Z. Yang, J. C. Lorenz and Y. Shi, Tetrahedron Lett., 1998, 39, 8621–8624; (b) J. C. Lorenz, J. Long, Z. Yang, S. Xue, Y. Xie and Y. Shi, J. Org. Chem., 2004, 69, 327–334.

(5)   A. B. Charette, S. Francoeur, J. Martel and N. Wilb, Angew. Chem., Int. Ed., 2000, 39, 4539–4542.

(6)   A. Voituriez, L. E. Zimmer and A. B. Charette, J. Org. Chem., 2010, 75, 1244–1250.

(7)   A. B. Charette, J.-F. Marcoux, C. Molinaro, A. Beauchemin, C. Brochu and E. Isabel, ´ J. Am. Chem. Soc., 2000, 122, 4508– 4509.

(8)   There is some conflicting data in the literature regarding the regioselectivity of Zn carbenoid addition to limonene; however, the most recent and comprehensive studies have found that mixtures of regioisomers are formed and that the product ratios depend on the reaction conditions: (a) S. D. Koch, R. M. Kliss, D. V. Lopiekes and R. J. Wineman, J. Org. Chem., 1961, 26, 3122–3125; (b) H. E. Simmons, E. P. Blanchard and R. D. Smith, J. Am. Chem. Soc., 1964, 86, 1347–1356; (c) E. C. Friedrich and F. NiyatiShirkhodaee, J. Org. Chem., 1991, 56, 2202–2205.

(9)   (a) A. H. Hoveyda, D. A. Evans and G. C. Fu, Chem. Rev., 1993, 93, 1307–1370; (b) H. Lebel, J.-F. Marcoux, C. Molinaro and A. B. Charette, Chem. Rev., 2003, 103, 977–1050.

(10)   (a) H. Nozaki, S. Moriuti, M. Yamabe and R. Noyori, Tetrahedron Lett., 1966, 7, 59–63; (b) M. P. Doyle, Chem. Rev., 1986, 86, 919–939; (c) M. P. Doyle, M. A. McKervey and T. Ye, Modern catalytic methods for organic synthesis with diazo compounds, Wiley, 1998; (d) H. Pellissier, Tetrahedron, 2008, 64, 7041–7095.

(11)   Photoredox catalysts for reductive cyclopropanation reactions: (a) A. M. del Hoyo, A. G. Herraiz and M. G. Suero, Angew. Chem., Int. Ed., 2017, 56, 1610–1613; (b) A. M. del Hoyo and M. García Suero, Eur. J. Org. Chem., 2017, 2017, 2122–2125.

(12)   (a) H. Takahashi, M. Yoshioka, M. Ohno and S. Kobayashi, Tetrahedron Lett., 1992, 33, 2575–2578; (b) A. B. Charette and C. Brochu, J. Am. Chem. Soc., 1995, 117, 11367–11368; (c) S. E. Denmark and S. P. O'Connor, J. Org. Chem., 1997, 62, 584–594; (d) A. B. Charette, C. Molinaro and C. Brochu, J. Am. Chem. Soc., 2001, 123, 12168–12175; (e) H. Shitama and T. Katsuki, Angew. Chem., Int. Ed., 2008, 47, 2450– 2453; (f) J. Balsells and P. J. Walsh, J. Org. Chem., 2000, 65, 5005–5008.

(13)   J. Long, H. Du, K. Li and Y. Shi, Tetrahedron Lett., 2005, 46, 2737–2740.

(14)   Y.-Y. Zhou and C. Uyeda, Angew. Chem., Int. Ed., 2016, 55, 3171–3175.

(15)   S. Pal, Y.-Y. Zhou and C. Uyeda, J. Am. Chem. Soc., 2017, 139, 11686–11689.

(16)   Seminal studies and selected reviews of catalytic reactions using (PDI)Co complexes: (a) B. L. Small, M. Brookhart and A. M. A. Bennett, J. Am. Chem. Soc., 1998, 120, 4049–4050; (b) G. J. P. Britovsek, V. C. Gibson, S. J. McTavish, G. A. Solan, A. J. P. White, D. J. Williams, G. J. P. Britovsek, B. S. Kimberley and P. J. Maddox, Chem. Commun., 1998, 849–850; (c) V. C. Gibson, C. Redshaw and G. A. Solan, Chem. Rev., 2007, 107, 1745–1776; (d) C. Bianchini, G. Giambastiani, L. Luconi and A. Meli, Coord. Chem. Rev., 2010, 254, 431–455; (e) Z. Flisak and W.-H. Sun, ACS Catal., 2015, 5, 4713–4724; (f) P. J. Chirik, Angew. Chem., Int. Ed., 2017, 56, 5170–5181.

(17)   U. Burger and R. Huisgen, Tetrahedron Lett., 1970, 11, 3057– 3060.

(18)   E. C. Friedrich, S. E. Lunetta and E. J. Lewis, J. Org. Chem., 1989, 54, 2388–2390.

(19)   K. Maruoka, Y. Fukutani and H. Yamamoto, J. Org. Chem., 1985, 50, 4412–4414.

(20)   (a) T. Hudlicky, T. M. Kutchan and S. M. Naqvi, Org. React., 1985, 33, 247–335; (b) J. E. Baldwin, Chem. Rev., 2003, 103, 1197–1212; (c) T. Hudlicky and J. W. Reed, Angew. Chem., Int. Ed., 2010, 49, 4864–4876; (d) Y. Gao, X.-F. Fu and Z.-X. Yu, in CC Bond Activation, Springer, 2014, pp. 195– 231; (e) L. Souillart and N. Cramer, Chem. Rev., 2015, 115, 9410–9464.

(21)   A. J. Anciaux, A. Demonceau, A. F. Noels, R. Warin, A. J. Hubert and P. Teyssi´e, Tetrahedron, 1983, 39, 2169– 2173.

(22)   M. J. Humphries, K. P. Tellmann, V. C. Gibson, A. J. P. White and D. J. Williams, Organometallics, 2005, 24, 2039–2050.

(23)   (a) E. Nakamura, A. Hirai and M. Nakamura, J. Am. Chem. Soc., 1998, 120, 5844–5845; (b) M. Nakamura, A. Hirai and E. Nakamura, J. Am. Chem. Soc., 2003, 125, 2341–2350.

CHAPTER 2. COBALT-CATALYZED REDUCTIVE DIMETHYLCYCLOPROPANATION OF 1,3-DIENES

2.1 Abstract

Dimethylcyclopropanes are valuable synthetic targets that are challenging to access in high yield using Zn carbenoid reagents. Here, we describe a cobalt-catalyzed variant of the Simmons–Smith reaction that enables the efficient dimethylcyclopropanation of 1,3-dienes using a Me_2CCl_2/Zn reagent mixture. The reactions proceed with high regioselectivity based on the substitution pattern of the 1,3-diene. The products are vinylcyclopropanes, which serve as substrates for transition-metal catalyzed ring-opening reactions, including 1,3-rearrangements and [5 + 2]-cycloadditions. Preliminary studies indicate that moderately activated monoalkenes are also amenable to dimethylcyclopropanation under the cobalt-catalyzed conditions.

2.2 Introduction

Geminal dimethylation is a common substitution pattern in polycyclic terpene natural products. Medicinal chemists have also explored the installation of dimethyl groups in biologically active compounds as a strategy to improve their potency or to eliminate metabolic liabilities. There are now over 50 clinically approved pharmaceutical compounds that feature these motifs (Figure 1). The presence of *gem*-dimethylation in a target compound introduces significant synthetic complexity in that a hindered tetrasubstituted carbon atom must be generated. The most common routes utilize classical carbonyl chemistry and entail either a double α-alkylation reaction or a double addition of a methyl nucleophile to a carboxylic acid derivative.
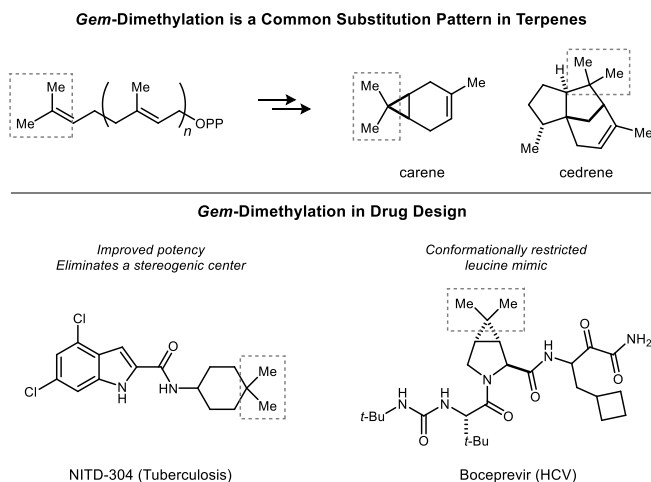
Figure 2.1 Rings containing *gem*-dimethyl groups, including dimethylcyclopropanes, are found in biologically active compounds of natural and synthetic origins.

It is attractive to consider an alternative approach based on the formation of dimethylcyclopropanes, which are themselves common in biologically active compounds but may also be diversified into other frameworks through strain-induced ring-opening reactions. The Simmons–Smith reaction is potentially well-suited to addressing these structures; however, it is known that the efficiency of Zn carbenoid-based cyclopropanations decreases significantly when using disubstituted *gem*-dihaloalkanes. For example, the addition of 2,2-diiodopropane under Furukawa conditions has only been demonstrated for two simple substrates, cyclopentene and cyclohexene, which provide yields up to 59% after a reaction time of 5 days. A notable advance in this area was reported by Charette, who showed that directing group effects can be leveraged to achieve a high-yielding dimethylcyclopropanation of allylic alcohols. Additionally, the Corey–Chaykovsky-type dimethylcyclopropanation of α,β-unsaturated carbonyl compounds has been developed (Figure 2).
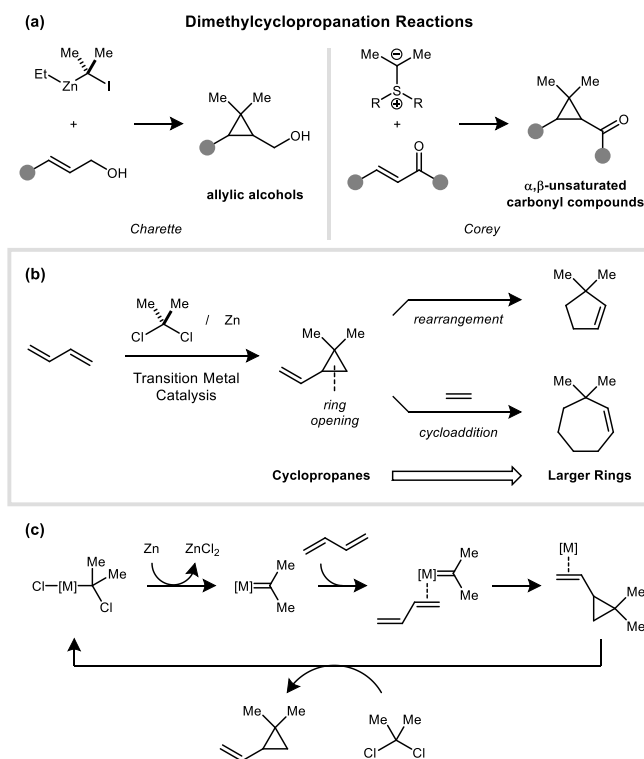
Figure 2.2 (a) Simmons–Smith-type dimethylcyclopropanation reactions of allylic alcohols and Corey–Chaykovsky dimethylcyclopropanation reactions of α,β-unsaturated carbonyl compounds. (b) Transition metal catalyzed reductive dimethylcyclopropanation reactions of 1,3-dienes and ring-opening reactions to generate 5- and 7-membered rings. (c) Proposed mechanism for a transition metal catalyzed reductive dimethylcyclopropanation reaction.

2.3   Catalyst Optimization

We recently found that [PDI]Co (PDI = pyridine–diimine) complexes function as catalysts for Simmons–Smith-type cyclopropanation reactions and generate a reactive carbene equivalent of significantly altered selectivity properties from Zn carbenoids. Motivated by this finding, we became interested in using transition metal catalysis to address the dimethylcyclopropanation reaction. Here, we report a cobalt-catalyzed dimethylcyclopropanation of 1,3-dienes using Me_2CCl_2/Zn as a source of isopropylidene equivalents.

The [$^{2,6-i-Pr}$PDI]CoBr$_2$ complex was previously shown to be an effective catalyst for cyclopropanation reactions using CH_2Br_2/Zn; however, it afforded negligible yields in the analogous reactions using Me_2CCl_2/Zn (Table 1, entry 7). We reasoned that the more hindered

dimethylcarbene fragment may require the steric profile of the PDI ligand to be correspondingly adjusted. Accordingly, a series of ligands was prepared by varying the size of the flanking aryl substituents (**L1**–**L4**). The 2-*t*-BuPh derived catalyst was identified as being optimal (entry 4), and the dimethylcyclopropanation of a model 1,3-diene (**1**) provided **2** in 93% yield as a single regioisomer. Zn is not capable of directly activating Me_2CCl_2, and in the absence of the Co catalyst, there is no conversion (entry 1). Despite the fact that $ZnCl_2$ is generated as a stoichiometric byproduct, the presence of $ZnBr_2$ at the start of the reaction provided a modest beneficial effect on yield (entry 14). $ZnBr_2$ accelerates the initial reduction of the yellow Co(II) complex to a violet Co(I) species, which is then capable of activating Me_2CCl_2. Finally, other classes of bidentate and tridentate ligands containing combinations of pyridine and imine donors were ineffective relative to PDI (entries 10–13). As a point of comparison, the non-catalytic dimethylcyclopropanation of **1** under Furukawa-type Simmons–Smith conditions (I_2CMe_2/Et_2Zn) provided **2** in a moderate yield of 45% along with several inseparable side products (see Supporting Information for experimental details).

Table 2.1 Catalyst Optimization Studies. Reactions were run on a 0.14 mmol scale of the 1,3-diene in THF (1 mL). Yields of **2** were determined by GC analysis against an internal standard. [b] Modifications from standard conditions: without ZnBr$_2$. [c] Modifications from standard conditions: 1.1 equiv of Me$_2$CCl$_2$. [d] Modifications from standard conditions: 2.0 equiv of Me$_2$CBr$_2$.

entry	metal source	ligand	yield **2**
1	–	–	< 1
2	–	2-*t*-BuPDI (**L1**)	< 1
3	CoBr$_2$	–	< 1
4	CoBr$_2$	2-*t*-BuPDI (**L1**)	93
5	CoBr$_2$	2,4,6-MePDI (**L2**)	77
6	CoBr$_2$	3,5-*t*-BuPDI (**L3**)	8
7	CoBr$_2$	2,6-*i*-PrPDI (**L4**)	2
8	NiBr$_2$	2-*t*-BuPDI (**L1**)	5
9	FeBr$_2$	2-*t*-BuPDI (**L1**)	4
10	CoBr$_2$	2,6-*i*-PrIP (**L5**)	2
11	CoBr$_2$	2,6-*i*-PrDAD (**L6**)	<1
12	CoBr$_2$	bpy (**L7**)	4
13	CoBr$_2$	terpy (**L8**)	1
14[b]	CoBr$_2$	2-*t*-BuPDI (**L1**)	87
15[c]	CoBr$_2$	2-*t*-BuPDI (**L1**)	78
16[d]	CoBr$_2$	2-*t*-BuPDI (**L1**)	79

2.4   Substrate Scope Exploration

With optimized conditions in hand, we next evaluated the substrate scope of the dimethylcyclopropanation reaction (Figure 3). A variety of 1-substituted, 1,2-disubstituted, and 1,3-disubstituted dienes are viable substrates. In all cases, cyclopropanation occurs at the terminal double bond with high regioselectivity (rr >19:1). Notably, there is no detectable secondary cyclopropanation of the product alkene despite the presence of excess Me_2CCl_2 and Zn in the reaction mixture. Common functional handles for further synthetic elaboration are tolerated, including a protected amine (**8**), BPin group (**9**), ester (**13**), and a free alcohol (**18**). The activation of Me_2CCl_2 by the Co catalyst is relatively facile such that aryl chlorides (**4**) present in the substrate are tolerated. The TBS-protected variant of Danishefsky's diene afforded a protected cyclopropanol derivative in high yield (**14**).

Unlike the Simmons–Smith reaction, the cobalt-catalyzed process is relatively insensitive to the electronic properties of the diene. For example, the presence of an electron-withdrawing group, such as a phosphonate ester (**11**), a ketone (**12**), or an ester (**13**), does not significantly decrease the rate of the reaction nor does it result in poor yields of the product. Additionally, the cobalt catalyst does not appear to interact strongly with alcohol directing groups. The diene **16** is selectively monocyclopropanated at the terminal double bond (rr = >19:1) as expected based solely on steric considerations. By contrast, Furukawa-type conditions using I_2CMe_2/Et_2Zn afford selectivity for the internal double bond, which is proximal to the alcohol.

Synthetic ethyl chrysanthemate is prepared on industrial scales by the addition of ethyl diazoacetate to 2,5-dimethyl-2,4-hexadiene. A limitation of this process is that the cyclopropane is formed as a mixture of cis and trans diastereomers, whereas natural pyrethrins are found only with the trans relative stereochemistry. Using the cobalt-catalyzed cyclopropanation, ethyl (E)-5-methyl-2,4-hexadienoate reacts at the less hindered internal alkene with >19:1 trans selectivity (**19**). This approach was applied to the synthesis of the commercial pesticide phenothrin (**20**) and unnatural pyrethrin analogues that contain other alkyl (**25**), cycloalkyl (**21**–**23**), or aryl (**24**) substituents in the place of the terminal methyl groups.

28
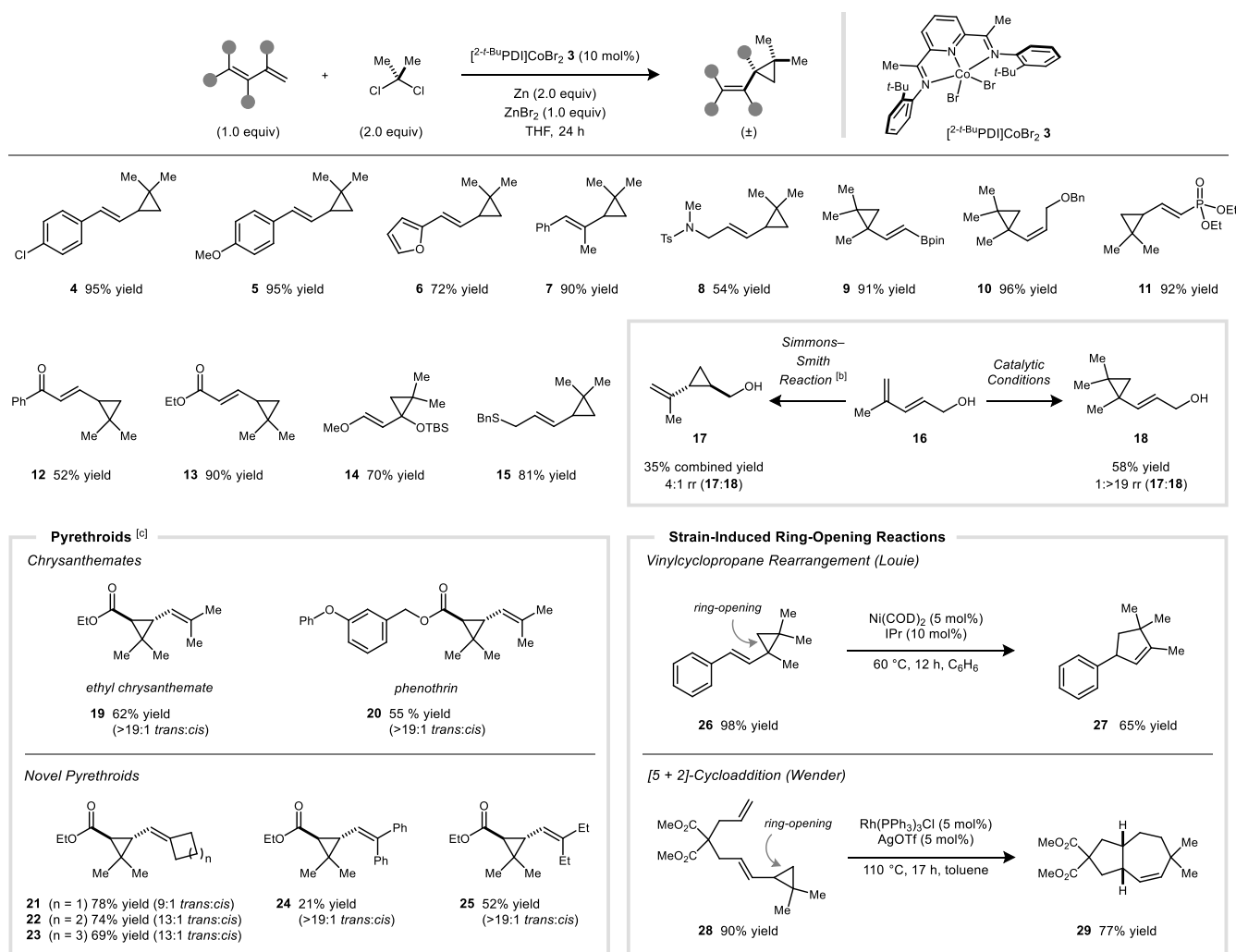
Figure 2.3 Substrate scope studies. [a] Standard reaction conditions: 0.14 mmol scale of the 1,3-diene (1.0 equiv), Me_2CCl_2 (2.0 equiv), Zn (2.0 equiv), $ZnBr_2$ (1.0 equiv), [$^{2\text{-}t\text{-}Bu}$PDI]CoBr$_2$ (**3**) (10 mol%), and THF (1 mL); 22 °C for 24 h. [b] Simmons–Smith reaction conditions: $ZnEt_2$ (4.0 equiv), I_2CMe_2 (4.0 equiv), and CH_2Cl_2 (1.0 mL). [c] Modifications to standard conditions: DCE (1.0 mL) instead of THF, Me_2CBr_2 (2.0 equiv) instead of Me_2CCl_2.

We considered the possibility that the vinyl cyclopropane products generated by this method might serve as substrates for transition metal-catalyzed ring-opening reactions; however, it was unknown at the outset whether the steric hindrance imposed by a *gem*-dimethyl group would be tolerated. Vinylcyclopropane **26** was prepared from the corresponding 1,3-diene precursor in 98% yield. Heating **26** at 60 °C for 12 h in the presence of a IPr/Ni(COD)$_2$ catalyst provided the rearranged vinylcyclopentene product **27** in 65% yield. The position of the alkene in **27** indicates that only the less hindered C–C bond is activated by the catalyst.

A substrate containing both a 1,3-diene and an isolated alkene was cyclopropanated under the cobalt-catalyzed conditions to yield a single regioisomer of the monocyclopropane product (**28**). When **28** was subjected to the Rh-catalyzed [5 + 2]-cycloaddition conditions developed by Wender, the bicyclic product **29** was formed in 77% yield. Like the 1,3-rearrangement reaction, the ring-opening proceeds with high regioselectivity to furnish a single isomer of the product.

Finally, it was of interest to test whether the catalytic conditions developed for the dimethylcyclopropanation of 1,3-dienes could be applied to isolated alkenes. Simple, unactivated alkenes such as 1-octene or cyclohexene were unreactive (<2% yield); however, substrates possessing a moderate degree of strain proved to be viable. For example, cyclopentene is cyclopropanated in 87% yield under the standard optimized conditions (**30**). This result represents a significant improvement in yield and reaction time over the only previously reported attempt to carry out this transformation (45% yield after 5 days using I$_2$CMe$_2$/Et$_2$Zn). Additionally, cyclooctene (**31**), indene (**32**), and norbornene (**33**) react in high yield. In the latter case, the exo-addition product is formed exclusively. *N*-Boc-2,5-dihydropyrrole (**34**) is cyclopropanated in 90% yield to generate **35**, which is a protected precursor to the HCV protease inhibitor boceprevir. The process-scale route to this bicyclic amine consists of a multi-step sequence in which the *gem*-dimethylcyclopropane unit is ultimately derived from ethyl chrysanthemate.
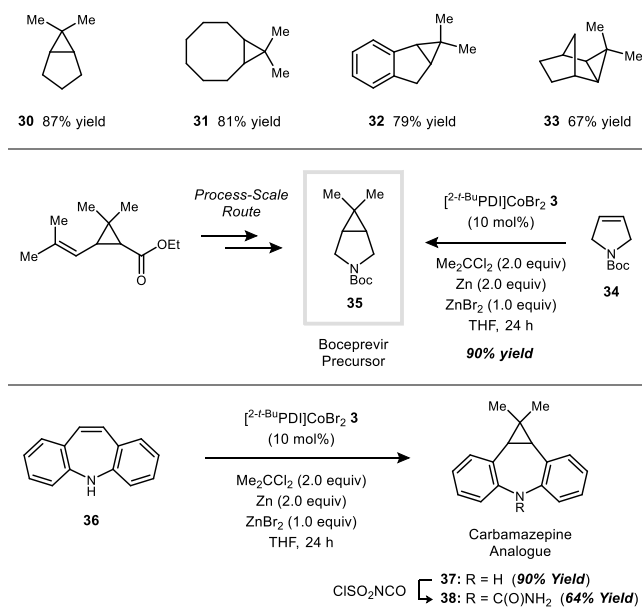
Figure 2.4 Dimethylcyclopropanations of activated alkenes, including applications to the synthesis of a boceprevir precursor and an analogue of carbamazepine. Standard dimethylcyclopropanation conditions: 0.14 mmol scale of the 1,3-diene (1.0 equiv), Me_2CCl_2 (2.0 equiv), Zn (2.0 equiv), $ZnBr_2$ (1.0 equiv), $[^{2-t-Bu}PDI]CoBr_2$ (**3**) (10 mol%), and THF (1 mL); 22 °C for 24 h.

In summary, cobalt catalysis enables the synthesis of dimethylcyclopropanes that were not previously accessible in high yield using the Simmons–Smith reaction. In particular, the regioselective dimethylcyclopropanation of 1,3-dienes yields polysubstituted vinyl cyclopropanes, which participate in strain-induced ring-opening reactions. Moderately activated monoalkenes are also cyclopropanated efficiently to generate building blocks for medicinal chemistry. These studies collectively highlight the unique properties of transition metal carbenoids over their Zn counterparts as reactive species in cyclopropanation chemistry.

2.5   References

(1)   a) T. J. Maimone, P. S. Baran, Nat. Chem. Biol. 2007, 3, 396; b) J. Gershenzon, N. Dudareva, Nat. Chem. Biol. 2007, 3, 408.

(2)   T. T. Talele, J. Med. Chem. 2018, 61, 2166 – 2210.

(3)   For examples of synthetic routes to gem-dimethyl groups in biologically active compounds, see: a) P. A. Glossop, C. A. L. Lane, D. A. Price, M. E. Bunnage, R. A. Lewthwaite, K. James, A. D. Brown, M. Yeadon, C. Perros-Huguet, M. A. Trevethick, N. P. Clarke, R. Webster, R. M. Jones, J. L. Burrows, N. Feeder, S. C. J. Taylor, F. J. Spence, J. Med. Chem. 2010, 53, 6640 – 6652; b) A. L. Gottumukkala, K. Matcha, M. Lutz, J. G. de Vries, A. J. Minnaard, Chem. Eur. J. 2012, 18, 6907 – 6914; c) J. Wang, R. Tong, J. Org. Chem. 2016, 81, 4325 – 4339; d) E. Kick, R. Martin, Y. Xie, B. Flatt, E. Schweiger, T.-L. Wang, B. Busch, M. Nyman, X.-H. Gu, G. Yan, B. Wagner, M. Nanao, L. Nguyen, T. Stout, A. Plonowski, I. Schulman, J. Ostrowski, T. Kirchgessner, R. Wexler, R. Mohan, Bioorg. Med. Chem. Lett. 2015, 25, 372 – 377.

(4)   For recent studies on dimethylcyclopropane synthesis, see: a) L. Dian, D. S. Müller, I. Marek, Angew. Chem. Int. Ed. 2017, 56, 6783 – 6787; Angew. Chem. 2017, 129, 6887 – 6891; b) H. Cang, R. A. Moss, K. Krogh-Jespersen, J. Am. Chem. Soc. 2015, 137, 2730 – 2737.

(5)   T. T. Talele, J. Med. Chem. 2016, 59, 8712 – 8756.

(6)   a) M. Meazza, H. Guo, R. Rios, Org. Biomol. Chem. 2017, 15, 2479 – 2490; b) L. Souillart, N. Cramer, Chem. Rev. 2015, 115, 9410 – 9464; c) P.-h. Chen, B. A. Billett, T. Tsukamoto, G. Dong, ACS Catal. 2017, 7, 1340 – 1360.

(7)   S. Sengmany, E. Léonel, J. P. Paugam, J.-Y. Nédélec, Tetrahedron 2002, 58, 271 – 277.

(8)   K.-J. Stahl, W. Hertzsch, H. Musso, Liebigs Ann. Chem. 1985, 1474 – 1484.

(9)   A. B. Charette, N. Wilb, Synlett 2002, 176 – 178.

(10)   E. J. Corey, M. Jautelat, J. Am. Chem. Soc. 1967, 89, 3912 – 3914.

(11)   P. J. Chirik, Angew. Chem. Int. Ed. 2017, 56, 5170 – 5181; Angew. Chem. 2017, 129, 5252 – 5265.

(12)   H. Kanai, H. Matsuda, J. Mol. Catal. 1985, 29, 157 – 164.

(13)   J. Werth, C. Uyeda, Chem. Sci. 2018, 9, 1604 – 1609

(14)   a) A. B. Charette, A. Beauchemin, Org. React. 2001, 58, 1 – 415; b) W. B. Motherwell, C. J. Nutley, Contemp. Org. Synth. 1994, 1, 219 – 241.

(15)   a) A. H. Hoveyda, D. A. Evans, G. C. Fu, Chem. Rev. 1993, 93, 1307 – 1370; b) C. D. Poulter, E. C. Friedrich, S. Winstein, J. Am. Chem. Soc. 1969, 91, 6892 – 6894.

(16)   M. P. Doyle, Chem. Rev. 1986, 86, 919 – 939.

(17)   K. Fujmoto, N. Itaya, Y. Okuno, T. Kadota, T. Yamaguchi, Agric. Biol. Chem. 1973, 37, 2681 – 2682.

(18)   G. Zuo, J. Louie, Angew. Chem. Int. Ed. 2004, 43, 2277 – 2279; Angew. Chem. 2004, 116, 2327 – 2329.

(19)   P. A. Wender, C. O. Husfeld, E. Langkopf, J. A. Love, J. Am. Chem. Soc. 1998, 120, 1940 – 1941.

(20)   T. Li, J. Liang, A. Ambrogelly, T. Brennan, G. Gloor, G. Huisman, J. Lalonde, A. Lekhal, B. Mijts, S. Muley, L. Newman, M. Tobin, G. Wong, A. Zaks, X. Zhang, J. Am. Chem. Soc. 2012, 134, 6467 – 6472.

(21)   a) H. Singh, N. Gupta, P. Kumar, S. K. Dubey, P. K. Sharma, Org. Process Res. Dev. 2009, 13, 870 – 874; b) M. Tian, A. Abdelrahman, S. Weinhausen, S. Hinz, S. Weyer, S. Dosa, A. El-Tayeb, C. E. Müller, Bioorg. Med. Chem. 2014, 22, 1077 – 1088.

(22)   K. Kawashima, Y. Kawano, Chem. Pharm. Bull. 1976, 24, 2751 – 2760.

(23)   B. Ravinder, S. Rajeshwar Reddy, M. Sridhar, M. Murali Mohan, K. Srinivas, A. Panasa Reddy, R. Bandichhor, Tetrahedron Lett. 2013, 54, 2841 – 2844

APPENDIX A. SUPPORTING INFORMATION FOR CHAPTER 1

1. General Information

General considerations. All manipulations were carried out using standard Schlenk or glovebox techniques under an atmosphere of N_2. THF was dried and degassed by passing through a column of activated alumina and sparging with Ar gas. $CDCl_3$ was purchased from Cambridge Isotope Laboratories, Inc., degassed, and stored over activated 3 Å molecular sieves prior to use. All other reagents and starting materials were purchased from commercial vendors and used without further purification unless otherwise noted. PDI ligands and the [$^{i\text{-Pr}}$PDI]CoBr$_2$ complex **1** were synthesized according to reported methods.[1,2] Liquid reagents were degassed and stored over activated 3 Å molecular sieves prior to use. Zn powder (325 mesh, 99.9%) and CoBr$_2$ were purchased from Strem. CoBr$_2$ was dried in the oven and stored in the glovebox.

Physical methods. ^{1}H and ^{13}C{^{1}H} NMR spectra were collected at room temperature on a Varian INOVA 300 MHz spectrometer or a Bruker Avance 500 MHz spectrometer. ^{1}H and ^{13}C{^{1}H} NMR spectra are reported in parts per million relative to tetramethylsilane, using the residual solvent resonances as an internal standard. High-resolution mass data were obtained using an Agilent 6320 Trap LC/MS, Agilent 5975C GC/MS, or Thermo Electron Corporation MAT 95XP-Trap. ATR-IR data were collected on a Thermo Scientific Nicolet Nexus spectrometer. Elemental analysis was performed by Midwest Microlab (Indianapolis, IN).

X-ray crystallography. Single-crystal X-ray diffraction studies were carried out at the Purdue University X-ray crystallography facility.

Procedure for XRD data collected using the Bruker Quest instrument (Cu Source). Single crystals of were coated with mineral oil and quickly transferred to the goniometer head of a Bruker Quest diffractometer with kappa geometry, an I-μ-S microsource X-ray tube, laterally graded multilayer (Goebel) mirror single crystal for monochromatization, a Photon2 CMOS area detector and an Oxford Cryosystems low temperature device. Examination and data collection were performed with Cu Kα radiation ($\lambda = 1.54178$ Å) at 150 K. Data were collected, reflections were indexed and processed, and the files scaled and corrected for absorption using APEX3.[3]

Structure Solution and Refinement. The space groups were assigned and the structures were solved by direct methods using XPREP within the SHELXTL suite of programs[4] and refined by full matrix least squares against F^2 with all reflections using Shelxl2016[5] using the graphical interface Shelxle.[6] If not specified otherwise H atoms attached to carbon atoms were positioned geometrically and constrained to ride on their parent atoms, with carbon hydrogen bond distances of 0.95 Å for aromatic C-H, 1.00, 0.99 and 0.98 Å for aliphatic C-H, CH$_2$ and CH$_3$ moieties, respectively. Methyl H atoms were allowed to rotate but not to tip to best fit the experimental electron density. U$_{iso}$(H) values were set to a multiple of U$_{eq}$(C) with 1.5 for CH$_3$, and 1.2 for C-H

units, respectively. Additional data collection and refinement details, including description of disorder can be found in Section 9 of the Supporting Information.

2. Procedures for Zn and Al Carbenoid Cyclopropanations

Figure S1. Comparison studies of Zn and Al carbenoid cyclopropanations.

entry	reaction conditions	yield (3 + 4)	rr (3:4)	yield 5
1	CH_2I_2 (1.0 equiv), Et_2Zn (0.5 equiv)	28%	1:6.7	3%
2	CH_2I_2 (1.0 equiv), Et_2Zn (1.0 equiv)	33%	1:4.6	5%
3	CH_2I_2 (2.0 equiv), Et_2Zn (2.0 equiv)	53%	1:6.5	16%
4	CH_2I_2 (2.0 equiv), Et_2Zn (2.0 equiv) 3,5-difluorobenzoic acid (2.0 equiv)	28%	1:3.5	19%
5	CH_2I_2 (2.0 equiv), Et_2Zn (2.0 equiv), $TiCl_4$ (20 mol%)	13%	1:4.6	1%
6	CH_2I_2 (1.2 equiv), $AlEt_3$ (1.2 equiv)	38%	1:3.1	9%

Entry 1. In an N_2-filled glovebox, a 5-mL vial was charged with olefin (0.14 mmol, 1.0 equiv), Et_2Zn (8.7 mg, 0.070 mmol, 0.50 equiv), CH_2Cl_2 (0.5 mL), and a magnetic stir bar. A solution of CH_2I_2 (38 mg, 0.14 mmol, 1.0 equiv) in CH_2Cl_2 (0.5 mL) was added dropwise, and the reaction mixture was stirred at room temperature for 24 h. After 24 h, CH_2Cl_2 was added to dilute the solution and an aliquot was used for GC analysis.

Entries 2 and 3. See procedure for Entry 1 with appropriate modifications to the equivalents of CH_2I_2 and Et_2Zn.

Entry 4. In an N_2-filled glovebox, a 5-mL vial was charged with olefin (0.14 mmol, 1.0 equiv), Et_2Zn (35 mg, 0.28 mmol, 2.0 equiv), CH_2Cl_2 (0.5 mL), and a magnetic stir bar. 3,5-Difluorobenzoic acid (43 mg, 0.28 mmol, 2.0 equiv) was added in portions to slow evolution of ethane gas. A solution of CH_2I_2 (75 mg, 0.28 mmol, 2.0 equiv) in CH_2Cl_2 (0.5 mL) was added dropwise, and the reaction mixture was stirred at room temperature for 24 h. After 24 h, CH_2Cl_2 was added to dilute the solution and an aliquot was used for GC analysis.

Entry 5. In an N_2-filled glovebox, a 5-mL vial was charged with olefin (0.14 mmol, 1.0 equiv), Et_2Zn (35 mg, 0.28 mmol, 2.0 equiv), CH_2Cl_2 (0.5 mL), and a magnetic stir bar. A solution of CH_2I_2 (75 mg, 0.28 mmol, 2.0 equiv) in CH_2Cl_2 (0.5 mL) was added dropwise. $TiCl_4$ (5.3 mg, 0.028 mmol, 0.2 equiv) was added dropwise, and the reaction mixture was stirred at room temperature for 24 h. After 24 h, CH_2Cl_2 was added to dilute the solution and an aliquot was used for GC analysis.

Entry 6. In an N_2-filled glovebox, a 5-mL vial was charged with olefin (0.14 mmol, 1.0 equiv), Et_3Al (20 mg, 0.17 mmol, 1.2 equiv), CH_2Cl_2 (0.5 mL), and a magnetic stir bar. A solution of

CH$_2$I$_2$ (45 mg, 0.17 mmol, 1.2 equiv) in CH$_2$Cl$_2$ (0.5 mL) was added dropwise, and the reaction mixture was stirred at room temperature for 24 h. After 24 h, CH$_2$Cl$_2$ was added to dilute the solution and an aliquot was used for GC analysis.

Entry 1

Peak#	Ret.Time	Area	Height
1	8.727	101196	36842
2	8.989	15143	6950
3	9.127	477195	171955
4	11.981	13560	2722
Total		607094	218469
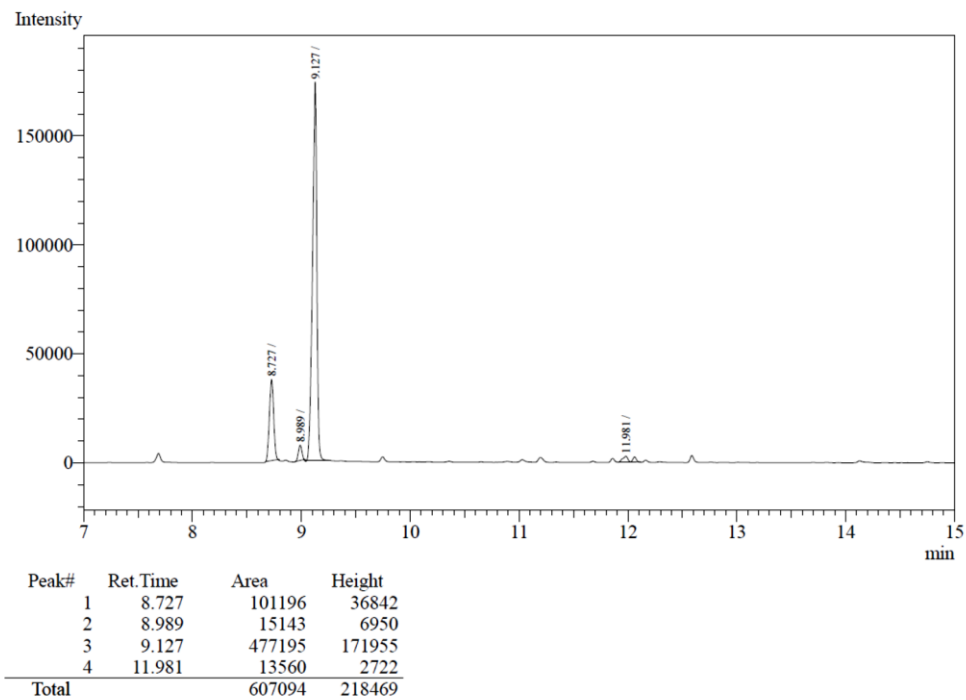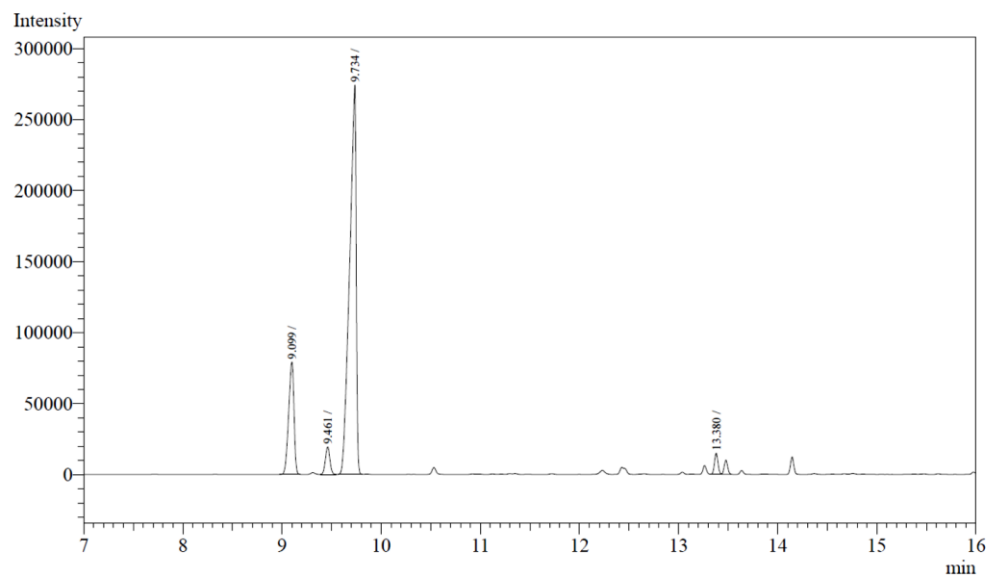
Entry 2

Peak#	Ret.Time	Area	Height
1	9.099	297373	78921
2	9.461	64586	19550
3	9.734	1255396	272338
4	13.380	60218	14604
Total		1677573	385413

Entry 3
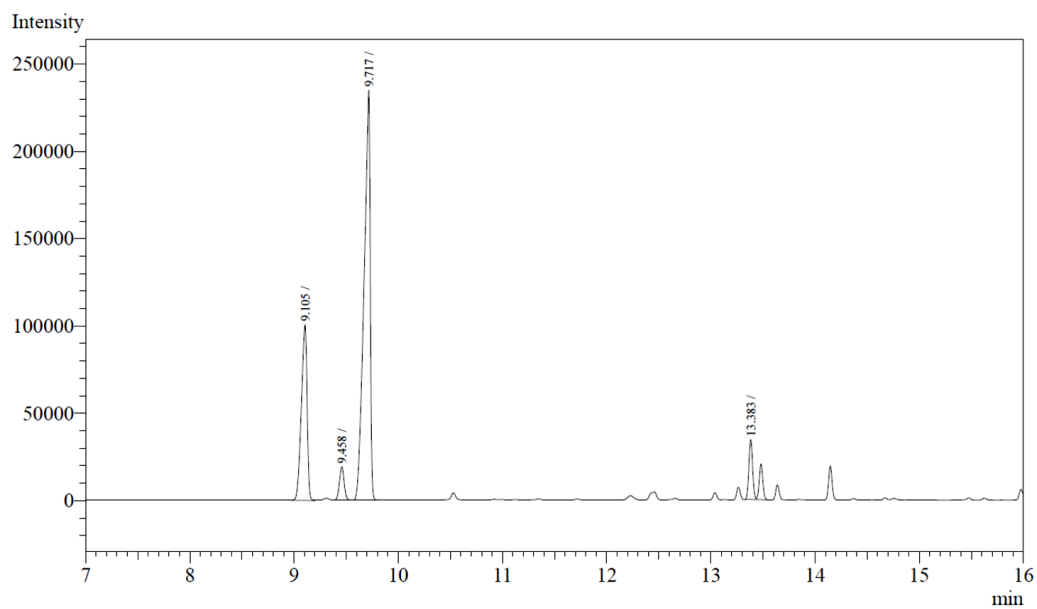
Peak#	Ret.Time	Area	Height
1	9.105	385361	100093
2	9.458	58944	18895
3	9.717	961668	232079
4	13.383	133669	34217
Total		1539642	385284

Entry 4
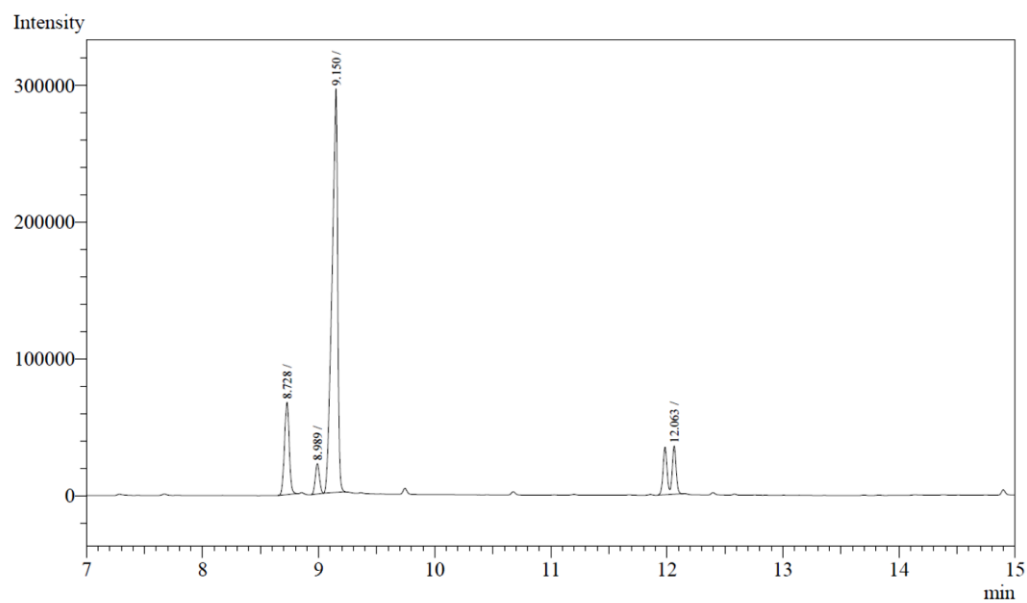
Peak#	Ret.Time	Area	Height
1	8.728	192745	66693
2	8.989	55303	22053
3	9.150	999362	293992
4	12.063	163995	34994
Total		1411405	417732

Entry 5

Peak#	Ret.Time	Area	Height
1	8.716	43219	15347
2	8.982	9459	3931
3	9.120	467288	165720
4	11.975	5659	1225
Total		525625	186223

Entry 6

Peak#	Ret.Time	Area	Height
1	8.725	124858	44144
2	8.987	40612	17567
3	9.126	493344	176963
4	11.980	40457	8866
Total		699271	247540

entry	reaction conditions[a]	yield (a + b)	rr (a:b)	yield c
1	CH$_2$I$_2$ (1.0 equiv), Et$_2$Zn (0.5 equiv)	35%	1:1.6	9%
2	CH$_2$I$_2$ (2.0 equiv), Et$_2$Zn (2.0 equiv) 3,5-difluorobenzoic acid (2.0 equiv)	39%	2.1:1	32%
3	CH$_2$I$_2$ (2.0 equiv), Et$_2$Zn (2.0 equiv), TiCl$_4$ (20 mol%)	35%	1:1.7	27%
4	CH$_2$I$_2$ (1.2 equiv), AlEt$_3$ (1.2 equiv)	45%	1.6:1	46%

[a]conducted using the same procedues as for 4-vinylcyclohexene)

Figure S2. GC data for Zn and Al carbenoid cyclopropanations.

Entry 1

Peak#	Ret.Time	Area	Height
1	7.539	357444	204052
2	8.666	83761	29133
3	9.069	53387	33763
4	9.414	35706	12978
Total		530298	279926

Entry 2

Peak#	Ret.Time	Area	Height
1	7.546	705695	355398
2	8.664	100337	33171
3	9.071	207278	127873
4	9.417	254091	97258
Total		1267401	613700

Entry 3
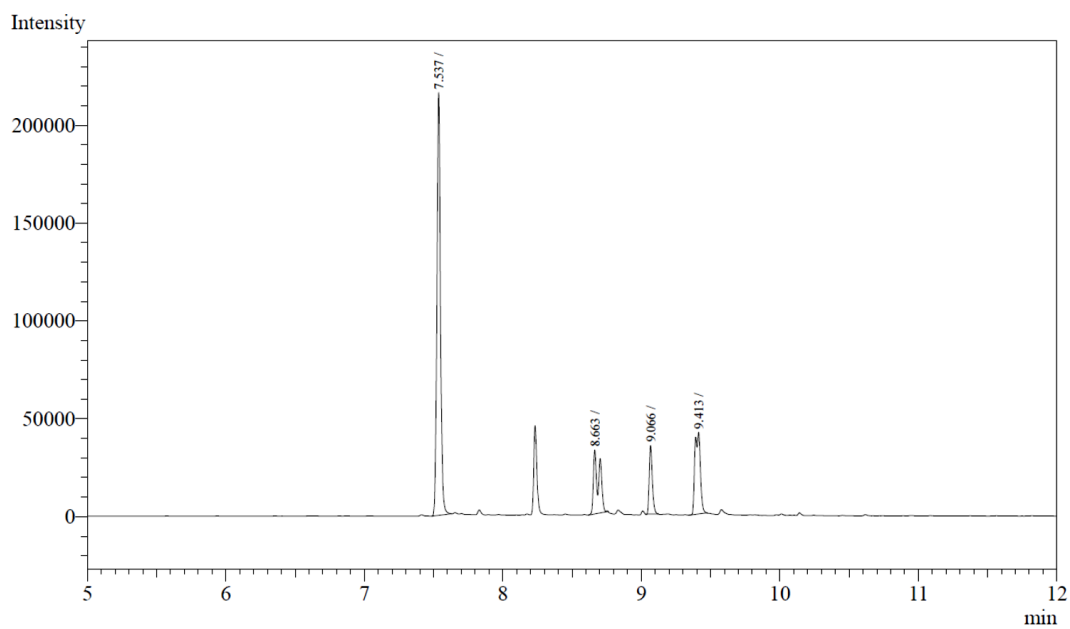
Peak#	Ret.Time	Area	Height
1	7.537	381855	212434
2	8.663	92874	31986
3	9.066	53781	34663
4	9.413	114968	41006
Total		643478	320089

Entry 4
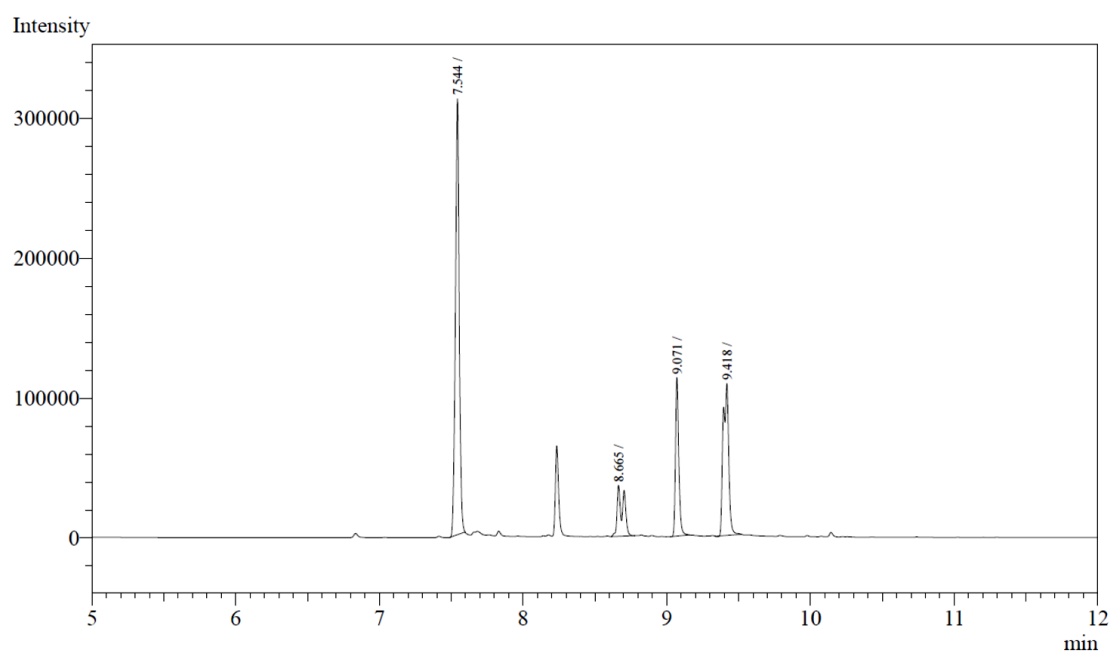
Peak#	Ret.Time	Area	Height
1	7.544	573759	307795
2	8.665	108866	36058
3	9.071	179599	112211
4	9.418	291031	105018
Total		1153255	561082

3. Optimization Studies for Transition Metal-Catalyzed Cyclopropanations

entry	metal source	ligand	yield (**3** +**4**)	rr (**3:4**)	yield **5**
1	–	–	<1%	–	<1%
2	CoBr$_2$	–	<1%	–	<1%
3	Co(DME)Br$_2$	–	<1%	–	<1%
4	–	$^{i\text{-Pr}}$PDI	<1%	–	<1%
5	CoBr$_2$	$^{i\text{-Pr}}$PDI	81%	>50:1	<1%
6	CoBr$_2$	^{Me}PDI	58%	>50:1	<1%
7	CoBr$_2$	^{Ph}PDI	4%	–	<1%
8	CoBr$_2$	$^{i\text{-Pr}}$DAD	<1%	–	<1%
9	CoBr$_2$	$^{i\text{-Pr}}$IP	2%	–	<1%
10	CoBr$_2$	terpyridine	4%	–	<1%
11	CoBr$_2$	(*S*)-$^{t\text{-Bu}}$PyBOX	<1%	–	<1%
12	CoBr$_2$	(*S*)-^{Ph}PyBOX	<1%	–	<1%
13	CoBr$_2$	[PPh$_3$]$_2$	<1%	–	0%
14	FeBr$_2$	$^{i\text{-Pr}}$PDI	3%	–	<1%
15	NiBr$_2$	$^{i\text{-Pr}}$PDI	<1%	–	<1%

Figure S3. Optimization studies probing metal and ligand sources.

General Procedure. In an N₂-filled glovebox, a 3-mL vial was charged with the metal source (0.0084 mmol, 0.060 equiv), ligand (0.0084 mmol, 0.060 equiv), THF (0.5 mL), and a magnetic stir bar. The catalyst mixture was allowed to stir at room temperature for 24 h. After this premixing period, 4-vinylcyclohexene (0.14 mmol, 1.0 equiv), CH_2Br_2 (27 mg, 0.15 mmol, 1.1 equiv), Zn powder (18 mg, 0.28 mmol, 2.0 equiv), mesitylene internal standard, and THF (0.5 mL) were added. The reaction mixture was stirred at room temperature for 24 h. After 24 h, CH_2Cl_2 was added to dilute the solution and an aliquot was used for GC analysis.

Peak#	Ret.Time	Area	Height
1	9.536	1150313	280109
2	9.772	1625979	334056
Total		2776292	614165
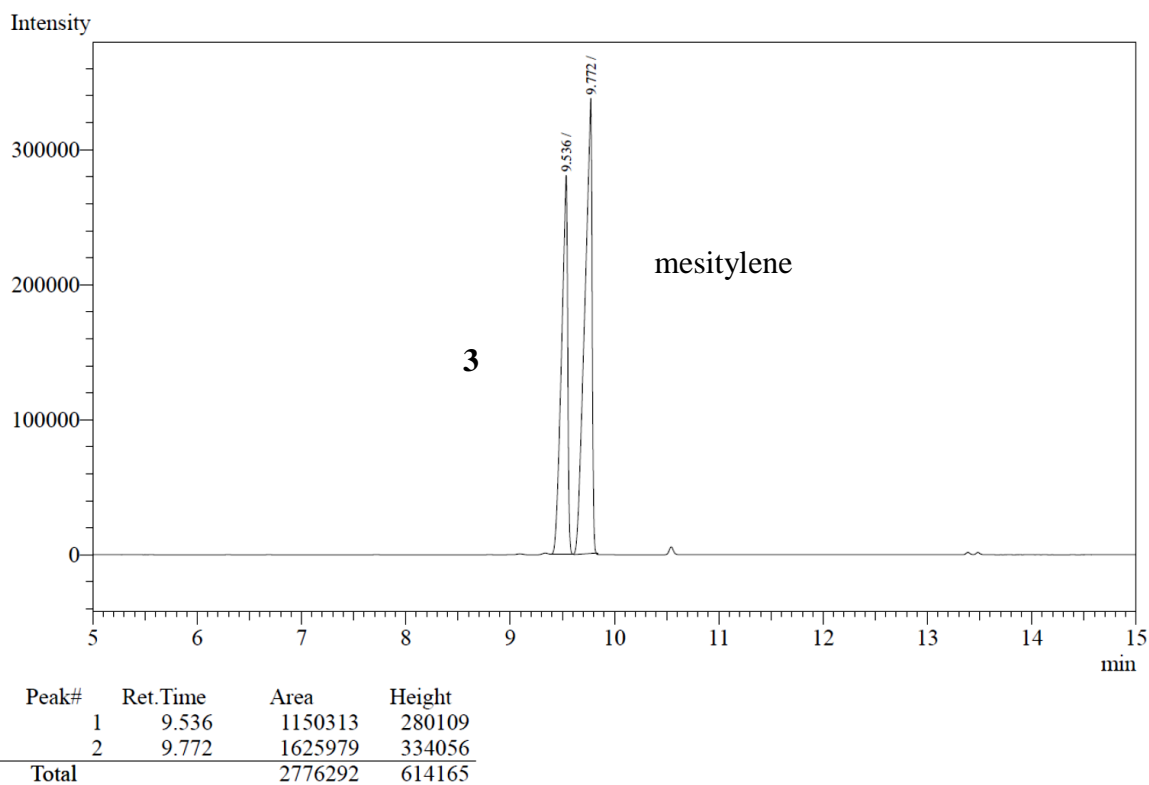
Figure S4. GC data for entry 5 in Figure S3.

4. Procedures for Competition Experiments

In an N$_2$-filled glovebox, a 3-mL vial was charged with [$^{i\text{-}Pr}$PDI]CoBr$_2$ (5.9 mg, 0.0084 mmol, 0.06 equiv), each alkene (0.14 mmol, 1.0 equiv), CH$_2$Br$_2$ (24 mg, 0.14 mmol, 1.0 equiv), Zn powder (18 mg, 0.28 mmol, 2.0 equiv), THF (1.0 mL), and a magnetic stir bar. The reaction was stirred for 24h. An aliquot was diluted with CH$_2$Cl$_2$ and used for GC analysis. Relative response factors of all products were assumed to be the same. Retention times were determined using authentic samples of each cyclopropane product.
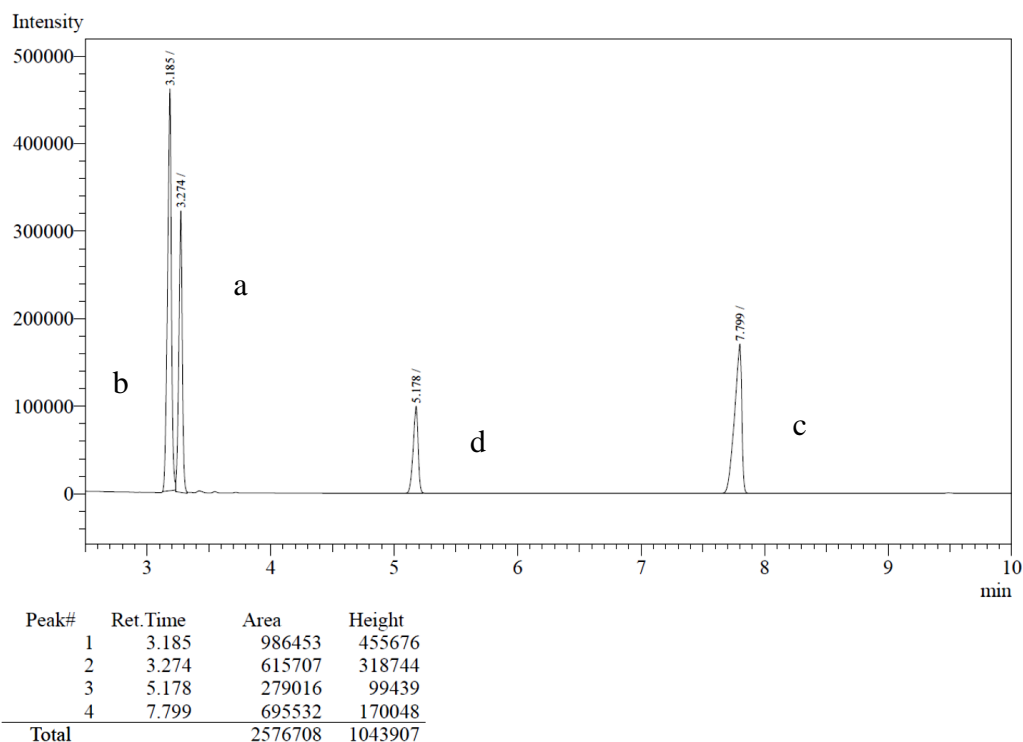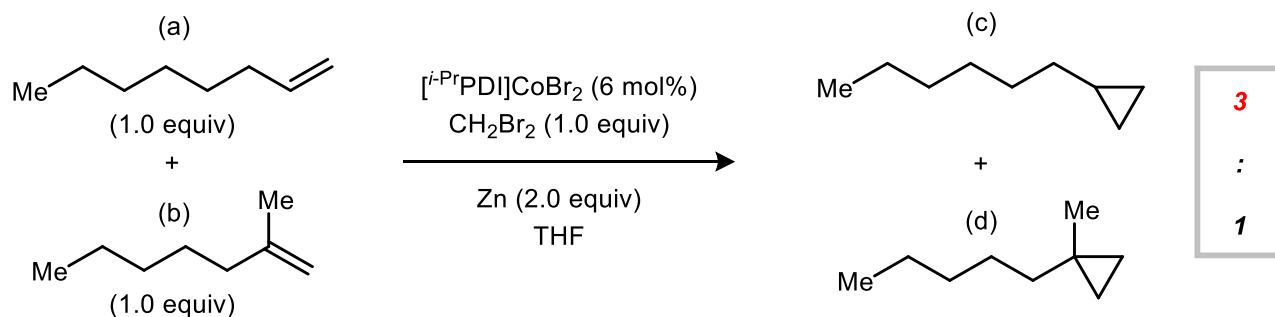
Figure S5. GC data for the competition experiment between 1-octene and 2-methyl-1-hepetene.
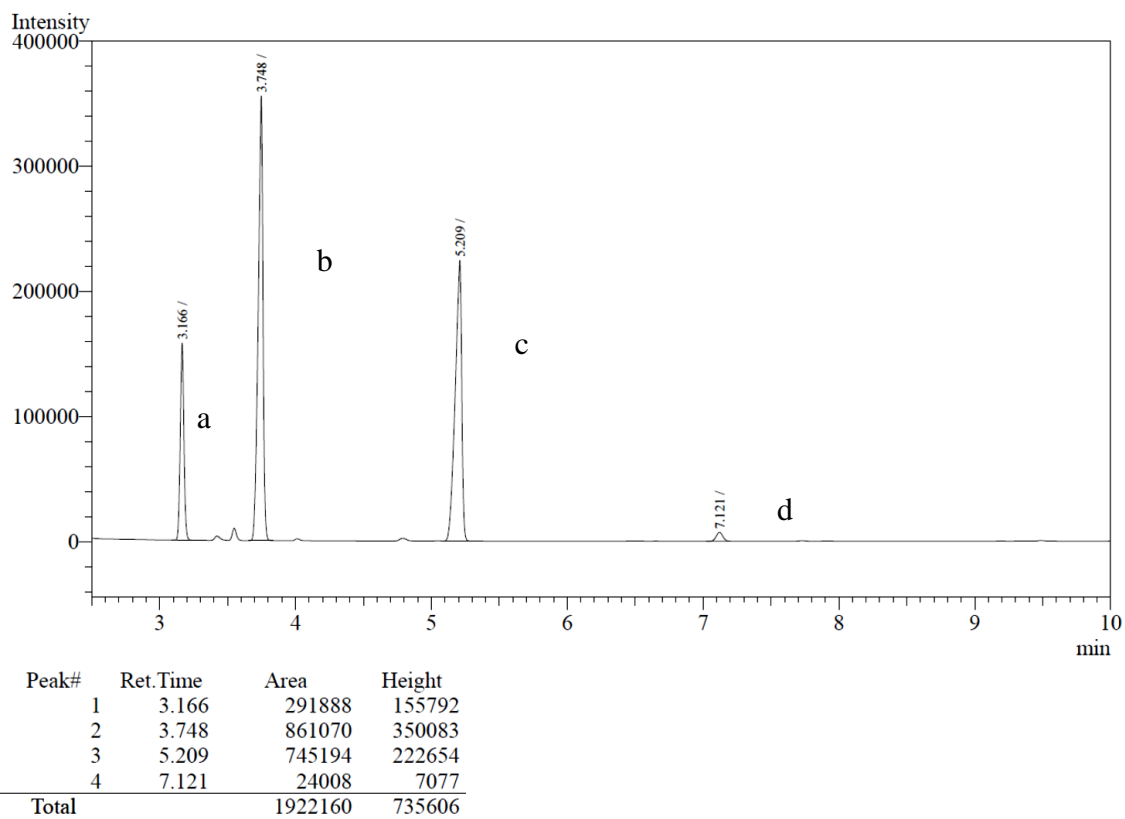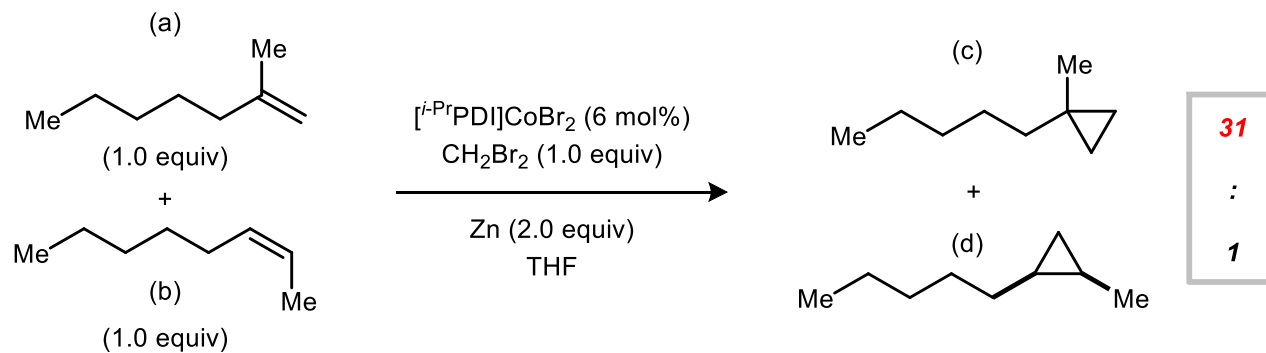
Figure S6. GC data for the competition experiment between 2-methyl-1-hepetene and (*Z*)-2-octene.
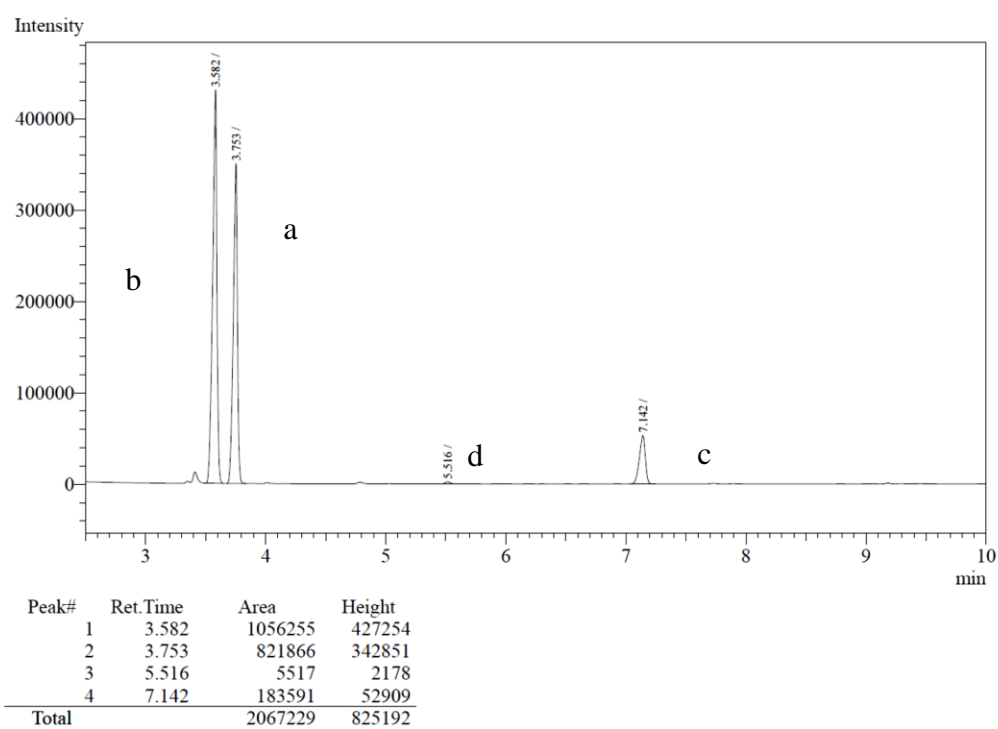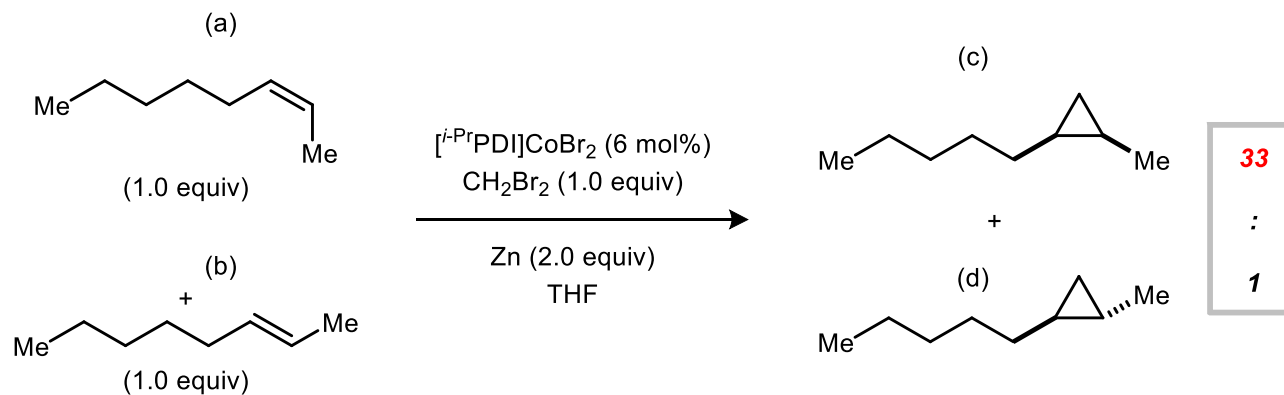
Figure S7. GC data for the competition experiment between (Z)-2-octene and (E)-2-octene using 1.0 equiv of CH₂Br₂.
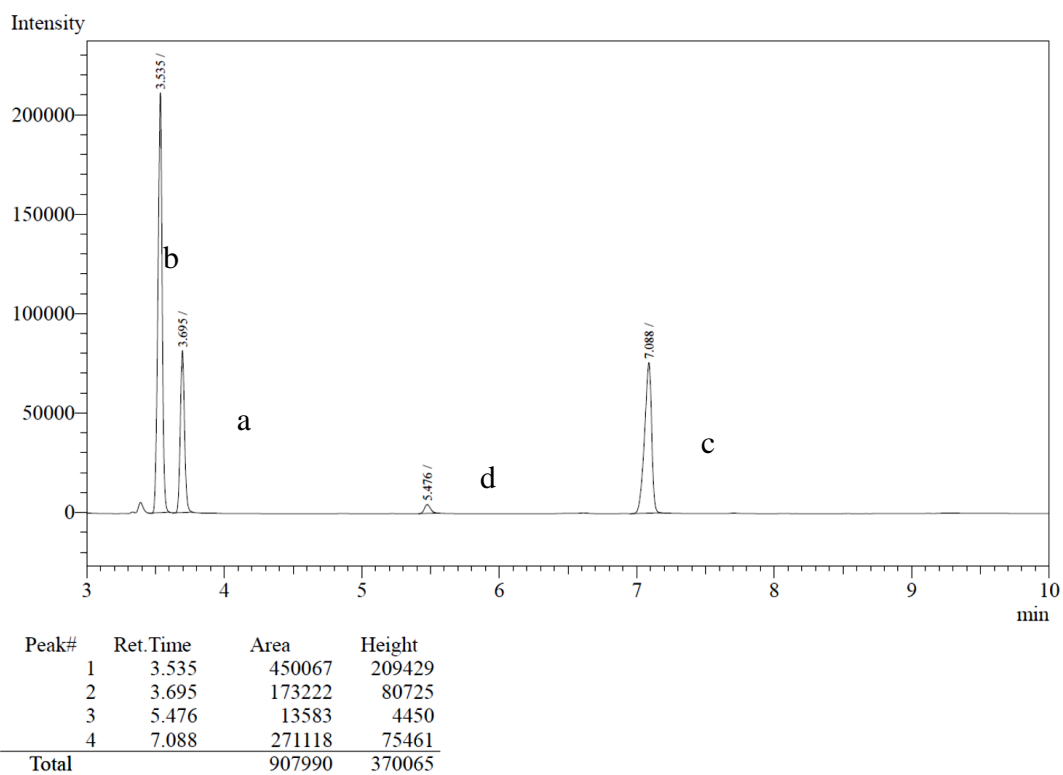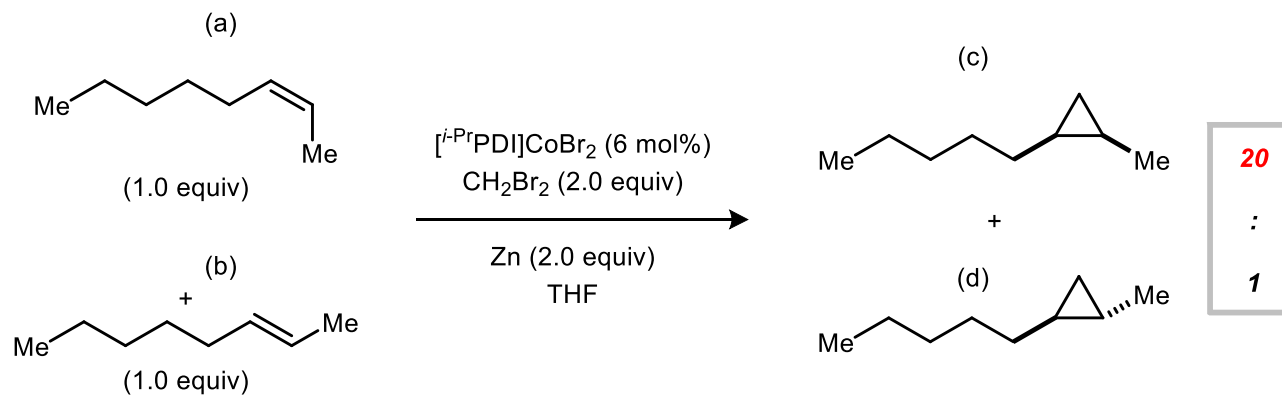
Figure S8. GC data for the competition experiment between (*Z*)-2-octene and (*E*)-2-octene using 2.0 equiv of CH$_2$Br$_2$.

5. Procedures for Regioselective Monocyclopropanation Reactions

General Procedure. In an N_2-filled glovebox, a 3-mL vial was charged with [$^{i\text{-Pr}}$PDI]CoBr$_2$ (5.9 mg, 0.0084 mmol, 0.06 equiv), the substrate (0.14 mmol, 1.0 equiv), CH$_2$Br$_2$ (37 mg, 0.21 mmol, 1.5 equiv), Zn powder (18 mg, 0.28 mmol, 2.0 equiv), THF (1.0 mL), and a magnetic stir bar. The reaction was stirred at room temperature. After 24 h, the reaction mixture was concentrated under reduced pressure, and the crude residue was directly loaded onto a column for purification.
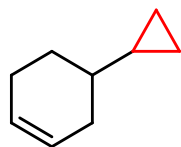
(4). The reaction was conducted using 4-vinylcyclohexene (18 µL) without modification from the general procedure to provide **4** as a colorless oil.

NMR Yield: Run 1: 88% yield. Run 2: 81% yield.

Isolated Yield: 11.7 mg (68% yield)

Purification: SiO$_2$ column; pentane

^{1}H NMR (300 MHz, CDCl$_3$) δ 5.65 (s, 2H), 2.18-1.98 (m, 3H), 1.90-1.80 (m, 2H), 1.45-1.31 (m, 1H), 0.84-0.72 (m, 1H), 0.63-0.53 (m, 1H), 0.42-0.37 (m, 2H), 0.10-0.06 (m, 2H).

^{13}C{^{1}H} NMR (126 MHz, CDCl$_3$) δ 127.0, 126.7, 39.0, 31.6, 28.6, 25.3, 16.9, 3.2, 3.0.

HRMS (EI) calc. for C$_9$H$_{14}^+$: m/z=122.1090, found: m/z=122.1091
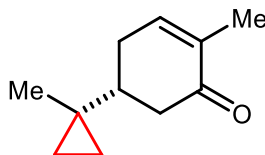
(6). The reaction was conducted using (–)-Carvone (19 µL) without modification from the general procedure to provide **6** as a yellow oil.

Run 1: 19.1 mg (83% yield). Run 2: 21.2 mg (92% yield). 1g scale: 922 mg (91% yield)

Purification: SiO$_2$ column; CH$_2$Cl$_2$

^{1}H NMR (300 MHz, CDCl$_3$) δ 6.76-6.73 (m, 1H), 2.47 (dd, J = 3.78, 16.05 Hz, 1H), 2.34-2.24 (m, 3H), 1.74 (q, J = 1.69 Hz, 3H), 1.41-1.28 (m, 1H), 0.96 (s, 3H), 0.27 (s, 4H).

^{13}C{^{1}H} NMR (126 MHz, CDCl$_3$) δ 200.6, 145.3, 135.3, 44.2, 42.2, 29.6, 19.1, 18.3, 15.7, 12.3, 12.3.

HRMS (ESI) calc. for C$_{11}$H$_{17}$O: m/z=165.1280, found: m/z=165.1274
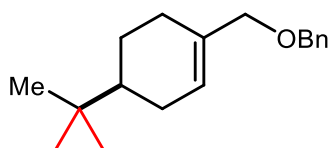
(7). The reaction was conducted using benzyloxylimonene[7] (34 mg) without modification from the general procedure to provide **7** as a colorless oil.

Run 1: 33.7 mg (94% yield). Run 2: 35.5 mg (99% yield).

Purification: SiO_2 column; CH_2Cl_2

^{1}H NMR (300 MHz, CDCl$_3$) δ 7.36-7.27 (m, 5H), 5.73 (s, 1H), 4.47 (s, 2H), 3.89 (s, 2H), 2.21-2.12 (m, 1H), 2.09-2.00 (m, 3H), 1.86-1.77 (m, 1H), 1.49-1.37 (m, 1H), 0.95 (s, 3H), 0.90-0.82 (m, 1H), 0.30-0.21 (m, 4H).

^{13}C{^{1}H} NMR (126 MHz, CDCl$_3$) δ 138.7, 134.7, 128.3, 127.7, 127.4, 125.3, 74.7, 71.6, 42.2, 28.3, 27.1, 26.3, 19.2, 18.7, 12.4, 12.3.

HRMS (ESI) calc. for $C_{18}H_{25}O$: m/z=257.1906, found: m/z=257.1903
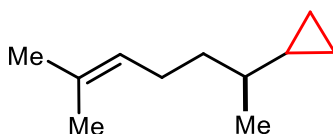
(8). The reaction was conducted using (+)-β-citronellene (25 µL) without modification from the general procedure to provide **8** as a colorless oil.

Run 1: 19.8 mg (93% yield). Run 2: 18.5 mg (87% yield).

Purification: SiO_2 column; pentane

^{1}H NMR (300 MHz, CDCl$_3$) δ 5.10 (t, J = 7.09 Hz, 1H), 2.03 (q, J = 7.65, 2H), 1.68 (s, 3H), 1.61 (s, 3H), 1.51-1.39 (m, 1H), 1.35-1.23 (m, 2H), 0.95, (d, J = 6.6 Hz, 3H), 0.73-0.61 (m, 1H), 0.52-0.30 (m, 2H), 0.12-(-0.07) (m, 2H).

^{13}C{^{1}H} NMR (126 MHz, CDCl$_3$) δ 131.0, 125.2, 38.2, 37.5, 25.8, 25.7, 19.8, 18.0, 17.6, 4.4, 2.9.

HRMS (EI) calc. for $C_{11}H_{20}{}^+$: m/z=152.1560, found: m/z=152.1563
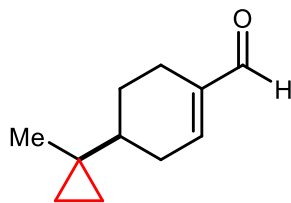
(9). The reaction was conducted using (–)-perillaldehyde (22 µL) without modification from the general procedure to provide **9** as a light yellow oil.

Run 1: 22.3 mg (97% yield). Run 2: 22.5 mg (98% yield).

Purification: SiO$_2$ column; CH$_2$Cl$_2$

^{1}H NMR (300 MHz, CDCl$_3$) δ 9.41 (s, 1H), 6.83-6.80 (m, 1H), 2.52-2.44 (m, 1H), 2.33-2.23 (m, 1H), 2.07-1.92 (m, 1H), 1.89-1.82 (m, 1H), 1.41-1.14 (m, 2H), 0.95 (s, 3H), 0.93-0.86 (m, 1H), 0.28-0.17 (m, 4H).

^{13}C{^{1}H} NMR (126 MHz, CDCl$_3$) δ 194.1, 151.6, 141.5, 42.1, 29.8, 25.3, 22.2, 18.9, 18.4, 12.5.

HRMS (ESI) calc. for C$_{11}$H$_{17}$O: m/z=165.1280, found: m/z=165.1273
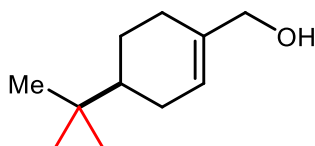
(10). The reaction was conducted using (–)-perillyl alcohol (22 µL) without modification from the general procedure to provide **10** as a light yellow oil.

Run 1: 13.0 mg (56% yield). Run 2: 15.8 mg (68% yield).

Purification: SiO$_2$ column; CH$_2$Cl$_2$

^{1}H NMR (300 MHz, CDCl$_3$) δ 5.68 (s, 1H), 3.98 (s, 2H), 2.10-2.06 (m, 1H), 2.00-1.95 (m, 2H), 1.83-1.76 (m, 1H), 1.48-1.33 (m, 2H), 1.26-1.13 (m, 1H), 0.93 (s, 3H), 0.89-0.79 (m, 1H), 0.28-0.15 (m, 4H).

^{13}C{^{1}H} NMR (126 MHz, CDCl$_3$) δ 137.3, 123.1, 67.4, 42.2, 28.2, 26.7, 26.3, 19.2, 18.7, 12.4, 12.3.

HRMS (EI) calc. for C$_{11}$H$_{18}$O$^+$: m/z=166.1352, found: m/z=166.1352
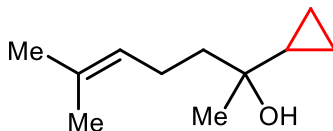
(11). The reaction was conducted using linalool (25 µL) without modification from the general procedure to provide **11** as a light yellow oil.

Run 1: 13.4 mg (57% yield). Run 2: 14.4 mg (61% yield).

Purification: SiO_2 column; pentane/CH_2Cl_2

^{1}H NMR (300 MHz, CDCl$_3$) δ 5.18-5.11 (m, 1H), 2.13 (q, $J = 7.05$, 2H), 1.69 (s, 3H), 1.63 (s, 3H), 1.59-1.53 (m, 2H), 1.11 (s, 3H), 1.09 (s, 1H), 0.95-0.86 (m, 1H), 0.39-0.25 (m, 4H).

^{13}C{^{1}H} NMR (126 MHz, CDCl$_3$) δ 131.7, 124.6, 71.2, 42.9, 25.9, 22.8, 21.0, 17.7, 0.5.

HRMS (EI) calc. for $C_{11}H_{21}$: m/z=169.1593, found: m/z=169.1587
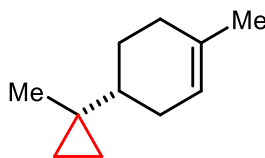
(12). The reaction was conducted using (+)-limonene (23 µL) without modification from the general procedure to provide **12** as a colorless oil.

Run 1: 17.0 mg (81% yield). Run 2: 16.6 mg (79% yield). 1.5 g scale: 1.49 g (90% yield)

Purification: SiO_2 column; pentane

^{1}H NMR (300 MHz, CDCl$_3$) δ 5.38 (s, 1H), 2.04-1.88 (m, 4H), 1.75-1.65 (m, 1H), 1.63 (s, 3H), 1.48-1.32 (m, 1H), 0.92 (s, 3H), 0.88-0.77 (m, 1H), 0.27-0.17 (m, 4H).

^{13}C{^{1}H} NMR (126 MHz, CDCl$_3$) δ 133.9, 121.1, 42.1, 31.1, 29.7, 28.5, 26.7, 23.5, 19.3, 18.7, 12.4, 12.3.

HRMS (EI) calc. for $C_{11}H_{18}^+$: m/z=150.1403, found: m/z=150.1408

Gram-scale catalytic cyclopropanation of (+)-Limonene. In an N_2-filled glovebox, a 250-mL round-bottom flask was charged with CoBr$_2$ (144 mg, 0.66 mmol, 0.060 equiv), the $^{i\text{-Pr}}$PDI ligand (318 mg, 0.66 mmol, 0.060 equiv), THF (50 mL), and a magnetic stir bar. The catalyst mixture was allowed to stir at room temperature for 24 h. After this premixing period, (+)-limonene (1.5 g, 11 mmol, 1.0 equiv), CH$_2$Br$_2$ (2.85 g, 16.5 mmol, 1.5 equiv), and Zn powder (1.43 mg, 22 mmol, 2.0 equiv) were added. The reaction mixture was stirred at room temperature. After 24 h, the reaction mixture was concentrated under reduced pressure, and the crude residue was directly loaded onto a column for purification. (1.49 g, 90% yield)
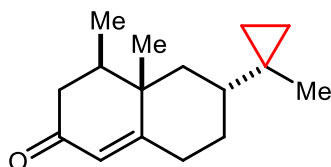
(13). The reaction was conducted using (+)-nootkatone (31 mg) without modification from the general procedure to provide **13** as an off-white solid.

Run 1: 27.3 mg (84% yield). Run 2: 29.9 mg (92% yield).

Purification: SiO_2 column; CH_2Cl_2

^{1}H NMR (300 MHz, CDCl3) δ 5.74 (s, 1H), 2.46-2.31 (m, 2H), 2.27-2.18 (m, 2H), 2.07-1.94 (m, 1H), 1.90-1.74 (m, 2H), 1.40-1.30 (m, 1H), 1.28-1.17 (m, 1H), 1.14-1.10 (m, 1H), 1.01 (s, 3H), 0.98 (d, $J = 6.79$ Hz, 3H), 0.88 (s, 3H), 0.28-0.21 (m, 4H).

^{13}C{^{1}H} NMR (126 MHz, CDCl3) δ 199.7, 171.3, 124.6, 42.3, 42.1, 41.4, 40.6, 39.2, 33.2, 29.9, 18.9, 18.8, 16.9, 15.0, 13.0, 12.9.

HRMS (ESI) calc. for $C_{16}H_{25}O$: m/z=233.1906, found: m/z=233.1901
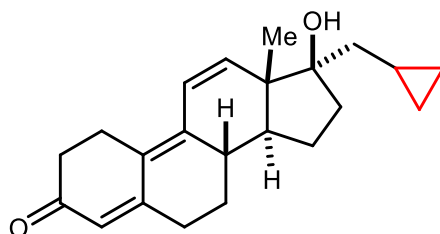
(14). The reaction was conducted using altrenogest (43 mg) without modification from the general procedure to provide **14** as a yellow oil.

Run 1: 37.2 mg (82% yield). Run 2: 39.1 mg (86% yield).

Purification: SiO_2 column; 3:2 EtOAc/hexane

^{1}H NMR (300 MHz, CDCl3) δ 6.44 (d, $J = 9.93$ Hz, 1H), 6.29 (d, $J = 10.02$ Hz, 1H), 5.77 (s, 1H), 2.83-2.76 (m, 2H), 2.61-2.52 (m, 2H), 2.46 (t, $J = 7.21$ Hz, 3H), 2.31-2.21 (m, 1H), 2.10 (s, 1H), 1.94-1.86 (m, 1H), 1.80-1.63 (m, 3H), 1.55-1.47 (m, 2H), 1.39-1.21 (m, 2H), 1.02 (s, 3H), 0.90-0.79 (m, 1H), 0.54 (dd, $J = 8.0, 1.25$ Hz, 2H), 0.16-0.04 (m, 2H).

^{13}C{^{1}H} NMR (126 MHz, CDCl3) δ 199.2, 156.5, 142.0, 141.8, 126.9, 123.8, 123.6, 82.7, 49.0, 47.7, 42.7, 38.3, 36.7, 35.1, 31.5, 27.1, 24.3, 23.1, 16.5, 5.6, 4.5, 4.1.

HRMS (ESI) calc. for $C_{22}H_{29}O_2$: m/z=325.2168, found: m/z=325.2163

6. Procedures for Regioselective Monocyclopropanations of 1,3-Dienes

General Procedure. In an N_2-filled glovebox, a 3-mL vial was charged with [$^{i\text{-Pr}}$PDI]CoBr$_2$ (5.9 mg, 0.0084 mmol, 0.06 equiv), the substrate (0.14 mmol, 1.0 equiv), CH_2Br_2 (37 mg, 0.21 mmol, 1.5 equiv), Zn powder (18 mg, 0.28 mmol, 2.0 equiv), THF (1.0 mL), and a magnetic stir bar. The reaction was stirred at room temperature. After 24 h, the reaction mixture was concentrated under reduced pressure, and the crude residue was directly loaded onto a column for purification.
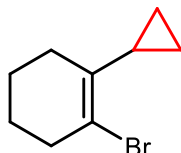
(15). The reaction was conducted using 1-bromo-2-vinylcyclohex-1-ene[8] (26 mg) without modification from the general procedure to provide **15** as a yellow oil.

Run 1: 17.7 mg (63% yield). Run 2: 18.0 mg (64% yield).

Purification: SiO$_2$ column; CH$_2$Cl$_2$

^{1}H NMR (300 MHz, CDCl$_3$) δ 2.54-2.49 (m, 2H), 2.06-1.97 (m, 1H), 1.68-1.66 (m, 4H), 1.64-1.57 (m, 2H), 0.68-0.51 (m, 4H)

^{13}C{^{1}H} NMR (126 MHz, CDCl$_3$) δ 134.6, 119.8, 37.0, 25.9, 24.8, 22.2, 17.0, 14.1, 3.9.

HRMS (ESI) calc. for C$_9$H$_{13}$Br$^+$: m/z=199.0121, found: m/z=199.0116
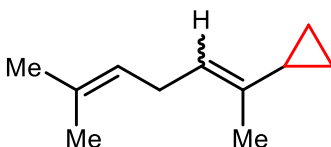
(16). The reaction was conducted using ocimene (2.3:1 *E/Z* ratio) (24 μL) without modification from the general procedure to provide **16** as a colorless oil.

Run 1: 16.6 mg (79% yield). Run 2: 17.5 mg (83% yield).

Purification: SiO$_2$ column; pentane

^{1}H NMR (300 MHz, CDCl$_3$) δ 5.18 (t, *J* = 7.21 Hz, 1H), 5.14-5.07 (m, 1H), 2.86-2.67 (m, 2H), 1.70-1.69 (m, 3H), 1.65-1.63 (m, 3H), 1.51-1.41 (m, 3H), 1.39-1.26 (m, 1H), 0.64-0.40 (m, 4H).

^{13}C{^{1}H} NMR (126 MHz, CDCl$_3$) δ 135.4, 134.6, 131.3, 124.5, 123.4, 123.3, 121.9, 27.0, 26.6, 25.7, 18.9, 18.7, 17.7, 13.8, 12.3, 4.2, 4.0.

HRMS (ESI) calc. for C$_{11}$H$_{17}$: m/z=149.1330, found: m/z=149.1324
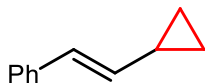
(17). The reaction was conducted using (*E*)-buta-1,3-dien-1-ylbenzene[9] (18 mg) without modification from the general procedure to provide **17** as a colorless oil.

Run 1: 17.0 mg (84% yield). Run 2: 17.4 mg (86% yield).

Purification: SiO_2 column; pentane

^{1}H NMR (300 MHz, CDCl$_3$) δ 7.33-7.14 (m, 5H), 6.49 (d, *J* = 15.8 Hz), 5.79-5.70 (m, 1H), 1.64-1.53 (m, 1H), 0.88-0.78 (m, 2H), 0.55-0.50 (m, 2H).

^{13}C{^{1}H} NMR (126 MHz, CDCl$_3$) δ 137.8, 134.9, 128.5, 127.4, 126.5, 125.6, 14.6, 7.3.

HRMS (CI) calc. for $C_{11}H_{12}^+$: m/z=144.0934, found: m/z=144.0932
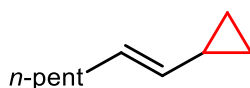
(18). The reaction was conducted using (*E*)-nona-1,3-diene[9] (17 mg) without modification from the general procedure to provide **18** as a colorless oil.

Run 1: 12.6 mg (65% yield). Run 2: 13.9 mg (72% yield).

Purification: SiO_2 column; pentane

^{1}H NMR (300 MHz, CDCl$_3$) δ 5.51 (dt, *J* = 6.76 Hz, 15.24 Hz, 1H), 4.95 (ddt, *J* = 15.2, 8.5, 1.5 Hz, 1H), 2.00-1.93 (m, 2H), 1.39-1.31 (m, 3H), 1.30-1.24 (m, 4H), 0.88 (t, *J* = 6.69 Hz, 3H), 0.68-0.61 (m, 2H), 0.33-0.28 (m, 2H).

^{13}C{^{1}H} NMR (126 MHz, CDCl$_3$) δ 133.6, 128.4, 32.5, 31.4, 29.4, 22.6, 14.1, 13.5, 6.3.

HRMS (CI) calc. for $C_{10}H_{18}^+$: m/z=138.1409, found: m/z=138.1406
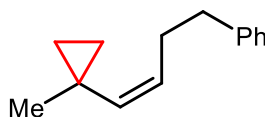
(19). The reaction was conducted using (Z)-(4-(1-methylcyclopropyl)but-3-en-1-yl)benzene[10] (24 mg) without modification from the general procedure to provide **19** as a colorless oil.

Run 1: 20.9 mg (80% yield). Run 2: 18.5 mg (71% yield).

Purification: SiO_2 column; pentane

^{1}H NMR (300 MHz, CDCl$_3$) δ 7.35-7.19 (m, 5H), 5.53 (d, *J* = 10.81 Hz, 1H), 5.42-5.34 (m, 1H), 2.73-2.68 (m, 2H), 2.62-2.54 (m, 2H), 1.14 (s, 3H), 0.54-0.43 (m, 4H).

^{13}C{^{1}H} NMR (126 MHz, CDCl$_3$) δ 142.2, 135.1, 131.1, 128.5, 128.3, 125.8, 36.1, 30.3, 25.0, 14.9, 14.6.

HRMS (APCI) calc. for $C_{16}H_{19}$: m/z=187.1481, found: m/z=187.1483
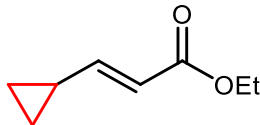
(20). The reaction was conducted using ethyl (*E*)-penta-2,4-dienoate[11] (18 mg) without modification from the general procedure to provide **20** as a colorless oil.

Run 1: 15.1 mg (77% yield). Run 2: 14.9 mg (76% yield).

Purification: SiO_2 column; CH_2Cl_2

^{1}H NMR (300 MHz, CDCl$_3$) δ 6.41 (dd, *J* = 10.07, 15.42 Hz, 1H), 5.88 (d, *J* = 15.42, 1H), 4.16, (q, *J* = 7.13 Hz, 2H), 1.62-1.50 (m, 1H), 1.27 (t, *J* = 7.15 Hz, 3H), 0.96-0.90 (m, 2H), 0.65-0.60 (m, 2H).

^{13}C{^{1}H} NMR (126 MHz, CDCl$_3$) δ 166.7, 154.0, 118.2, 60.0, 14.3, 14.3, 8.6.

HRMS (CI) calc. for $C_8H_{12}O_2$: m/z=141.0910, found: m/z=141.0912
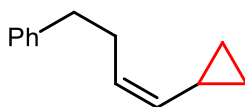
(21). The reaction was conducted using (Z)-hexa-3,5-dien-1-ylbenzene[12] (22 mg) without modification from the general procedure to provide **21** as a colorless oil.

Run 1: 22.9 mg (95% yield). Run 2: 21.9 mg (91% yield).

Purification: SiO_2 column; pentane

^{1}H NMR (300 MHz, CDCl$_3$) δ 7.34-7.19 (m, 5H), 5.42-5.33 (m, 1H), 4.79 (t, *J* = 9.83 Hz, 1H), 2.77-2.72 (m, 2H), 2.52 (q, *J* = 7.82 Hz, 2H), 1.59-1.46 (m, 1H), 0.75-0.69 (m, 2H), 0.34-0.29 (m, 2H).

^{13}C{^{1}H} NMR (126 MHz, CDCl$_3$) δ 142.2, 134.6, 128.5, 128.3, 127.1, 125.8, 36.1, 29.5, 9.7, 6.9.

HRMS (EI) calc. for $C_{13}H_{16}^+$: m/z=172.1247, found: m/z=172.1242
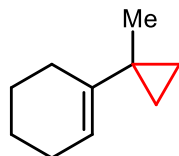
(22). The reaction was conducted using 1-(prop-1-en-2-yl)cyclohex-1-ene[13] (17 mg) without modification from the general procedure to provide **22** as a colorless oil.

Run 1: 12.0 mg (63% yield). Run 2: 13.5 mg (71% yield).

Purification: SiO_2 column; pentane

^{1}H NMR (300 MHz, CDCl$_3$) δ 5.50-5.48 (m, 1H), 2.02-1.89 (m, 4H), 1.64-1.50 (m, 4H), 1.13 (s, 3H), 0.58-0.55 (m, 2H), 0.34-0.31 (m, 2H).

^{13}C{^{1}H} NMR (126 MHz, CDCl$_3$) δ 141.2, 120.1, 25.9, 25.3, 23.9, 23.1, 22.6, 21.3, 12.5.

HRMS (EI) calc. for C$_{10}$H$_{15}$: m/z=135.1168, found: m/z=135.1165
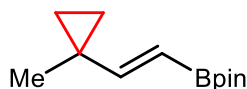
(23). The reaction was conducted using (E)-4,4,5,5-tetramethyl-2-(3-methylbuta-1,3-dien-1-yl)-1,3,2-dioxaborolane[14] (27 mg) without modification from the general procedure to provide **23** as a clear oil.

Run 1: 25.3 mg (87% yield). Run 2: 25.1 mg (86% yield).

Purification: SiO_2 column; CH_2Cl_2

^{1}H NMR (300 MHz, CDCl$_3$) δ 6.16 (d, J = 18.1 Hz, 1H), 5.37 (d, J = 18.1 Hz, 1H), 1.25 (s, 12H), 1.17, (s, 3H), 0.74-0.64, (m, 4H).

^{13}C{^{1}H} NMR (126 MHz, CDCl$_3$) δ 161.9, 82.9, 24.8, 20.2, 19.7, 16.2.

^{11}B NMR (96 MHz, CDCl$_3$): δ 30.0.

HRMS (ESI) calc. for C$_{12}$H$_{21}$BO$_2$$^+$: m/z=208.1749, found: m/z=208.1744
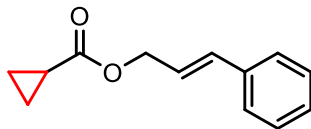
The reaction was conducted using cinnamyl acrylate[15] without modification from the general procedure to provide product **S1** as a yellow oil.

Run 1: 26.3 mg (93% yield). Run 2: 24.3 mg (86% yield).

Purification: SiO_2 column; CH_2Cl_2

^{1}H NMR (300 MHz, CDCl$_3$): 7.42-7.39 (m, 2H), 7.36-7.33 (m, 2H), 7.31-7.27 (m, 1H),

6.67 (d, J = 15.6 Hz, 1H), 6.31 (dt, J = 6.42, 15.87 Hz, 1H), 4.75 (dd, J = 1.26, 6.42 Hz, 2H),

1.71-1.63 (m, 1H), 1.07-1.02 (m, 2H), 0.92-0.86 (m, 2H),

^{13}C NMR (126 MHz, CDCl$_3$):174.7, 136.3, 134.0, 128.6, 128.0, 126.6, 123.4, 65.1, 12.9, 8.6

HRMS (EI) calc. for $C_{13}H_{14}O_2^+$: m/z= 202.0988, found: m/z 202.0994

7. CV Data
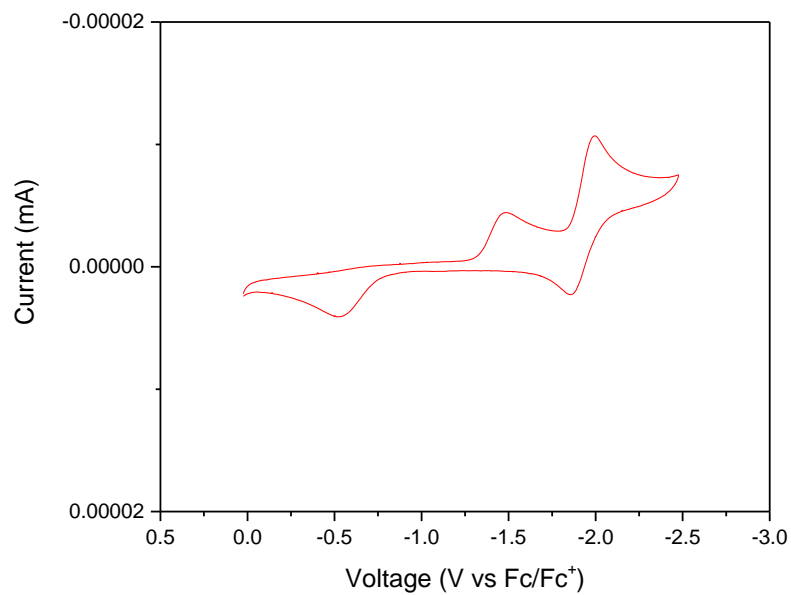
Figure S9. Cyclic voltammetry data for **1** (0.3 M [*n*-Bu$_4$N][PF$_6$] supporting electrolyte in THF, glassy carbon working electrode, 100 mV/s scan rate, N$_2$ atmosphere).

8. Synthesis and Characterization of the Co/Zn Complex 31
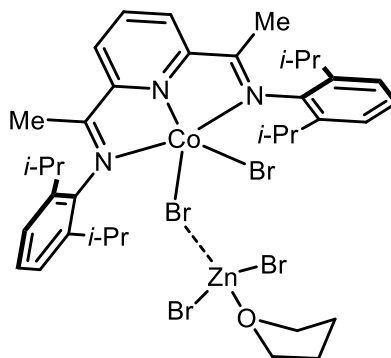
[$^{i\text{-Pr}}$PDI]CoBr$_2$Zn(THF/Et$_2$O)Br$_2$ (31). In an N$_2$-filled glovebox, a 20-mL vial was charged with [$^{i\text{-Pr}}$PDI]CoBr$_2$ (20 mg, 0.029 mmol, 1.0 equiv), ZnBr$_2$ (6.5 mg, 0.029 mmol, 1.0 equiv), THF (10-mL) and a magnetic stir bar. The reaction mixture was stirred at room temperature for 1 h to ensure complete complete dissolution and consumption of ZnBr$_2$. The reaction mixture was concentrated to dryness under reduced pressure. Ether was added to the residue, and the mixture was filtered through a glass fiber pad to produce a green solution. Slow-cooling of the solution (–30 °C) produced dark-green crystals (7 mg, 0.007 mmol, 24% yield). Single crystals obtained by this procedure were suitable for XRD analysis. Complex **31** is NMR silent.

Anal. Calc. for **31** (C$_{37}$H$_{51}$Br$_4$CoN$_3$OZn): C 44.54%, H 5.15%, N 4.21%; found: C 44.22%, H 5.24%, N 4.14%. In the solid state structure, there is a solvent molecule bound to Zn that is disordered between Et$_2$O and THF. The calculated elemental analysis is shown assuming 100% THF; however, the found values are also adequately modeled using 100% Et$_2$O due to the similarity in the elemental composition of the two solvents.
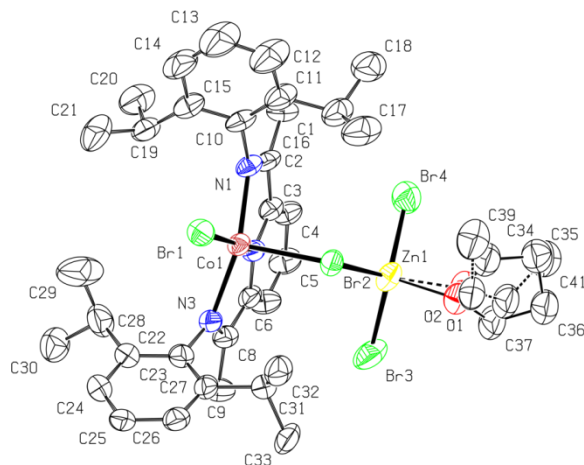
JJWIV_142_CoBr2PDI_0m

Crystal data	
Chemical formula	$C_{37}H_{51.88}Br_4CoN_3OZn$
M_r	998.64
Crystal system, space group	Orthorhombic, $P2_12_12_1$
Temperature (K)	150
a, b, c (Å)	12.6608 (8), 17.5590 (13), 18.5345 (14)
V (Å^3)	4120.4 (5)
Z	4
Radiation type	Cu $K\alpha$
μ (mm^{-1})	8.65
Crystal size (mm)	$0.23 \times 0.13 \times 0.10$
Data collection	
Diffractometer	Bruker AXS D8 Quest CMOS diffractometer

Absorption correction	Multi-scan
	SADABS 2016/2: Krause, L., Herbst-Irmer, R., Sheldrick G.M. & Stalke D., J. Appl. Cryst. 48 (2015) 3-10
T_{min}, T_{max}	0.429, 0.753
No. of measured, independent and observed [$I > 2\sigma(I)$] reflections	23175, 7493, 6130
R_{int}	0.064
Refinement	
$R[F^2 > 2\sigma(F^2)]$, $wR(F^2)$, S	0.048, 0.123, 1.02
No. of reflections	7493
No. of parameters	485
No. of restraints	131
H-atom treatment	H-atom parameters constrained
$\Delta\rho_{max}$, $\Delta\rho_{min}$ (e Å^{-3})	1.23, −0.96
Absolute structure	Flack x determined using 2262 quotients [(I+)-(I-)]/[(I+)+(I-)] (Parsons, Flack and Wagner, Acta Cryst. B69 (2013) 249-259).
Flack parameter	−0.011 (4)

A THF and an ether molecule are disordered at a Zn coordinated site. Equivalent bonds in the disordered moieties were restrained to have similar bond distances, and the ether CH_2-CH_3 bonds were restrained to 1.54(2) Angstrom. Uij components of ADPs for disordered atoms closer to each other than 1.7 Angstrom were restrained to be similar. Subject to these conditions the occupancy ratio refined to 0.558(13) to 0.442(13) in favor of THF.

9. Mechanistic Experiments
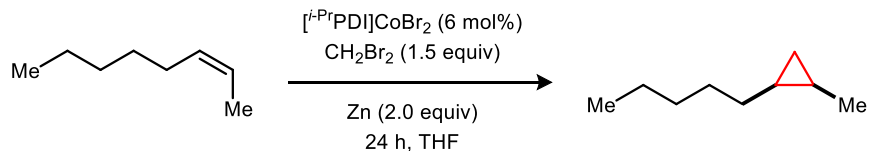
Stereospecificity. In an N_2-filled glovebox, a 3-mL vial was charged with [$^{i\text{-Pr}}$PDI]CoBr$_2$ (5.9 mg, 0.0084 mmol, 0.06 equiv), *cis*-2-octene (0.14 mmol, 1.0 equiv), CH_2Br_2 (37 mg, 0.21 mmol, 1.5 equiv), Zn powder (18 mg, 0.28 mmol, 2 equiv), mesitylene as an internal standard, THF (1 mL), and a magnetic stir bar. The reaction mixture was stirred at room temperature. After 24 h, CH_2Cl_2 was added to dilute the solution, and an aliquot of the mixture was removed and analyzed by GC. (95% yield, >50:1 *E*/*Z* ratio)
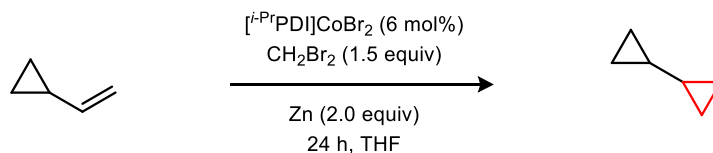
Radical Clock Experiment. In an N_2-filled glovebox, a 3-mL vial was charged with [$^{i\text{-Pr}}$PDI]CoBr$_2$ (5.9 mg, 0.0084 mmol, 0.06 equiv), vinylcyclopropane[16] (0.14 mmol, 1.0 equiv), CH_2Br_2 (37 mg, 0.21 mmol, 1.5 equiv), Zn powder (18 mg, 0.28 mmol, 2.0 equiv), mesitylene as an internal standard, THF (1.0 mL), and a magnetic stir bar. The reaction mixture was stirred at room temperature. After 24 h, an aliquot was removed and analyzed by ^{1}H NMR spectroscopy. No ring-opened product was observed by the limit of detection in the NMR.

NMR Yields: Run 1: 70% yield. Run 2: 72% yield.

^{1}H NMR (300 MHz, CDCl$_3$): 0.81-0.70 (m, 2H), 0.32-0.23 (m, 4H), 0.02-(-0.04) (m, 4H).
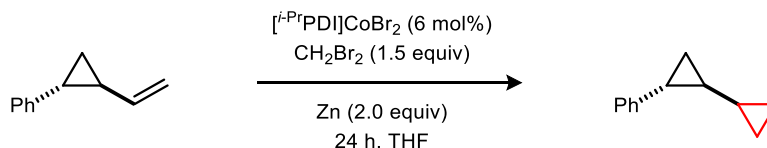
Radical Clock Experiment. In an N_2-filled glovebox, a 3-mL vial was charged with [$^{i\text{-}Pr}$PDI]CoBr$_2$ (5.9 mg, 0.0084 mmol, 0.06 equiv), (2-vinylcyclopropyl)benzene[17] (20 mg, 0.14 mmol, 1.0 equiv), CH_2Br_2 (37 mg, 0.21 mmol, 1.5 equiv), Zn powder (18 mg, 0.28 mmol, 2.0 equiv), THF (1.0 mL), and a magnetic stir bar. The reaction was stirred at room temperature. After 24 h, the reaction mixture was concentrated under reduced pressure. The crude residue directly purified by column chromatography to provide **29** as a colorless oil.

Run 1: 21.5 mg (97% yield). Run 2: 19.3 mg (87% yield).

Purification: SiO_2 column; pentane

^{1}H NMR (300 MHz, CDCl$_3$) δ 7.31-7.23 (m, 2H), 7.17-7.11 (m, 1H), 7.07-7.04 (m, 2H), 1.71-1.65 (m, 1H), 1.21-1.13 (m, 1H), 1.02-0.92 (m, 1H), 0.85-0.74 (m, 2H), 0.50-0.37 (m, 2H), 0.24-0.11 (m, 2H).

^{13}C{^{1}H} NMR (126 MHz, CDCl$_3$) δ 143.7, 128.2, 125.6, 125.2, 25.4, 21.7, 13.8, 12.4, 3.4, 2.6.

HRMS (EI) calc. for $C_{12}H_{14}^+$: m/z=158.1090, found: m/z=158.1085
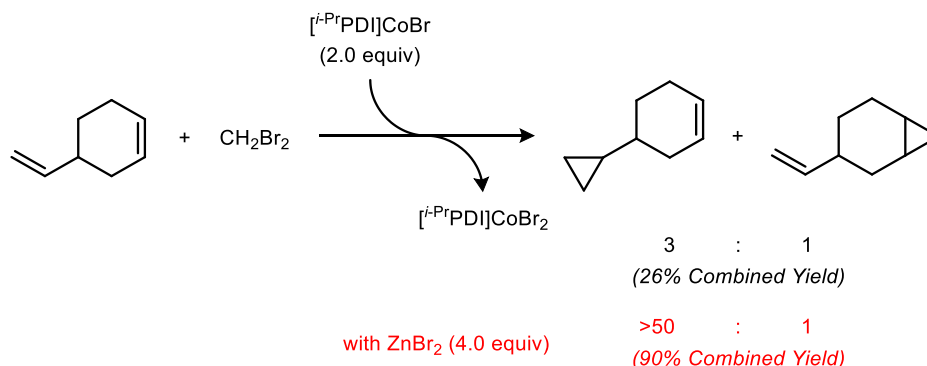
Stoichiometric Cyclopropanation with [$^{i\text{-}Pr}$PDI]CoBr. In an N_2-filled glovebox, a 3-mL vial was charged with [$^{i\text{-}Pr}$PDI]CoBr (5.2 mg, 0.0084 mmol, 0.06 equiv), 4-vinylcyclohexene (0.14 mmol, 1 equiv), CH_2Br_2 (27 mg, 0.15 mmol, 1.1 equiv), mesitylene as an internal standard, THF (1 mL), and a magnetic stir bar. The reaction mixture was stirred at room temperature. After 24 h, CH_2Cl_2 was added to dilute the solution and an aliquot was removed and analyzed by GC. The same procedure was repeated in the presence of $ZnBr_2$ (3.8 mg, 0.017 mmol, 0.12 equiv).

The yields were determined assuming that two equivalents of the [$^{i\text{-}Pr}$PDI]CoBr complex are required for each equivalent of cyclopropane that is generated.

10. NMR Spectra
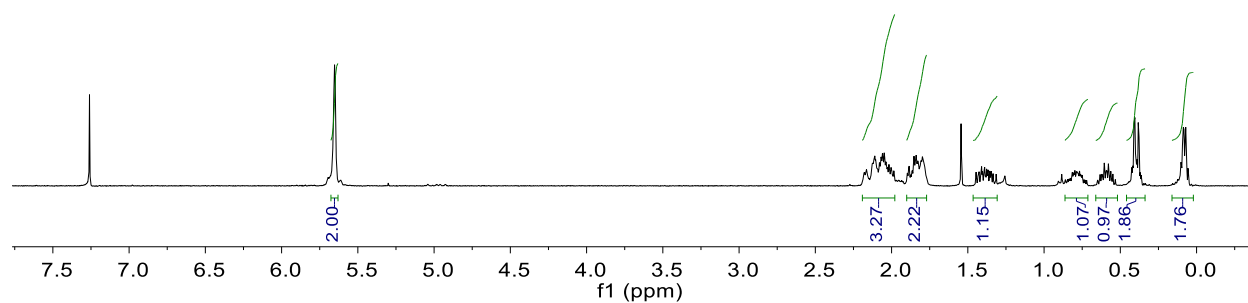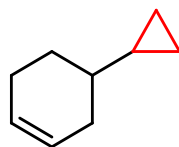
Figure S10. ^{1}H NMR spectrum for **4** (CDCl$_3$, 295 K).
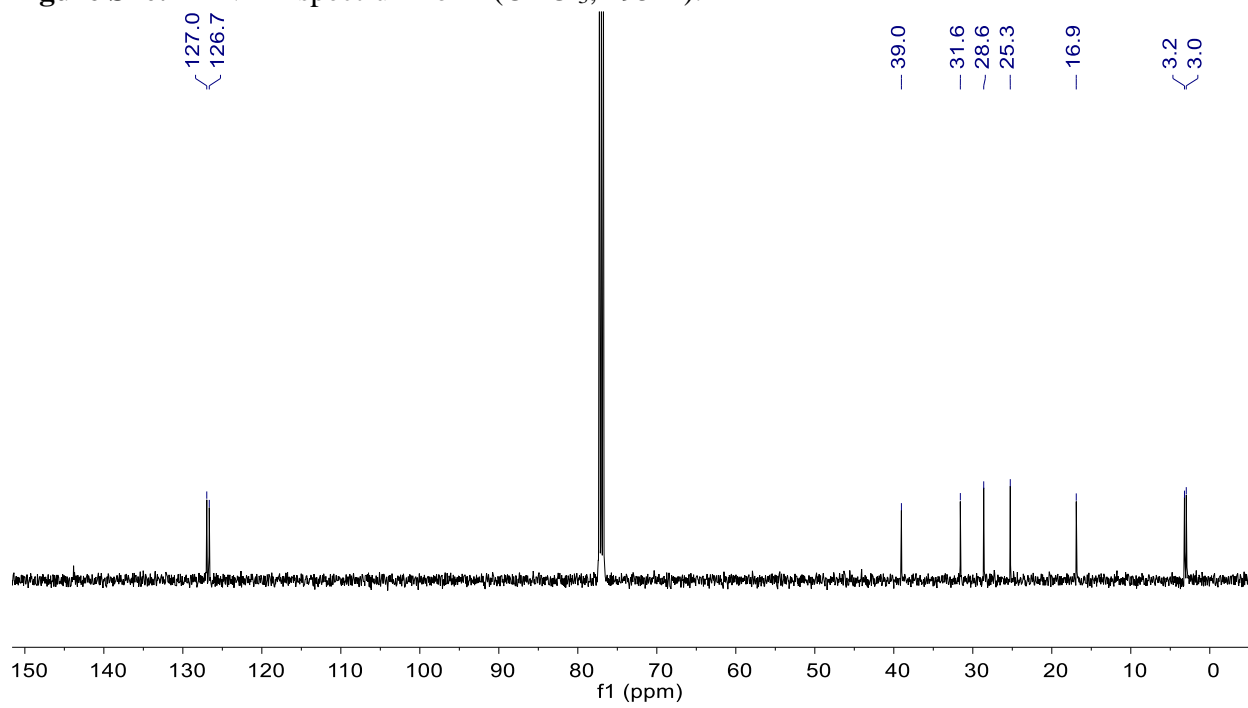
**Figure S11.** ^{13}C NMR spectrum for **4** (CDCl$_3$, 295 K).
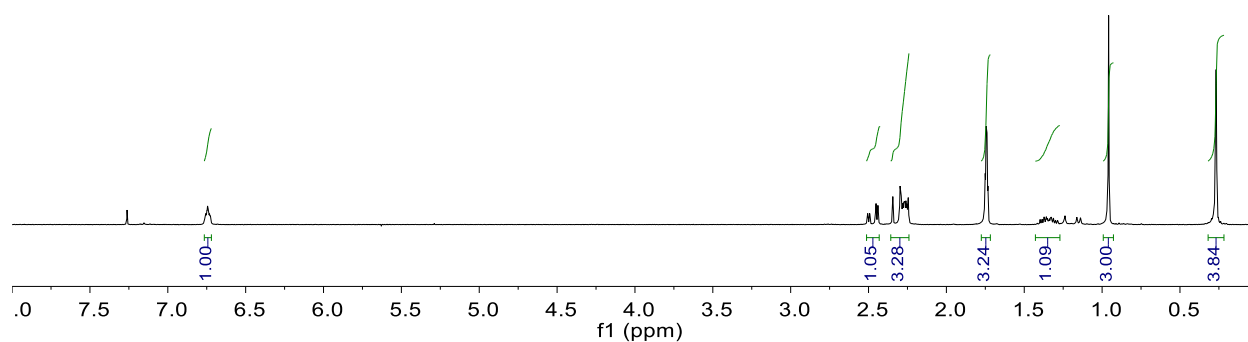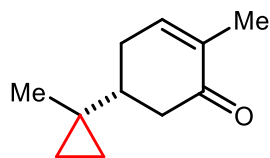
**Figure S12.** ^{1}H NMR spectrum for **6** (CDCl$_3$, 295 K).
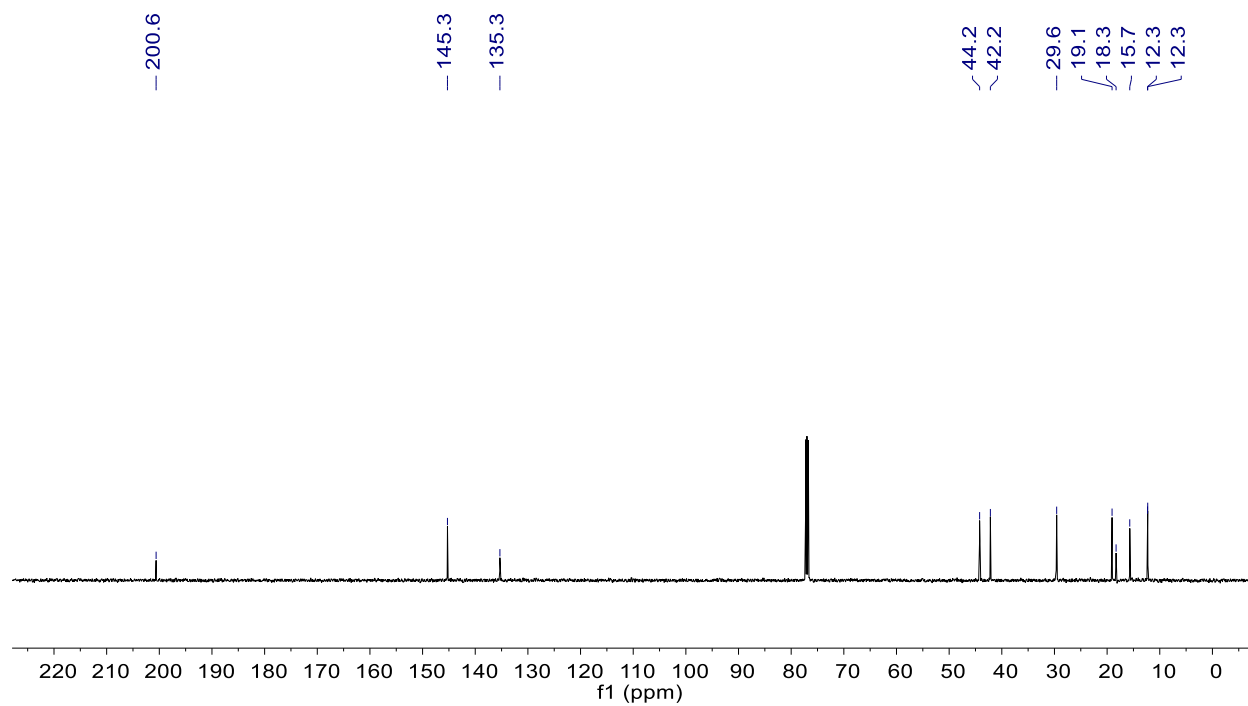
Figure S13. ^{13}C NMR spectrum for **6** (CDCl$_3$, 295 K).
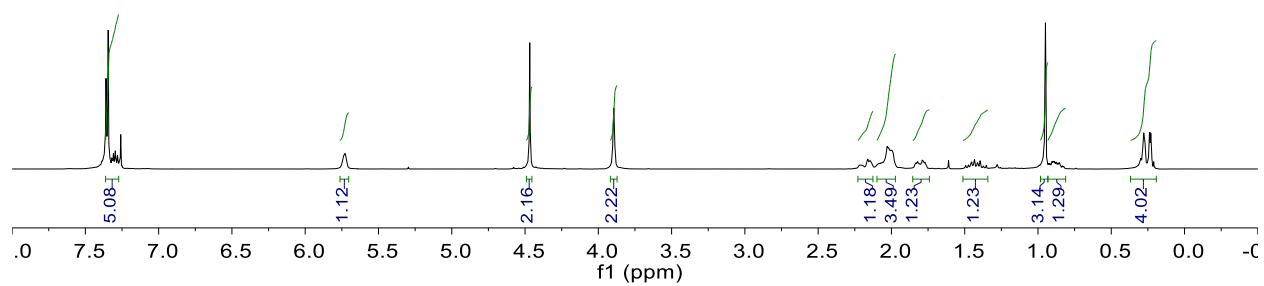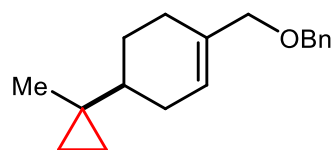
Figure S14. ^{1}H NMR spectrum for **7** (CDCl$_3$, 295 K).
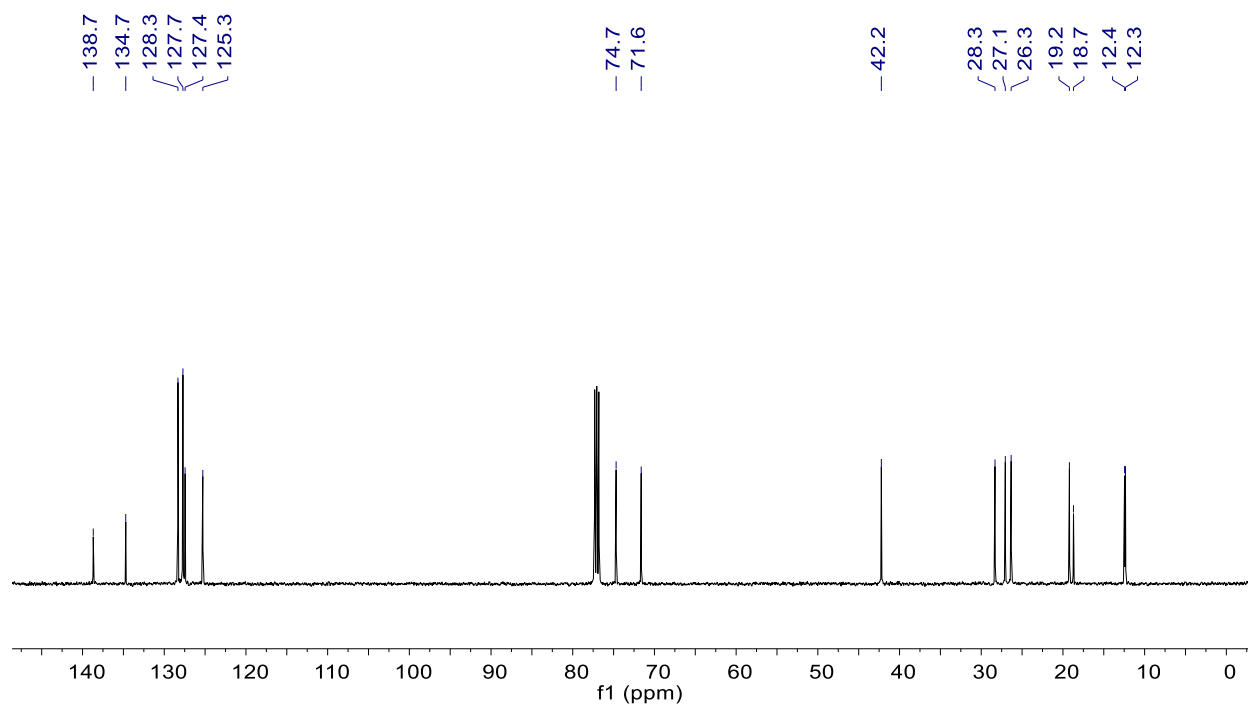
Figure S15. ^{13}C NMR spectrum for **7** (CDCl$_3$, 295 K).
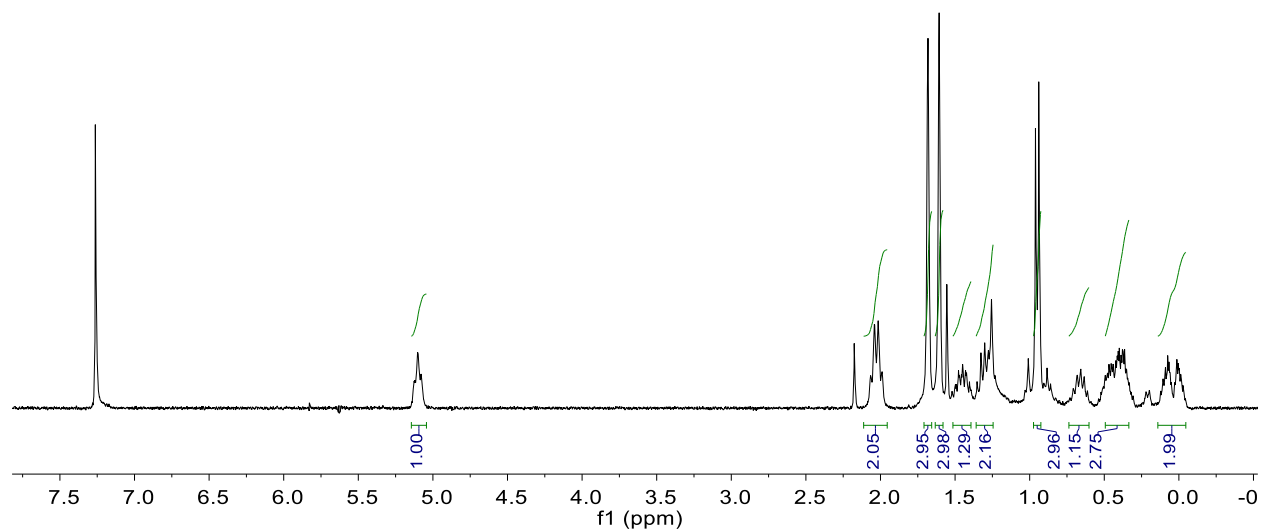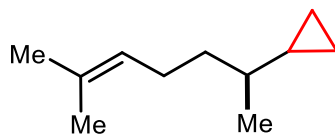
Figure S16. ^{1}H NMR spectrum for **8** (CDCl$_3$, 295 K).
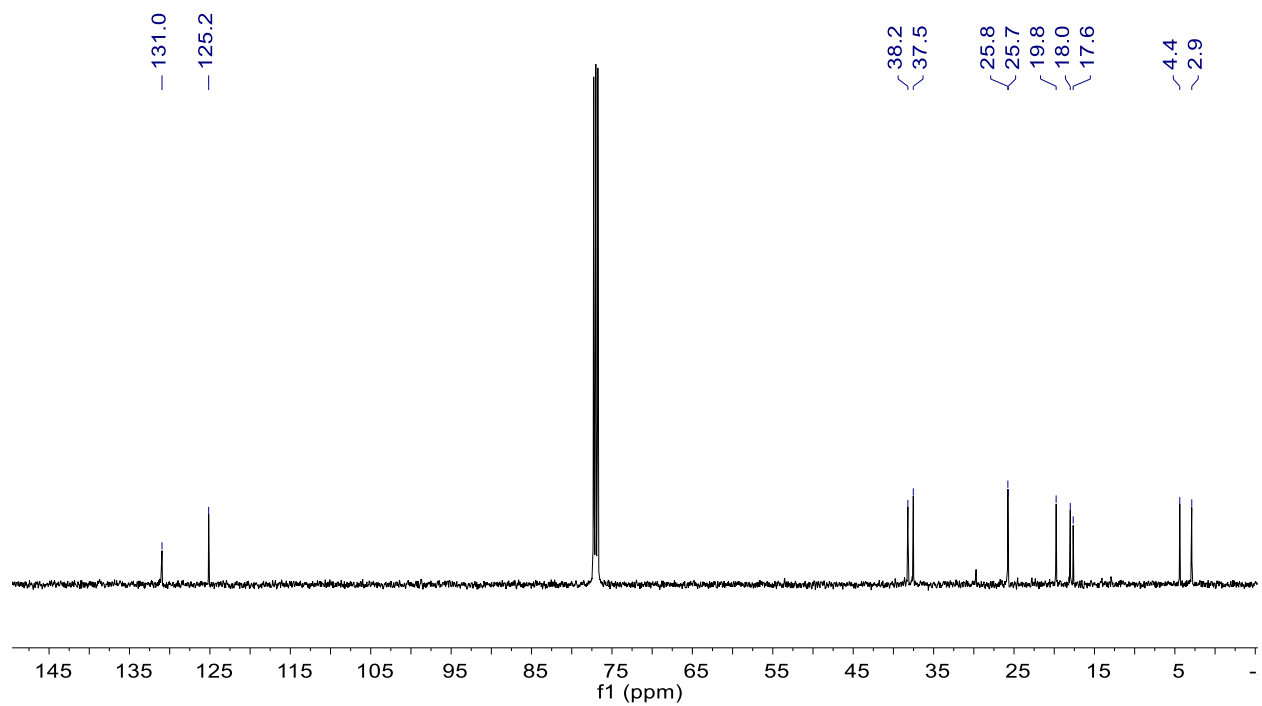
Figure S17. ^{13}C NMR spectrum for **8** (CDCl$_3$, 295 K).

Figure S18. ^{1}H NMR spectrum for **9** (CDCl$_3$, 295 K).

Figure S19. ^{13}C NMR spectrum for **9** (CDCl$_3$, 295 K).
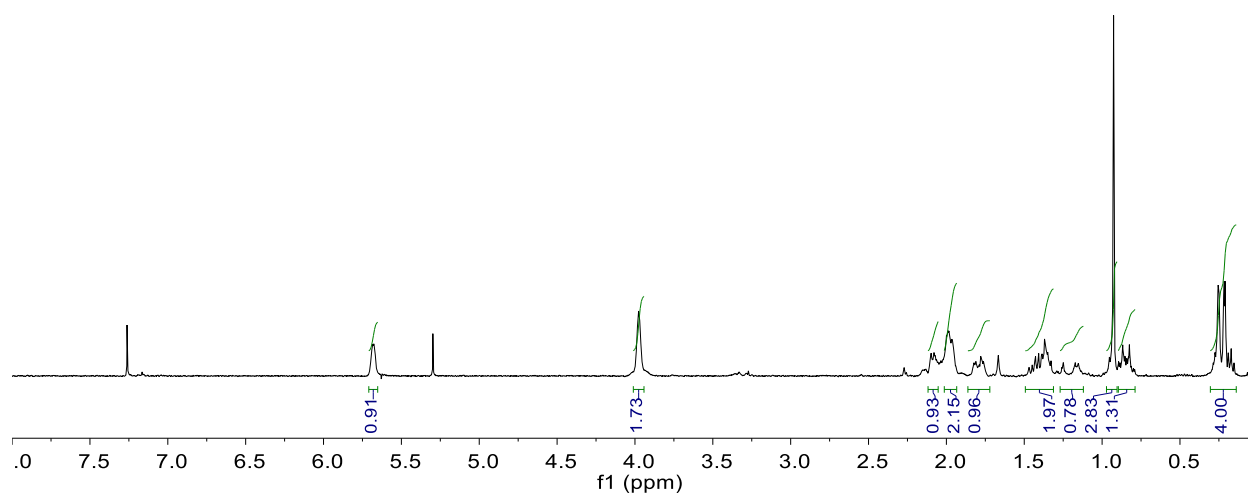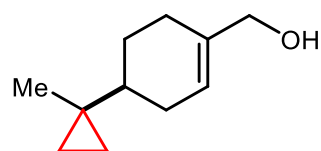
Figure S20. ^{1}H NMR spectrum for **10** (CDCl$_3$, 295 K).^{i}
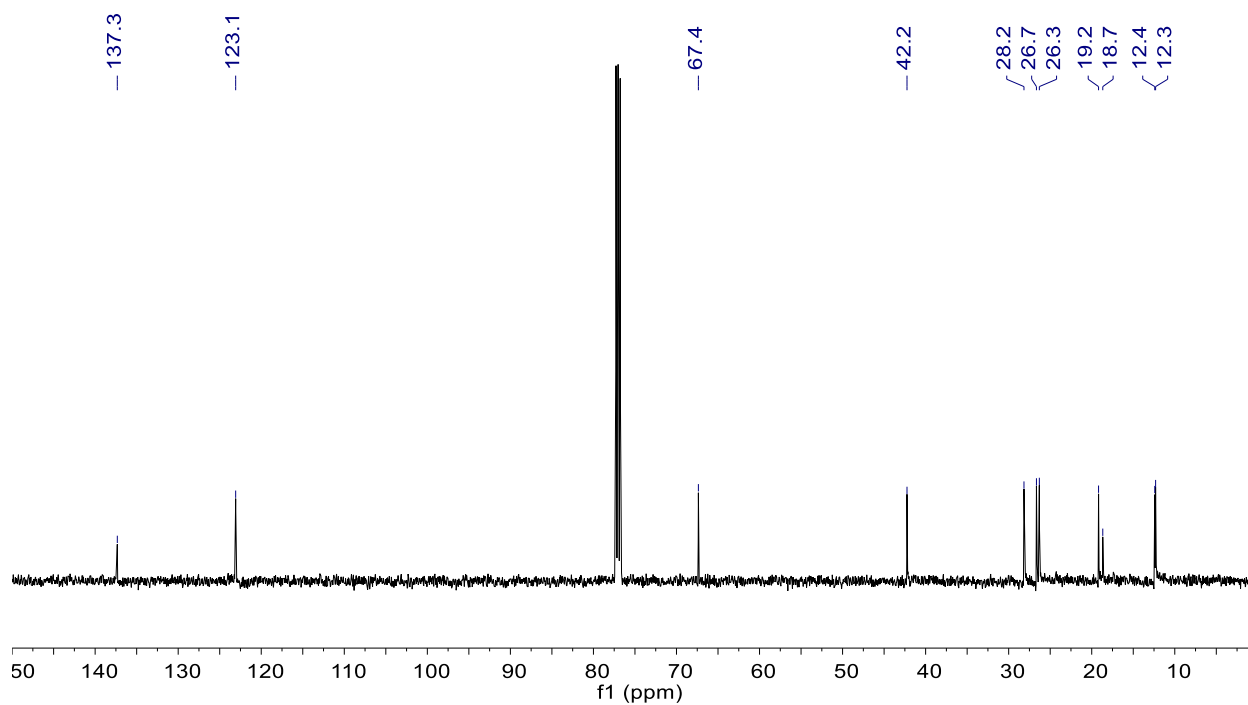
Figure S21. ^{13}C NMR spectrum for **10** (CDCl$_3$, 295 K).
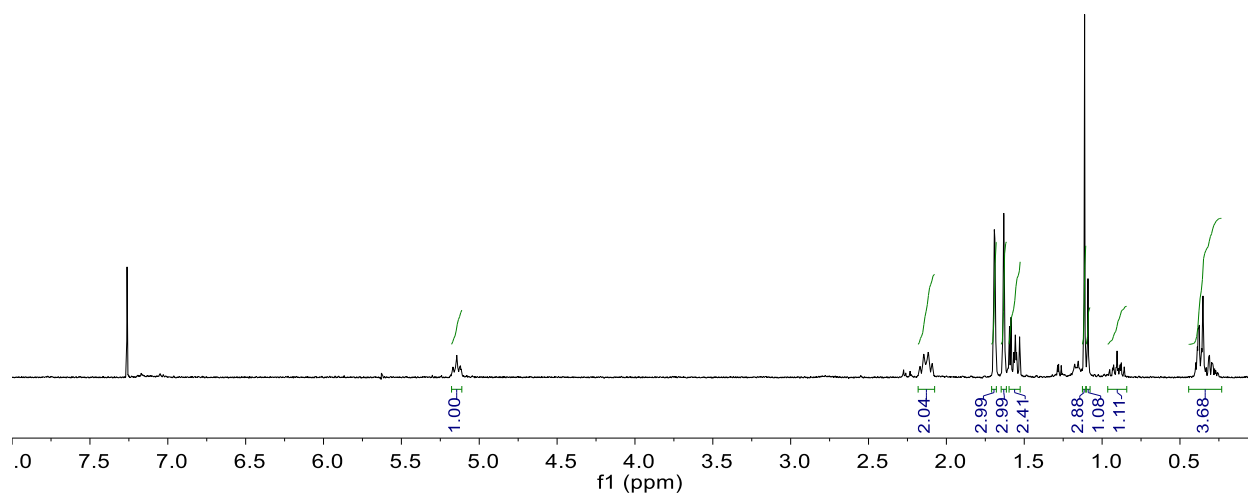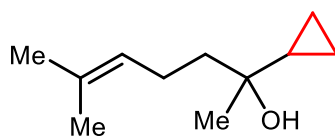
Figure S22. ^{1}H NMR spectrum for **11** (CDCl$_3$, 295 K).
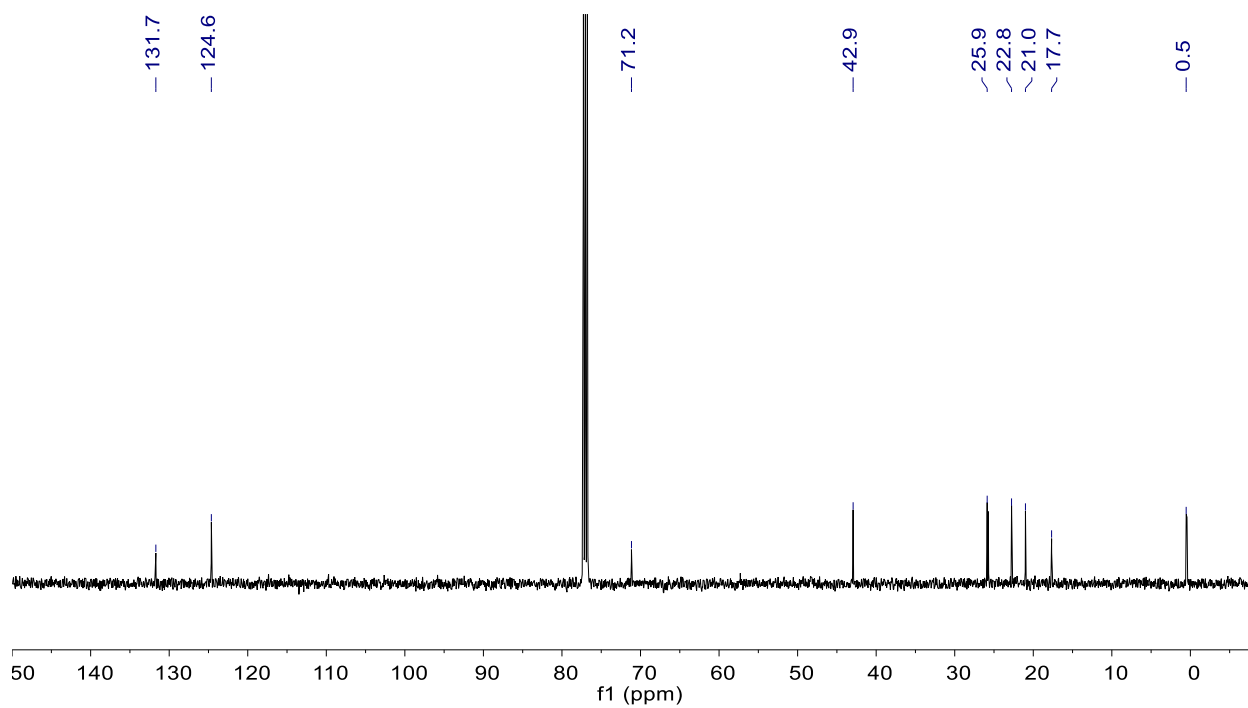
Figure S23. ^{13}C NMR spectrum for **11** (CDCl$_3$, 295 K).
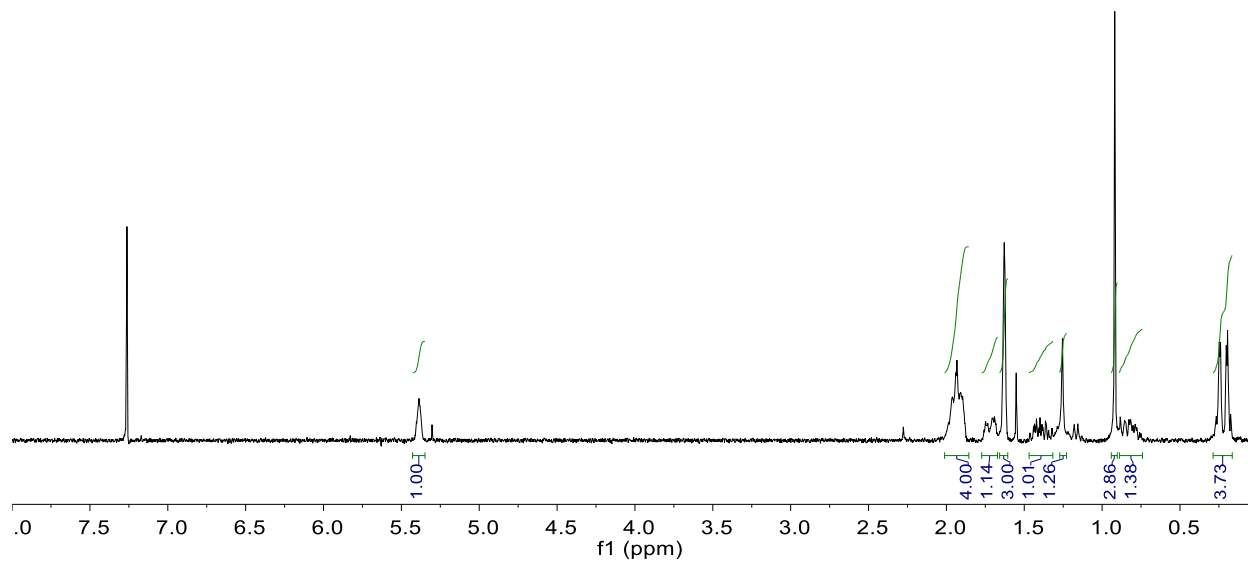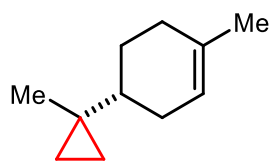
Figure S24. ^{1}H NMR spectrum for **12** (CDCl$_3$, 295 K).
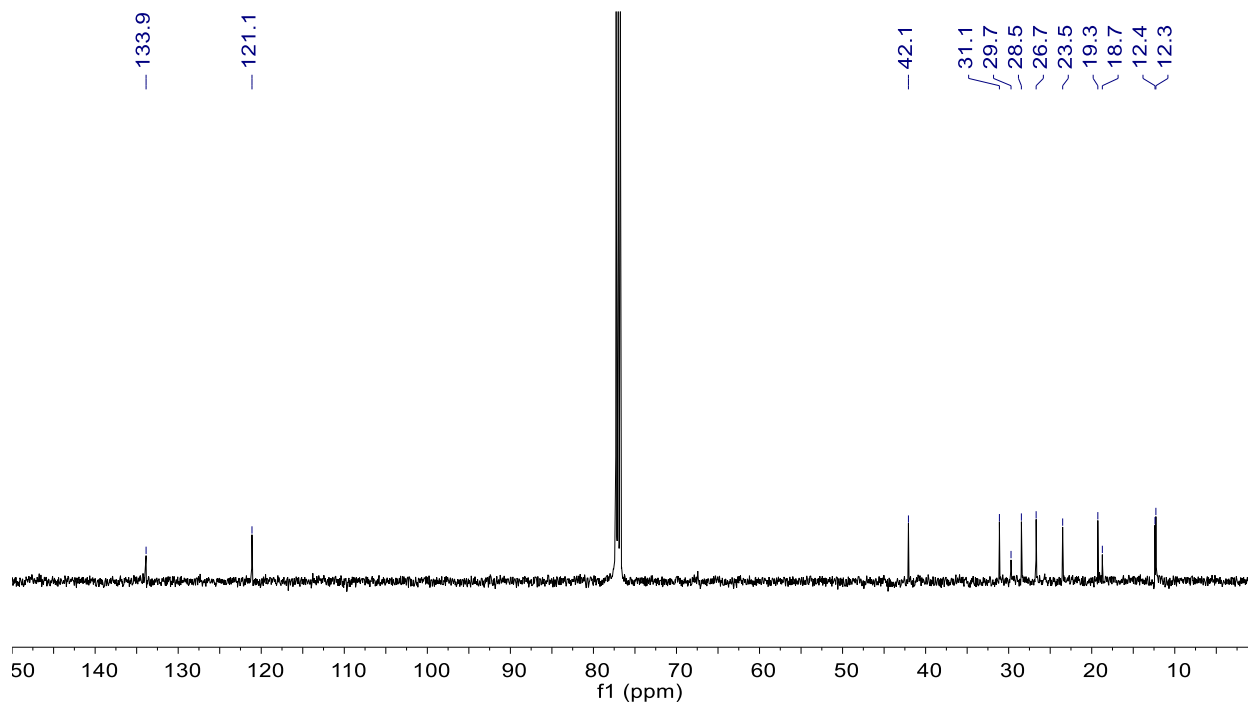
Figure S25. ^{13}C NMR spectrum for **12** (CDCl$_3$, 295 K).
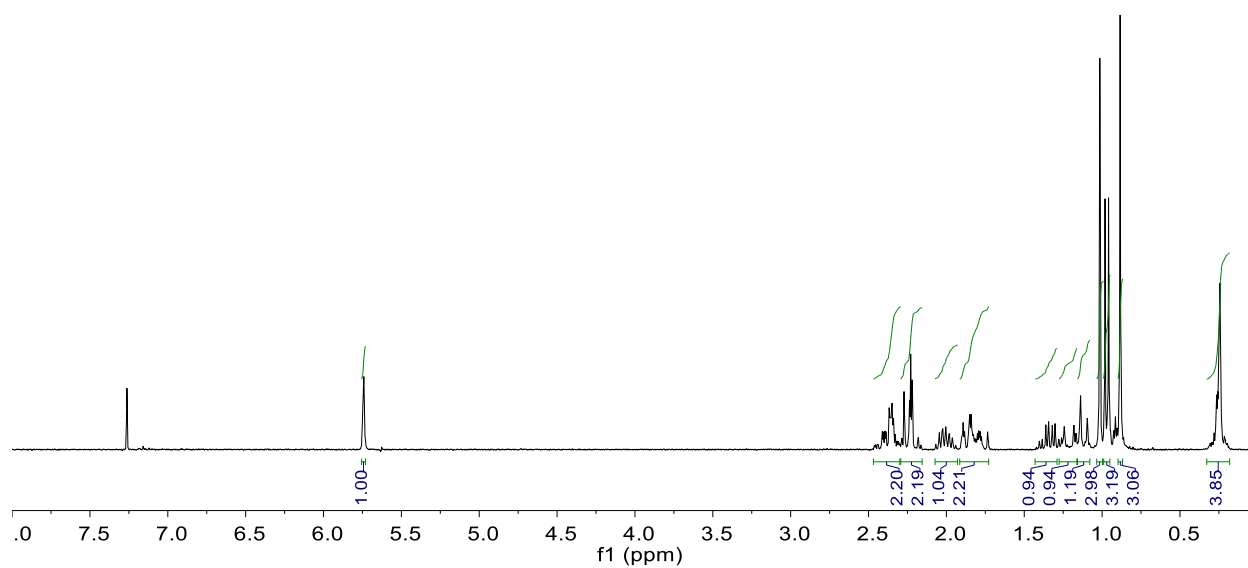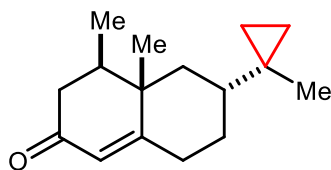
Figure S26. ^{1}H NMR spectrum for **13** (CDCl$_3$, 295 K).
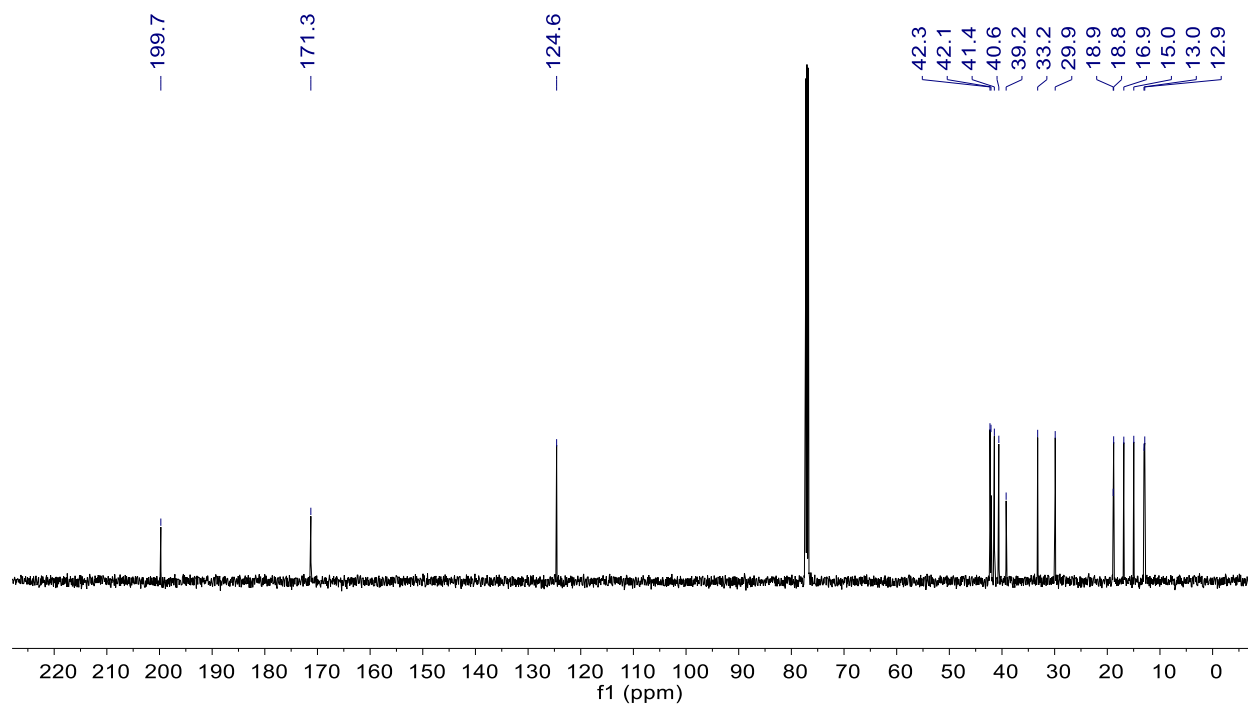
Figure S27. ^{13}C NMR spectrum for **13** (CDCl$_3$, 295 K).
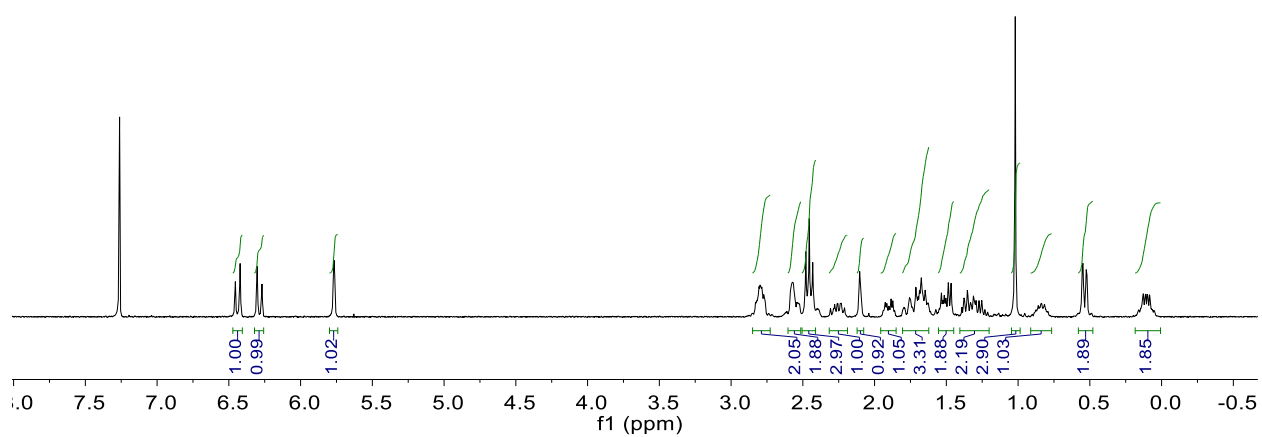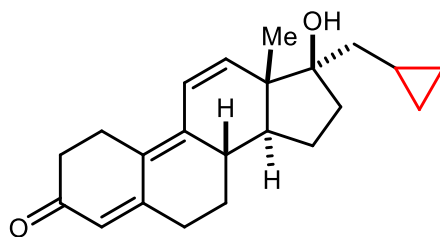
Figure S28. ^{1}H NMR spectrum for **14** (CDCl$_3$, 295 K).
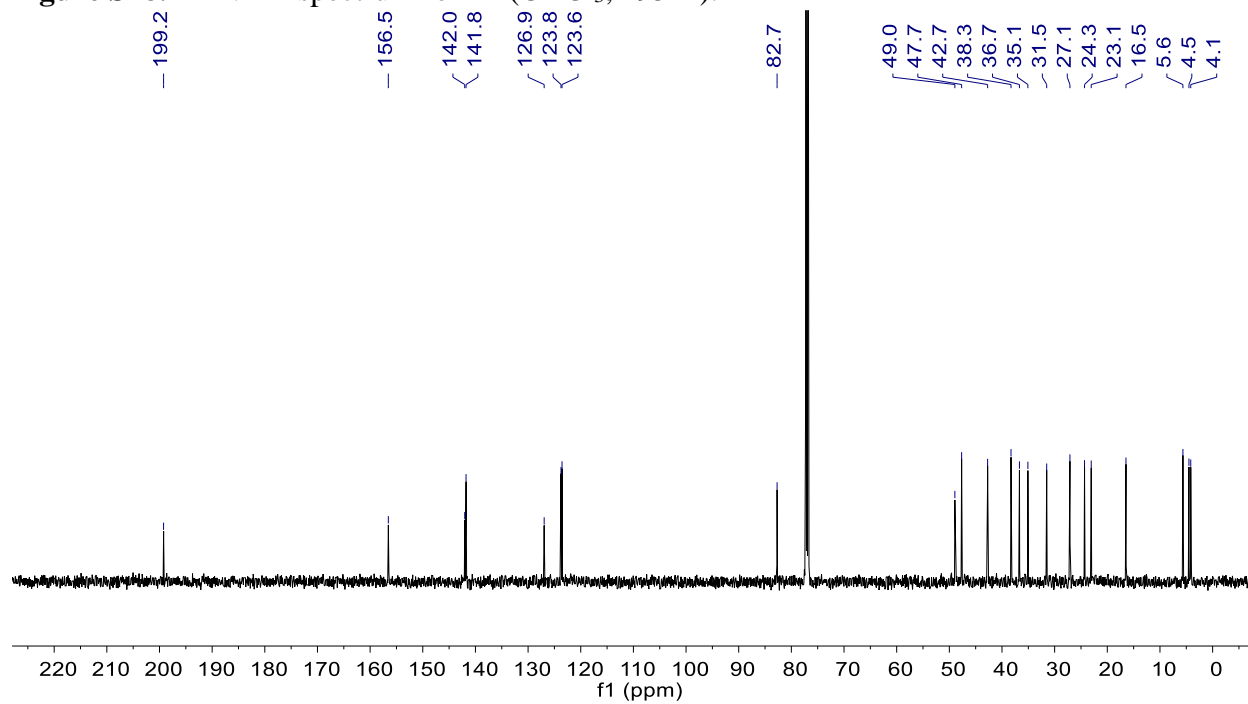
Figure S29. ^{13}C NMR spectrum for **14** (CDCl$_3$, 295 K).
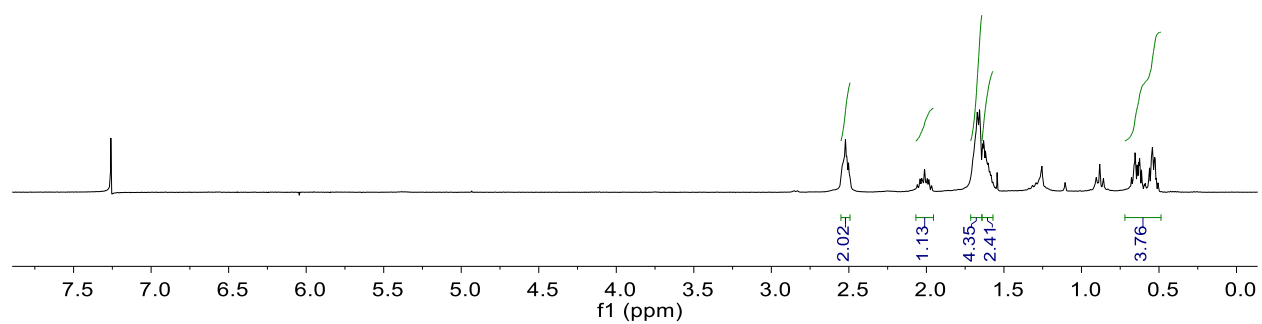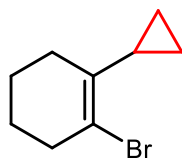
Figure S30. ^{1}H NMR spectrum for **15** (CDCl$_3$, 295 K).
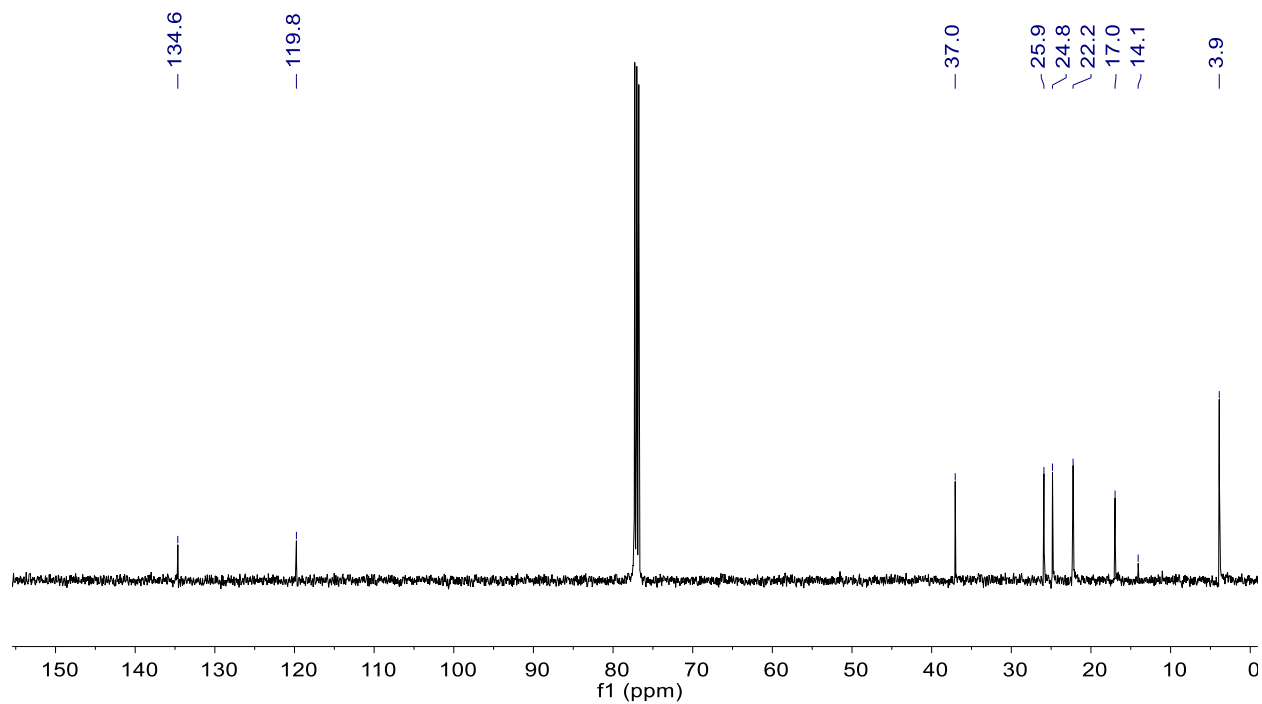
Figure S31. ^{13}C NMR spectrum for **15** (CDCl$_3$, 295 K).
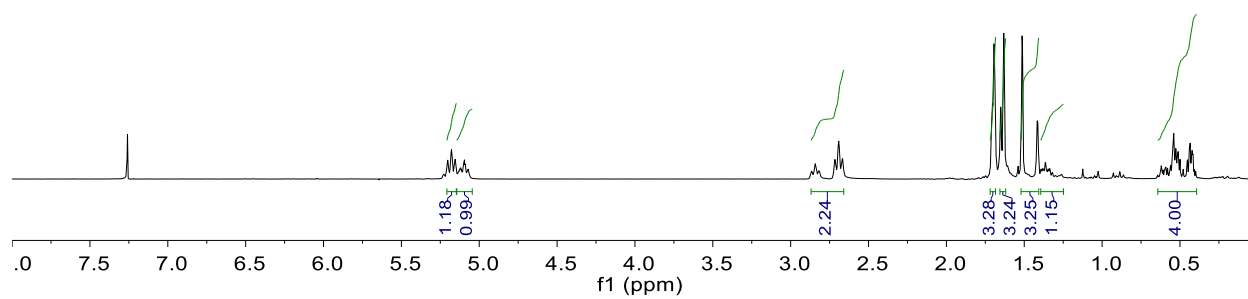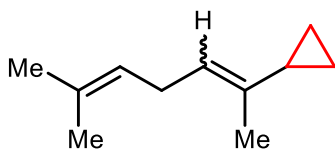
Figure S32. ^{1}H NMR spectrum for **16** (CDCl$_3$, 295 K).
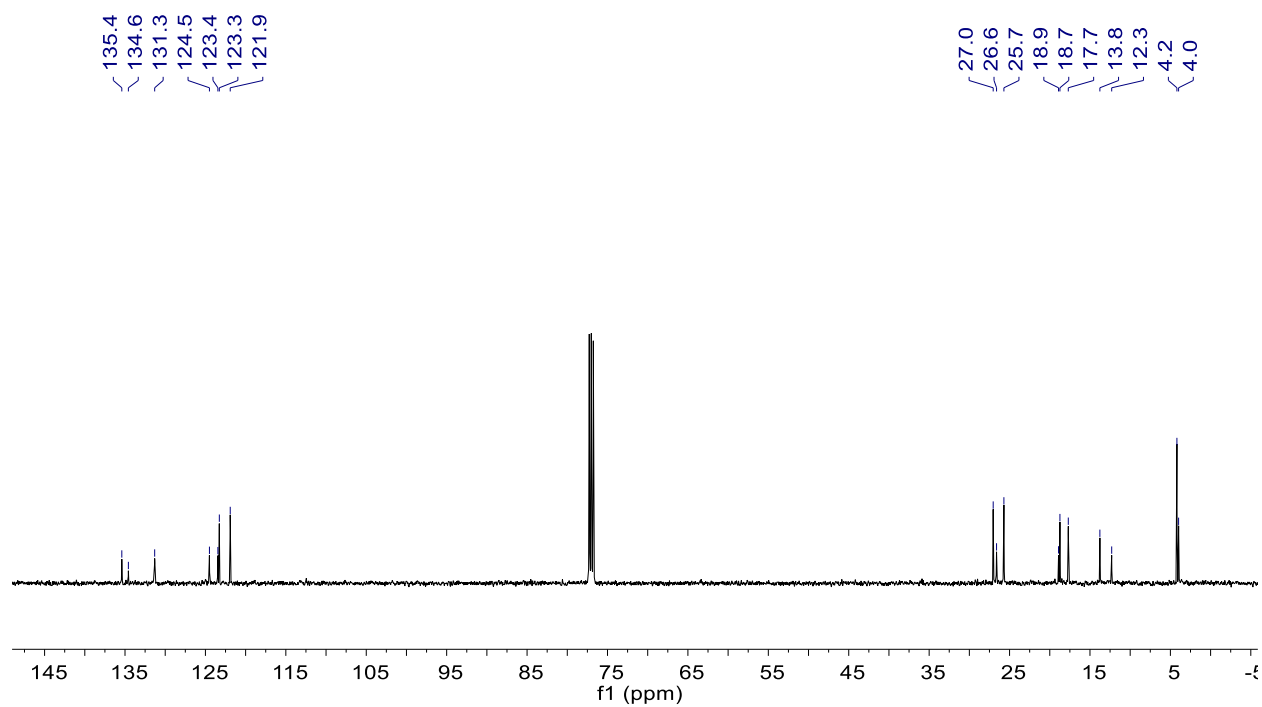
Figure S33. ^{13}C NMR spectrum for **16** (CDCl$_3$, 295 K).
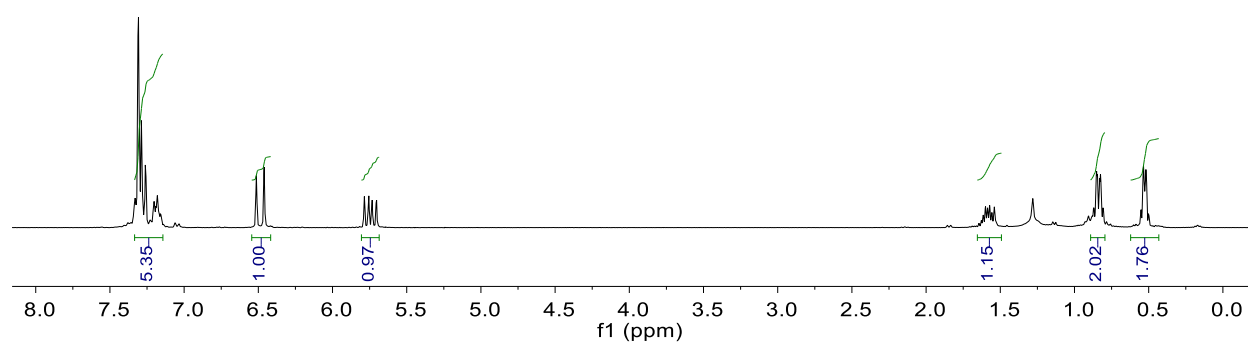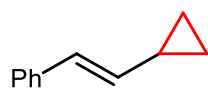
Figure S34. ^{1}H NMR spectrum for **17** (CDCl$_3$, 295 K).
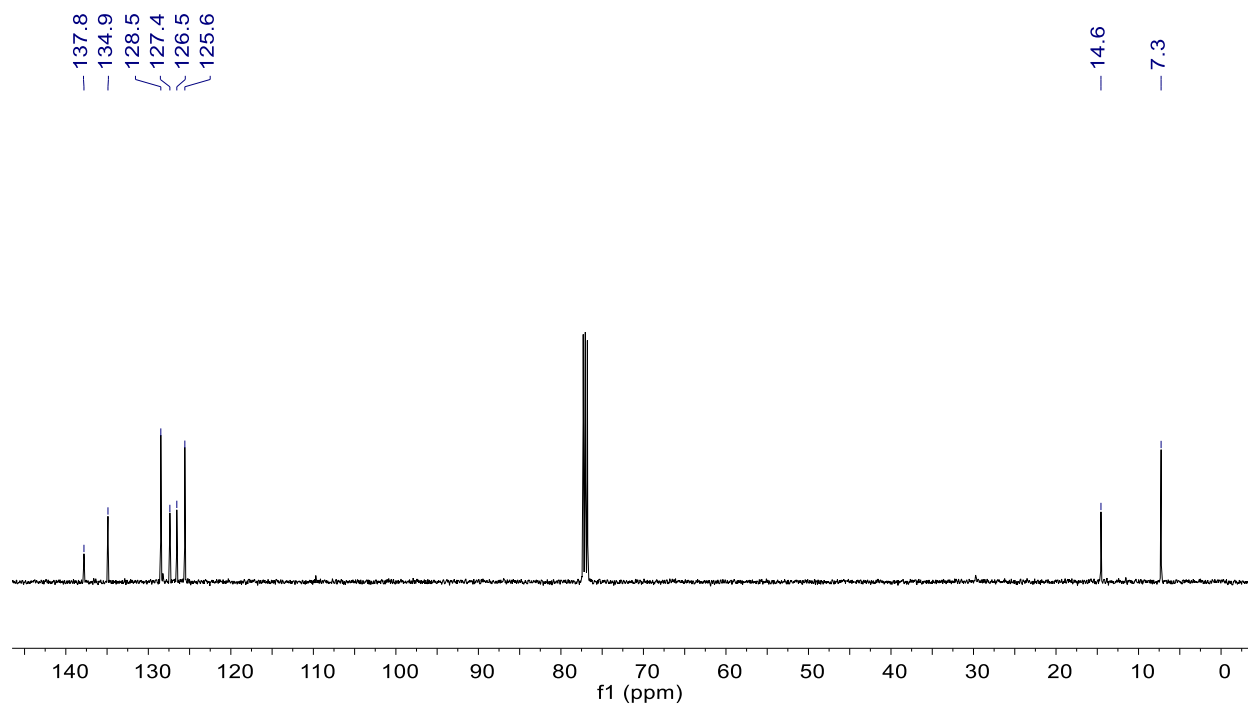
Figure S35. ^{13}C NMR spectrum for **17** (CDCl$_3$, 295 K)
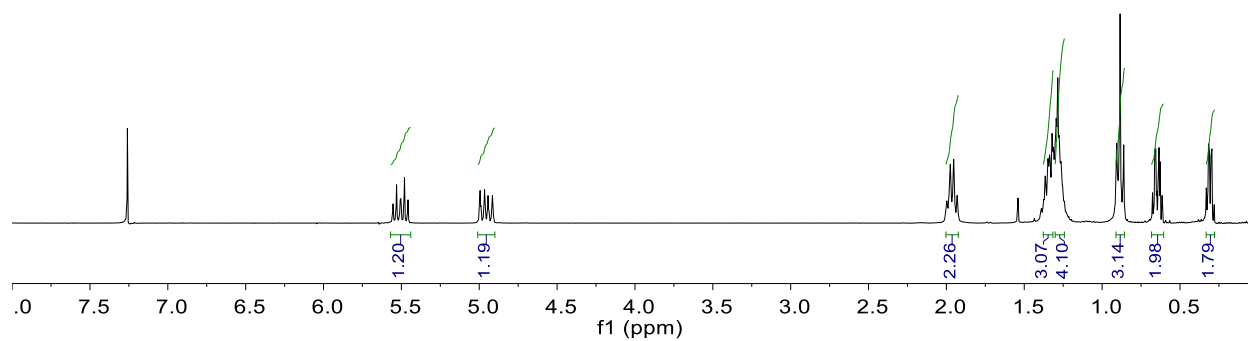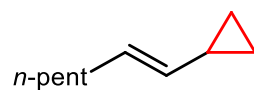
Figure S36. ^{1}H NMR spectrum for **18** (CDCl$_3$, 295 K)
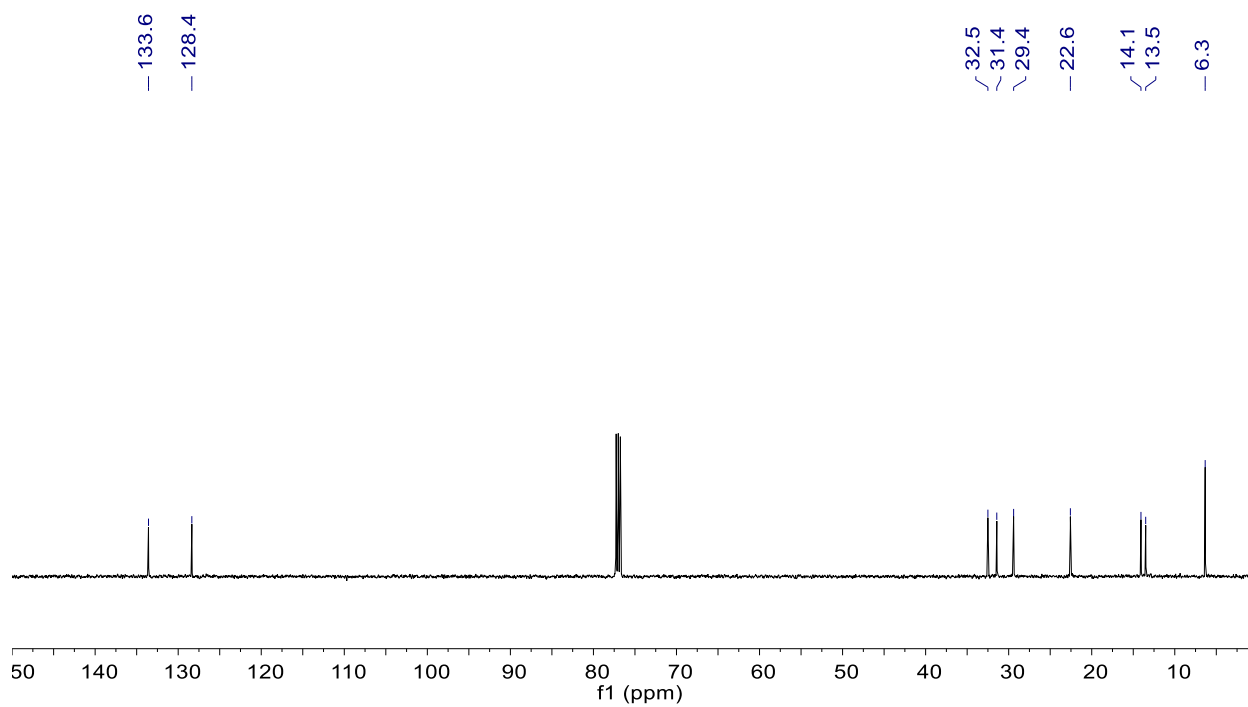
Figure S37. ^{13}C NMR spectrum for **18** (CDCl$_3$, 295 K)
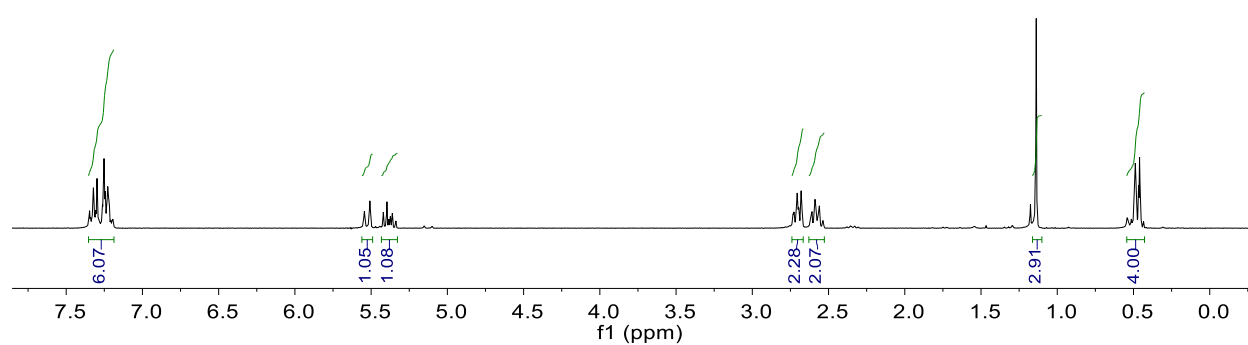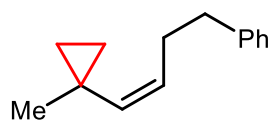
Figure S38. ^{1}H NMR spectrum for **19** (CDCl$_3$, 295 K)
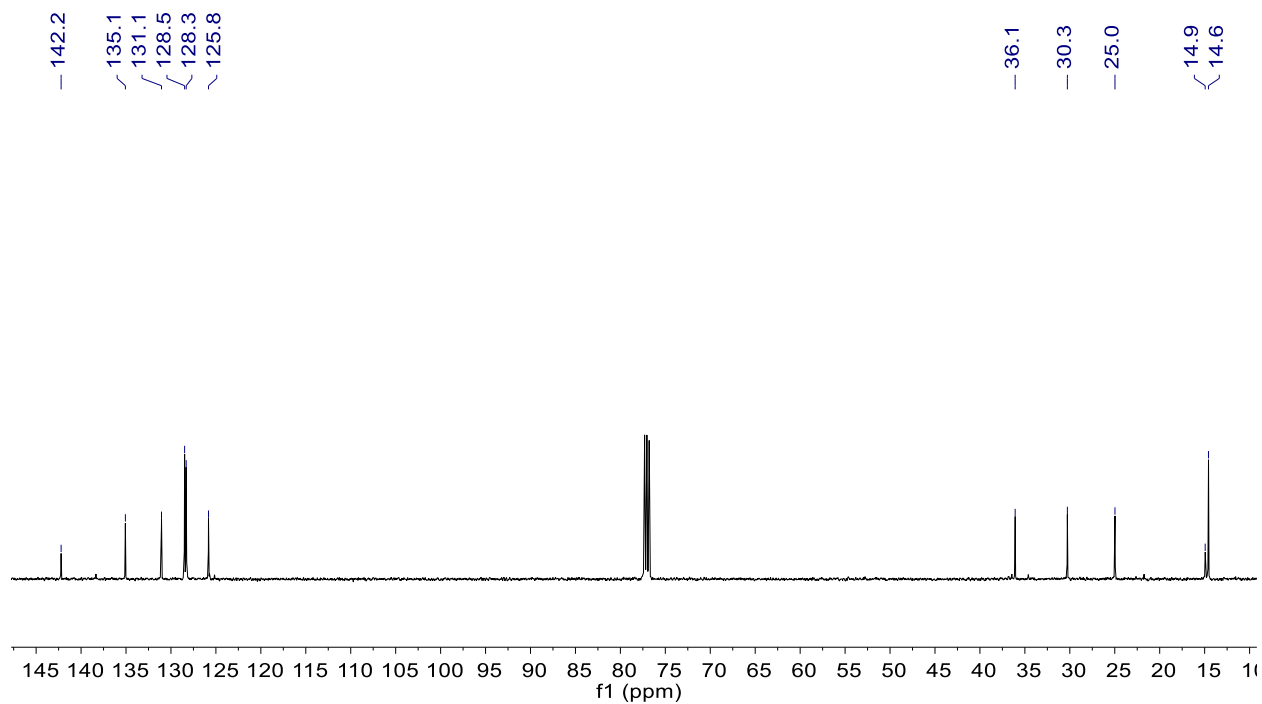
Figure S39. ^{13}C NMR spectrum for **19** (CDCl$_3$, 295 K)

Figure S40. ^{1}H NMR spectrum for **20** (CDCl$_3$, 295 K)

Figure S41. ^{13}C NMR spectrum for **20** (CDCl$_3$, 295 K)
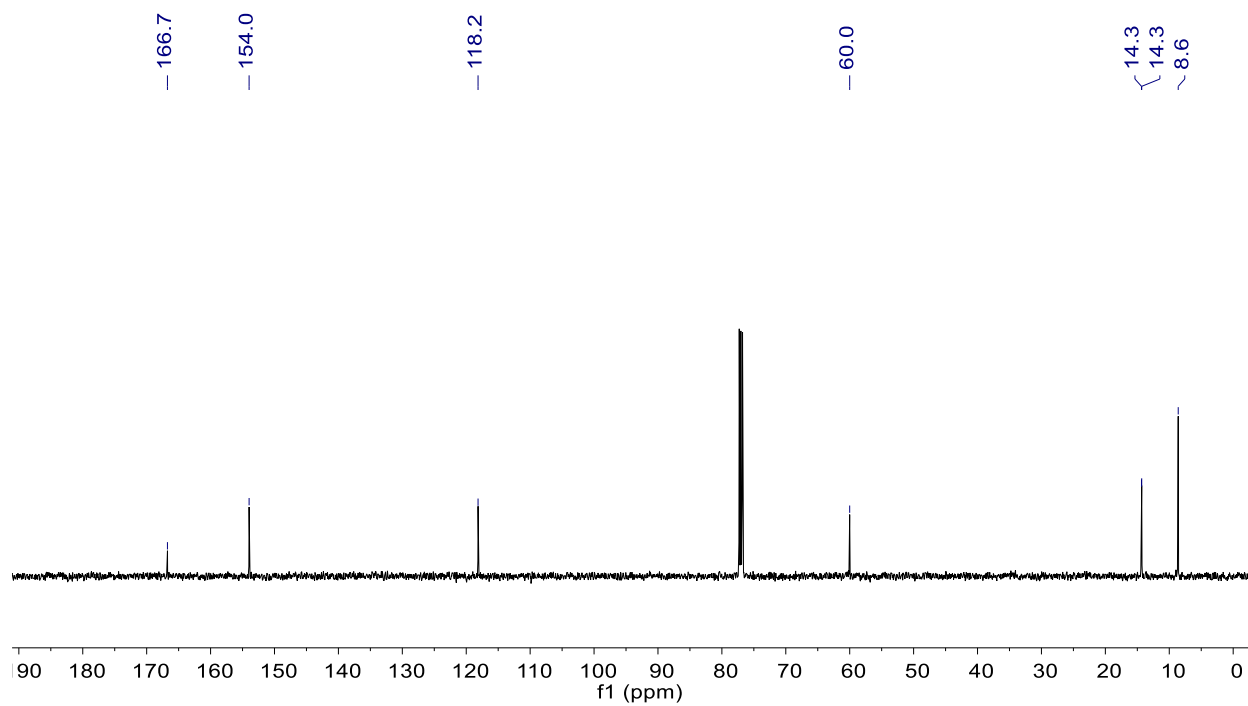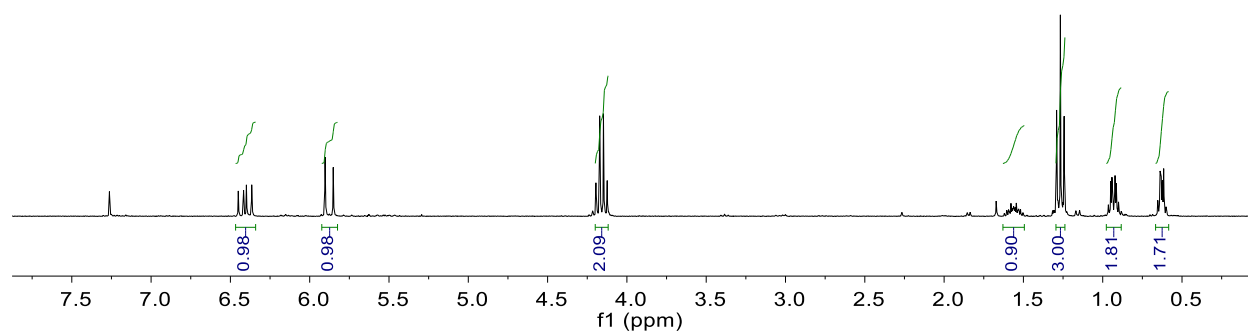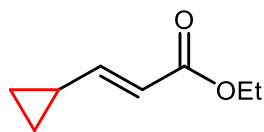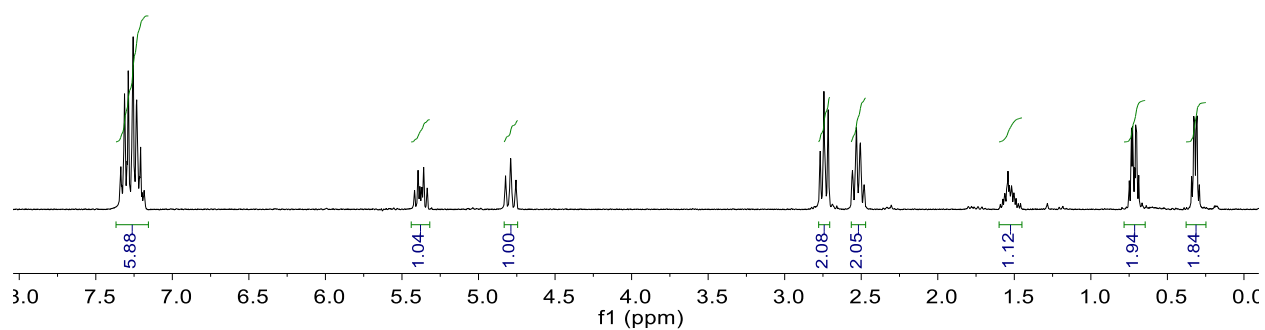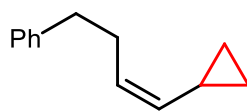
Figure S42. ^{1}H NMR spectrum for **21** (CDCl$_3$, 295 K)
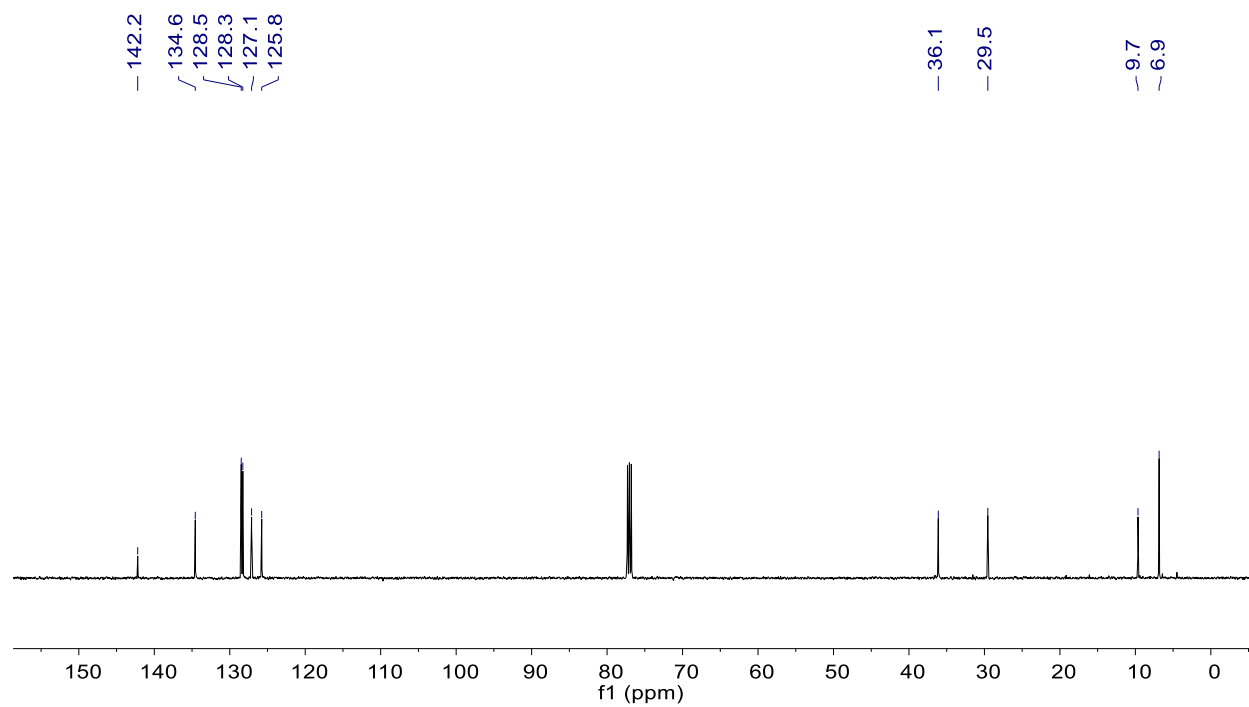
Figure S43. ^{13}C NMR spectrum for **21** (CDCl$_3$, 295 K)
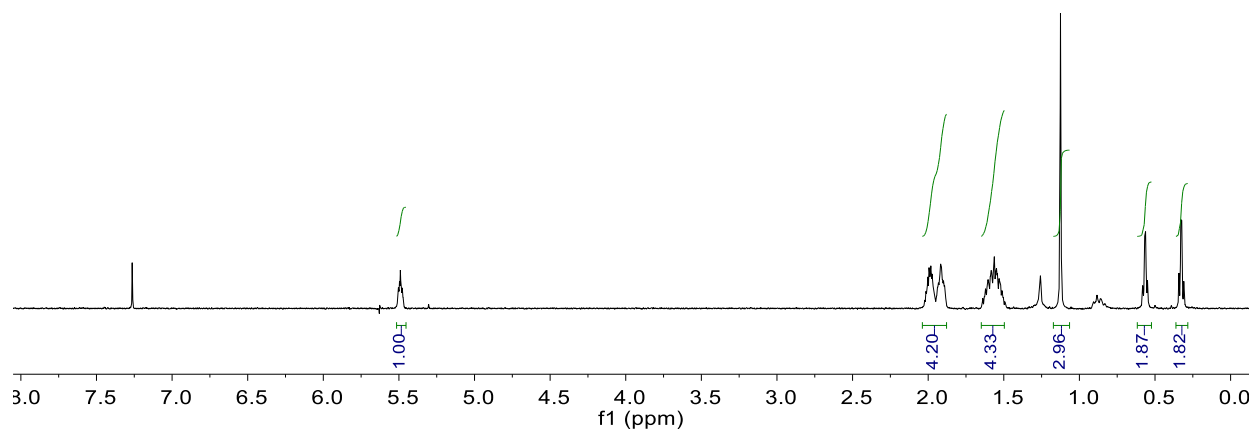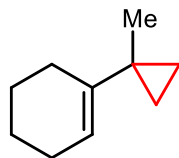
Figure S44. ^{1}H NMR spectrum for **22** (CDCl$_3$, 295 K)
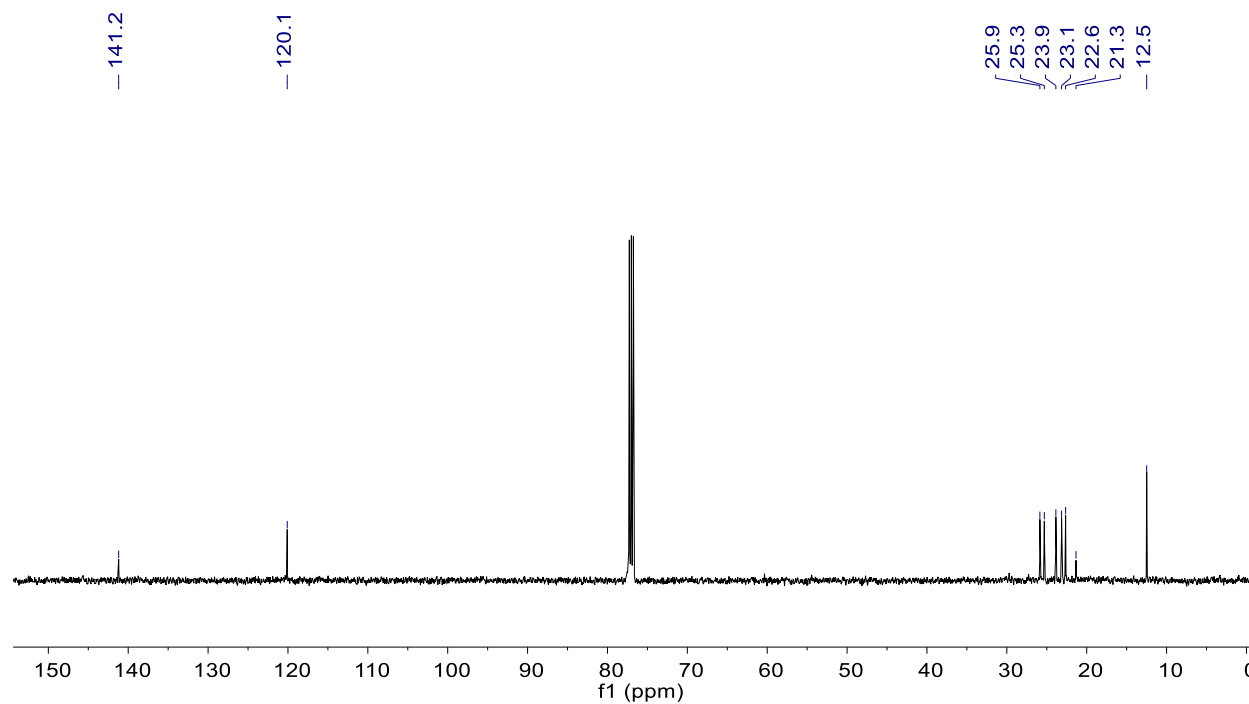
Figure S45. ^{13}C NMR spectrum for **22** (CDCl$_3$, 295 K)
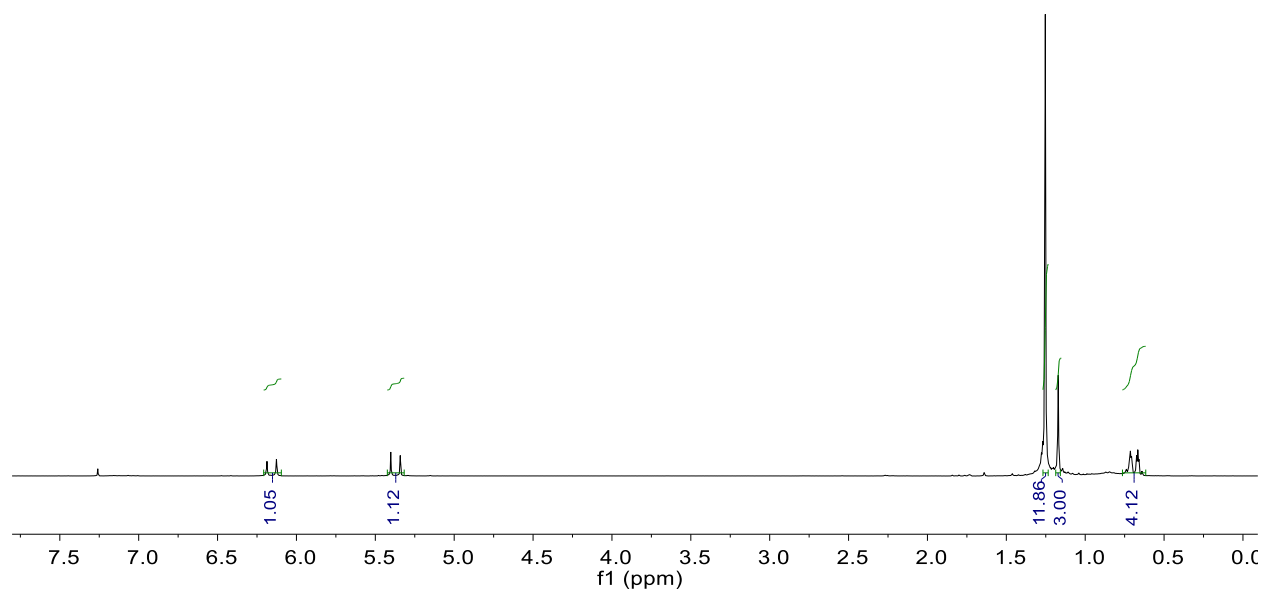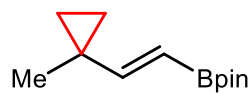
Figure S46. ^{1}H NMR spectrum for **23** (CDCl$_3$, 295 K)
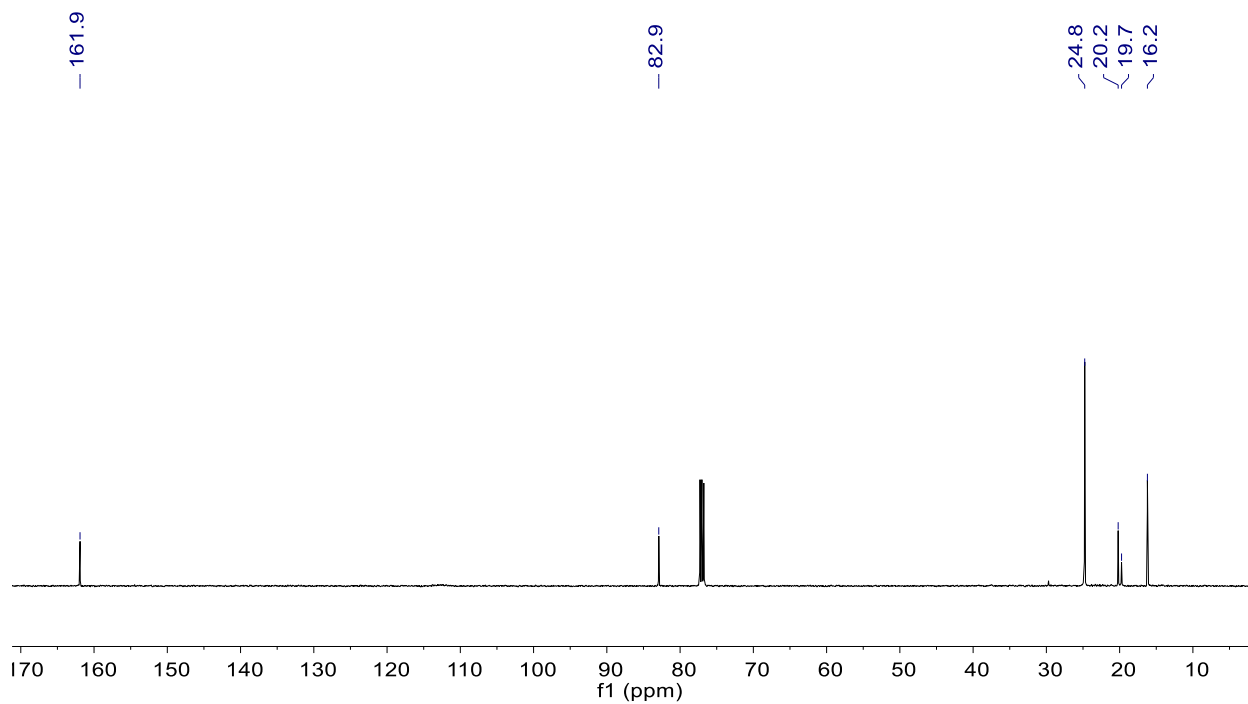
Figure S47. ^{13}C NMR spectrum for **23** (CDCl$_3$, 295 K)
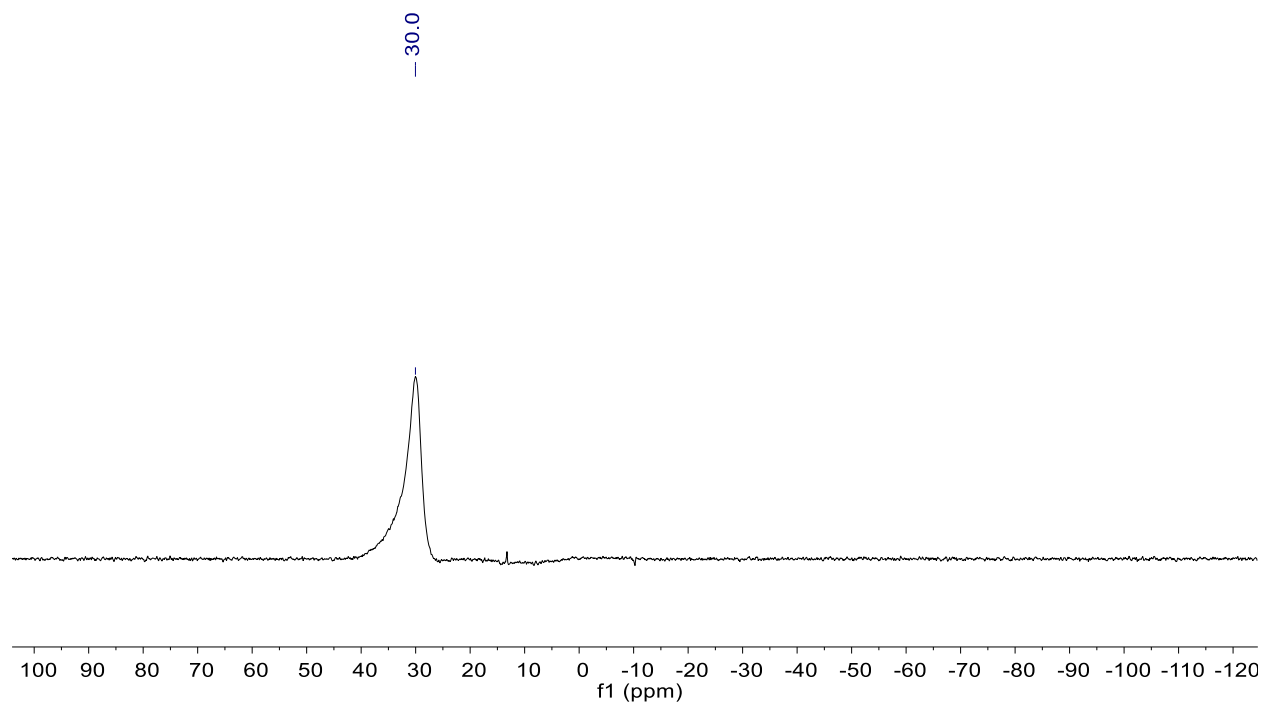
Figure S48. ^{11}B NMR spectrum for **23** (CDCl$_3$, 295 K)
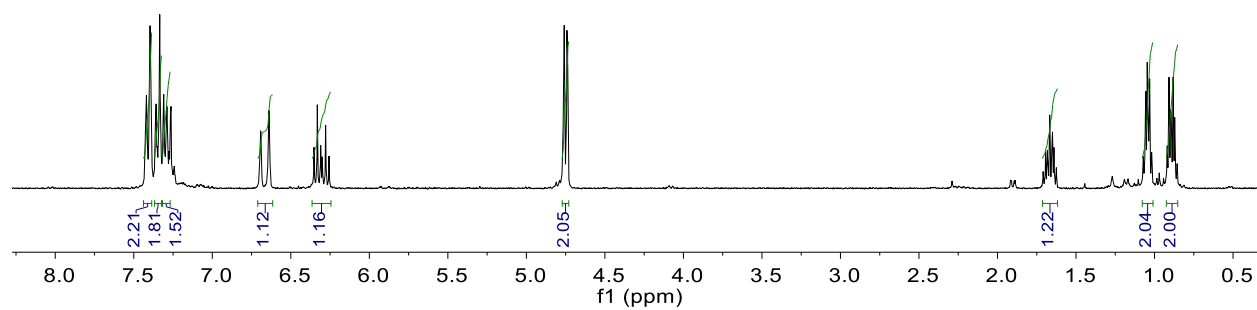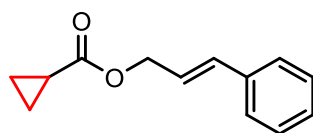
Figure S49. ^{1}H NMR spectrum for **S1** (CDCl$_3$, 295 K)
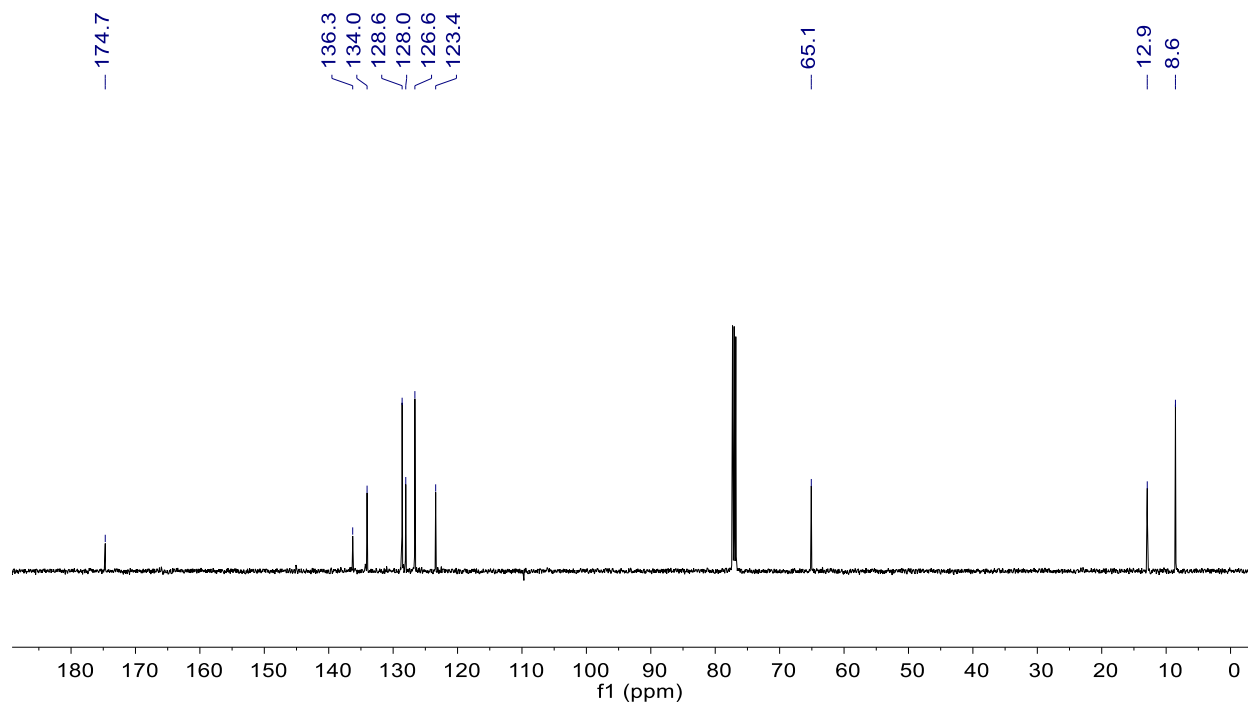
Figure S50. ^{13}C NMR spectrum for **S1** (CDCl$_3$, 295 K)
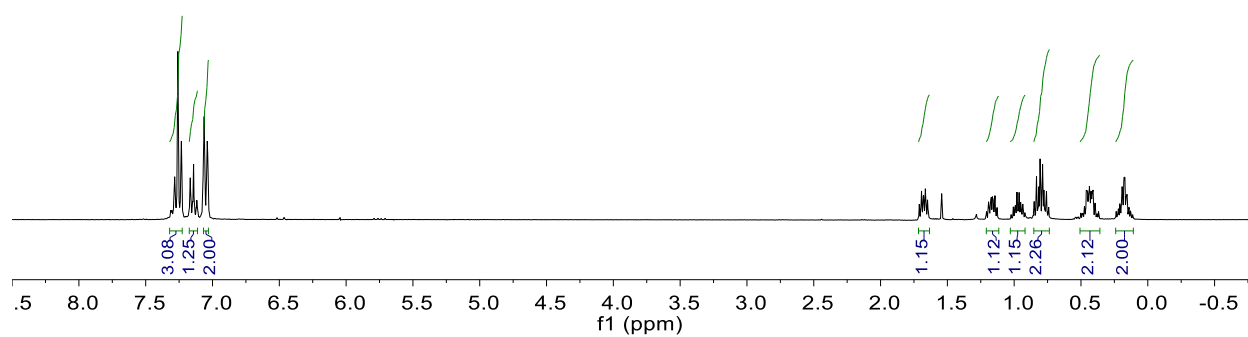
Figure S51. ^{1}H NMR spectrum for **29** (CDCl$_3$, 295 K)
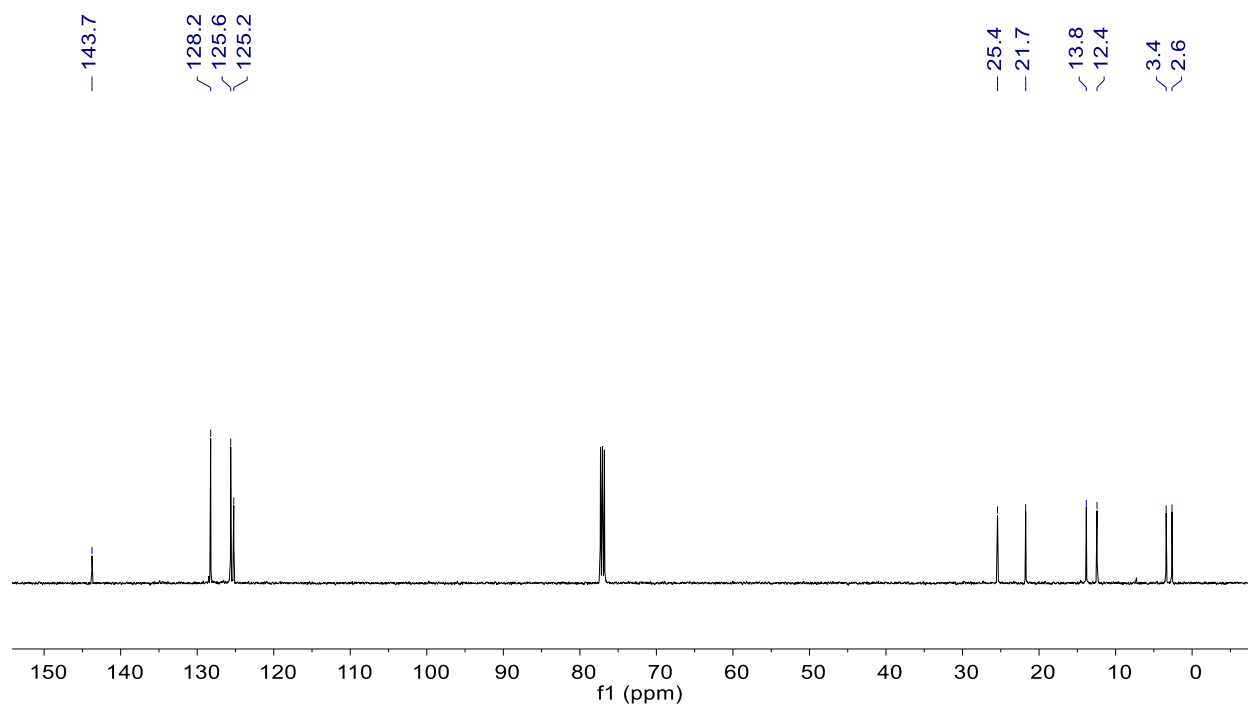
**Figure S52.** ^{13}C NMR spectrum for **29** (CDCl$_3$, 295 K)

11. IR Spectra
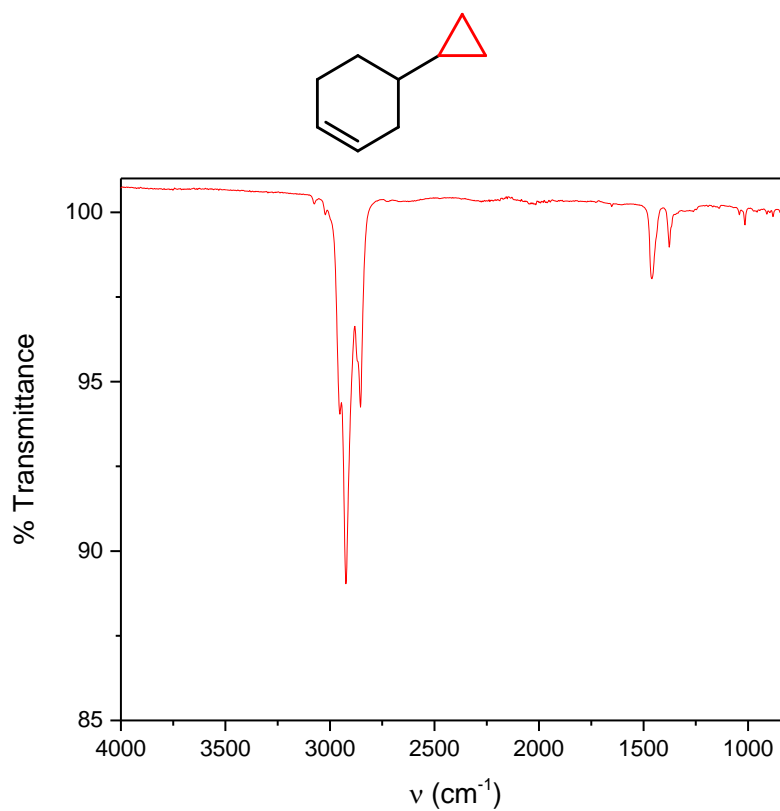
Figure S53. ATR-IR spectrum for **5**.
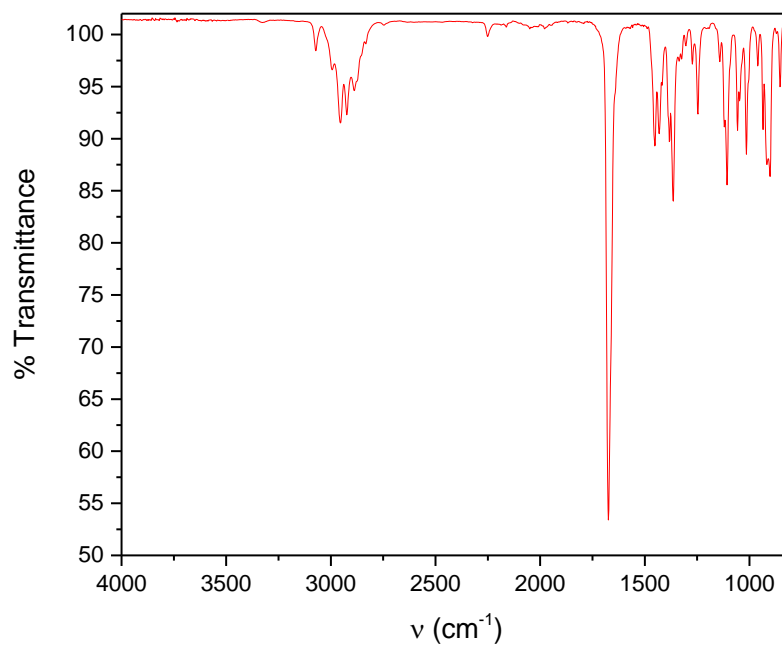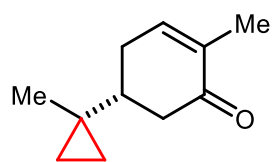
Figure S54. ATR-IR spectrum for **6**.
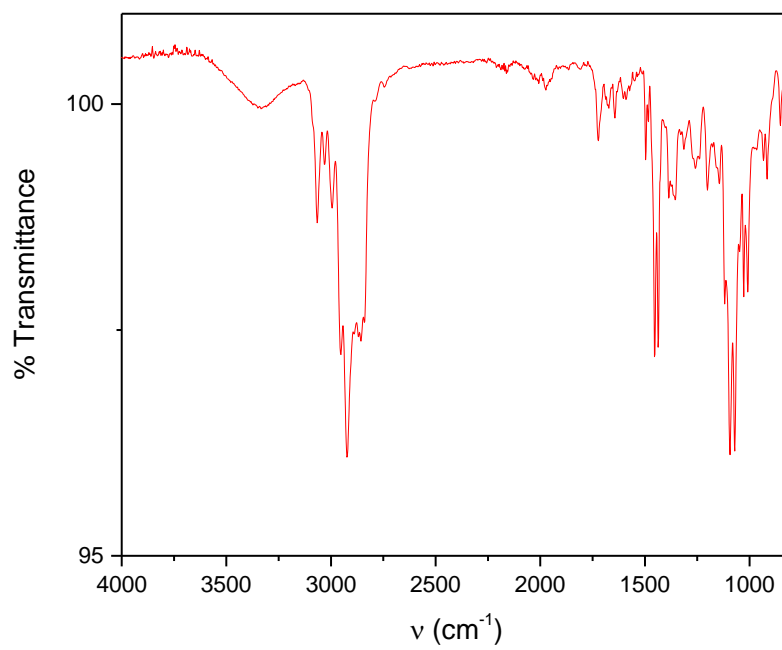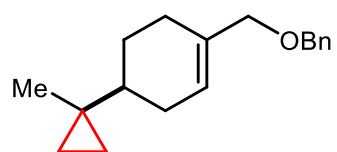
Figure S55. ATR-IR spectrum for **7**.
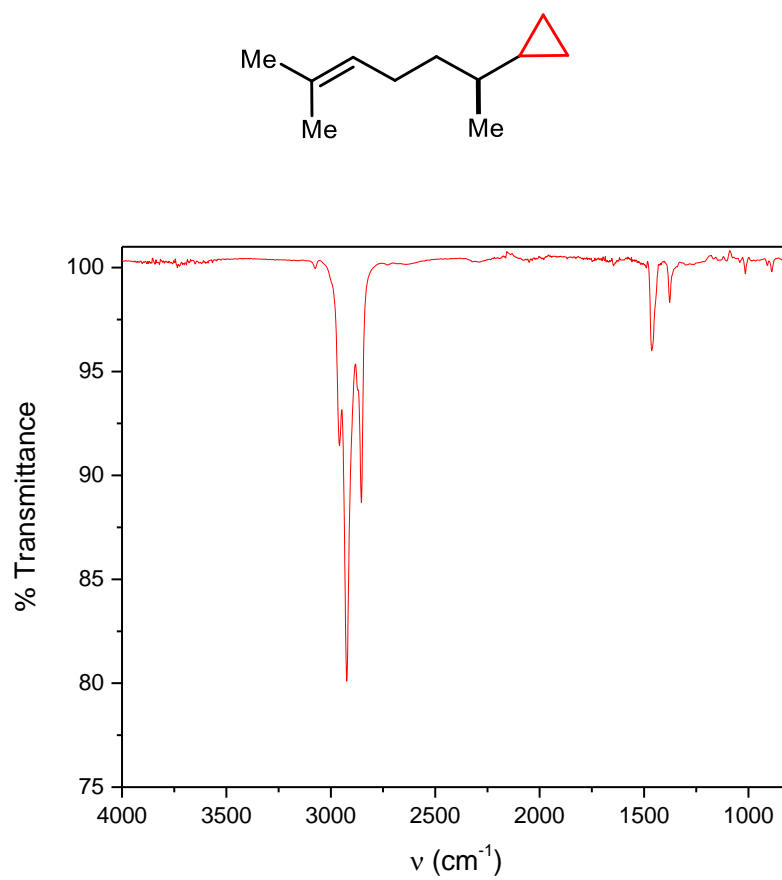
Figure S56. ATR-IR spectrum for **8**.
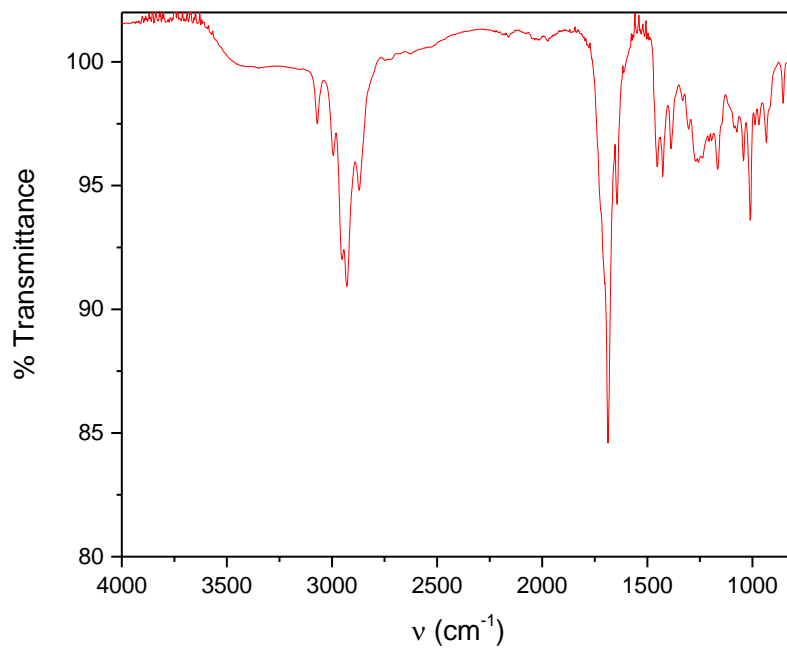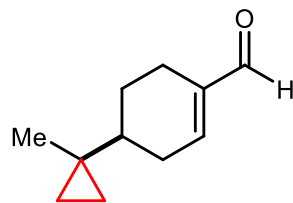
Figure S567. ATR-IR spectrum for **9**.
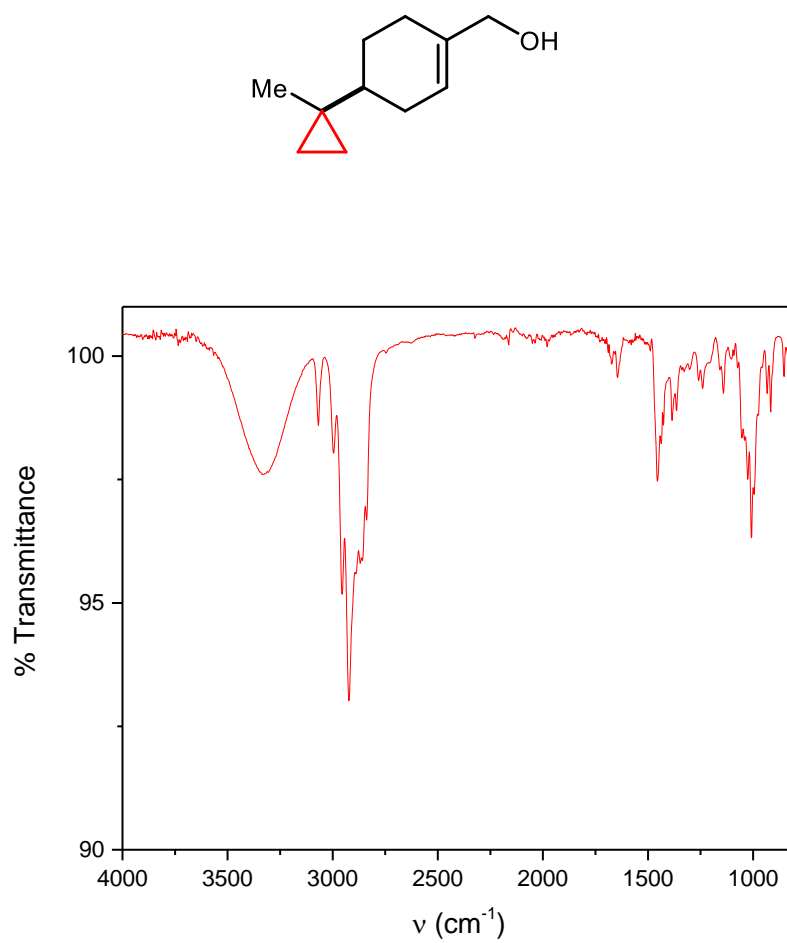
Figure S58. ATR-IR spectrum for **10**.
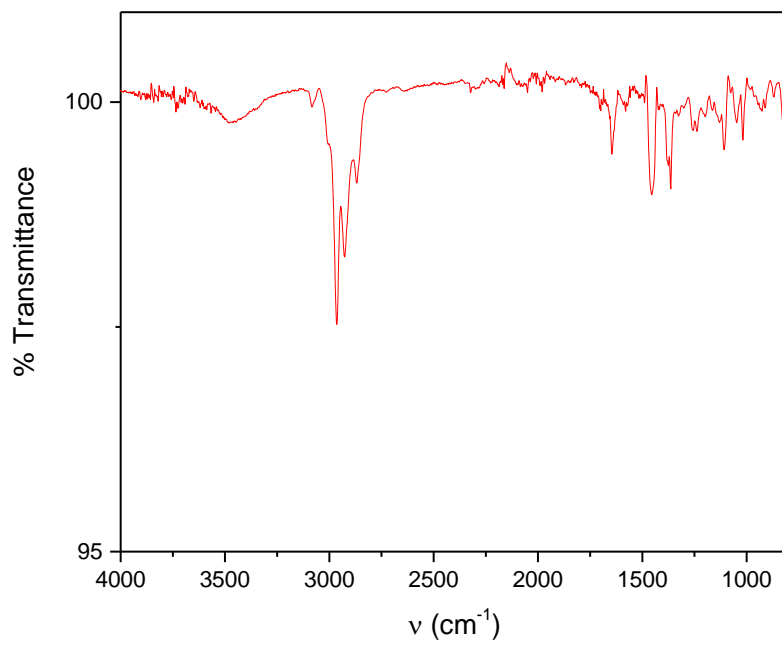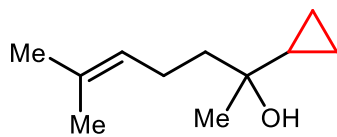
**Figure S59.** ATR-IR spectrum for **11**.
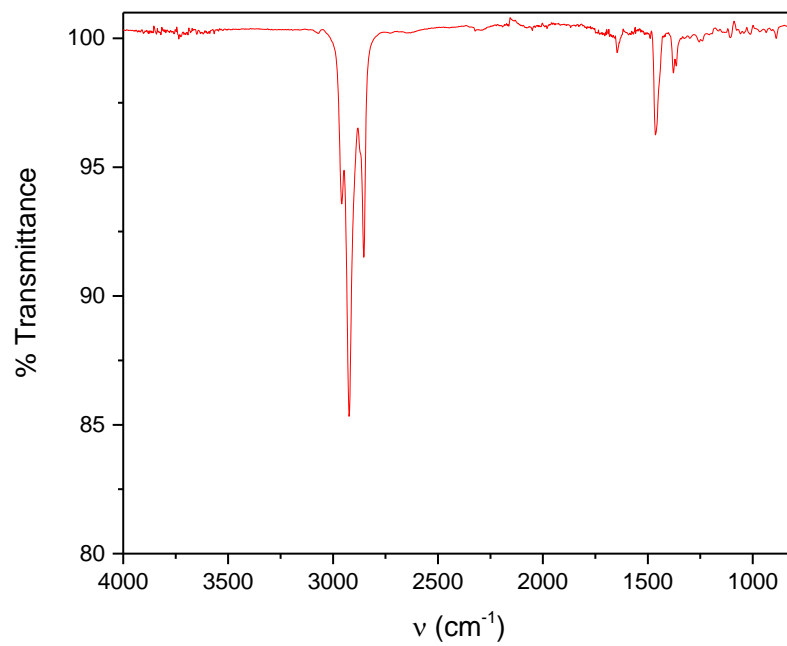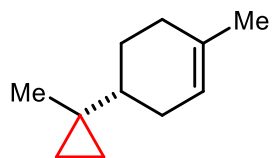
Figure S60. ATR-IR spectrum for **12**.
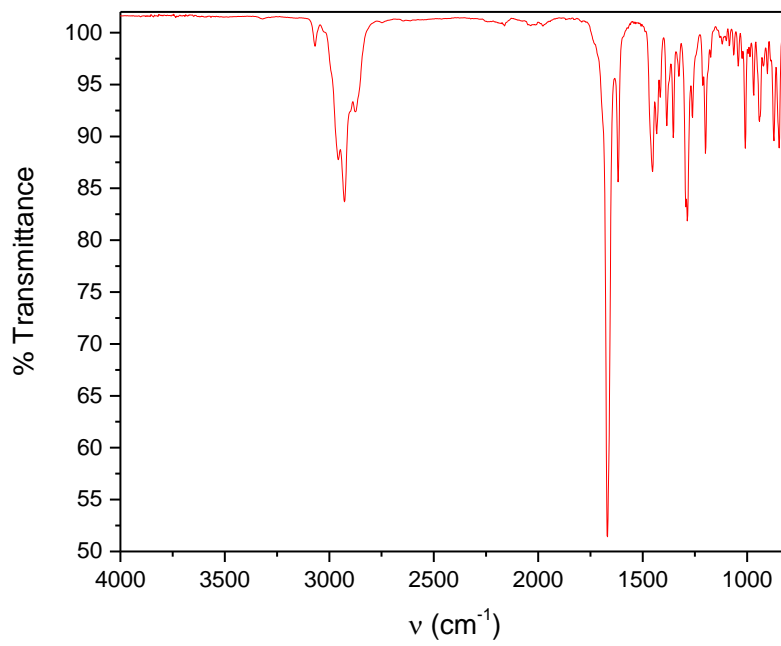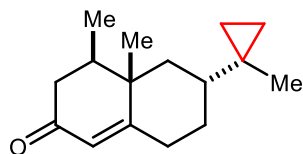
Figure S61. ATR-IR spectrum for **13**.
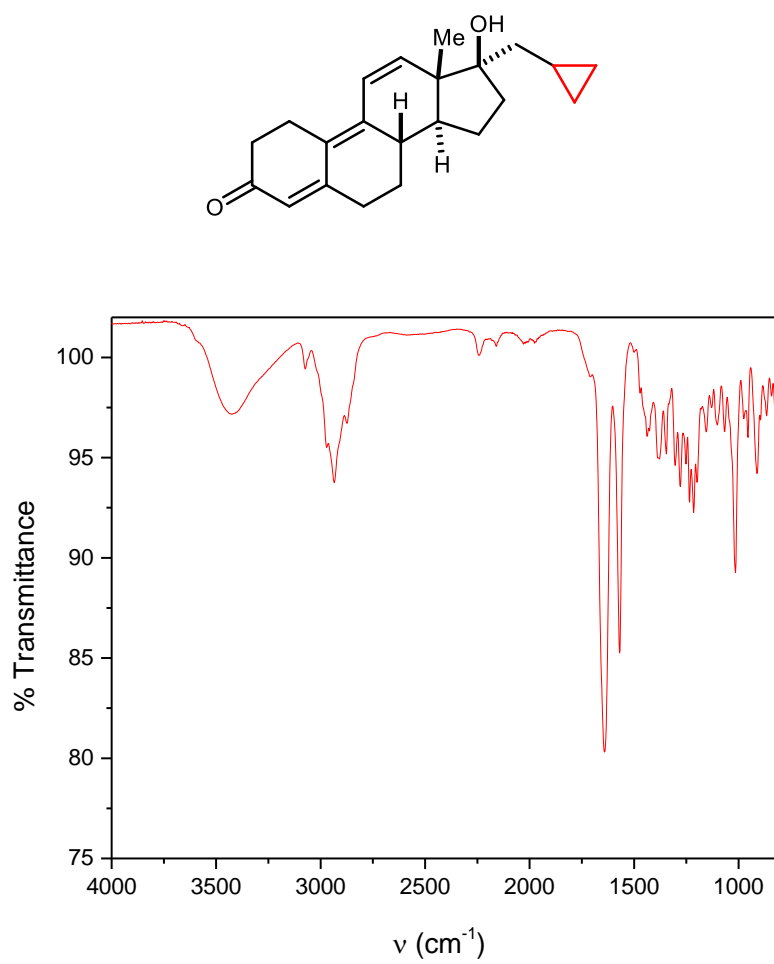
Figure S62. ATR-IR spectrum for **14**.
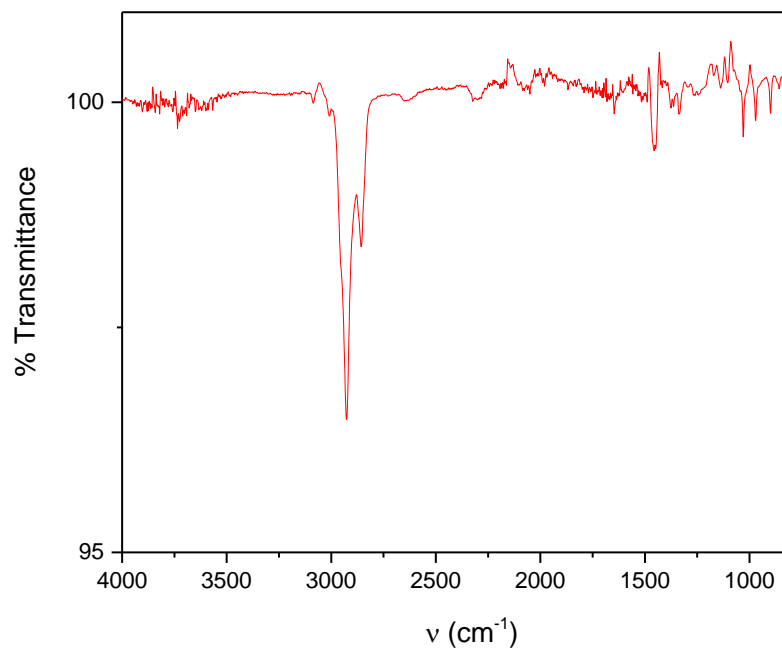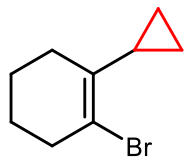
Figure S63. ATR-IR spectrum for **15**.
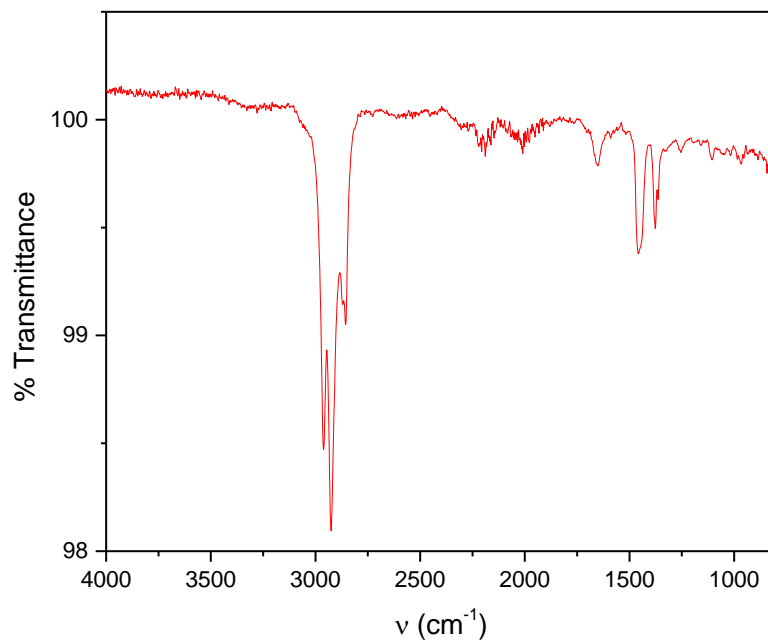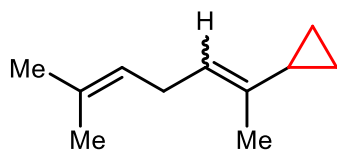
Figure S64. ATR-IR spectrum for **16**.
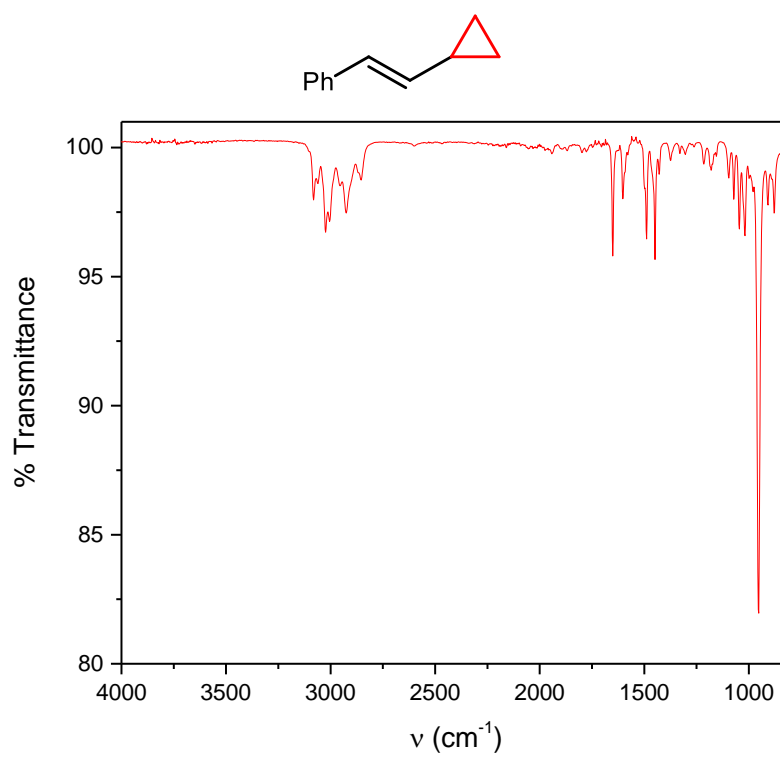
Figure S65. ATR-IR spectrum for **17**.
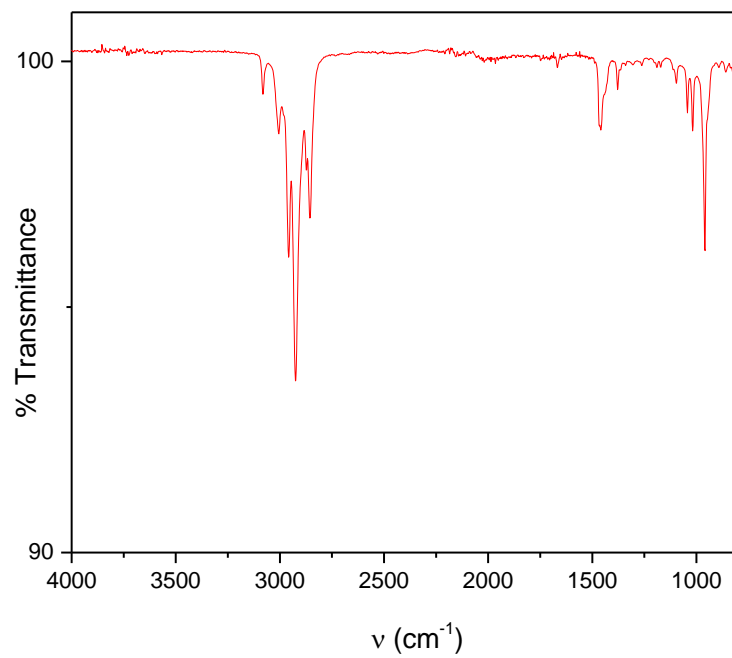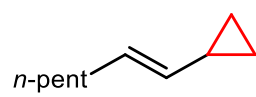
Figure S66. ATR-IR spectrum for **18**.
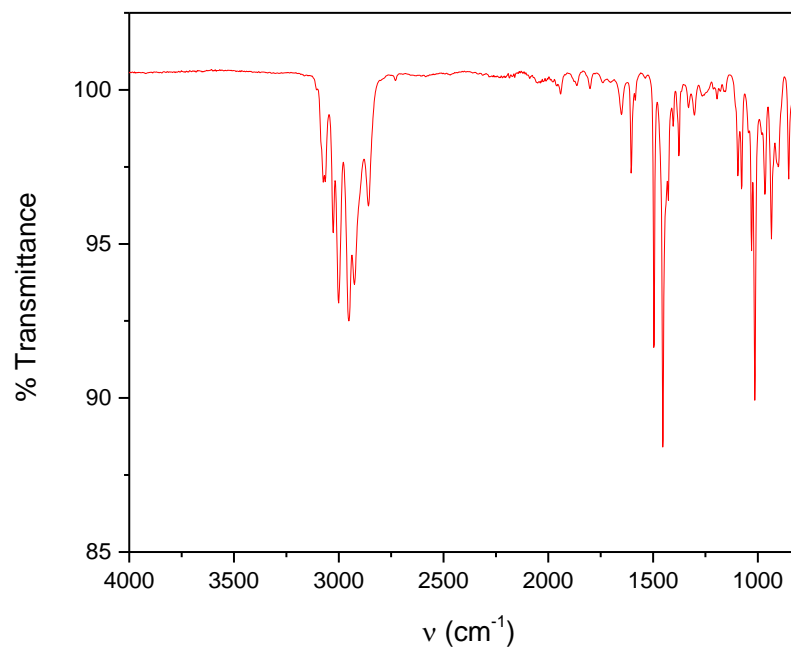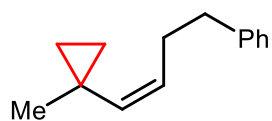
Figure S67. ATR-IR spectrum for **19**.
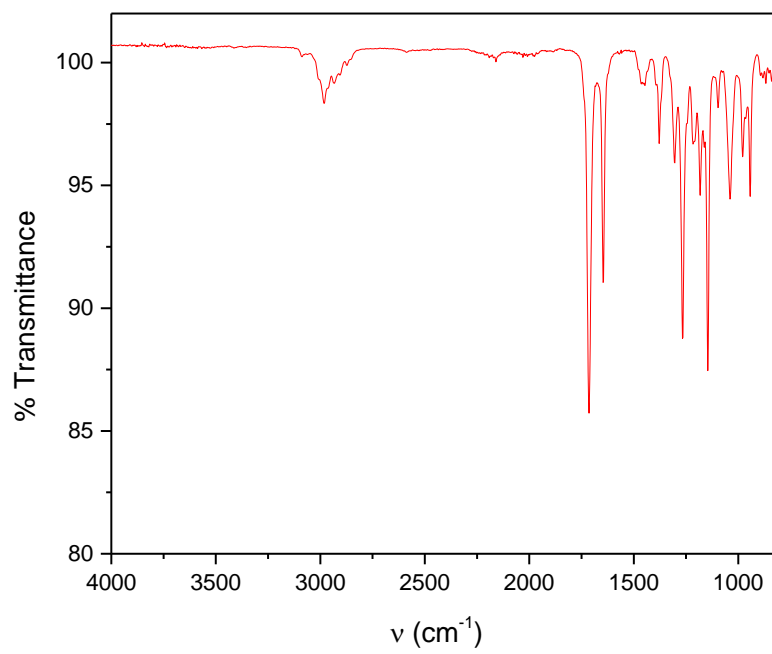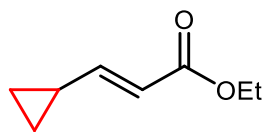
Figure S68. ATR-IR spectrum for **20**.
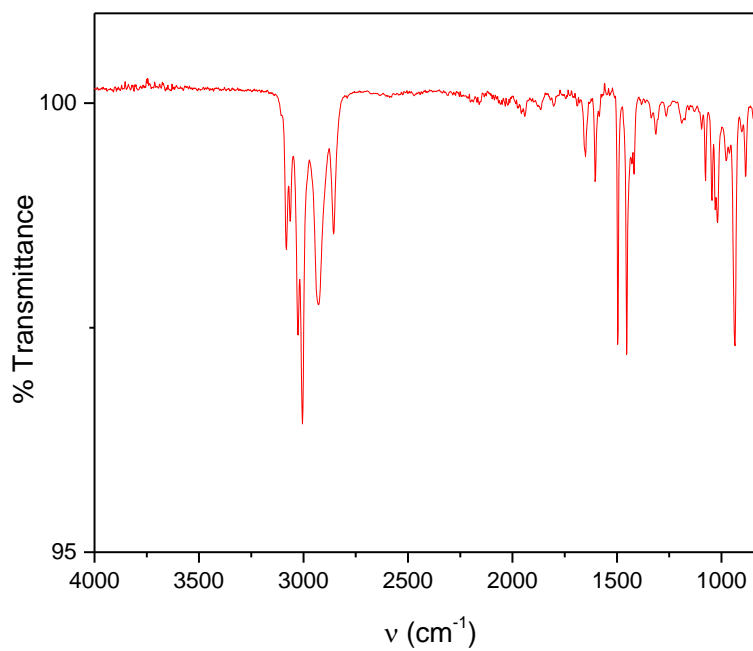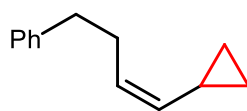
Figure S69. ATR-IR spectrum for **21**.
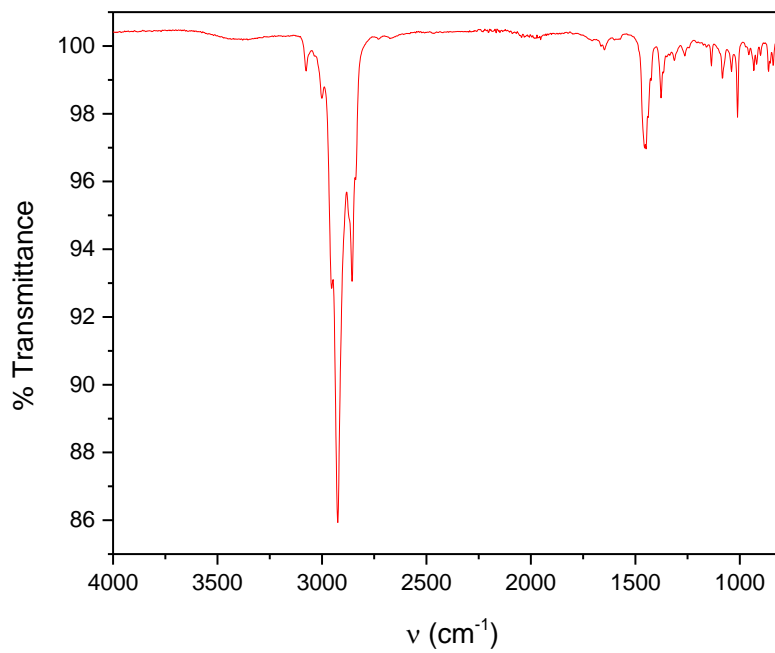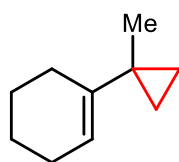
Figure S70. ATR-IR spectrum for **22**.
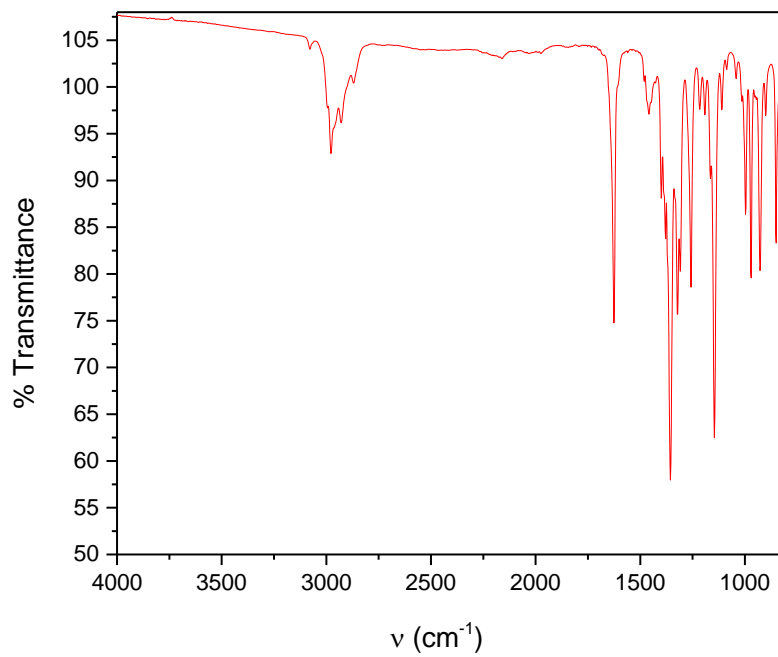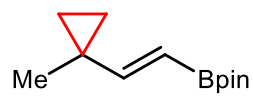
Figure S71. ATR-IR spectrum for **23**.
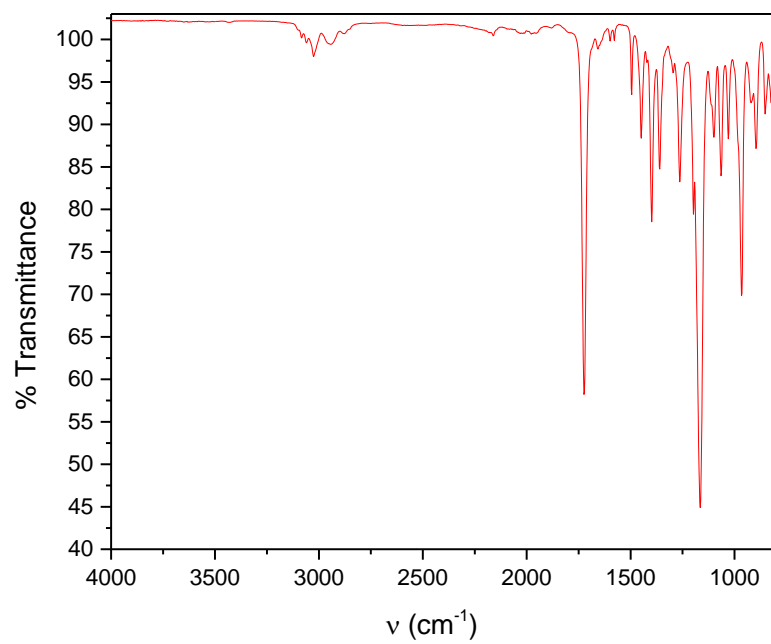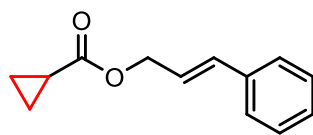
Figure S72. ATR-IR spectrum for **S1**.
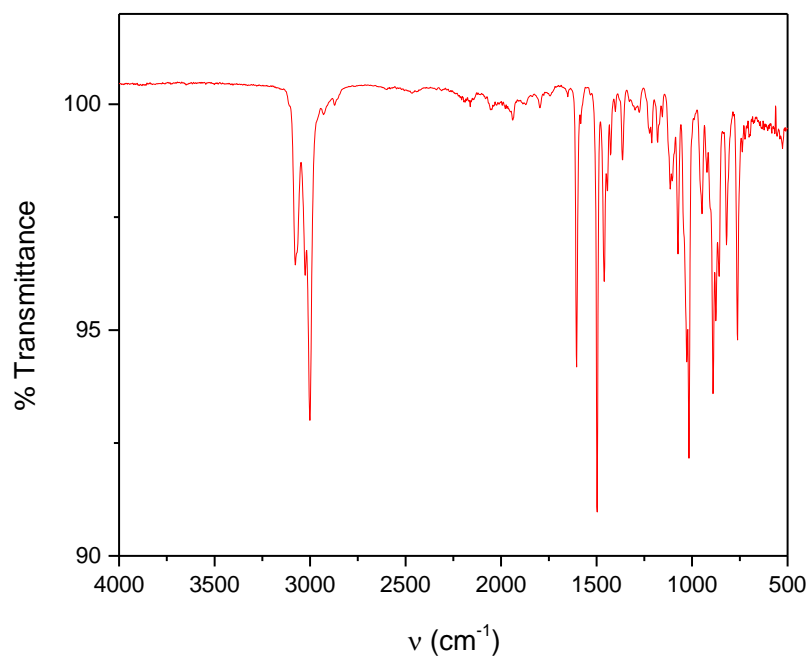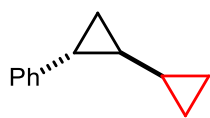
Figure S73. ATR-IR spectrum for **29**.

10. References

[1] Wei, L.; Yang, Y.; Fan, R.; Wang, P.; Li, L.; Yu, J.; Yang, B.; Cao, W. *RSC. Adv*. **2013**. 3, 25908-25916.

[2] A. M. A. Bennett (DuPont), *WO Pat*., 98/27124, 1998

[3] Bruker (2016). Apex3 v2016.9-0, Saint V8.34A, SAINT V8.37A, Bruker AXS Inc.: Madison (WI), USA, 2013/2014.

[4] (a) SHELXTL suite of programs, Version 6.14, 2000-2003, Bruker Advanced X-ray Solutions, Bruker AXS Inc., Madison, Wisconsin: USA; (b) Sheldrick, G. M. *Acta Crystallogr A*. **2008**, *64*, 112–122.

[5] Sheldrick, G. M. *Acta Crystallogr Sect C Struct Chem.* **2015**, *71*, 3–8.

[6] Hübschle, C. B.; Sheldrick, G. M.; Dittrich, B. *J. Appl. Crystallogr.* **2011**, *44*, 1281–1284.

[7] Arora, A.; Teegardin, K.A.; Weaver, J.D. *Org. Lett*. **2015**, 17, 3722-3725.

[8] Percy, J.M.; Emerson,H.; Fyfe, J.W.B.; Kennedy, A.R.; Maciuk, S.; Orr, D.; Rathouská, L.; Redmond, J.M.; Wilson, P.G. *Chem. Eur. J.* **2016**, 22, 12166-12175.

[9] Zheng, M.; Huang, L.; Wu, W.; Jiang, H. *Org. Lett.* **2013**, 15, 1838-1841.

[10] Tamura, R.; Saegusa, K.; Kakihana, M.; Oda, D. *J. Org. Chem.* **1988**, 53, 2723-2728.

[11] Zhao, D.; Lied, F.; Glorius, F. *Chem. Sci*. **2014**, 5, 2869.

[12] Kilman, L.T.; Mlynarski, S. N.; Ferris, G. E.; Morken, J. P. *Angew. Chem. Int. Ed*. **2012**, 51, 521-524.

[13] Niu, G.; Hou, C.; Chuang, G.J.; Wu, C.; Liao, C. *Eur. J. Org. Chem*. **2014**, 3794-3801.

[14] Cannillo, A.; Norsikian, S.; Retailleau, P.; Dau, M.T.H.; Iorga, B.I.; Beau, J. *Chem. Eur. J*. **2013**, 19, 9127-9131.

[15] Kalyva, M.; Zografos, A.L.; Kapourani, E.; Giambazolias, E.; Devel, L.; Papakyriakou, A.; Dive, V.; Lazarou, Y.G.; Georgiadis, D. *Chem. Eur. J*. **2015**, 21, 3278-3289.

[16] Coombs, J. R.; Haeffner, F.; Kilman, L.T.; Morken, J. P. *J. Am. Chem. Soc*. **2013**, 135, 11222-11231.

[17] Jang, Y.H.; Youn, S.W. *Org. Lett*., **2014**, 16, 3720-3723.

APPENDIX B. SUPPORTING INFORMATION FOR CHAPTER 2

1. General Information

General considerations. All manipulations were carried out using standard Schlenk or glovebox techniques under an atmosphere of N_2. THF was dried and degassed by passage through a column of activated alumina and sparging with Ar gas. $CDCl_3$ was purchased from Cambridge Isotope Laboratories, Inc., degassed, and stored over activated 3 Å molecular sieves prior to use. All other reagents and starting materials were purchased from commercial vendors and used without further purification unless otherwise noted. PDI ligands were synthesized according to reported methods.[1,2] Zn powder (325 mesh, 99.9%) and $CoBr_2$ were purchased from Strem. $ZnBr_2$ was purchased from Sigma-Aldrich. $CoBr_2$ was dried in the oven and stored in the glovebox.

Physical methods. ^{1}H and ^{13}C{^{1}H} NMR spectra were collected at room temperature on a Varian INOVA 300 MHz spectrometer, Bruker Avance 400 MHz spectrometer, or Bruker Avance 500 MHz spectrometer. ^{1}H and ^{13}C{^{1}H} NMR spectra are reported in parts per million relative to tetramethylsilane, using the residual solvent resonances as an internal standard. High-resolution mass data were obtained using an Agilent 6320 Trap LC/MS, Agilent 5975C GC/MS, or Thermo Electron Corporation MAT 95XP-Trap instrument. ATR-IR data were collected on a Thermo Scientific Nicolet Nexus spectrometer.

2. Reaction Optimization Studies

General Procedure for Optimization Study. In an N_2-filled glovebox, a 2-dram vial was charged with the metal salt (0.014 mmol, 0.10 equiv), ligand (0.014 mmol, 0.10 equiv), THF (0.5 mL) and a magnetic stir bar. The metal complex was allowed to form by stirring at room temperature for 24 h. Then, Zn powder (18 mg, 0.28 mmol, 2.0 equiv), $ZnBr_2$ (18 mg, 0.28 mmol, 1.0 equiv), and a stock solution of the substrate (0.14 mmol, 1.0 equiv) and a mesitylene standard dissolved in THF (0.5 mL) were added. The reaction mixture was stirred at room temperature for approximately 15 min, during which time a deep violet color developed. Me_2CCl_2 (31.6 mg, 0.28 mmol, 2.0 equiv) was added, and stirring was continued at room temperature. After 24 h, the reaction mixture was diluted with CH_2Cl_2, and an aliquot was analyzed by GC (FID detector).

Metal Source (10 mol%)
Ligand (10 mol%)
$Cl_2C(Me)_2$ (2 eq.)
Zn (2 eq.)
$ZnBr_2$ (1 eq.)

THF, 24 h

1 → **2**

Entry	Metal Source	Ligand	Yield **2** [%]
1	–	–	< 1
2	–	2-t-BuPDI (**L1**)	< 1
3	CoBr₂	–	< 1
4	CoBr₂	2-t-BuPDI (**L1**)	93
5	CoBr₂	2,4,6-MePDI (**L2**)	77
6	CoBr₂	3,5-t-BuPDI (**L3**)	8
7	CoBr₂	2,6-i-PrPDI (**L4**)	2
8	NiBr₂	2-t-BuPDI (**L1**)	5
9	FeBr₂	2-t-BuPDI (**L1**)	4
10	CoBr₂	2,6-i-PrIP (**L5**)	2
11	CoBr₂	2,6-i-PrDAD (**L6**)	<1
12	CoBr₂	bpy (**L7**)	4
13	CoBr₂	terpy (**L8**)	1
14	CoBr₂	Chiral PDI (**L9**)	9
15	CoBr₂	Chiral PDI (**L10**)	17
16[b]	CoBr₂	2-t-BuPDI (**L1**)	87
17[c]	CoBr₂	2-t-BuPDI (**L1**)	78
18[d]	CoBr₂	2-t-BuPDI (**L1**)	79
19[e]	CoBr₂	2-t-BuPDI (**L1**)	26
20[f]	CoBr₂	2-t-BuPDI (**L1**)	>99

| 21[g] | CoBr$_2$ | 2-t-BuPDI (**L1**) | 7 |
| 22[h] | CoBr$_2$ | 2-t-BuPDI (**L1**) | 11 |

L9   **L10**
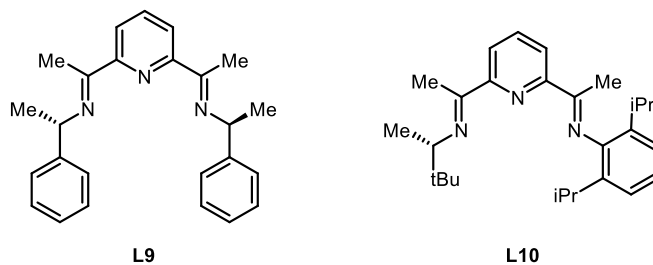
Figure S1. Optimization studies probing metal and ligand sources. [b] Modifications from standard conditions: without ZnBr$_2$. [c] Modifications from standard conditions: 1.1 equiv of Me$_2$CCl$_2$. [d] Modifications from standard conditions: 2.0 equiv of Me$_2$CBr$_2$. [e] Modifications from standard conditions: 2.0 equiv of I$_2$CMe$_2$. [f] Modifications from standard conditions: 1.1 equiv of Zn. [g] Modifications from standard conditions: 1 equiv of MgBr$_2$ (No ZnBr$_2$). [h] Modifications from standard conditions: 1 equiv of LiCl (No ZnBr$_2$).
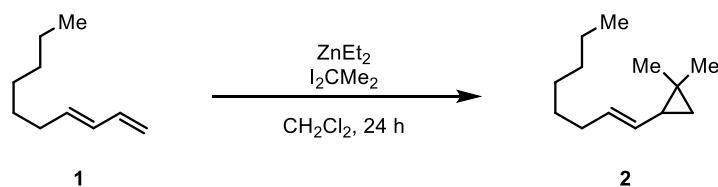
General Procedure for Zinc Carbenoid Dimethylcyclopropanation.[3] In an N_2-filled glovebox, a 2-dram vial was charged with **1** (0.14 mmol, 1.0 equiv), CH_2Cl_2 (1.0 mL), mesitylene, and a magnetic stir bar. Et_2Zn (69 mg, 0.56 mmol, 4.0 equiv) was added dropwise to the solution at –30 °C. I_2CMe_2[4] (166 mg, 0.56 mmol, 4.0 equiv) was added dropwise, and the reaction was allowed to warm to room temperature and stirred for 24 h. The crude reaction mixture was diluted with CH_2Cl_2, and an aliquot was analyzed by GC (FID detector). Conversion of **1**: 70%. Yield of **2**: 45%.
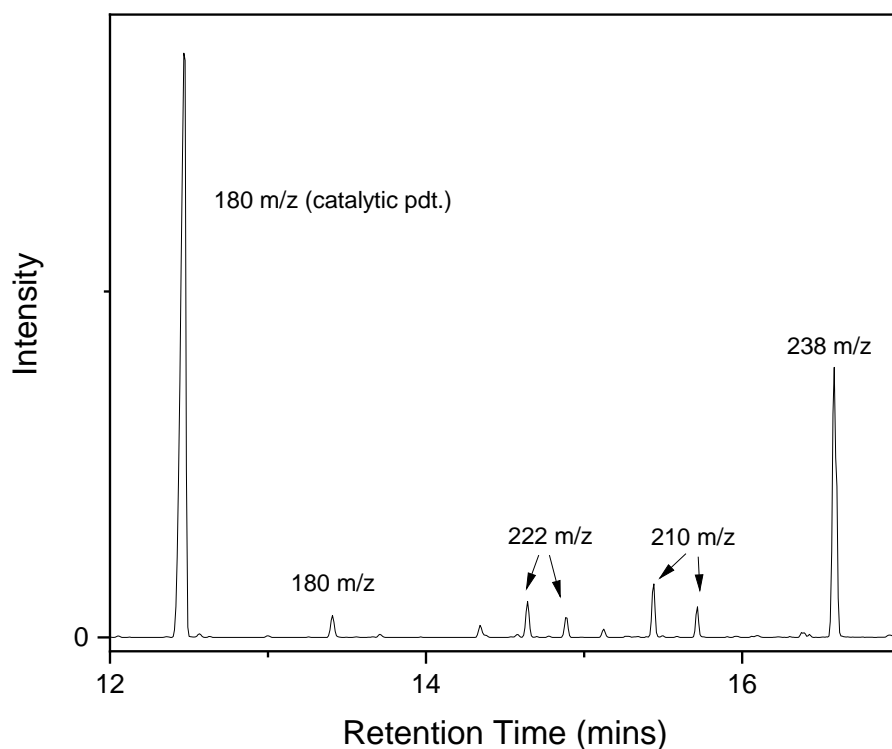
Figure S2. GC/MS analysis of the crude reaction mixture (**1** + I_2CMe_2/Et_2Zn). Additional products correspond to isomers of **2**, products containing two Me_2C fragments, and products containing additional Et groups.

Catalytic Conditions

Simmons-Smith Conditions

f1 (ppm)
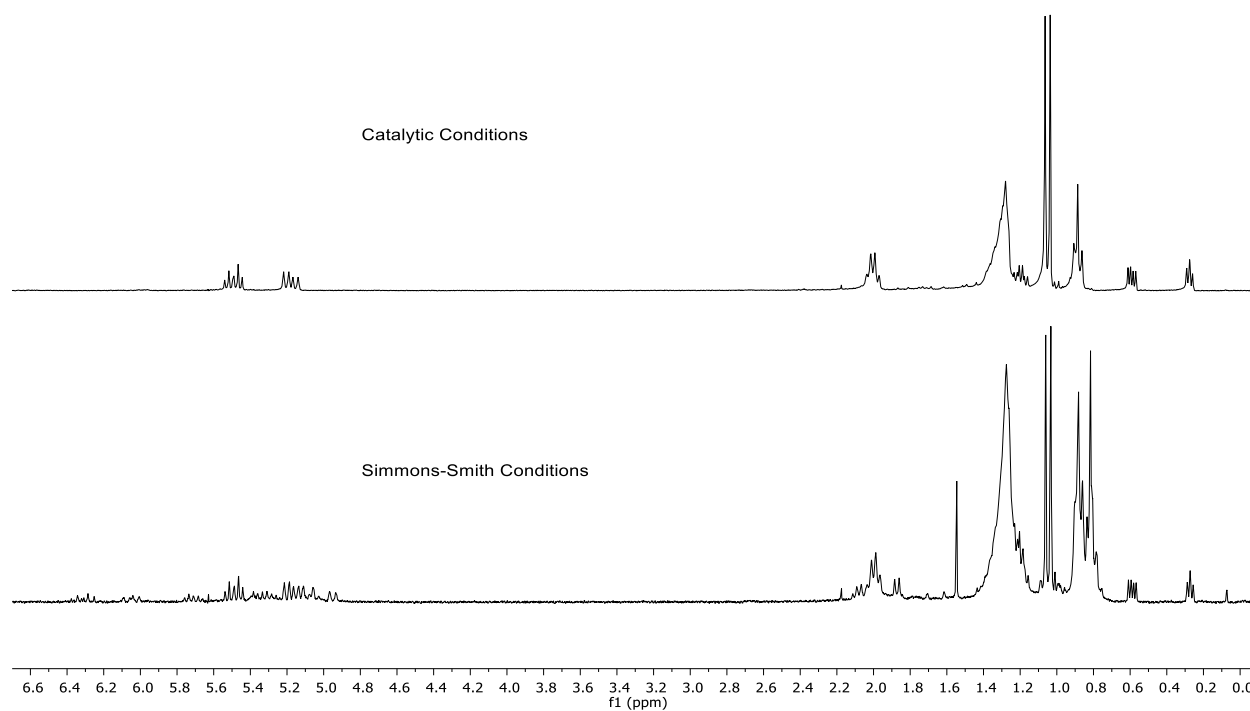
Figure S3. A ^{1}H NMR comparison of the crude reaction mixtures for the cobalt-catalyzed cyclopropanation of **1** (top) and the non-catalytic Furukawa-type Simmons–Smith reaction of **1** (bottom).

3. Procedures for the Dimethylcyclopropanation of 1,3-Dienes

Preparation of [$^{2\text{-}tBu}$PDI]CoBr$_2$ (3). In an N$_2$-filled glovebox, a 5-dram vial was charged with $^{2\text{-}tBu}$PDI[5] (100 mg, 0.23 mmol, 1.0 equiv), CoBr$_2$ (anhydrous) (50.1 mg, 0.23 mmol, 1.0 equiv), THF (7.0 mL) and a magnetic stir bar. The mixture was stirred at room temperature for 24 h. After 24 h, the mixture was concentrated to dryness under vacuum to produce a mustard-yellow solid.
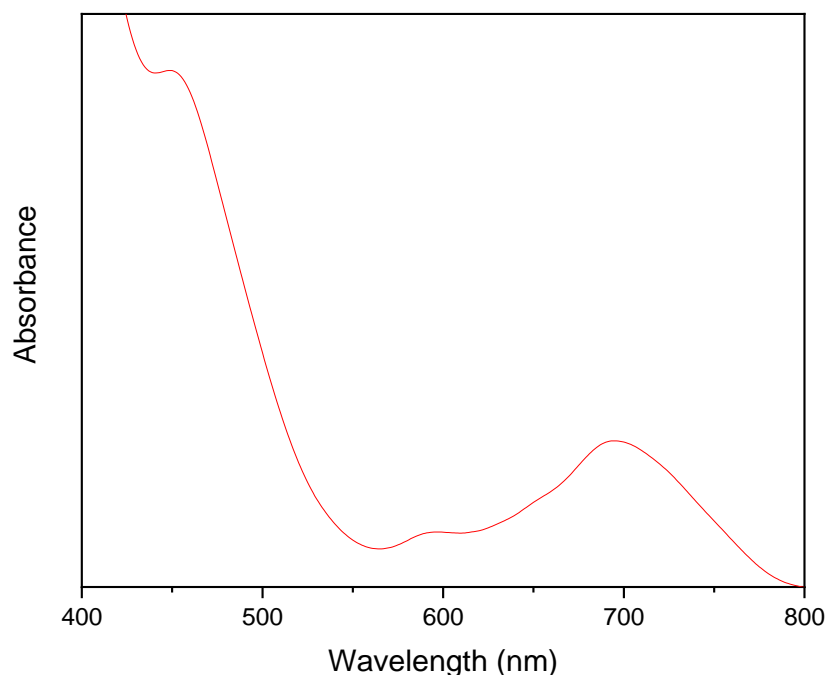
Figure S4. UV-Vis spectrum of [$^{2\text{-tBu}}$PDI]CoBr$_2$ (**3**).

General procedure for the dimethylcyclopropanation of 1,3-dienes. In an N$_2$-filled glovebox, a 2-dram vial was charged with the [$^{2\text{-}tBu}$PDI]CoBr$_2$ catalyst **3** (9.0 mg, 0.014 mmol, 0.10 equiv), the substrate (0.14 mmol, 1.0 equiv), Zn powder (18 mg, 0.28 mmol, 2.0 equiv), ZnBr$_2$ (31 mg, 0.14 mmol, 1.0 equiv), THF (1.0 mL), and a magnetic stir bar. The reaction mixture was stirred at room temperature for approximately 15 min during which time a deep violet color developed. Me$_2$CCl$_2$ (31.6 mg, 0.28 mmol, 2.0 equiv) was added, and stirring was continued at room temperature. After 24 h, the reaction mixture was concentrated under reduced pressure, and the crude residue was directly loaded onto a SiO$_2$ column for purification.

(2). The reaction was conducted using (*E*)-deca-1,3-diene[6] without modification from the general procedure to provide **2** as a colorless oil.

Run 1: 24.7 mg (98% yield). Run 2: 22.2 mg (88% yield).

Purification: SiO_2 column; pentane.

^{1}H NMR (300 MHz, CDCl$_3$) δ 5.54-5.44 (m, 1H), 5.22-5.14 (m, 1H), 2.00 (q, *J* = 6.52 Hz, 2H), 1.36-1.26 (m, 8H), 1.23-1.16 (m, 1H), 1.06 (s, 3H), 1.04 (s, 3H), 0.89 (t, *J* = 6.97 Hz, 3H), 0.61-0.57 (m, 1H), 0.28 (t, *J* = 4.71 Hz, 1H).

^{13}C{^{1}H} NMR (126 MHz, CDCl$_3$) δ 130.3, 130.1, 32.8, 31.8, 29.8, 28.9, 27.5, 27.0, 22.7, 21.0, 20.5, 18.0, 14.1.

HRMS (ESI) calc. for $C_{13}H_{23}$: m/z=179.1794, found: m/z=179.1792

IR (film): 3052, 3001, 2952, 2915, 2851, 1452, 1365, 963 cm^{-1}
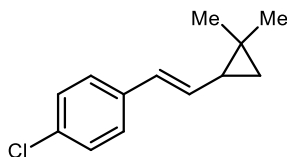
(4). The reaction was conducted using (*E*)-1-(buta-1,3-dien-1-yl)-4-chlorobenzene[7] without modification from the general procedure to provide **4** as a colorless oil.

Run 1: 27.8 mg (96% yield). Run 2: 27.2 mg (94% yield).

Purification: SiO_2 column; pentane

^{1}H NMR (300 MHz, CDCl$_3$) δ 7.25 (s, 4H), 6.42 (d, *J* = 15.70 Hz, 1H), 6.01-5.92 (m, 1H), 1.47-1.39 (m, 1H), 1.15 (s, 6H), 0.83-0.79 (m, 1H), 0.52 (t, *J* = 4.87 Hz, 1H).

^{13}C{^{1}H} NMR (126 MHz, CDCl$_3$) δ 136.5, 132.5, 131.9, 128.6, 128.0, 126.8, 28.6, 27.1, 22.5, 20.8, 19.9.

HRMS (ESI) calc. for $C_{13}H_{14}Cl$: m/z=205.0779, found: m/z=205.0781

IR (film): 3001, 2944, 2858, 1645, 1487, 1444, 1085, 971 cm^{-1}
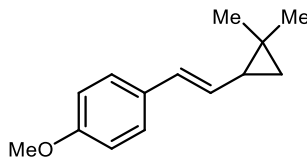
(5). The reaction was conducted using (*E*)-1-(buta-1,3-dien-1-yl)-4-methoxybenzene[8] without modification from the general procedure to provide **5** as a colorless oil.

Run 1: 26.6 mg (94% yield). Run 2: 26.9 mg (95% yield).

Purification: SiO_2 column; CH_2Cl_2

^{1}H NMR (300 MHz, CDCl$_3$) δ 7.27 (d, J = 8.50 Hz, 2H), 6.84 (d, J = 8.44 Hz, 2H), 6.43 (d, J = 15.69 Hz, 1H), 5.86 (dd, J = 8.87, 6.54 Hz, 1H), 3.81 (s, 3H), 1.45-1.37 (m, 1H), 1.14 (s, 6H), 0.79-0.75 (m, 1H), 0.48 (t, J = 4.78 Hz, 1H).

^{13}C{^{1}H} NMR (126 MHz, CDCl$_3$) δ 158.4, 130.9, 129.4, 128.6, 126.7, 113.9, 55.3, 28.5, 27.1, 22.1, 20.8, 19.4.

HRMS (ESI) calc. for C$_{14}$H$_{17}$O: m/z=201.1274, found: m/z=201.1277

IR (film): 2995, 2958, 1609, 1509, 1236, 1164, 1049, 934 cm^{-1}
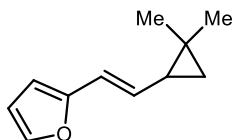
(6). The reaction was conducted using (*E*)-2-(buta-1,3-dien-1-yl)furan[9] without modification from the general procedure to provide **6** as a colorless oil.

Run 1: 16.8 mg (74% yield). Run 2: 15.9 mg (70% yield).

Purification: SiO$_2$ column; CH$_2$Cl$_2$

^{1}H NMR (300 MHz, CDCl$_3$) δ 7.29 (d, J = 1.62 Hz, 1H), 6.34 (dd, J = 1.84, 1.42 Hz, 1H), 6.29 (d, J = 15.73 Hz, 1H), 6.10 (d, J = 3.23 Hz, 1H), 5.94 (dd, J = 9.24, 6.48 Hz, 1H), 1.41-1.33 (m, 1H), 1.13-1.12 (m, 6H), 0.80-0.76 (m, 1H), 0.49 (t, J = 4.78 Hz, 1H).

^{13}C{^{1}H} NMR (126 MHz, CDCl$_3$) δ 153.5, 140.9, 130.8, 117.8, 111.1, 105.2, 28.4, 27.0, 22.5, 20.8, 19.9.

HRMS (ESI) calc. for C$_{11}$H$_{13}$O: m/z=161.0961, found: m/z=161.0960

IR (film): 2995, 2944, 2865, 1444, 1150, 1006, 949, 906 cm^{-1}
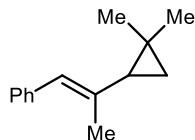
(7). The reaction was conducted using (*E*)-(2-methylbuta-1,3-dien-1-yl)benzene[10] without modification from the general procedure to provide **7** as a colorless oil.

Run 1: 23.7 mg (91% yield). Run 2: 23.0 mg (88% yield).

Purification: SiO$_2$ column; pentane

^{1}H NMR (300 MHz, CDCl$_3$) δ 7.36-7.27 (m, 3H), 7.27-7.17 (m, 2H), 6.19 (s, 1H), 1.95 (s, 3H), 1.36 (t, J = 6.97 Hz, 1H), 1.21 (s, 3H), 1.02 (s, 3H), 0.70 (t, J = 5.0 Hz, 1H), 0.60-0.56 (m, 1H).

^{13}C{^{1}H} NMR (126 MHz, CDCl$_3$) δ 138.6, 138.0, 128.8, 128.0, 125.8, 125.0, 34.4, 27.5, 20.1, 19.3, 18.4, 17.8.

HRMS (ESI) calc. for C$_{14}$H$_{17}$: m/z=185.1325, found: m/z=185.1323

IR (film): 3073, 2937, 2851, 1652, 1595, 1452, 1372, 1071, 913 cm^{-1}
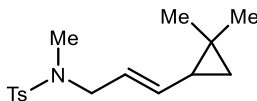
(8). The reaction was conducted using (*E*)-N,4-dimethyl-N-(penta-2,4-dien-1-yl)benzenesulfonamide[11] without modification from the general procedure to provide **8** as a yellow oil.

Run 1: 23.4 mg (57% yield). Run 2: 20.5 mg (50% yield).

Purification: SiO_2 column; hexane/EtOAc (80:20)

^{1}H NMR (300 MHz, CDCl$_3$) δ7.67 (d, *J* = 8.29 Hz, 2H), 7.32 (d, *J* = 8.44 Hz, 2H), 5.42-5.26 (m, 2H), 3.63-3.51 (m, 2H), 2.64 (s, 3H), 2.43 (s, 3H), 1.26-1.17 (m, 1H), 1.05 (s, 3H), 0.99 (s, 3H), 0.67-0.62 (m, 1H), 0.30 (t, *J* = 4.89 Hz, 1H).

^{13}C{^{1}H} NMR (126 MHz, CDCl$_3$) δ 143.2, 136.5, 134.6, 129.6, 127.5, 123.2, 52.5, 33.9, 27.2, 26.9, 21.6, 21.5, 20.5, 18.9.

HRMS (ESI) calc. for $C_{16}H_{23}NO_2SNa$: m/z=316.1342, found: m/z=316.1346

IR (film): 2966, 2915, 2872, 1430, 1336, 1164, 1078, 956, 906 cm^{-1}
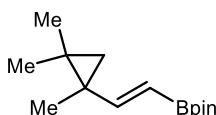
(9). The reaction was conducted using (*E*)-4,4,5,5-tetramethyl-2-(3-methylbuta-1,3-dien-1-yl)-1,3,2-dioxaborolane[12] without modification from the general procedure to provide **9** as a colorless oil.

Run 1: 29.8 mg (90% yield). Run 2: 30.1 mg (91% yield).

Purification: SiO_2 column; CH_2Cl_2

^{1}H NMR (300 MHz, CDCl$_3$) δ 6.54 (d, *J* = 18.07 Hz, 1H), 5.41 (d, *J* = 18.05 Hz, 1H), 1.25 (s, 12H), 1.19 (s, 3H), 1.13 (s, 6H), 0.79 (d, *J* = 4.38 Hz, 1H), 0.51 (d, *J* = 4.37 Hz, 1H).

^{13}C{^{1}H} NMR (126 MHz, CDCl$_3$) δ 160.1, 82.8, 29.9, 28.2, 24.8, 24.4, 22.8, 22.7, 17.4.

^{11}B NMR (96 MHz, CDCl$_3$) δ 29.85.

HRMS (ESI) calc. for $C_{14}H_{25}BO_2$: m/z=236.2057, found: m/z=236.2054

IR (film): 2973, 2937, 1609, 1344, 1307, 1164, 956 cm^{-1}
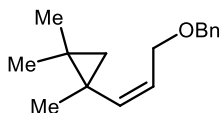
(10). The reaction was conducted using (*Z*)-(((4-methylpenta-2,4-dien-1-yl)oxy)methyl)benzene without modification from the general procedure to provide **10** as a colorless oil.

Run 1: 31.0 mg (96% yield). Run 2: 31.0 mg (96% yield).

Purification: SiO_2 column; CH_2Cl_2

^{1}H NMR (300 MHz, CDCl$_3$) δ 7.38-7.26 (m, 5H), 5.75-5.71 (m, 1H), 5.67-5.60 (m, 1H), 4.55 (s, 2H), 4.27-4.21 (m, 1H), 4.15-4.09 (m, 1H), 1.12 (s, 3H), 1.09 (s, 3H), 1.01 (s, 3H), 0.38 (d, J = 4.04 Hz, 1H), 0.33 (d, J = 4.04 Hz, 1H).

^{13}C{^{1}H} NMR (126 MHz, CDCl$_3$) δ 138.4, 137.0, 128.8, 128.4, 127.9, 127.6, 72.6, 66.9, 28.1, 23.8, 23.3, 21.3, 21.2, 20.1.

HRMS (ESI) calc. for C$_{16}$H$_{23}$O: m/z=231.1743, found: m/z=231.1741

IR (film): 3030, 2980, 2944, 2851, 1452, 1350, 1064, 1021, 934 cm^{-1}
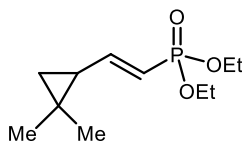
(11). The reaction was conducted using diethyl (*E*)-buta-1,3-dien-1-ylphosphonate**Error! Bookmark not defined.** without modification from the general procedure to provide **11** as a colorless oil.

Run 1: 30.2 mg (93% yield). Run 2: 29.6 mg (91% yield).

Purification: SiO$_2$ column; EtOAc

^{1}H NMR (300 MHz, CDCl$_3$) δ 6.71-6.55 (m, 1H), 5.65 (dd, J = 16.82, 5.6 Hz, 1H), 4.20-4.08 (m, 4H), 1.47-1.38 (m, 1H), 1.32 (t, J = 7.66 Hz, 6H), 1.17 (s, 3H), 1.11 (s, 3H), 0.94-0.90 (m, 1H), 0.75 (t, J = 4.85 Hz, 1H).

^{13}C{^{1}H} NMR (126 MHz, CDCl$_3$) δ 158.3, 111.9 (d, J = 194.2 Hz), 62.9, 30.4, 30.2, 26.9, 24.4, 22.7, 20.9, 16.3.

^{31}P NMR (121 MHz, CDCl$_3$) δ 20.8

HRMS (ESI) calc. for C$_{11}$H$_{22}$O$_3$P: m/z=233.1301, found: m/z=233.1303

IR (film): 2980, 2865, 1616, 1207, 1021, 956, 826 cm^{-1}
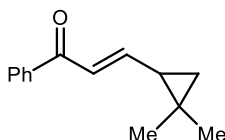
(12). The reaction was conducted using (*E*)-1-phenylpenta-2,4-dien-1-one[13] without modification from the general procedure to provide **12** as a colorless oil.

Run 1: 14.0 mg (50% yield). Run 2: 15.1 mg (54% yield).

Purification: SiO$_2$ column; hexane/EtOAc (95:5)

^{1}H NMR (300 MHz, CDCl$_3$) δ 7.96-7.93 (m, 2H), 7.58-7.52 (m, 1H), 7.49-7.43 (m, 2H), 7.03 (d, J = 15.05 Hz, 1H), 6.90-6.82 (m, 1H), 1.61-1.54 (m, 1H), 1.21 (s, 3H), 1.18 (s, 3H), 1.06-1.01 (m, 1H), 0.79 (t, J = 4.75 Hz, 1H).

^{13}C{^{1}H} NMR (126 MHz, CDCl$_3$) δ 189.7, 152.8, 138.3, 132.4, 128.4, 128.4 124.4, 29.5, 27.0, 25.2, 23.3, 21.1.

HRMS (APCI) calc. for C$_{14}$H$_{17}$O: m/z=201.1274, found: m/z=201.1276

IR (film): 3059, 2958, 2872, 1667, 1602, 1279, 1178, 1006, 920 cm^{-1}
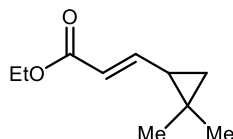
(13). The reaction was conducted using ethyl (*E*)-penta-2,4-dienoate[14] without modification from the general procedure to provide **13** as a colorless oil.

Run 1: 21.0 mg (89% yield). Run 2: 21.4 mg (91% yield).

Purification: SiO_2 column; hexane:CH_2Cl_2 (1:1)

^{1}H NMR (300 MHz, CDCl$_3$) δ 6.69 (dd, *J* = 14.80, 10.92 Hz, 1H), 5.88 (d, *J* = 15.35 Hz, 1H), 4.17 (q, *J* = 8.02 Hz, 2H), 1.46-1.38 (m, 1H), 1.28 (td, *J* = 7.13, 1.24 Hz, 3H), 1.15 (s, 3H), 1.13 (s, 3H), 0.94-0.90 (m, 1H), 0.66 (t, *J* = 4.92 Hz, 1H).

^{13}C{^{1}H} NMR (126 MHz, CDCl$_3$) δ 166.7, 151.3, 119.6, 60.0, 28.3, 26.9, 24.3, 22.3, 20.9, 14.3.

HRMS (ESI) calc. for C$_{10}$H$_{17}$O$_2$: m/z=169.1223, found: m/z=169.1221

IR (film): 2973, 2944, 2865, 1724, 1630, 1221, 1143, 1035 cm^{-1}
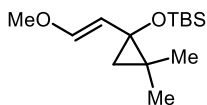
(14). The reaction was conducted using *trans*-3-(*tert*-Butyldimethylsilyloxy)-1-methoxy-1,3-butadienewithout modification from the general procedure to provide **14** as a colorless oil.

Run 1: 24.3 mg (68% yield). Run 2: 25.6 mg (72% yield).

Purification: SiO_2 column; CH_2Cl_2

^{1}H NMR (300 MHz, CDCl$_3$) δ 6.42 (d, *J* = 12.7 Hz, 1H), 5.04 (d, *J* = 12.6 Hz, 1H), 3.55 (s, 3H), 1.19 (s, 3H), 0.94 (s, 3H), 0.86 (s, 9H), 0.60 (d, *J* = 5.3 Hz, 1H), 0.42 (d, *J* = 5.3 Hz, 1H), 0.09 (d, *J* = 3.6 Hz, 6H).

^{13}C{^{1}H} NMR (126 MHz, CDCl$_3$) δ 149.6, 104.3, 61.5, 56.0, 25.9, 24.3, 22.3, 21.4, 20.2, 18.1.

HRMS (ESI) calc. for C$_{14}$H$_{27}$O$_2$Si: m/z=255.1775, found: m/z=255.1774

IR (film): 2952, 2923, 2844, 1645, 1458, 1258, 1135, 941 cm^{-1}
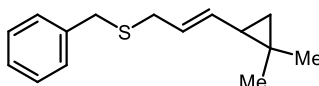
(15). The reaction was conducted using (*E*)-benzyl(penta-2,4-dien-1-yl)sulfane[15] without modification from the general procedure to provide **15** as a colorless oil.

Run 1: 25.7 mg (79% yield). Run 2: 27 mg (83% yield).

Purification: SiO_2 column; CH_2Cl_2

^{1}H NMR (300 MHz, CDCl$_3$) δ 7.36 – 7.20 (m, 5H), 5.50 (dt, *J* = 14.6, 7.2 Hz, 1H), 5.26 (dd, *J* = 15.0, 9.5 Hz, 1H), 3.68 (s, 2H), 3.03 (d, *J* = 7.2 Hz, 2H), 1.30 (dd, *J* = 8.4, 5.2 Hz, 1H), 1.10 (s, 3H), 1.08 (s, 3H), 0.69 (dd, *J* = 8.7, 4.3 Hz, 1H), 0.36 (t, *J* = 4.9 Hz, 1H).

^{13}C{^{1}H} NMR (126 MHz, CDCl$_3$) δ 138.5, 134.2, 128.9, 128.3, 126.7, 125.0, 34.8, 33.4, 27.3, 26.9, 21.5, 20.6, 18.6.

HRMS (ESI) calc. for C$_{15}$H$_{21}$S: m/z=233.1359, found: m/z=233.1358

IR (film): 3030, 2930, 2865, 1501, 1437, 963, 913 cm^{-1}
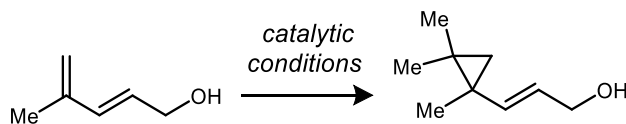
(18). The reaction was conducted using (*E*)-4-methylpenta-2,4-dien-1-ol **16**[16] without modification from the general procedure to provide **18** as a yellow oil.

Run 1: 11.2 mg (57% yield). Run 2: 11.4 mg (58% yield).

Purification: SiO$_2$ column; hexane/EtOAc (90:10)

^{1}H NMR (300 MHz, CDCl$_3$) δ 5.64-5.62 (m, 2H), 4.14-4.11 (m, 2H), 1.24-1.22 (m, 1H), 1.20 (s, 3H), 1.14 (s, 3H), 1.08 (s, 3H), 0.60 (d, *J* = 4.55 Hz, 1H), 0.42 (d, *J* = 4.39 Hz, 1H).

^{13}C{^{1}H} NMR (126 MHz, CDCl$_3$) δ 139.3, 126.5, 64.2, 28.4, 25.4, 22.9, 22.6, 22.3, 18.5.

HRMS (ESI) calc. for C$_9$H$_{15}$O: m/z=139.1117, found: m/z=139.1120

IR (film): 3324, 2980, 2923, 2858, 1659, 1452, 1379, 1085, 956, 906 cm^{-1}

4:1 rr (35% combined yield)
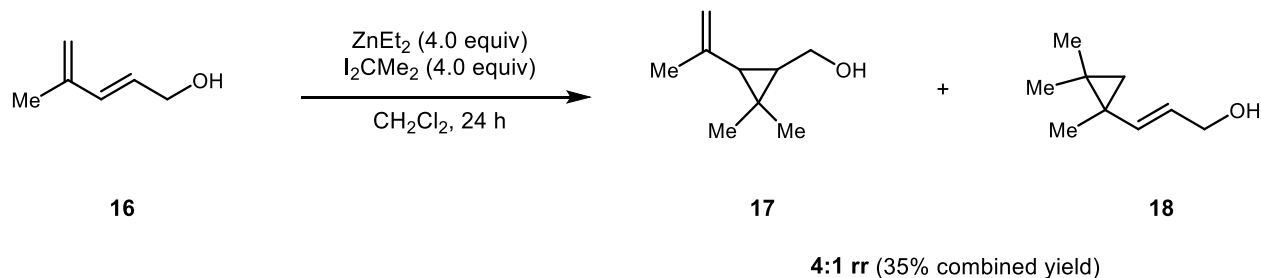
Non-Catalytic Furukawa-Type Simmons–Smith Cyclopropanation of 16. In an N$_2$-filled glovebox, a 2-dram vial was charged with **16** (0.14 mmol, 1.0 equiv), CH$_2$Cl$_2$ (1.0 mL), and a magnetic stir bar. Et$_2$Zn (69 mg, 0.56 mmol, 4.0 equiv) was added dropwise to the solution at –30 °C. I$_2$CMe$_2$ (166 mg, 0.56 mmol, 4.0 equiv) was added dropwise, and the reaction was allowed to warm to room temperature and stirred for 24 h. The reaction mixture was concentrated under reduced pressure, and the crude residue was directly loaded onto a SiO$_2$ column to obtain a mixture of **16**, **17**, and **18**. Combined Yield of **17** + **18**: 35%. Ratio **17:18** = 4:1.
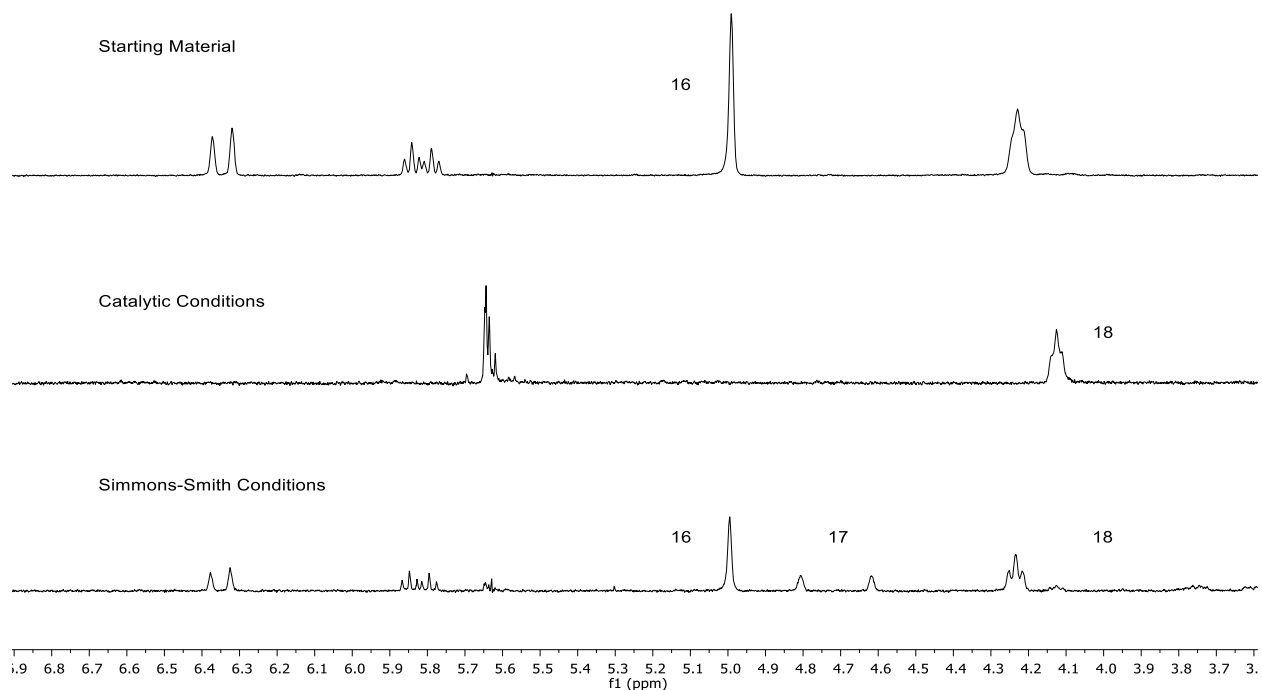
Figure S5. ^{1}H NMR comparison of product **18** obtained from the catalytic dimethylcyclopropanation (middle) and the mixture of **17**, **18**, and recovered starting material (**16**) obtained under the Furukawa-type Simmons–Smith conditions (bottom).
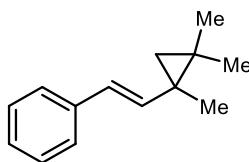
(26). The reaction was conducted using (*E*)-(3-methylbuta-1,3-dien-1-yl)benzene**Error! Bookmark not defined.** without modification from the general procedure to provide **26** as a colorless oil.

Run 1: 25.8 mg (99% yield). Run 2: 25.3 mg (97% yield).

Purification: SiO_2 column; pentane

^{1}H NMR (300 MHz, CDCl$_3$) δ 7.37-7.28 (m, 4H), 7.22-7.17 (m, 1H), 6.39 (d, *J* = 15.97 Hz, 1H), 6.24 (d, *J* = 15.97 Hz, 1H), 1.33 (s, 3H), 1.22 (s, 3H), 1.17 (s, 3H), 0.79 (d, *J* = 4.34 Hz, 1H), 0.53 (d, *J* = 4.41 Hz, 1H).

^{13}C{^{1}H} NMR (126 MHz, CDCl$_3$) δ 138.3, 137.0, 128.5, 127.4, 126.5, 125.7, 28.8, 26.4, 23.3, 23.1, 22.5, 18.7.

HRMS (ESI) calc. for $C_{14}H_{17}$: m/z=185.1325, found: m/z=185.1322

IR (film): 3016, 2987, 2944, 2865, 1630, 1444, 1114, 1064, 971 cm^{-1}
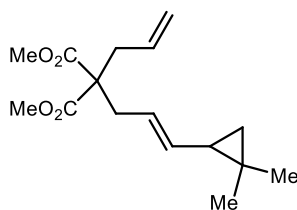
(28). The reaction was conducted using dimethyl (*E*)-2-allyl-2-(penta-2,4-dien-1-yl)malonate[17] without modification from the general procedure to provide **28** as a yellow oil.

Run 1: 35.7mg (91% yield). Run 2: 34.5 mg (88% yield).

Purification: SiO$_2$ column; hexane/EtOAc (95:5)

^{1}H NMR (300 MHz, CDCl$_3$) δ 5.72-5.57 (m, 1H), 5.27 (t, *J* = 5.99 Hz, 2H), 5.11 (d, *J* = 5.81 Hz, 1H), 5.06 (s, 1H), 3.70 (s, 6H), 2.65-2.59 (m, 4H), 1.22-1.15 (m, 1H), 1.04 (s, 3H), 1.01 (s, 3H), 0.63-0.59 (m, 1H), 0.27 (t, *J* = 4.67 Hz, 1H).

^{13}C{^{1}H} NMR (126 MHz, CDCl$_3$) δ 171.3, 135.7, 132.5, 122.6, 119.0, 58.0, 52.3, 36.8, 35.9, 27.5, 27.0, 21.4, 20.6, 18.5.

HRMS (ESI) calc. for C$_{16}$H$_{25}$O$_4$: m/z=281.1747, found: m/z=281.1746

IR (film): 2987, 2958, 2858, 1724, 1437, 1200, 963, 920 cm^{-1}

Additional Substrates Exhibiting Modest Yields:
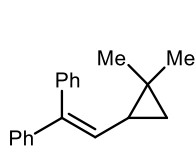

^{1}H NMR Yield: 9%
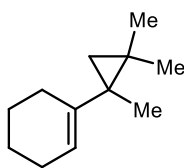
^{1}H NMR Yield: 19%
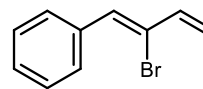

Messy NMR
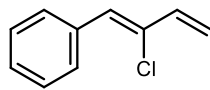
Messy NMR
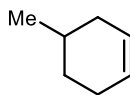
Low Conversion
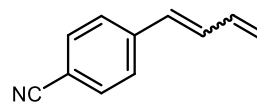
Low Conversion

4. Procedures for the Vinylcyclopropane Ring-Opening Reactions
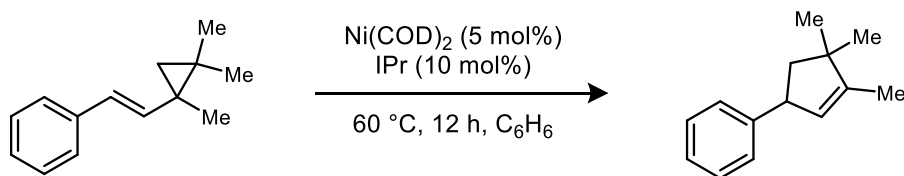
(27). The reaction was conducted using the procedure reported by Louie using **26** to provide **27** as a colorless oil (65% yield, 10.2 mg).[18]

Purification: SiO$_2$ column; pentane

^{1}H NMR (300 MHz, CDCl$_3$) δ 7.32-7.27 (m, 2H), 7.23-7.15 (m, 3H), 5.29 (t, J = 1.46 Hz, 1H), 3.88-3.78 (m, 1H), 2.25 (dd, J = 12.58, 8.01 Hz, 1H), 1.71 (dd, J = 1.55, 0.81, Hz, 3H), 1.61 (dd, J = 8.30, 4.25, Hz, 1H), 1.08 (s, 3H), 1.08 (s, 3H).

^{13}C{^{1}H} NMR (126 MHz, CDCl$_3$) δ 149.3, 147.0, 128.3, 127.3, 126.2, 125.8, 51.2, 48.0, 46.2, 27.6, 26.0, 12.3.

HRMS (APCI) calc. for C$_{14}$H$_{17}$: m/z=185.1325, found: m/z=185.1326

IR (film): 3023, 2944, 2930, 2844, 1602, 1501, 1444, 1358, 1035, 834 cm^{-1}
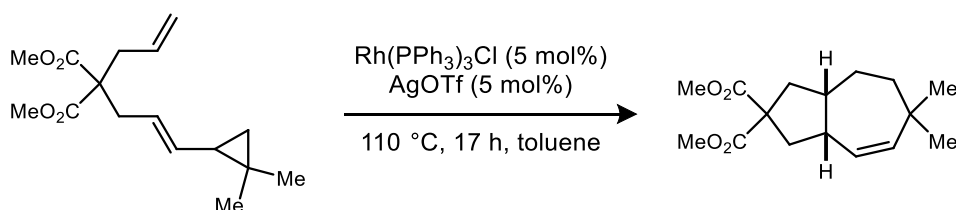
(29). The reaction was conducted using the procedure reported by Wender using **28** to provide **29** as a colorless oil (77% yield, 28.1 mg).[19]

Purification: SiO$_2$ column; hexane/EtOAc (95:5)

^{1}H NMR (300 MHz, CDCl$_3$) δ 5.18-5.14 (m, 2H), 3.71 (s, 6H), 2.86 (qd, J = 7.64, 2.48 Hz, 1H), 2.50-2.39 (m, 2H), 2.26-2.18 (m, 1H), 2.11 (dd, J = 7.95, 5.62 Hz, 1H), 1.95 (dd, J = 8.17, 5.12 Hz, 1H), 1.74 (d, J = 4.28 Hz, 1H), 1.66-1.60 (m, 1H), 1.51-1.48 (m, 2H), 0.99 (s, 3H), 0.96 (s, 3H).

^{13}C{^{1}H} NMR (126 MHz, CDCl$_3$) δ 173.2, 172.9, 139.6, 126.6, 59.0, 52.7, 52.7, 43.9, 41.4, 41.3, 40.8, 38.7, 37.5, 31.2, 29.8, 26.9.

HRMS (ESI) calc. for C$_{16}$H$_{25}$O$_4$: m/z=281.1747, found: m/z=281.1752.

IR (film): 3009, 2958, 2858, 1724, 1437, 1250, 1207, 1150, 1064 cm^{-1}

Stereochemical Assignment for 29. The relative stereochemistry of the ring fusion was assigned as cis by analogy to the products obtained by Wender. Additionally, **29** was hydrogenated using a Pd/C catalyst to obtain a mixture of the hydrogenated product and an alkene migration product. The hydrogenated product was assigned as the cis diastereomer based on the non-equivalency ^{1}H NMR signals corresponding to the two methyl groups and the two methyl esters.

10 wt% Pd/C

MeOH, H$_2$ (1 atm), 17h

1:2
78% combined yield
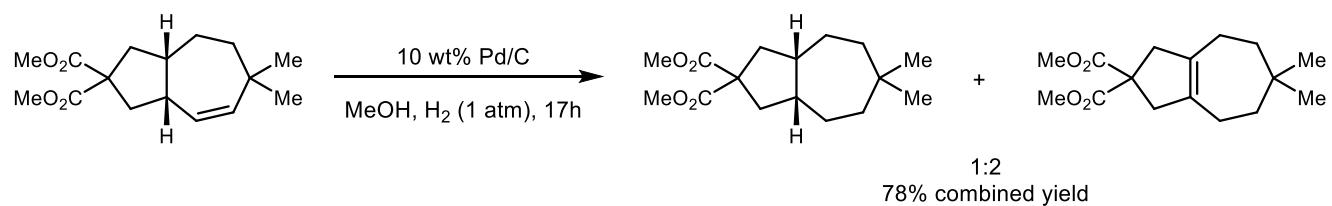
5. Synthesis and Characterization of Dienoic Esters

Procedure A[20,21]:
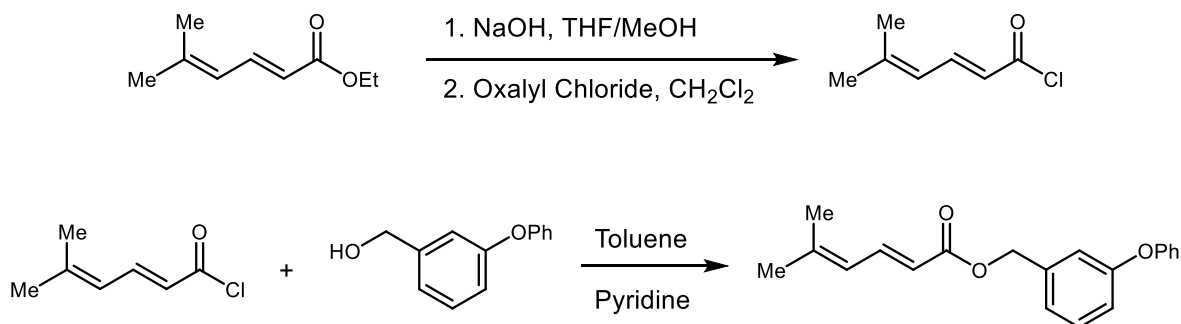
Step 1: A 100-mL round bottom flask was charged with the dienoic ester**Error! Bookmark not defined.** (4.1 mmol) and a THF/MeOH (1:2, 70 mL) solvent mixture. An aqueous solution of 2 M NaOH (19 mL) was added dropwise. The reaction mixture was heated at reflux for 4 h. The reaction mixture was cooled to room temperature and concentrated under reduced pressure. The crude product was dissolved in water (50 mL), and the aqueous phase was washed with Et_2O (3 × 20 mL). The aqueous phase was acidified with concentrated HCl (aq) and extracted with Et_2O (3 × 50 mL). The combined organic phases were washed with water (2 × 25 mL) then saturated aqueous NaCl (2 × 25 mL). The organic phase was dried over anhydrous Na_2SO_4 and filtered. The solvent was removed under vacuum to give provide the dienoic acid[22] (460 mg, 89% yield), which was carried forward without purification.

Step 2: To a solution of the dienoic acid (460 mg, 3.6 mmol) dissolved in anhydrous CH_2Cl_2 (20 mL) was added oxalyl chloride (0.65 mL, 7.2 mmol). The mixture was stirred at room temperature for 12 h. The solvent was evaporated under vacuum to provide the acid chloride (**S1**) (505 mg, 97%) as a yellow oil. The crude product was carried forward without further purification.
^{1}H NMR (300 MHz, CDCl$_3$) δ 7.74 (dd, J = 14.60, 11.72 Hz, 1H), 6.08 (d, J = 11.78 Hz, 1H), 5.98 (d, J = 14.55 Hz, 1H), 1.97 (s, 3H), 1.95 (s, 3H).

Step 3: To a solution of 3-phenoxy-benzenemethanol (505 mg, 3.5 mmol) in dry toluene (10 mL) was added pyridine (0.5 mL). Acid chloride **S1** was added dropwise, and the reaction mixture was stirred overnight at room temperature. The reaction was quenched with water (10 mL) and extracted with Et_2O (3 × 20 mL). The organic phase was washed with 1 M HCl then saturated NaCl (aq). The organic phase was dried over Na_2SO_4, filtered, and concentrated under vacuum. The crude residue was purified by column chromatography (hexane/CH_2Cl_2) to afford **S2** in an isomerically pure form (452 mg, 43% yield).
^{1}H NMR (300 MHz, CDCl$_3$) δ 7.62 (dd, J = 10.82, 3.56 Hz, 1H), 7.34 (q, J = 7.53 Hz, 3H), 7.15-7.09 (m, 2H), 7.05-7.01 (m, 3H), 6.97-6.93 (m, 1H), 6.00 (d, J = 11.61 Hz, 1H), 5.82 (d, J = 15.18 Hz, 1H), 5.17 (s, 2H), 1.89 (s, 6H).

$^{13}C\{^1H\}$ NMR (126 MHz, CDCl$_3$) δ 167.4, 157.5, 157.0, 146.9, 141.7, 138.4, 129.8, 123.7, 123.4, 122.6, 119.0, 118.2, 118.0, 65.4, 26.6, 19.0.

HRMS (ESI) calc. for C$_{20}$H$_{20}$O$_3$: m/z=309.1485, found: m/z=309.1481.

IR (film): 3052, 2901, 1695, 1566, 1466, 1258, 1207, 1121, 985 cm^{-1}

Procedure B:[23]
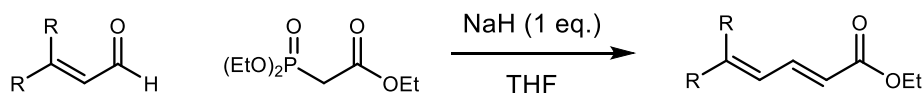

The following dienoic esters were synthesized using the Horner—Wadsworth—Emmons reaction following the literature procedure:
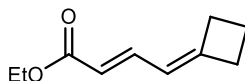
(S3). The reaction was conducted using 2-cyclobutylideneacetaldehyde[24] without modification from procedure B to provide **S3** as a colorless oil (56% yield)

^{1}H NMR (300 MHz, CDCl$_3$) δ 7.25 (dd, J = 15.32, 11.47, Hz, 1H), 5.97-5.86 (m, 1H), 5.70 (dt, J = 15.30, 0.81 Hz, 1H), 4.19 (q, J = 7.13 Hz, 2H), 2.89 (t, J = 7.99 Hz, 2H), 2.80 (t, J = 7.92 Hz, 2H), 2.05 (tt, J = 8.20, 7.39 Hz, 2H), 1.28 (t, J = 7.14 Hz, 3H).

^{13}C{^{1}H} NMR (126 MHz, CDCl$_3$) δ 167.6, 157.3, 140.8, 119.5, 117.5, 60.1, 32.1, 30.7, 16.9, 14.3.

HRMS (ESI) calc. for C$_{10}$H$_{15}$O$_2$: m/z=167.1067, found: m/z=167.1068

IR (film): 2973, 2937, 2908, 1716, 1652, 1616, 1258, 1186, 1129, 971 cm^{-1}
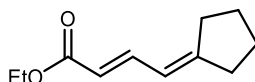
(S4). The reaction was conducted using 2-cyclopentylideneacetaldehyde**Error! Bookmark not defined.** without modification from procedure B to provide **S4** as a colorless oil (41% yield)

^{1}H NMR (300 MHz, CDCl$_3$) δ 7.44 (dd, J = 15.17, 11.66, Hz, 1H), 6.09 (d, J = 11.60 Hz, 1H), 5.71 (d, J = 15.24 Hz, 1H), 4.20 (q, J = 7.13 Hz, 2H), 2.49 (t, J = 6.85 Hz, 2H), 2.39 (t, J = 6.97 Hz, 2H), 1.74 (quintet, J = 6.78 Hz, 2H), 1.68 (quintet, J = 6.59 Hz, 2H), 1.29 (t, J = 7.12 Hz, 3H).

^{13}C{^{1}H} NMR (126 MHz, CDCl$_3$) δ 167.7, 159.1, 142.5, 119.1, 117.7, 60.1, 34.8, 30.2, 26.2, 26.0, 14.4.

HRMS (ESI) calc. for C$_{11}$H$_{17}$O$_2$: m/z=181.1223, found: m/z=181.1222.

IR (film): 2966, 2880, 1702, 1630, 1372, 1258, 1200, 1129, 963 cm^{-1}
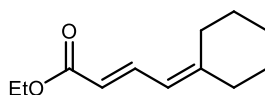
(S5). The reaction was conducted using 2-cyclohexylideneacetaldehyde[25] without modification from procedure B to provide **S5** as a colorless oil (38% yield)

^{1}H NMR (300 MHz, CDCl$_3$) δ 7.63 (dd, J = 15.20, 11.70, Hz, 1H), 5.93 (d, J = 11.56 Hz, 1H), 5.79 (d, J = 15.17 Hz, 1H), 4.20 (q, J = 7.12 Hz, 2H), 2.42-2.36 (m, 2H), 2.24-2.18 (m, 2H), 1.63-1.57 (m, 6H), 1.29 (t, J = 7.11 Hz, 3H).

^{13}C{^{1}H} NMR (126 MHz, CDCl$_3$) δ 167.8, 154.3, 140.4, 120.5, 118.8, 60.1, 37.8, 29.8, 28.5, 27.9, 26.5, 14.4.

HRMS (ESI) calc. for C$_{12}$H$_{19}$O$_2$: m/z=195.1380, found: m/z=195.1377

IR (film): 2930, 2844, 1702, 1624, 1301, 1272, 1164, 1129, 977, 870 cm^{-1}
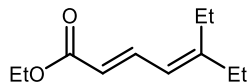
(S6). The reaction was conducted using 3-ethylpent-2-enal[26] without modification from procedure B to provide **S6** as a colorless oil (54% yield)

^{1}H NMR (300 MHz, CDCl$_3$) δ 7.63 (dd, J =15.12, 11.64, Hz, 1H), 5.94 (d, J = 11.78 Hz, 1H), 5.80 (d, J = 15.14 Hz, 1H), 4.21 (q, J = 7.13 Hz, 2H), 2.32 (q, J = 7.58 Hz, 2H), 2.19 (q, J = 7.49 Hz, 2H), 1.30 (dt, J = 7.13, 1.51 Hz, 3H), 1.06 (dq, J = 3.98, 1.49 Hz, 6H).

^{13}C{^{1}H} NMR (126 MHz, CDCl$_3$) δ 167.7, 157.4, 140.7, 121.3, 119.0, 60.1, 30.0, 24.4, 14.4, 13.8, 12.4.

HRMS (ESI) calc. for C$_{11}$H$_{19}$O$_2$: m/z=183.1380, found: m/z=183.1379.

IR (film): 2980, 2937, 2837, 1702, 1630, 1358, 1272, 1135, 985, 877 cm^{-1}

6. Procedures for the Dimethylcyclopropanation of Dienoic Esters

General procedure for the dimethylcyclopropanation of dienoic esters. In an N_2-filled glovebox, a 2-dram vial was charged with the [$^{2-tBu}$PDI]CoBr$_2$ catalyst **3** (9.0 mg, 0.014 mmol, 0.10 equiv), the substrate (0.14 mmol, 1.0 equiv), Zn powder (18 mg, 0.28 mmol, 2.0 equiv), ZnBr$_2$ (31 mg, 0.14 mmol, 1.0 equiv), 1,2-dichloroethane (1.0 mL), and a magnetic stir bar. The reaction mixture was stirred at room temperature for approximately 15 min during which time a deep violet color developed. Me$_2$CBr$_2$ (56.5 mg, 0.28 mmol, 2.0 equiv) was added, and stirring was continued at room temperature. After 24 h, the reaction mixture was concentrated under reduced pressure, and the crude residue was directly loaded onto a SiO$_2$ column for purification.
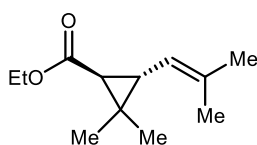
(19). The reaction was conducted using ethyl (*E*)-5-methylhexa-2,4-dienoate[27] without modification from the general procedure to provide **19** as a colorless oil.

Run 1: 17.9 mg (65% yield, >19:1 trans/cis). Run 2: 16.2 mg (59% yield, 13:1 trans/cis).

Purification: SiO$_2$ column; (1:1) CH$_2$Cl$_2$:Hexane

^{1}H NMR (300 MHz, CDCl$_3$) δ 4.88 (d, *J* = 9.44 Hz, 1H), 4.17-4.07 (m, 2H), 2.06-2.02 (m, 1H), 1.73-1.67 (m, 6H), 1.37 (d, *J* = 5.34 Hz, 1H), 1.25 (t, *J* = 7.25 Hz, 6H), 1.13 (s, 3H).

^{13}C{^{1}H} NMR (126 MHz, CDCl$_3$) δ 172.5, 135.4, 121.2, 60.2, 34.8, 32.6, 28.5, 25.6, 22.2, 20.4, 18.5, 14.4.

HRMS (ESI) calc. for C$_{12}$H$_{21}$O$_2$: m/z=197.1536, found: m/z=197.1538.

IR (film): 2958, 2915, 2880, 1731, 1150 cm^{-1}
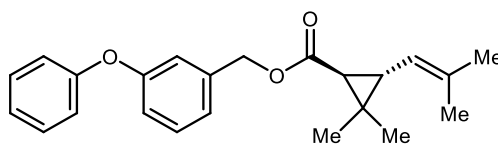
(20). The reaction was conducted using **S2** without modification from the general procedure to provide **20** as a colorless oil.

Run 1: 27.5 mg (56% yield, >19:1 trans/cis). Run 2: 26.5 mg (54% yield, 11:1 trans/cis).

Purification: SiO$_2$ column; (1:1) CH$_2$Cl$_2$:Hexane

^{1}H NMR (300 MHz, CDCl$_3$) δ 7.36-7.30 (m, 3H), 7.11 (q, *J* = 8.56 Hz, 2H), 7.03-7.01 (m, 3H), 6.95 (d, *J* = 7.96 Hz, 1H), 5.09 (s, 2H), 4.89 (d, *J* = 7.86 Hz, 1H), 2.09-2.07 (m, 1H), 1.72 (s, 3H), 1.70 (s, 3H), 1.45 (d, *J* = 5.33 Hz, 1H), 1.26 (s, 3H), 1.13 (s, 3H).

^{13}C{^{1}H} NMR (126 MHz, CDCl$_3$) δ 172.3, 157.5, 157.0, 138.4, 135.6, 129.8, 129.8, 123.4, 122.7, 121.0, 119.0, 118.3, 118.2, 65.6, 34.7, 33.0, 28.9, 25.6, 22.2, 20.5, 18.5.

HRMS (ESI) calc. for C$_{23}$H$_{27}$O$_3$: m/z=351.1955, found: m/z=351.1958.

IR (film): 3030, 2944, 2923, 2865, 1724, 1573, 1487, 1473, 1243, 1121 cm^{-1}
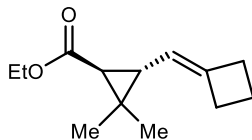
(21). The reaction was conducted using **S3** without modification from the general procedure to provide **21** as a colorless oil.

Run 1: 23.3 mg (80% yield, 8:1 trans/cis). Run 2: 21.9 mg (75% yield, 9:1 trans/cis).

Purification: SiO$_2$ column; (1:1) CH$_2$Cl$_2$:Hexane

^{1}H NMR (500 MHz, CDCl$_3$) δ 4.85-4.81 (m, 1H), 4.14-4.08 (m, 2H), 2.75-2.69 (m, 2H), 2.66 (t, J = 8.76 Hz, 2H), 1.96 (quintet, J = 7.84 Hz, 2H), 1.88 (dd, J = 8.86, 5.27, Hz, 1H), 1.41 (d, J = 5.31 Hz, 1H), 1.26 (d, J = 8.13 Hz, 3H), 1.24 (s, 3H), 1.14 (s, 3H).

^{13}C{^{1}H} NMR (126 MHz, CDCl$_3$) δ 172.4, 143.2, 117.1, 60.2, 34.4, 32.7, 31.2, 29.7, 28.2, 22.2, 20.3, 17.1, 14.4.

HRMS (ESI) calc. for C$_{13}$H$_{21}$O$_2$: m/z=209.1536, found: m/z=209.1532

IR (film): 2973, 2937, 2865, 1716, 1272, 1221, 1172, 841 cm^{-1}
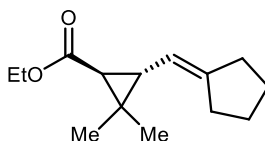
(22). The reaction was conducted using **S4** without modification from the general procedure to provide **22** as a colorless oil.

Run 1: 22.1 mg (71% yield, 13:1 trans/cis). Run 2: 23.7 mg (76% yield, 12:1 trans/cis).

Purification: SiO$_2$ column; (1:1) CH$_2$Cl$_2$:Hexane

^{1}H NMR (300 MHz, CDCl$_3$) δ 5.02 (dt, J = 2.20, 8.53 Hz, 1H), 4.12 (dq, J = 7.10, 2.87, Hz, 2H), 2.31-2.22 (m, 4H), 1.99 (dd, J = 8.55, 5.34, Hz, 1H), 1.70-1.57 (m, 4H), 1.39 (d, J = 5.32 Hz, 1H), 1.26 (t, J = 7.13 Hz, 6H), 1.14 (s, 3H).

^{13}C{^{1}H} NMR (126 MHz, CDCl$_3$) δ 172.5, 146.8, 116.6, 60.1, 34.8, 34.0, 33.8, 29.3, 28.4, 26.5, 26.4, 22.3, 20.5, 14.4.

HRMS (ESI) calc. for C$_{14}$H$_{23}$O$_2$: m/z=223.1693, found: m/z=223.1691

IR (film): 2952, 2858, 1710, 1365, 1236, 1172, 1135, 1028 cm^{-1}
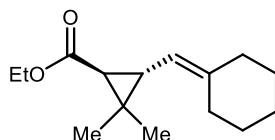
(23). The reaction was conducted using **S5** without modification from the general procedure to provide **23** as a colorless oil.

Run 1: 23.2 mg (70% yield, 13:1 trans/cis). Run 2: 22.5 mg (68% yield, 13:1 trans/cis).

Purification: SiO_2 column; (1:1) CH_2Cl_2:Hexane

^{1}H NMR (300 MHz, CDCl$_3$) δ 4.82 (d, J = 7.83 Hz, 1H), 4.17-4.05 (m, 2H), 2.21-2.16 (m, 2H), 2.08-2.04 (m, 3H), 1.57-1.48 (m, 6H), 1.36 (d, J = 5.23 Hz, 1H), 1.25 (t, J = 3.34 Hz, 6H), 1.12 (s, 3H).

^{13}C{^{1}H} NMR (126 MHz, CDCl$_3$) δ 172.6, 143.5, 117.8, 60.1, 36.8, 34.9, 31.7, 29.4, 28.6, 28.5, 27.7, 26.8, 22.2, 20.4, 14.4.

HRMS (ESI) calc. for $C_{15}H_{25}O_2$: m/z=237.1849, found: m/z=237.1847

IR (film): 2930, 2851, 1731, 1423, 1372, 1207, 1150, 1121, 834 cm^{-1}
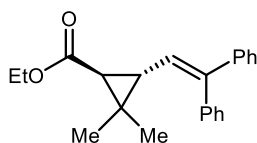
(24). The reaction was conducted using ethyl (E)-5,5-diphenylpenta-2,4-dienoate[28] without modification from the general procedure to provide **24** as a colorless oil.

Run 1: 9.9 mg (22% yield, >19:1 trans/cis). Run 2: 8.5 mg (19% yield, 16:1 trans/cis).

Purification: SiO_2 column; (1:1) CH_2Cl_2:Hexane

^{1}H NMR (300 MHz, CDCl$_3$) δ 7.41-7.29 (m, 4H), 7.24-7.21 (m, 6H), 6.50 (d, J =9.45 Hz, 1H), 4.15 (q, J = 7.0 Hz, 2H), 1.86 (t, J = 8.87 Hz, 1H), 1.68 (d, J = 8.56 Hz, 1H), 1.38 (s, 3H), 1.28 (t, J = 7.11 Hz, 3H), 1.14 (s, 3H).

^{13}C{^{1}H} NMR (126 MHz, CDCl$_3$) δ 171.2, 143.4, 142.6, 140.2, 130.4, 128.1, 128.1, 127.4, 127.0, 126.9, 123.8, 60.0, 34.0, 32.7, 28.3, 28.0, 15.1, 14.4.

HRMS (ESI) calc. for $C_{22}H_{25}O_2$: m/z=321.1849, found: m/z=321.1854

IR (film): 3052, 3030, 2952, 1724, 1200, 1143, 1100 cm^{-1}
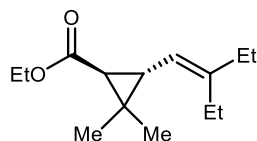
(25). The reaction was conducted using **S6** without modification from the general procedure to provide **25** as a colorless oil.

Run 1: 17.6 mg (56% yield, >19:1 trans/cis). Run 2: 15.1 mg (48% yield, >19:1 trans/cis).

Purification: SiO$_2$ column; (1:1) CH$_2$Cl$_2$:Hexane

^{1}H NMR (300 MHz, CDCl$_3$) δ 4.82 (d, J = 8.07 Hz, 1H), 4.16 – 4.09 (m, 2H), 2.16-2.09 (m, 5H), 1.39 (d, J = 5.34 Hz, 1H), 1.26 (t, J = 7.25 Hz, 6H), 1.13 (s, 3H), 0.98 (td, J = 7.50, 1.92 Hz, 6H)

^{13}C{^{1}H} NMR (126 MHz, CDCl$_3$) δ 172.5, 146.9, 119.2, 60.1, 35.1, 32.2, 29.2, 28.5, 23.9, 22.2, 20.4, 14.4, 13.2, 12.8.

HRMS (ESI) calc. for C$_{16}$H$_{25}$O$_2$: m/z=225.1849, found: m/z=225.1851

IR (film): 2958, 2930, 2887, 1716, 1458, 1365, 1200, 1150, 1100, 1035, 841 cm^{-1}

7. Procedure for the Dimethylcyclopropanation of Activated Alkenes

General procedure for the dimethylcyclopropanation of activated alkenes. In an N_2-filled glovebox, a 2-dram vial was charged with the [$^{2-tBu}$PDI]CoBr$_2$ catalyst **3** (9.0 mg, 0.014 mmol, 0.10 equiv), the substrate (0.14 mmol, 1.0 equiv), Zn powder (18 mg, 0.28 mmol, 2.0 equiv), ZnBr$_2$ (31 mg, 0.14 mmol, 1.0 equiv), THF (1.0 mL), and a magnetic stir bar. The reaction mixture was stirred at room temperature for approximately 15 min during which time a deep violet color developed. Me$_2$CCl$_2$ (31.6 mg, 0.28 mmol, 2.0 equiv) was added, and stirring was continued at room temperature. After 24 h, the reaction mixture was concentrated under reduced pressure, and the crude residue was directly loaded onto a SiO$_2$ column for purification.

(30). The reaction was conducted using cyclopentene without modification from the general procedure to provide **30** as a colorless oil.

Purification: SiO$_2$ column; pentane

^{1}H NMR Yield. Run 1: 88%; Run 2: 85%

^{1}H NMR (300 MHz, CDCl$_3$) δ 1.85-1.75 (m, 2H), 1.52-1.27 (m, 4H), 1.05 (d, J = 4.3 Hz, 2H), 0.95 (s, 3H), 0.90 (s, 3H).

^{13}C{^{1}H} NMR (126 MHz, CDCl$_3$) δ 31.5, 28.0, 27.8, 25.3, 14.5, 14.1.
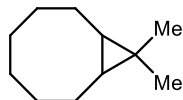
(31). The reaction was conducted using cyclooctene without modification from the general procedure to provide **31** as a colorless oil.

Purification: SiO$_2$ column; pentane

Yield 1: 83%, 17.7 mg; Yield 2: 78%, 16.6 mg

^{1}H NMR (300 MHz, CDCl$_3$) δ 1.76-1.55 (m, 6H), 1.40-1.29 (m, 4H), 1.08-1.02 (m, 1H), 1.01 (s, 3H), 0.99-0.97 (m, 1H), 0.92 (s, 3H), 0.34-0.25 (m, 2H).

^{13}C{^{1}H} NMR (126 MHz, CDCl$_3$) δ 29.7, 29.2, 26.6, 26.5, 22.4, 16.4, 15.1.

HRMS (APCI) calc. for C$_{11}$H$_{20}$: m/z=152.1560, found: m/z=152.1557

IR (film): 2923, 2844, 1452, 1372 cm^{-1}
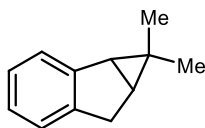
(32). The reaction was conducted using indene without modification from the general procedure to provide **32** as a colorless oil.

Purification: SiO$_2$ column; pentane

Yield 1: 75%, 16.7 mg; Yield 2: 82%, 18.3 mg

^{1}H NMR (300 MHz, CDCl$_3$) δ 7.24-7.22 (m, 1H), 7.12-7.07 (m, 3H), 3.10 (dd, J = 17.43, 7.26 Hz, 1H), 2.77 (d, J = 17.40 Hz, 1H), 2.24 (dd, J = 6.36, 1.23 Hz, 1H), 1.60 (t, J = 6.86 Hz, 1H), 1.16 (s, 3H) 0.63 (s, 3H).

^{13}C{^{1}H} NMR (126 MHz, CDCl$_3$) δ 145.0, 143.8, 125.8, 125.2, 124.3, 124.0, 37.2, 32.0, 29.1, 26.8, 21.4, 13.8.

HRMS (ESI) calc. for C$_{12}$H$_{15}$: m/z=159.1168, found: m/z=159.1166

IR (film): 3023, 2944, 2908, 2858, 1480, 1372, 1114, 884 cm^{-1}

(33). The reaction was conducted using norbornene without modification from the general procedure to provide **33** as a colorless oil.

Purification: SiO$_2$ column; pentane

Yield 1:66%, 12.7 mg; Yield 2: 67%, 12.8 mg

^{1}H NMR (300 MHz, CDCl$_3$) δ 2.32 (s, 2H), 1.46-1.35 (m, 3H), 1.25-1.19 (m, 2H), 1.17 (s, 3H), 0.88 (s, 3H), 0.64 (d, J = 10.64 Hz, 1H), 0.43 (s, 2H).

^{13}C{^{1}H} NMR (126 MHz, CDCl$_3$) δ 36.0, 31.1, 31.0, 30.8, 30.5, 18.6, 16.1.

HRMS (APCI) calc. for C$_{10}$H$_{17}$: m/z=137.1325, found: m/z=137.1320

IR (film): 2958, 2908, 2844, 1444 cm^{-1}
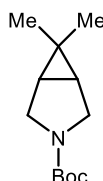
(35). The reaction was conducted using *N*-Boc-2,5-dihydro-1*H*-pyrrole without modification from the general procedure to provide **35** as a yellow oil.

Run 1: 26.2 mg (89% yield). Run 2: 26.6 mg (91% yield).

Purification: SiO$_2$ column; Hexane/EtOAc (80:20)

^{1}H NMR (300 MHz, CDCl$_3$) δ 3.48-3.38 (m, 2H), 3.35-3.24 (m, 2H), 1.42 (s, 9H), 1.29-1.27 (m, 2H), 1.00 (s, 3H), 0.90 (s, 3H).

^{13}C{^{1}H} NMR (126 MHz, CDCl$_3$) δ 153.9, 79.0, 46.1, 45.9, 28.5, 27.9, 27.1, 26.3, 18.9, 12.4.

HRMS (ESI) calc. for C$_{12}$H$_{21}$NO$_2$Na: m/z=234.1465, found: m/z=234.1467

IR (film): 2966, 2930, 2880, 1702, 1409, 1379, 1178, 1107, 870 cm^{-1}
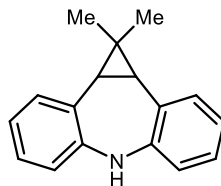
(37). The reaction was conducted using iminostilbene without modification from the general procedure to provide **37** as a white solid.

Run 1: 30.6 mg (93% yield). Run 2: 32.5 mg (99% yield).

Purification: SiO_2 column; hexane/EtOAc (95:5)

^{1}H NMR (300 MHz, CDCl$_3$) δ 7.27 (dd, J = 7.44, 1.18, Hz, 2H), 7.07 (td, J = 7.66, 1.67 Hz, 2H), 6.92 (td, J = 7.44, 1.28 Hz, 2H), 6.81 (dd, J = 7.93, 1.26 Hz, 2H), 5.55 (br s, 1H), 2.30 (s, 2H), 1.50 (s, 3H), 0.59 (s, 3H).

^{13}C{^{1}H} NMR (100 MHz, CDCl$_3$) δ 144.0, 133.3, 126.4, 125.7, 121.0, 119.5, 30.9, 28.7, 27.8, 18.5.

HRMS (ESI) calc. for $C_{17}H_{18}N$: m/z=236.1434, found: m/z=236.1436

IR (film): 3367, 2966, 2937, 2865, 1587, 1480, 1329, 1250, 1107, 1028, 913 cm^{-1}

m.p.: 133-136°C
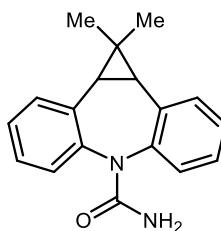
(38). The reaction was conducted using **37** under previously reported conditions[29] to provide **38** as a white solid.

Run 1: 23.3 mg (64% yield)

Purification: SiO_2 column; 100% EtOAc

^{1}H NMR (300 MHz, DMSO-d$_6$) δ 7.28-7.25 (m, 2H), 7.24-7.21 (m, 4H), 7.19-7.14 (m, 2H), 5.65 (br s, 2H), 2.20 (s, 2H), 1.40 (s, 3H), 0.42 (s, 3H).

^{13}C{^{1}H} NMR (100 MHz, DMSO-d$_6$) δ 157.5, 143.5, 135.4, 132.7, 129.3, 127.8, 127.4, 28.6, 28.1, 19.6, 19.0.

HRMS (ESI) calc. for $C_{18}H_{19}N_2O$: m/z=279.1492, found: m/z=279.1491

IR (film): 3475, 3318, 3203, 2930, 1673, 1581, 1480, 1393, 920 cm^{-1}

m.p.: 176-177 °C

8. NMR Spectra
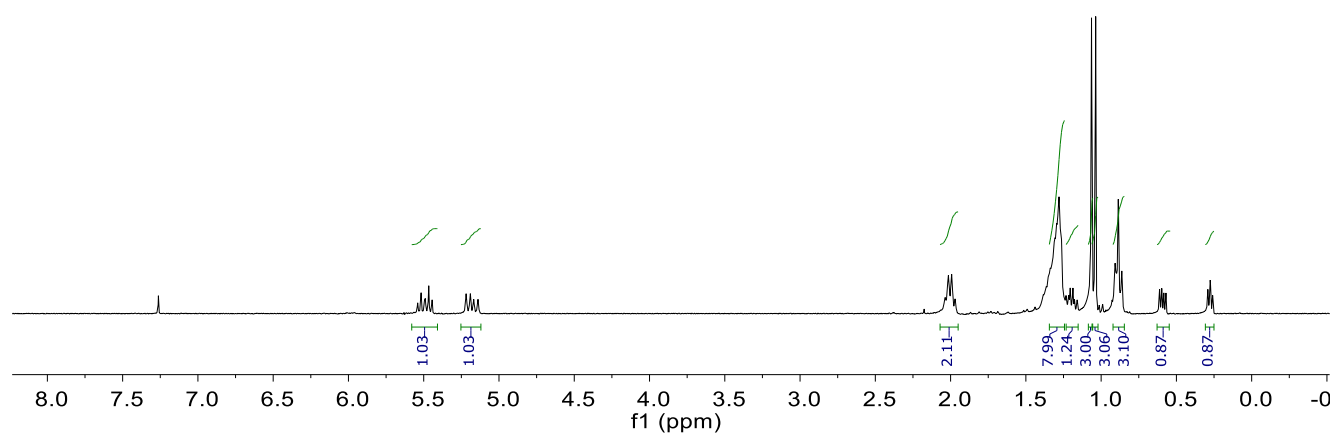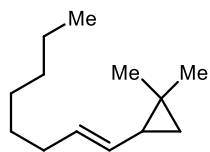
Figure S6. ^{1}H NMR spectrum for **2** (CDCl$_3$, 295 K)
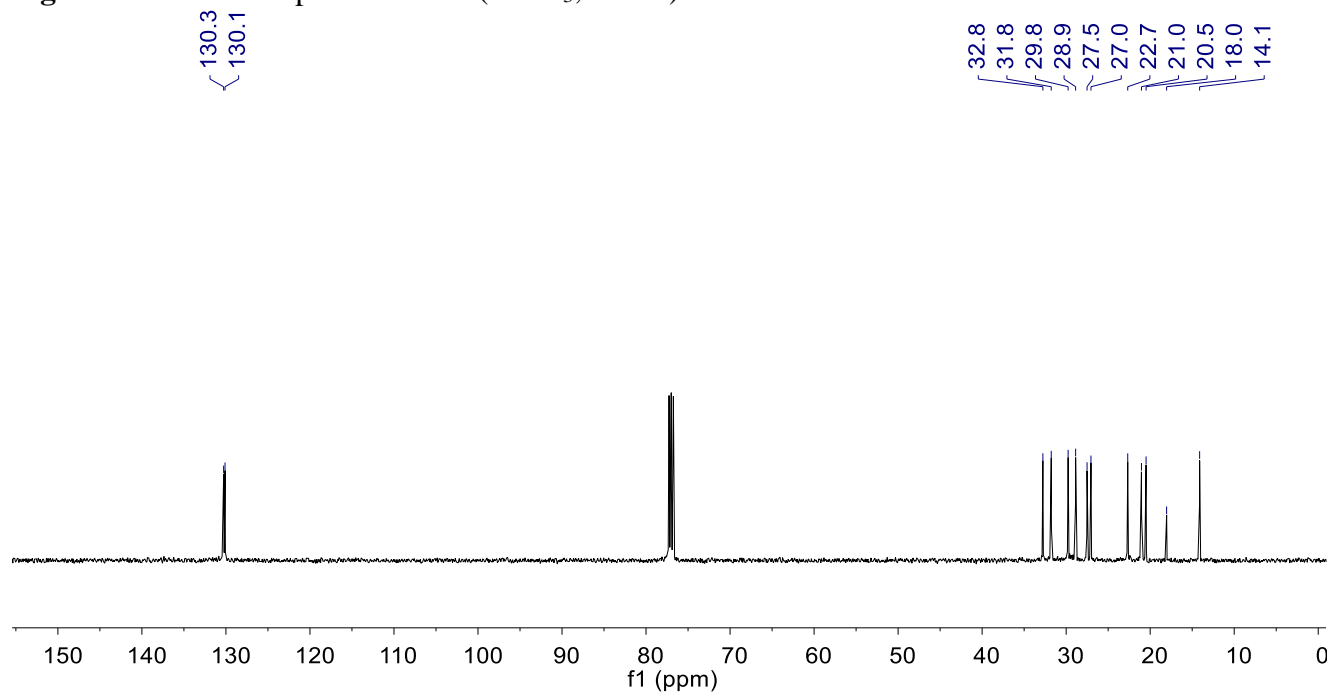
Figure S7. ^{13}C{^{1}H} NMR spectrum for **2** (CDCl$_3$, 295 K)
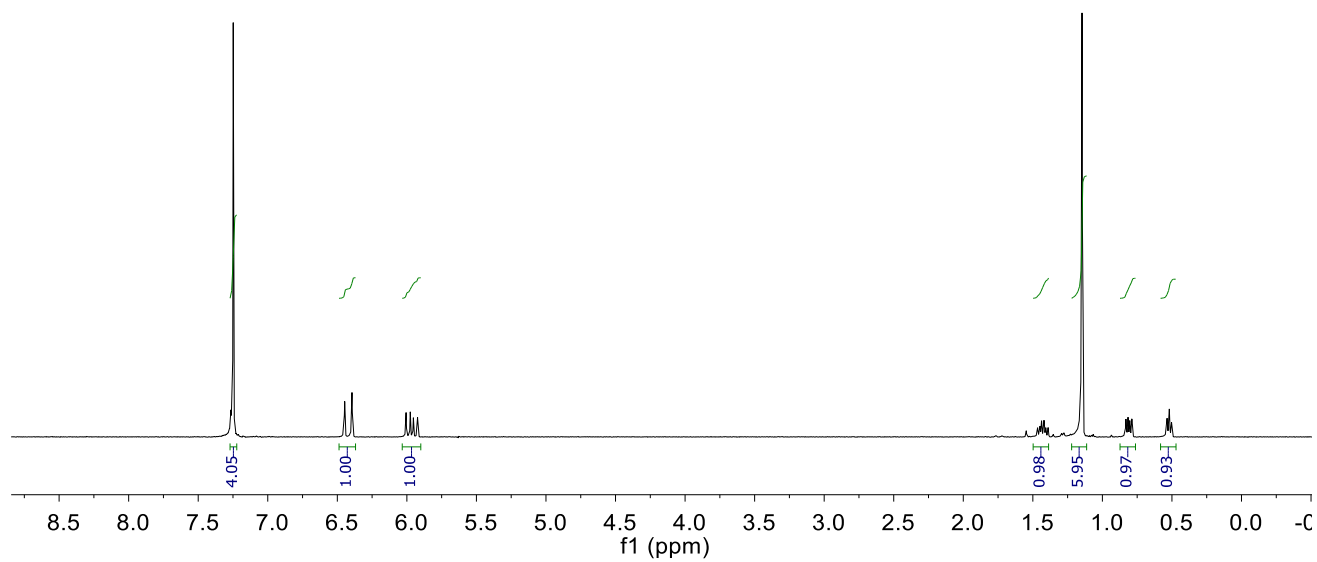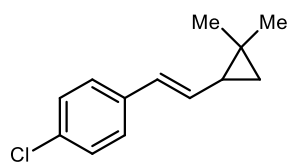
Figure S8: ^{1}H NMR spectrum for **4** (CDCl$_3$, 295 K)
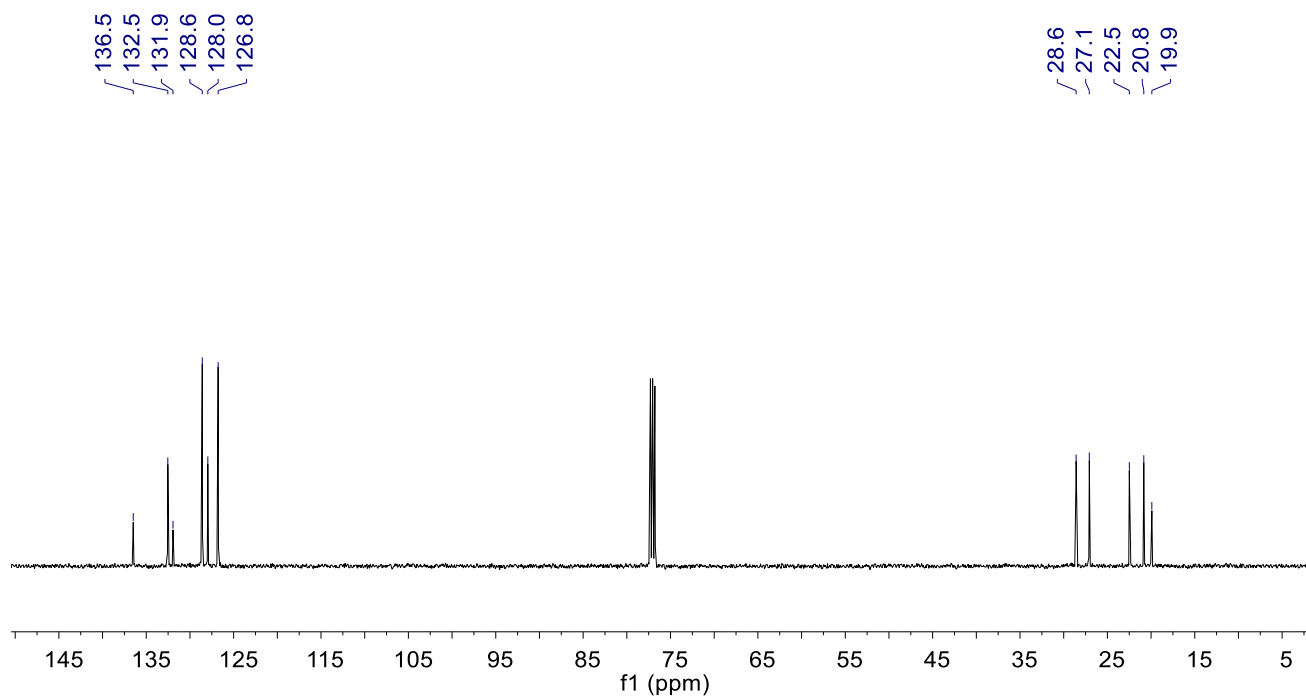
Figure S9: ^{13}C{^{1}H} NMR spectrum for **4** (CDCl$_3$, 295 K)
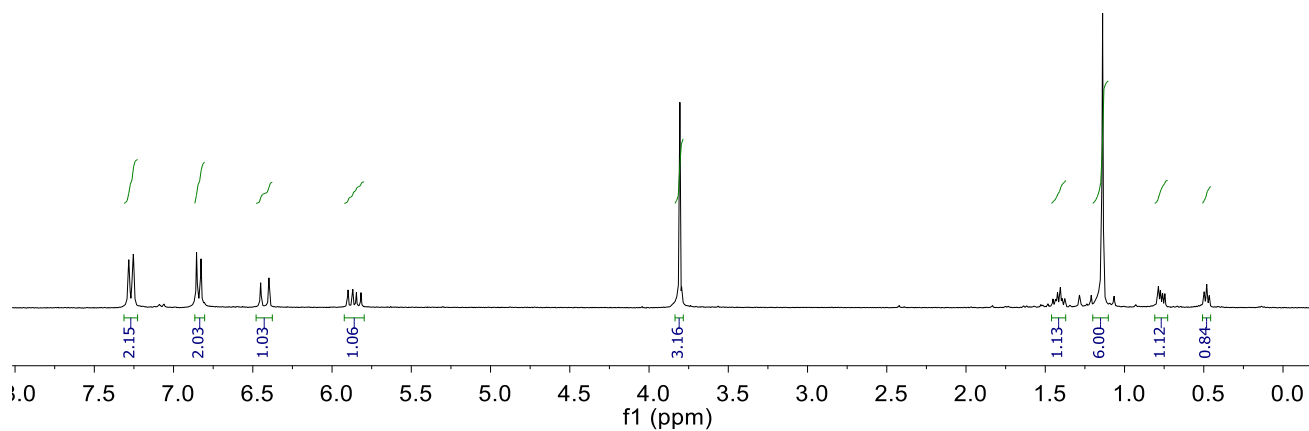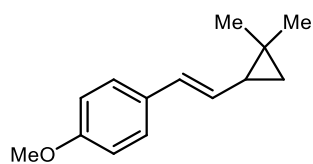
Figure S10: ^{1}H NMR spectrum for **5** (CDCl$_3$, 295 K)
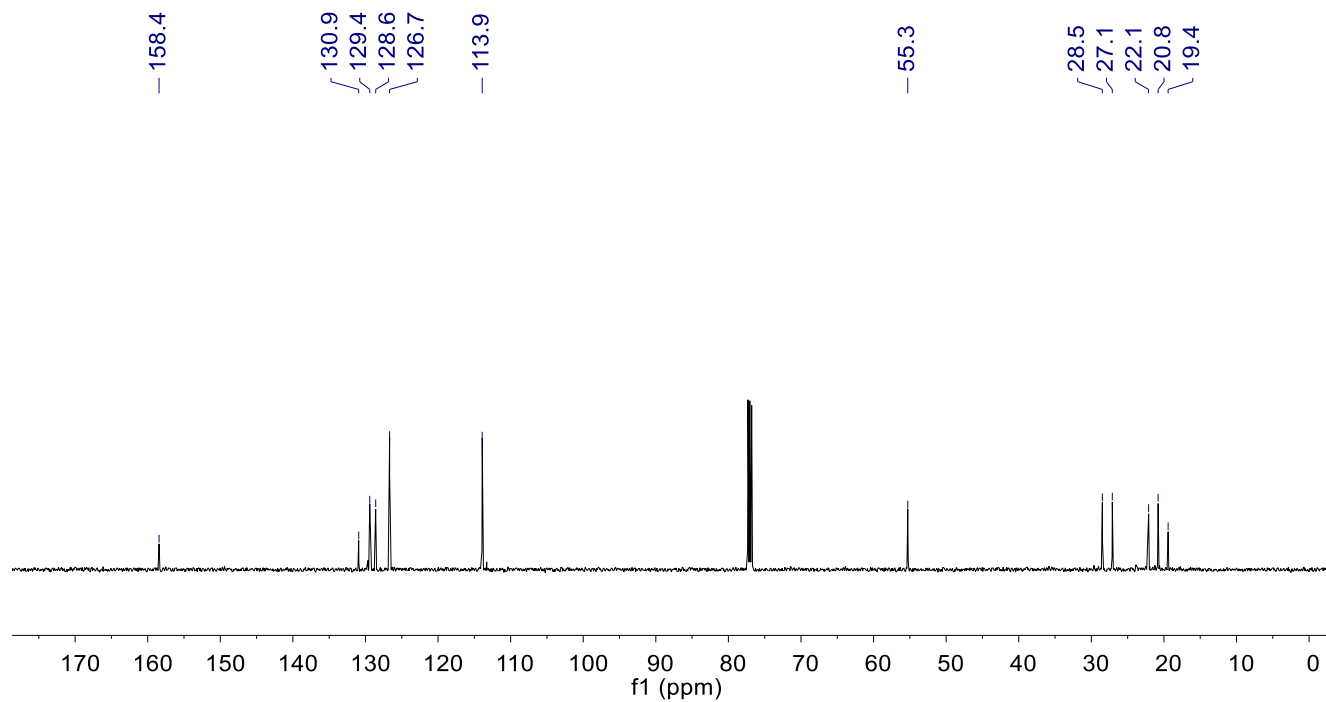
Figure S11: ^{13}C{^{1}H} NMR spectrum for **5** (CDCl$_3$, 295 K)
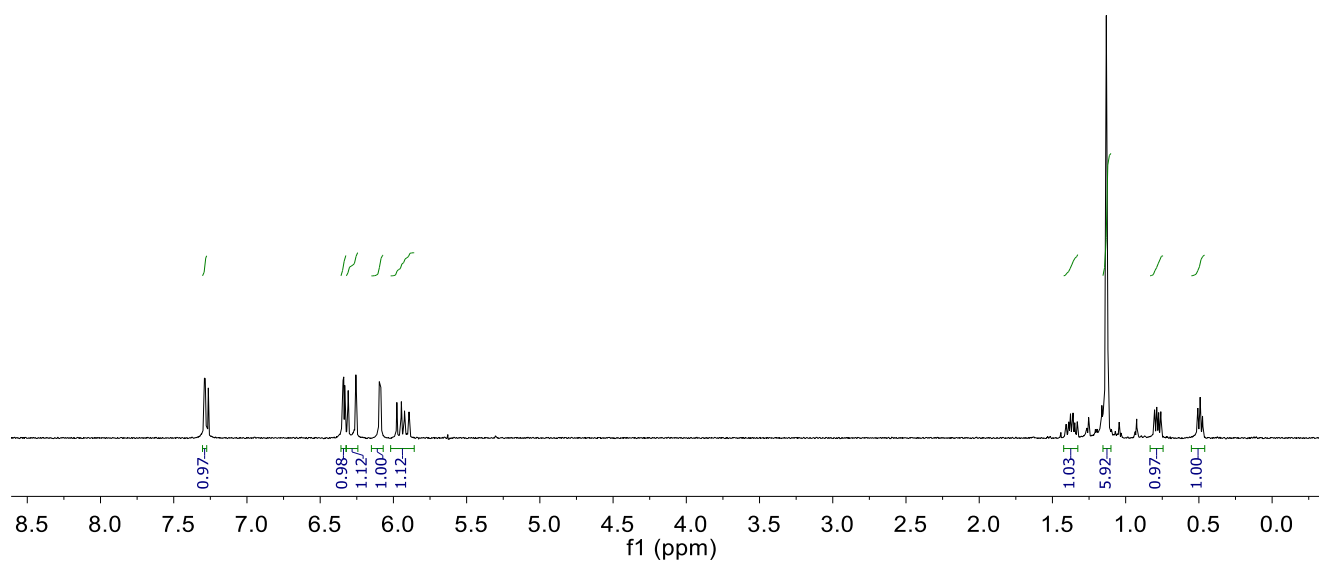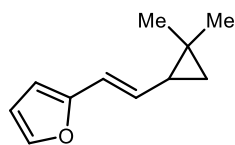
Figure S12: ^{1}H NMR spectrum for **6** (CDCl$_3$, 295 K)
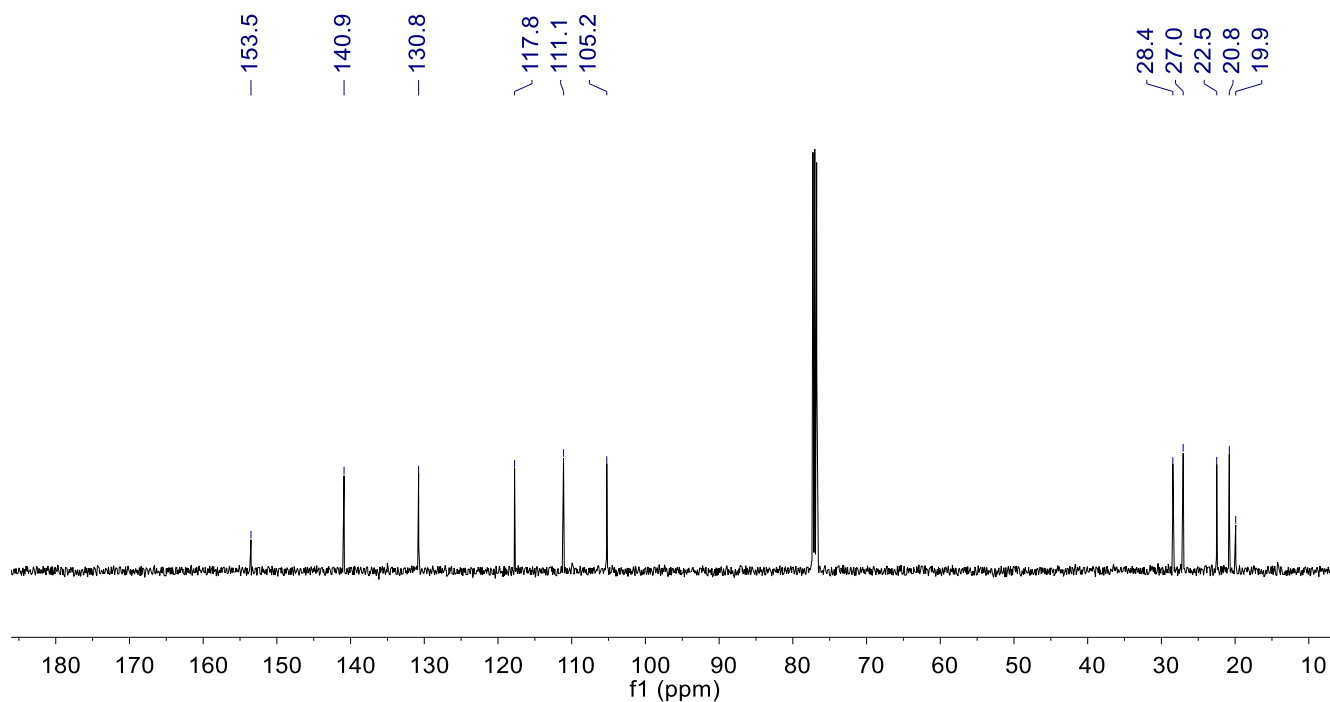
Figure S13: ^{13}C{^{1}H} NMR spectrum for **6** (CDCl$_3$, 295 K)
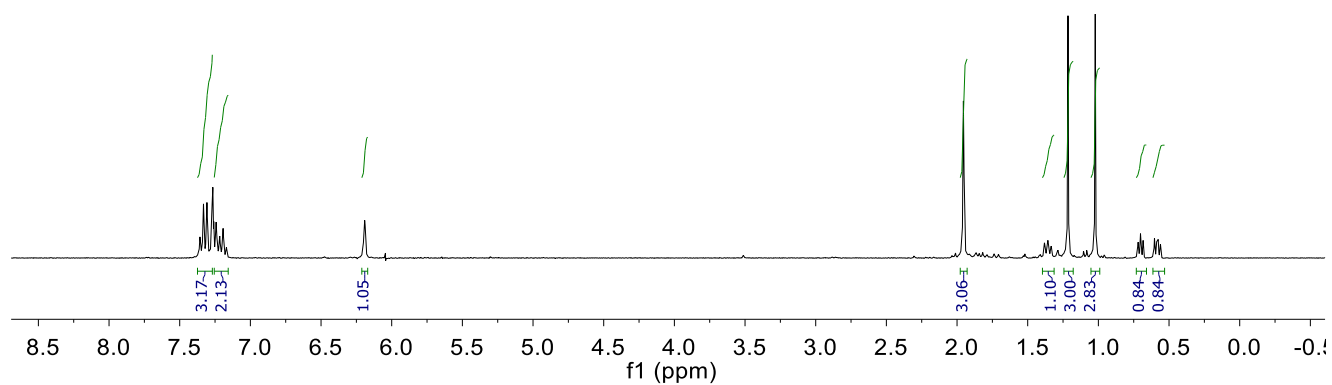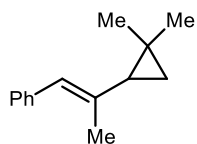
Figure S14: ^{1}H NMR spectrum for **7** (CDCl$_3$, 295 K)
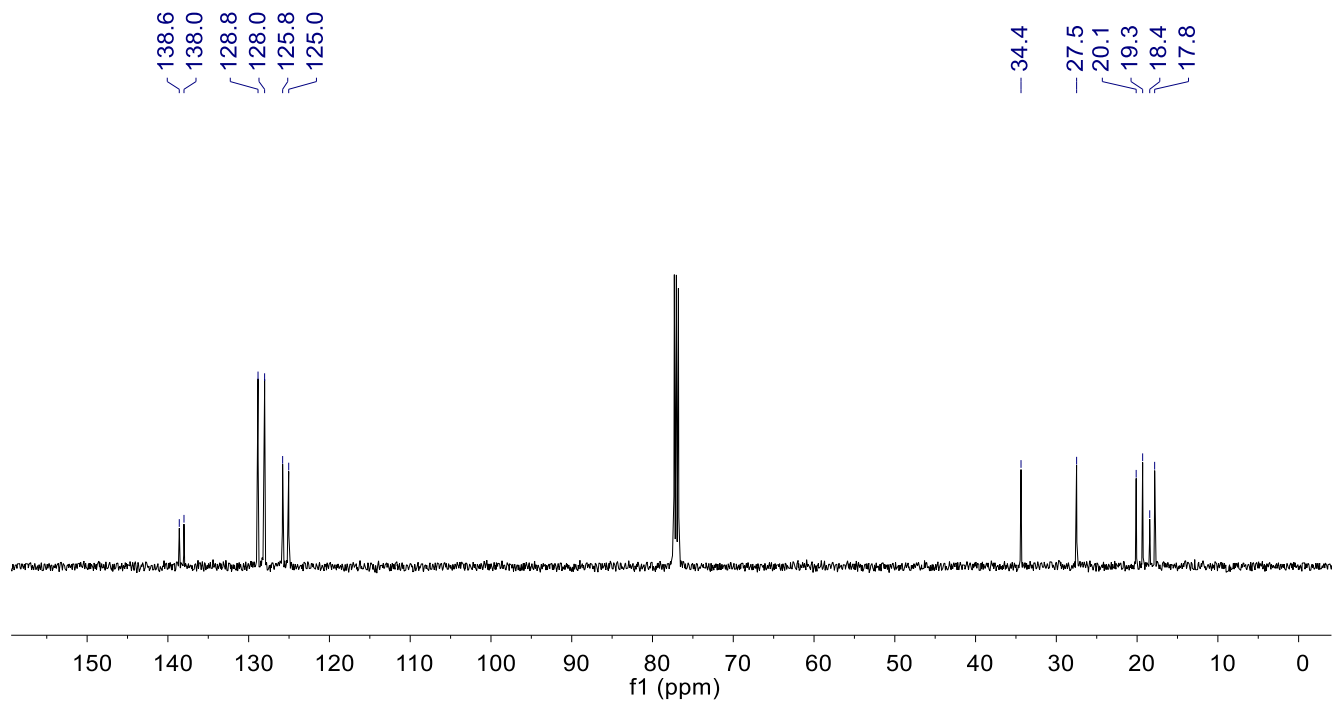
Figure S15: ^{13}C{^{1}H} NMR spectrum for **7** (CDCl$_3$, 295 K)
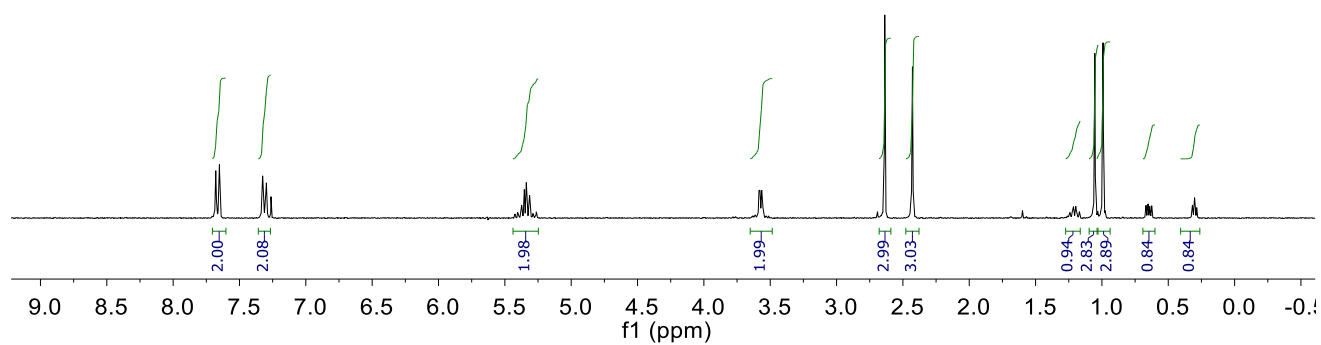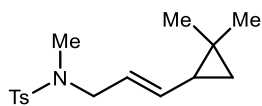
Figure S16: ^{1}H NMR spectrum for **8** (CDCl$_3$, 295 K)
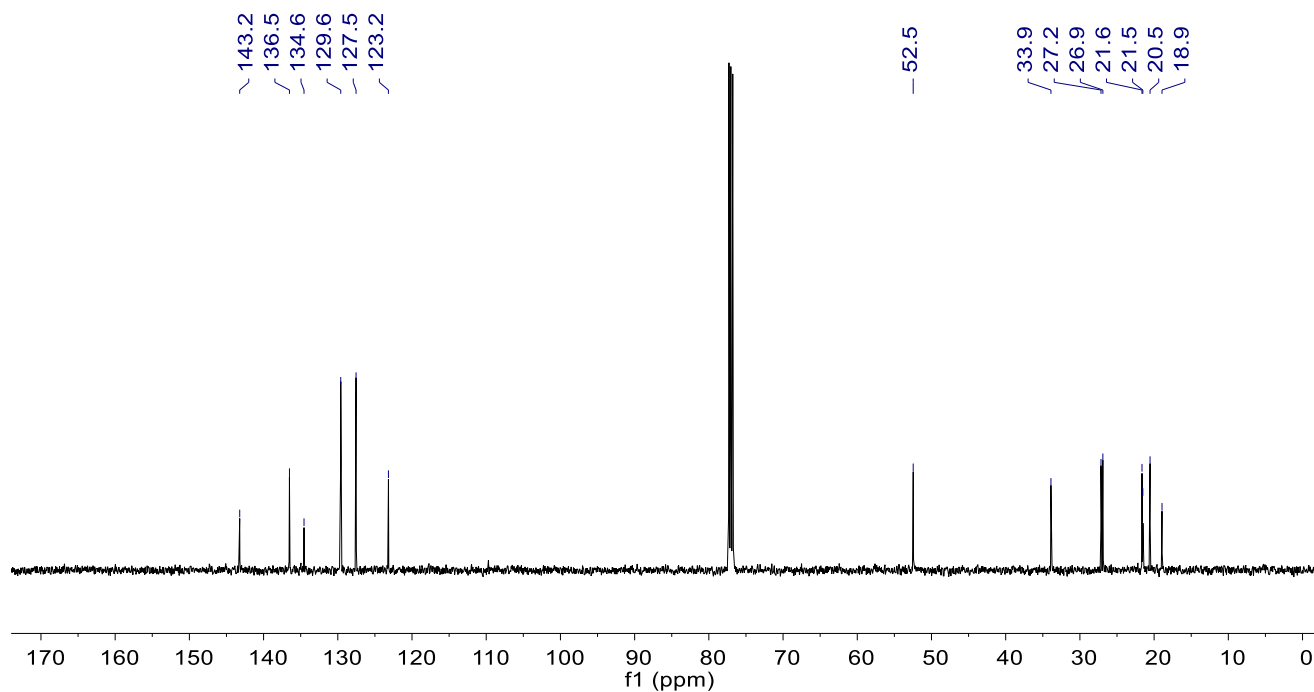
Figure S17: ^{13}C{^{1}H} NMR spectrum for **8** (CDCl$_3$, 295 K)
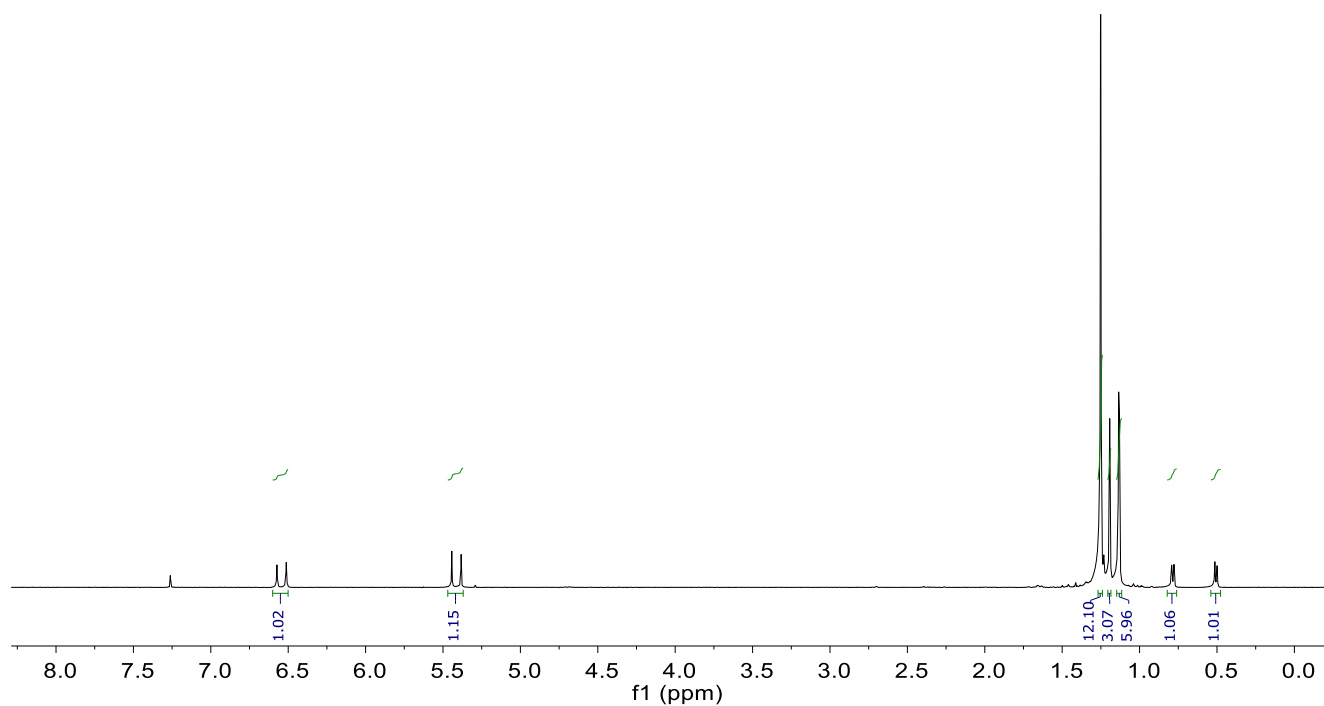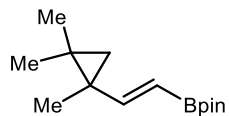
Figure S18: ^{1}H NMR spectrum for **9** (CDCl$_3$, 295 K)
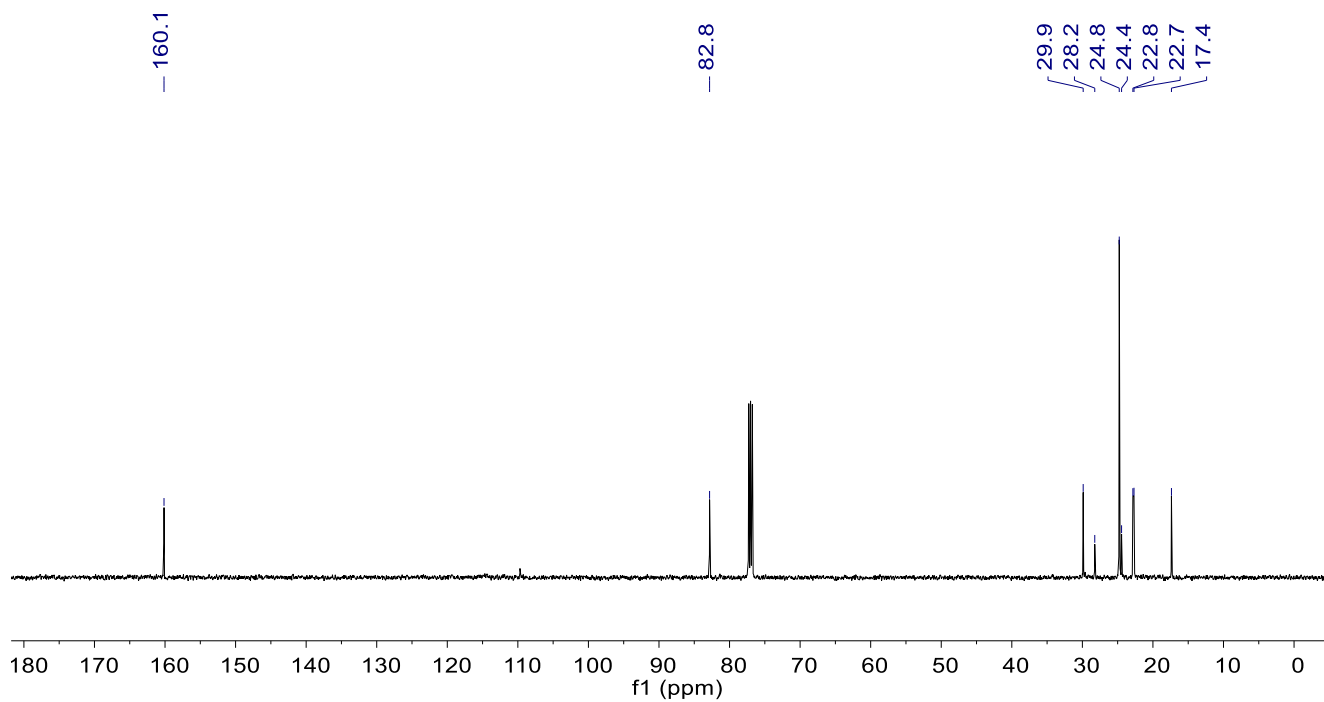
Figure S19: ^{13}C{^{1}H} NMR spectrum for **9** (CDCl$_3$, 295 K)

29.8
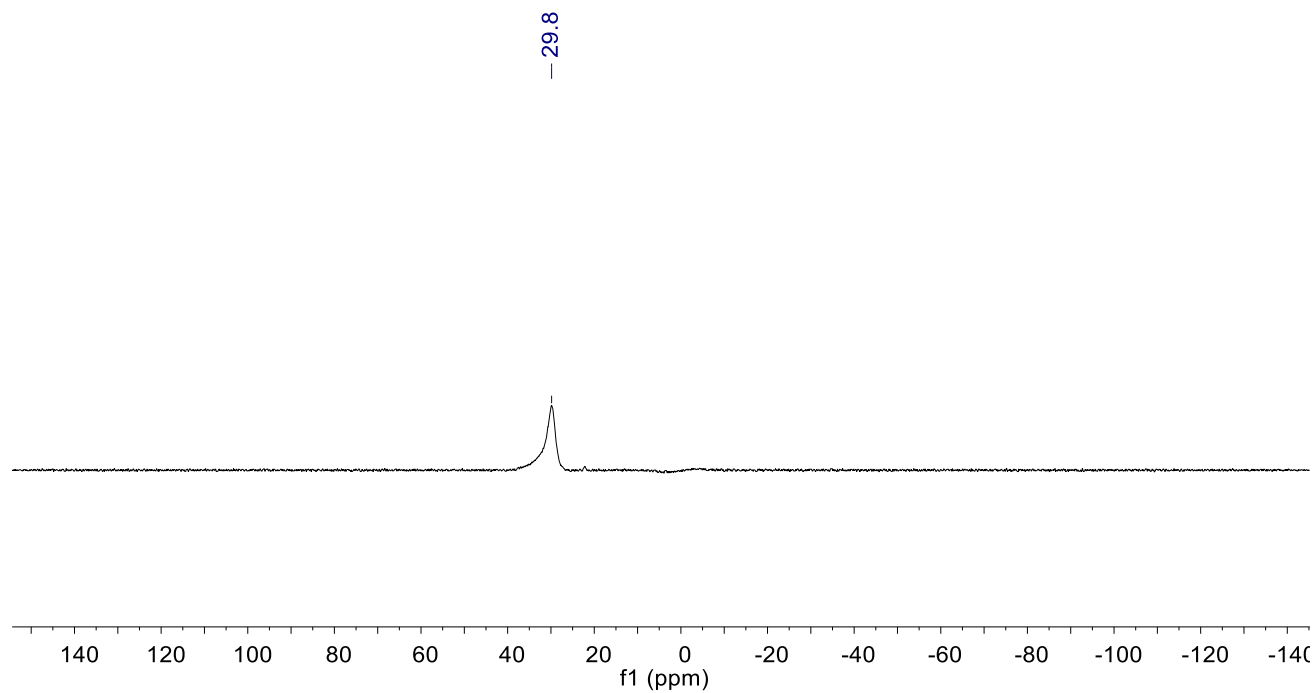
**Figure S20**: ^{11}B NMR spectrum for **9** (CDCl$_3$, 295 K)
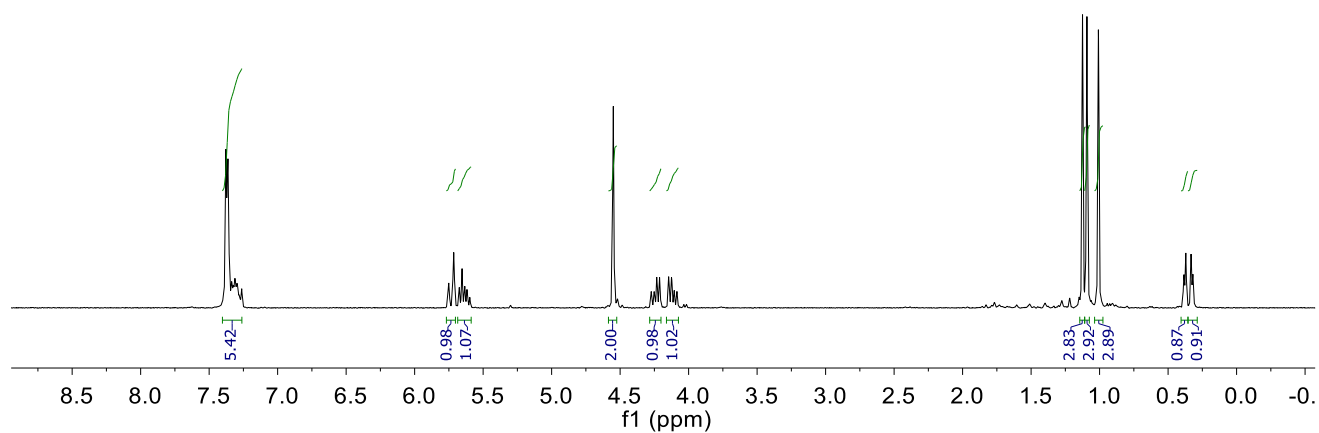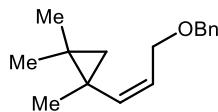
**Figure S21**: ^{1}H NMR spectrum for **10** (CDCl$_3$, 295 K)
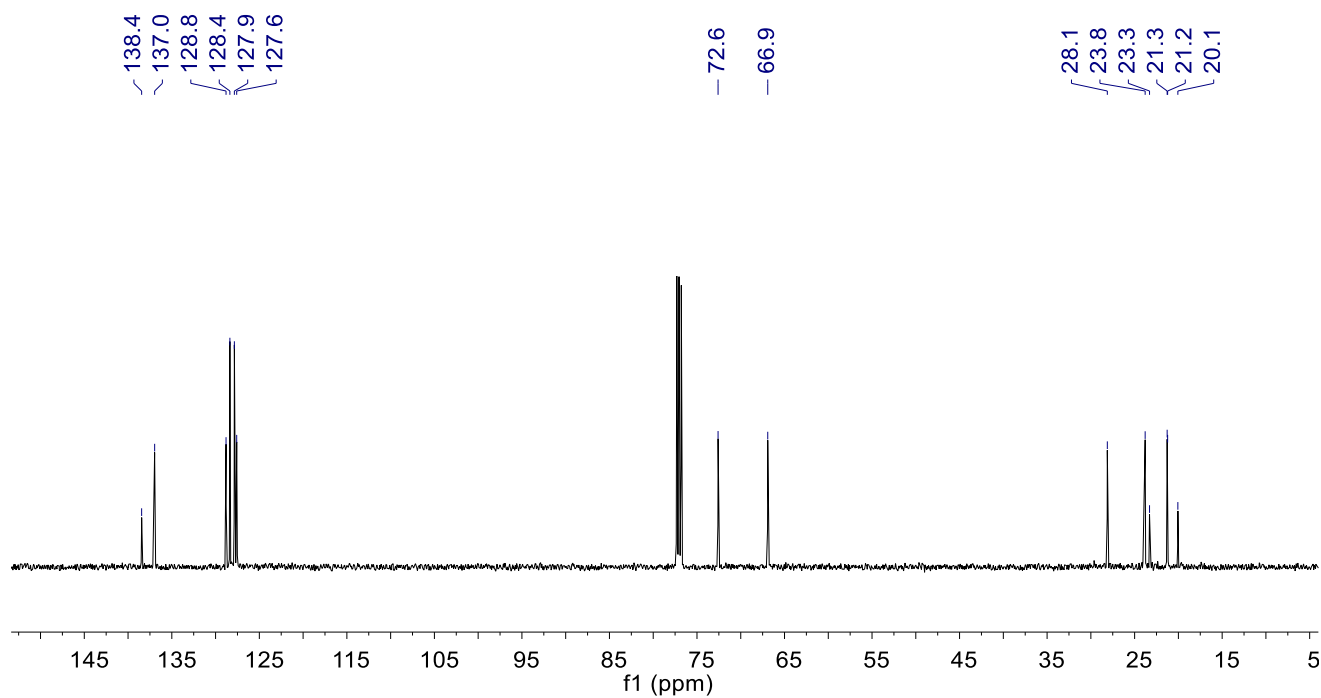
Figure S22: ^{13}C{^{1}H} NMR spectrum for **10** (CDCl$_3$, 295 K)
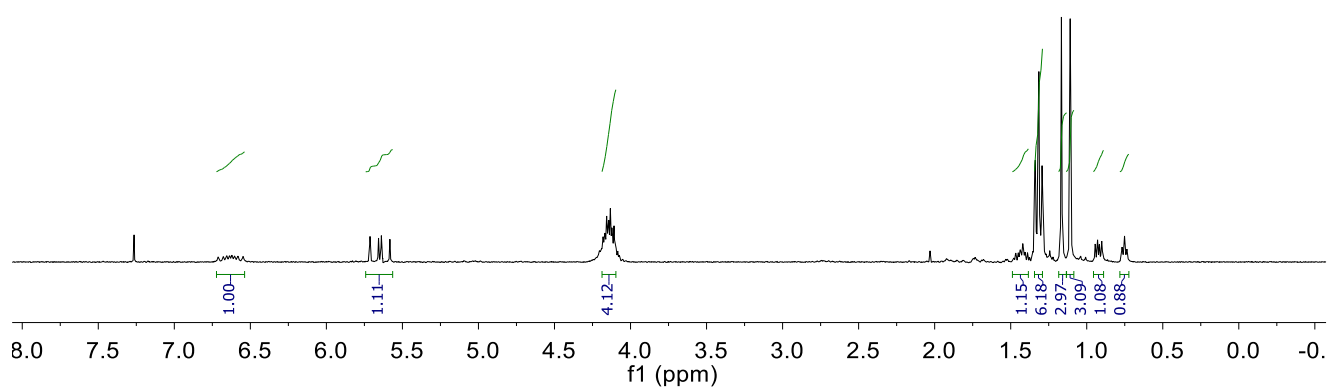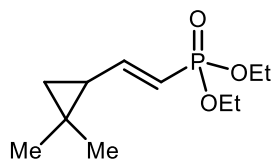
Figure S23: ^{1}H NMR spectrum for **11** (CDCl$_3$, 295 K)
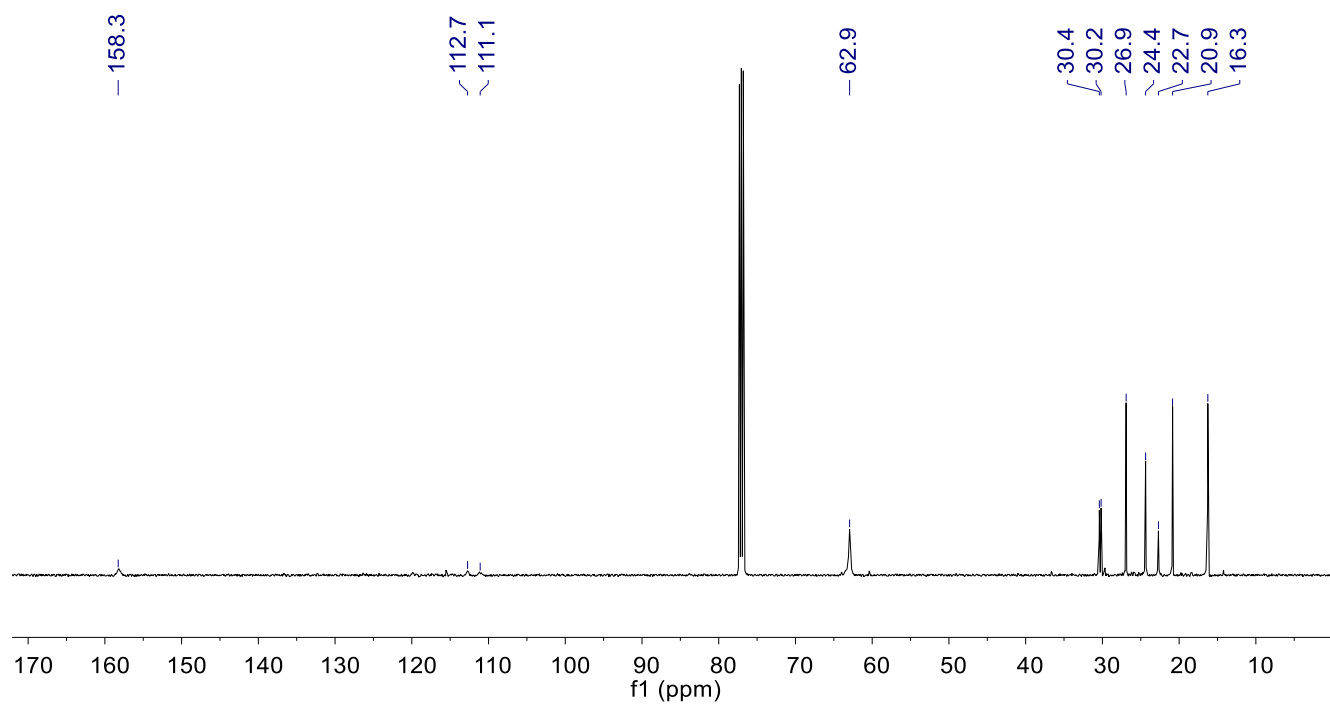
Figure S24: ^{13}C{^{1}H} NMR spectrum for **11** (CDCl$_3$, 295 K)
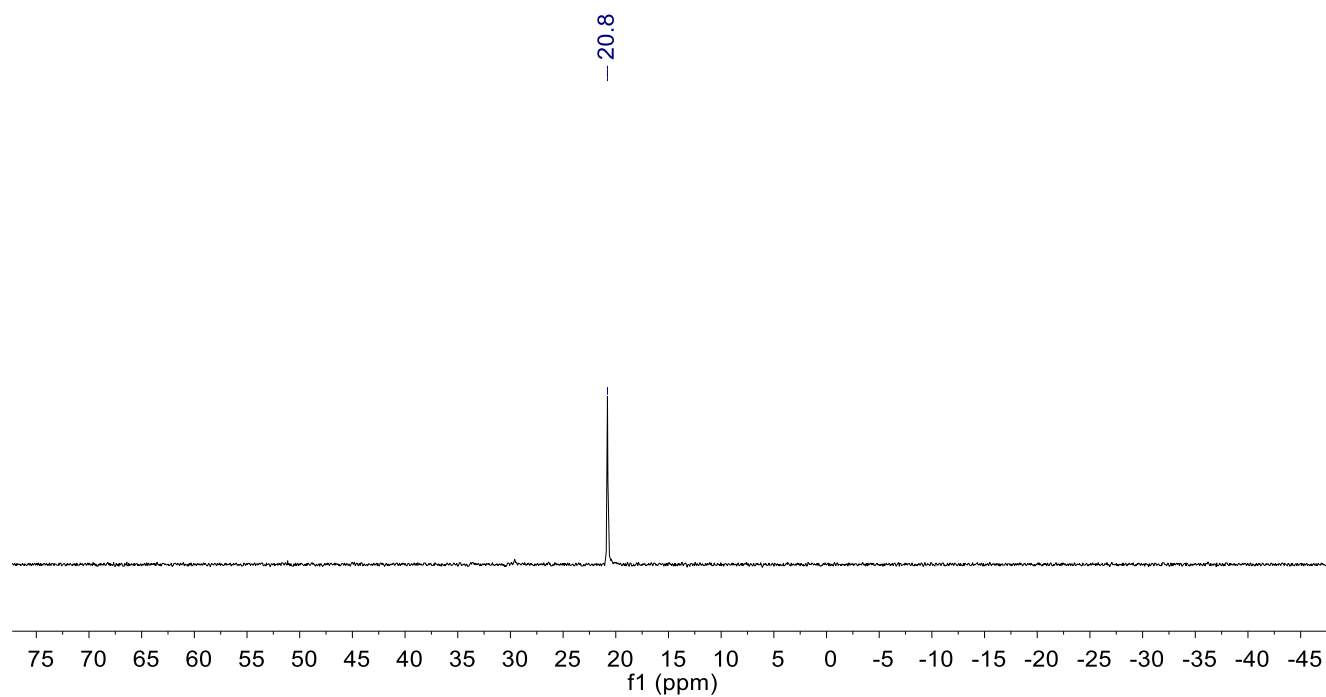
Figure S25: ^{31}P NMR spectrum for **11** (CDCl$_3$, 295 K)
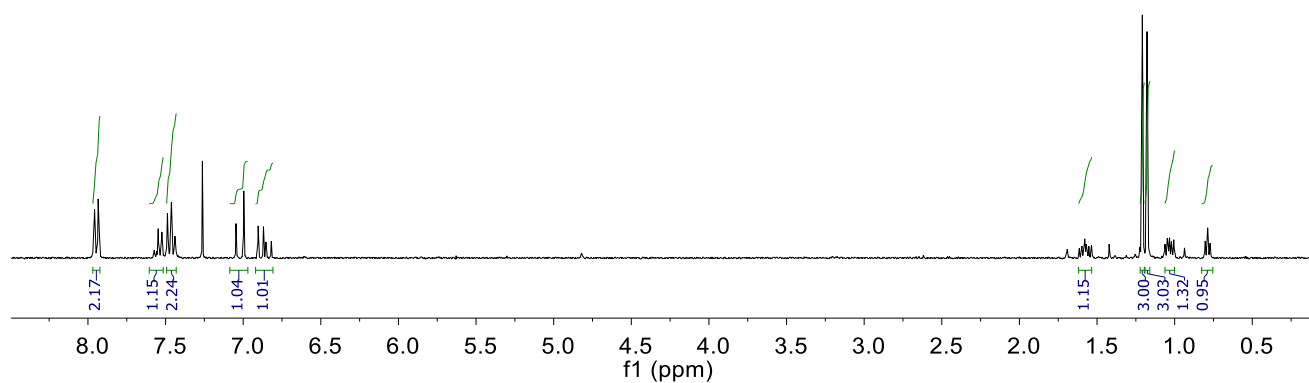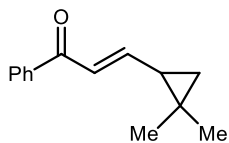
Figure S26: ^{1}H NMR spectrum for **12** (CDCl$_3$, 295 K)
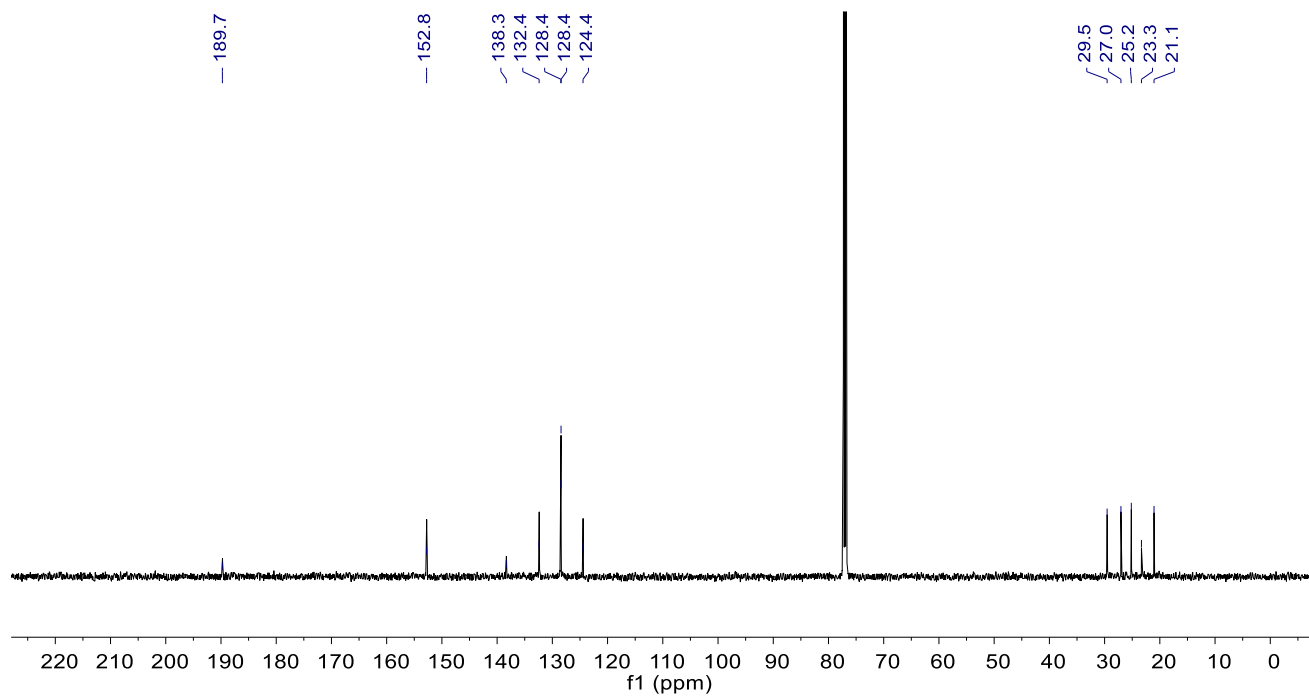
Figure S27: ^{13}C{^{1}H} NMR spectrum for **12** (CDCl$_3$, 295 K)
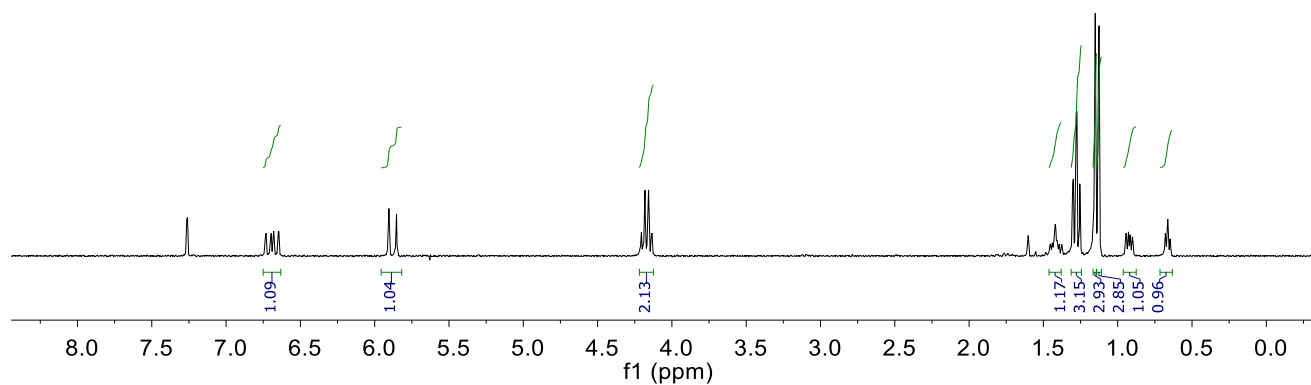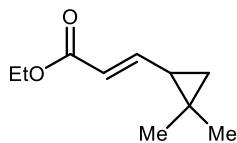
Figure S28: ^{1}H NMR spectrum for **13** (CDCl$_3$, 295 K)
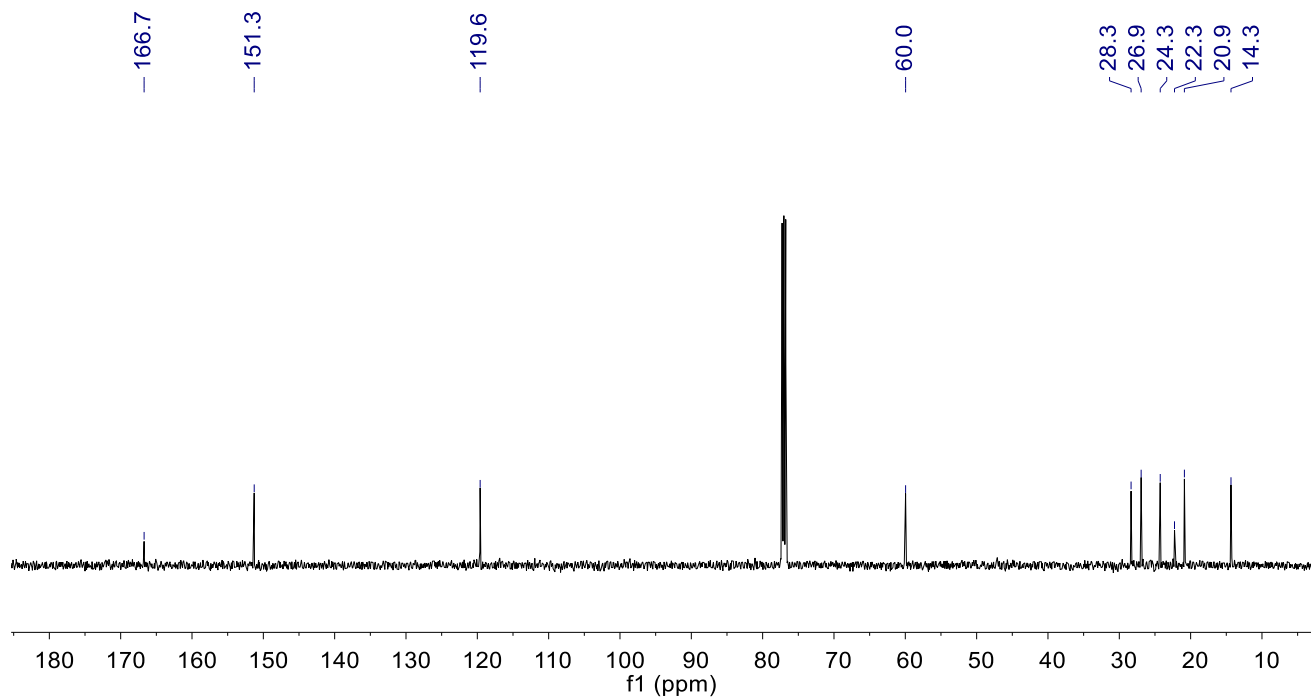
**Figure S29**: ^{13}C{^{1}H} NMR spectrum for **13** (CDCl$_3$, 295 K)
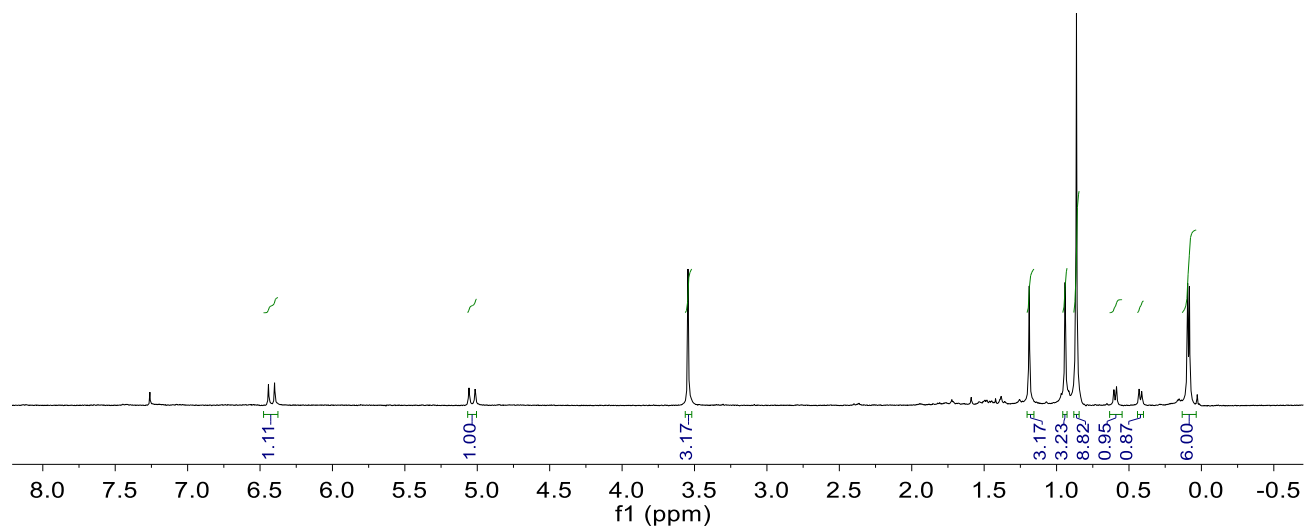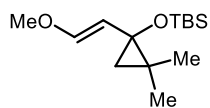
Figure S30: ^{1}H NMR spectrum for **14** (CDCl$_3$, 295 K)
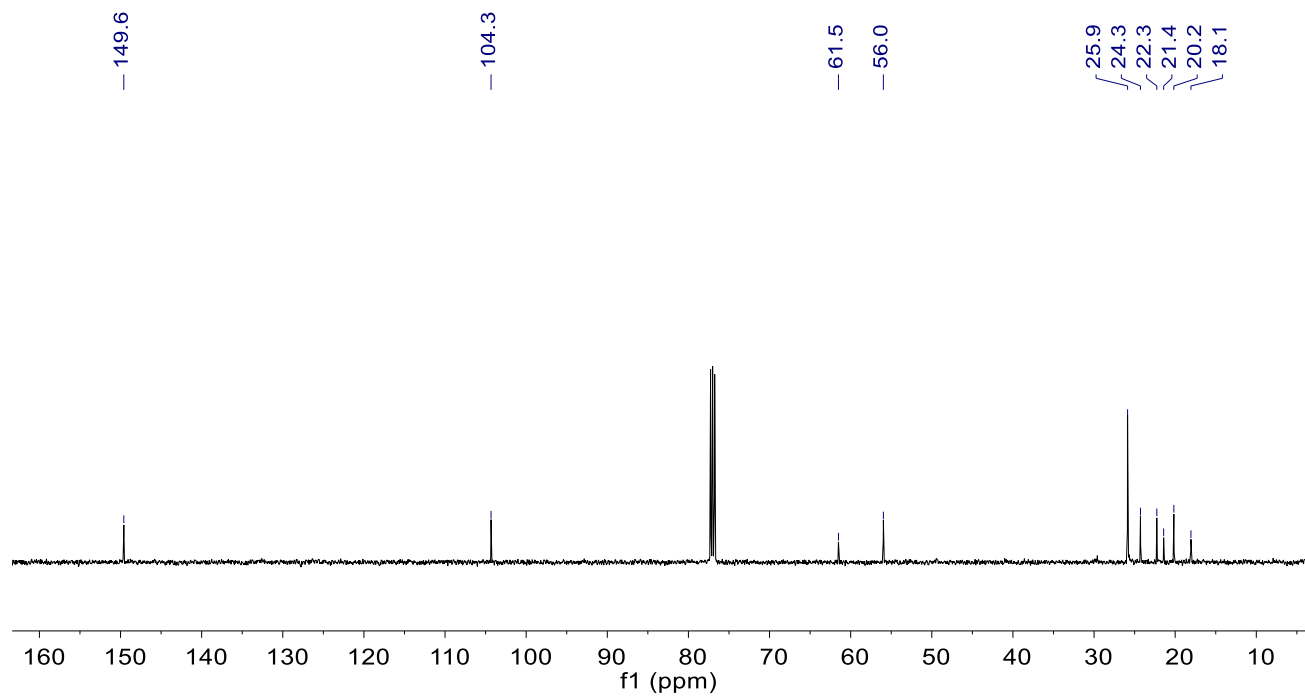
Figure S31: ^{13}C{^{1}H} NMR spectrum for **14** (CDCl$_3$, 295 K)
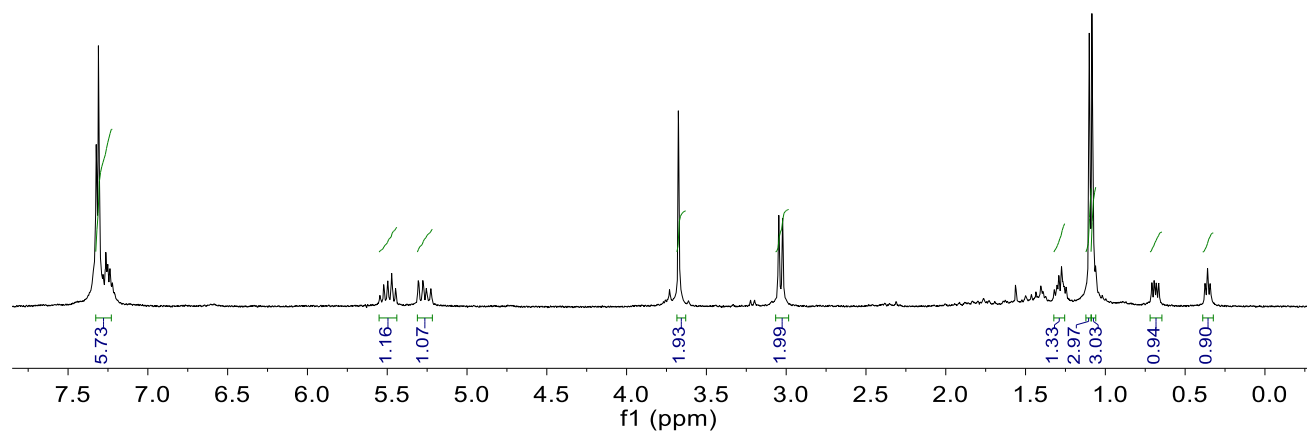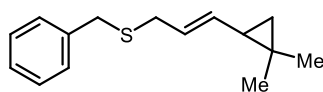
Figure S32: ^{1}H NMR spectrum for **15** (CDCl$_3$, 295 K)
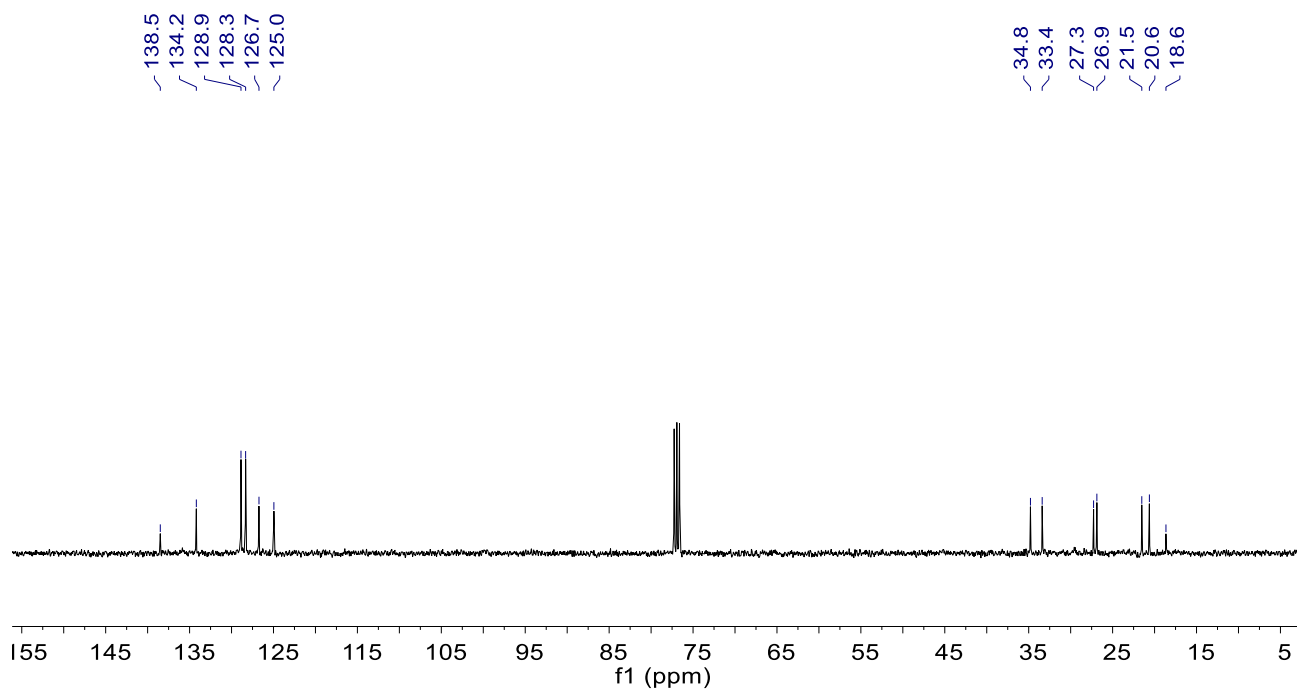
Figure S33: ^{13}C{^{1}H} NMR spectrum for **15** (CDCl$_3$, 295 K)
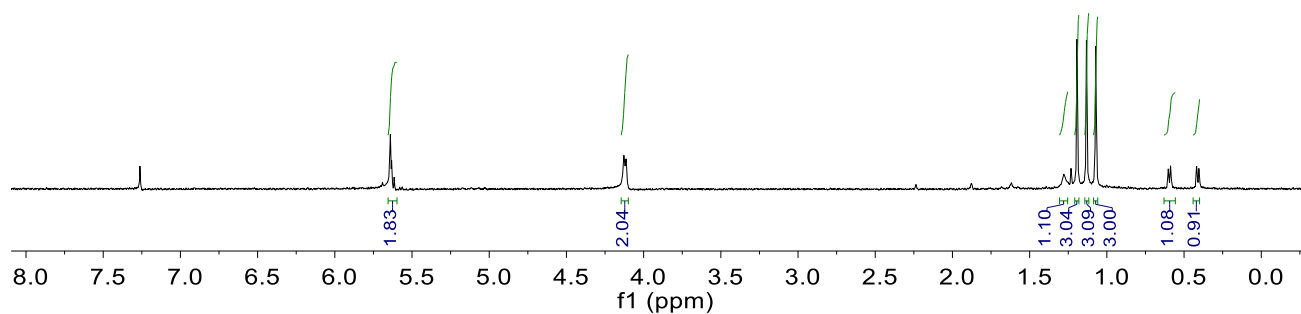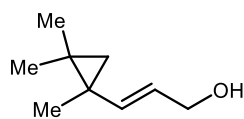
Figure S34: ^{1}H NMR spectrum for **18** (CDCl$_3$, 295 K)
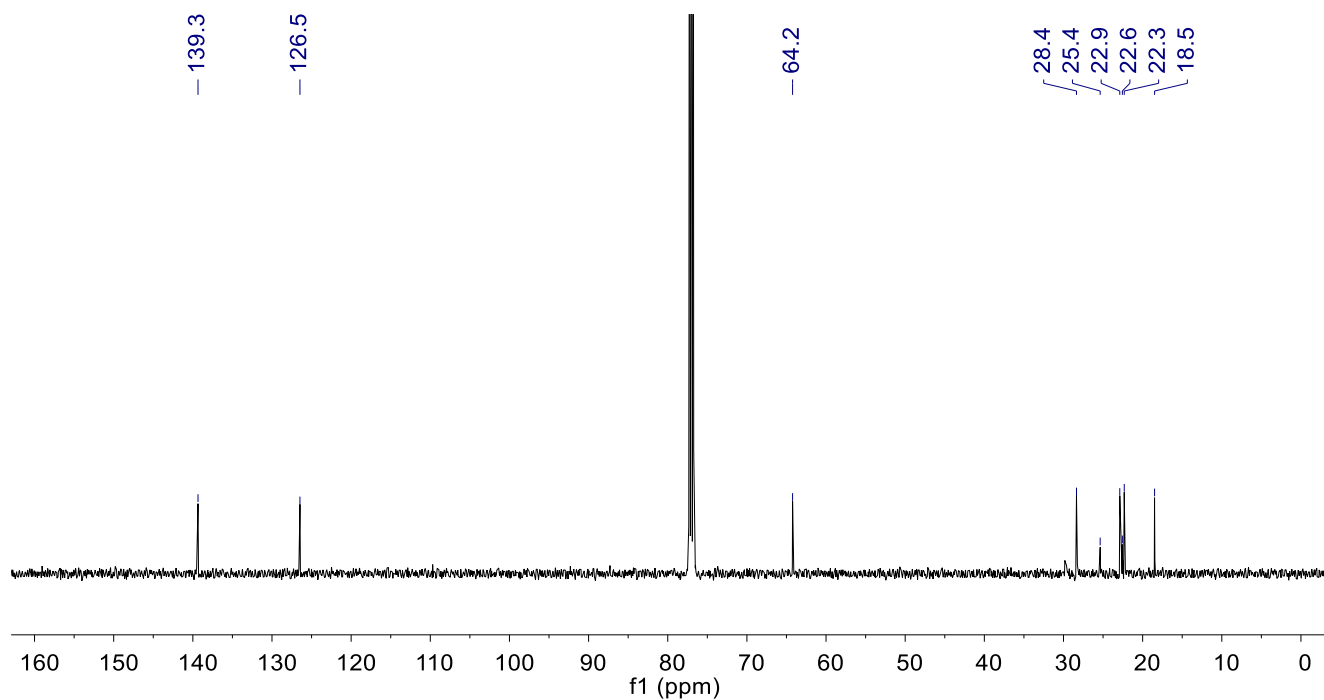
Figure S35: ^{13}C{^{1}H} NMR spectrum for **18** (CDCl$_3$, 295 K)
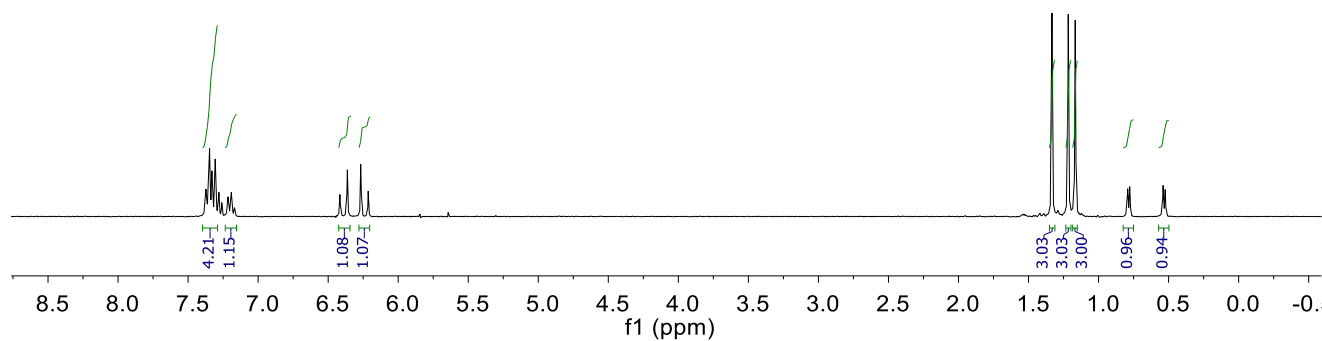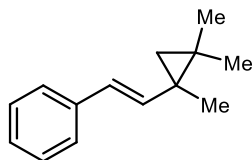
Figure S36: ^{1}H NMR spectrum for **26** (CDCl$_3$, 295 K)
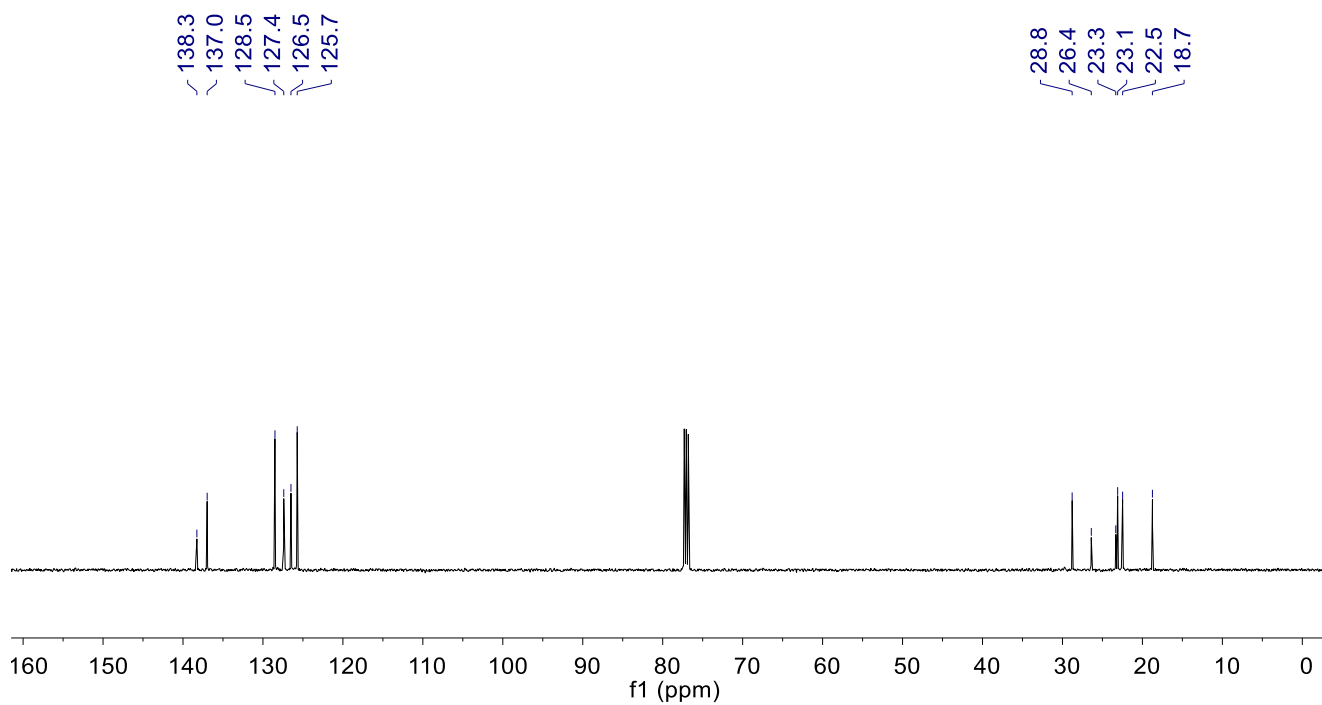
Figure S37: ^{13}C{^{1}H} NMR spectrum for **26** (CDCl$_3$, 295 K)
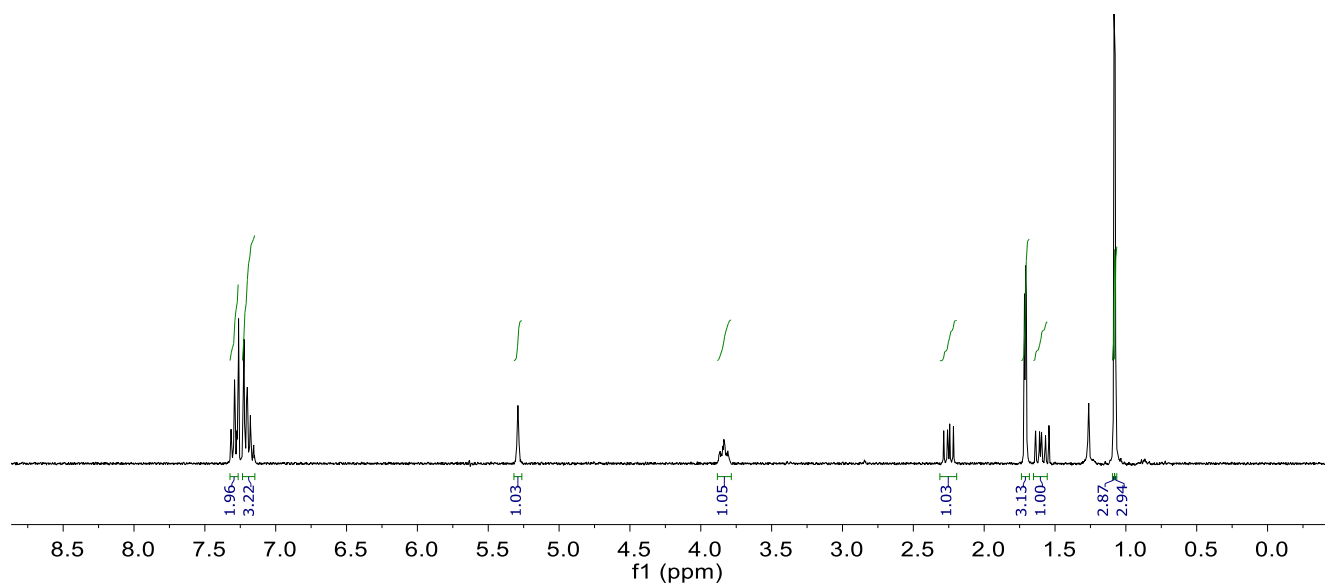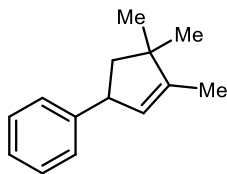
Figure S38: ^{1}H NMR spectrum for **27** (CDCl$_3$, 295 K)
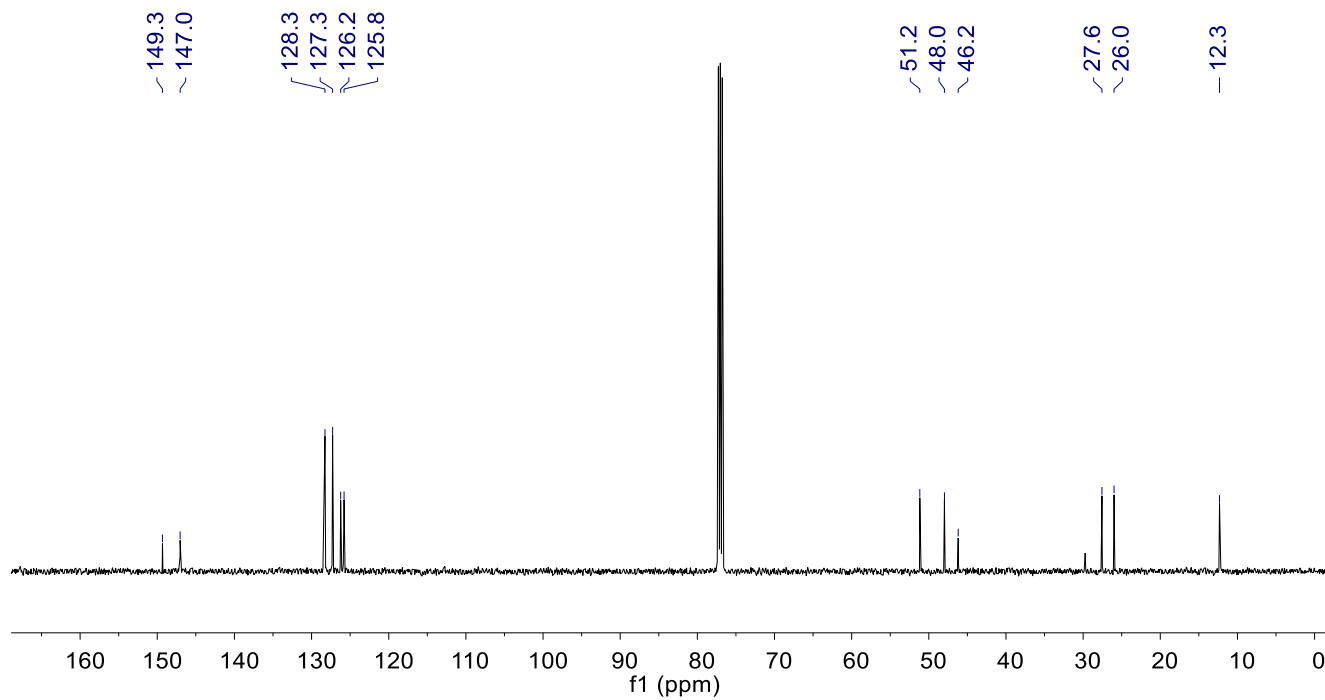
Figure S39: ^{13}C{^{1}H} NMR spectrum for **27** (CDCl$_3$, 295 K)
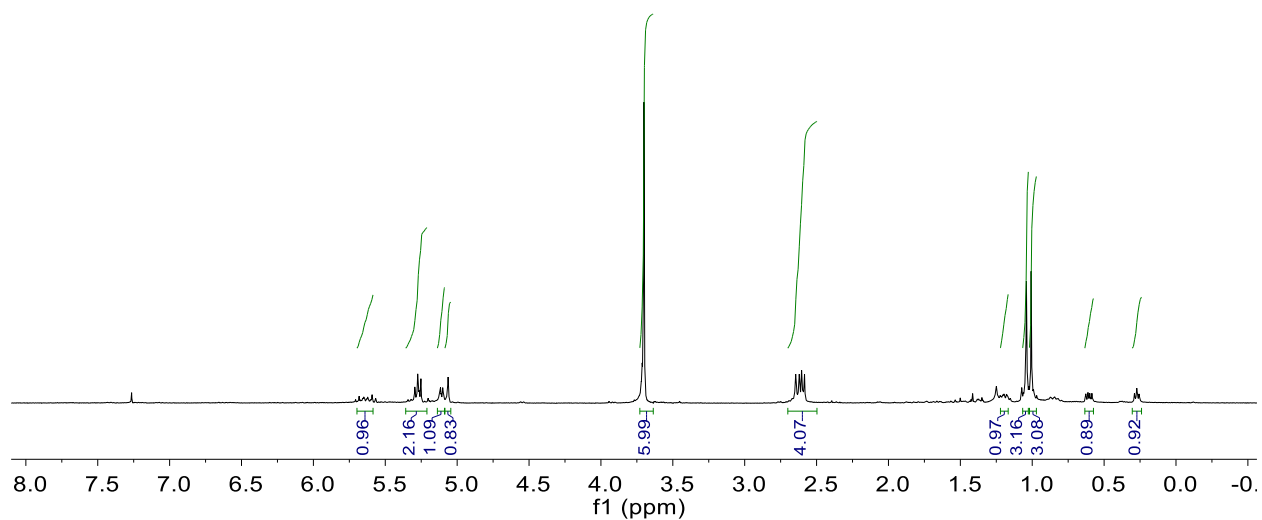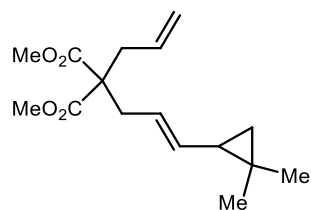
Figure S40: ^{1}H NMR spectrum for **28** (CDCl$_3$, 295 K)
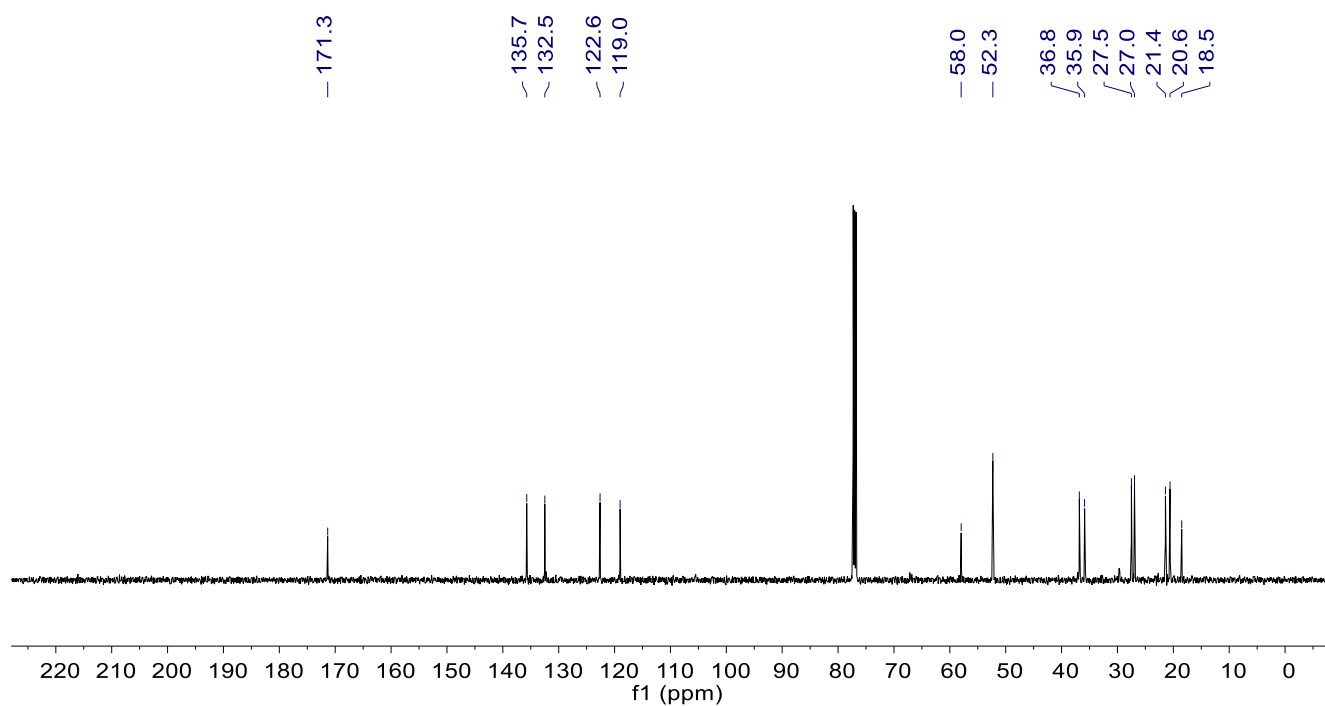
Figure S41: ^{13}C{^{1}H} NMR spectrum for **28** (CDCl$_3$, 295 K)
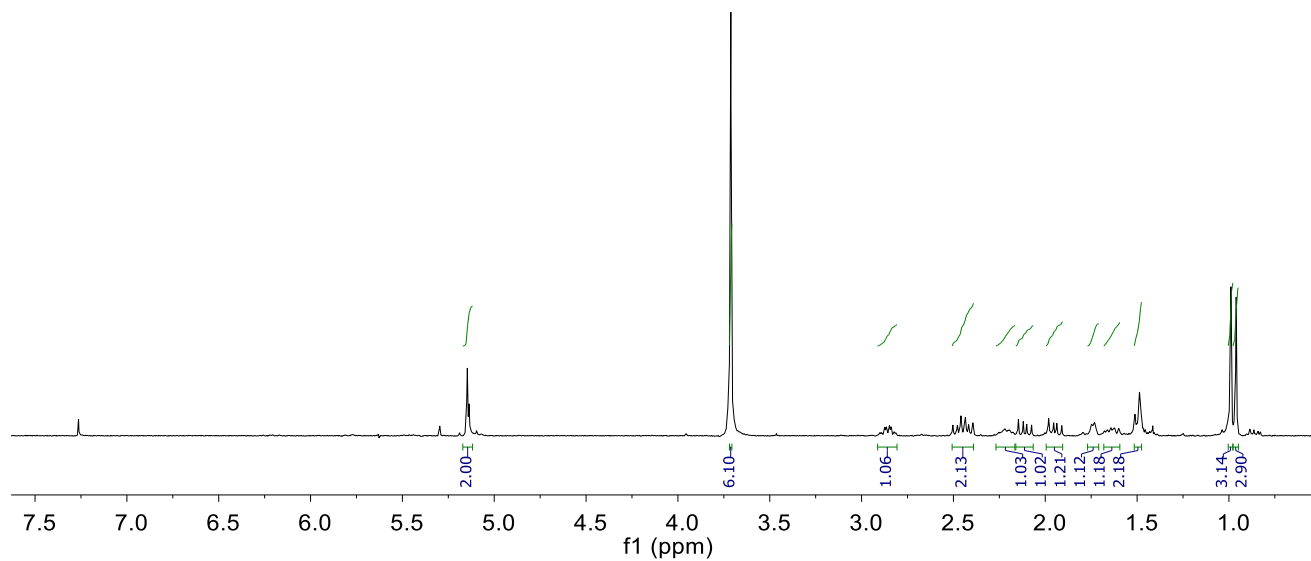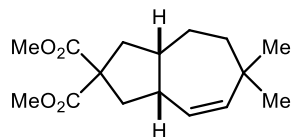
Figure S42: ^{1}H NMR spectrum for **29** (CDCl$_3$, 295 K)
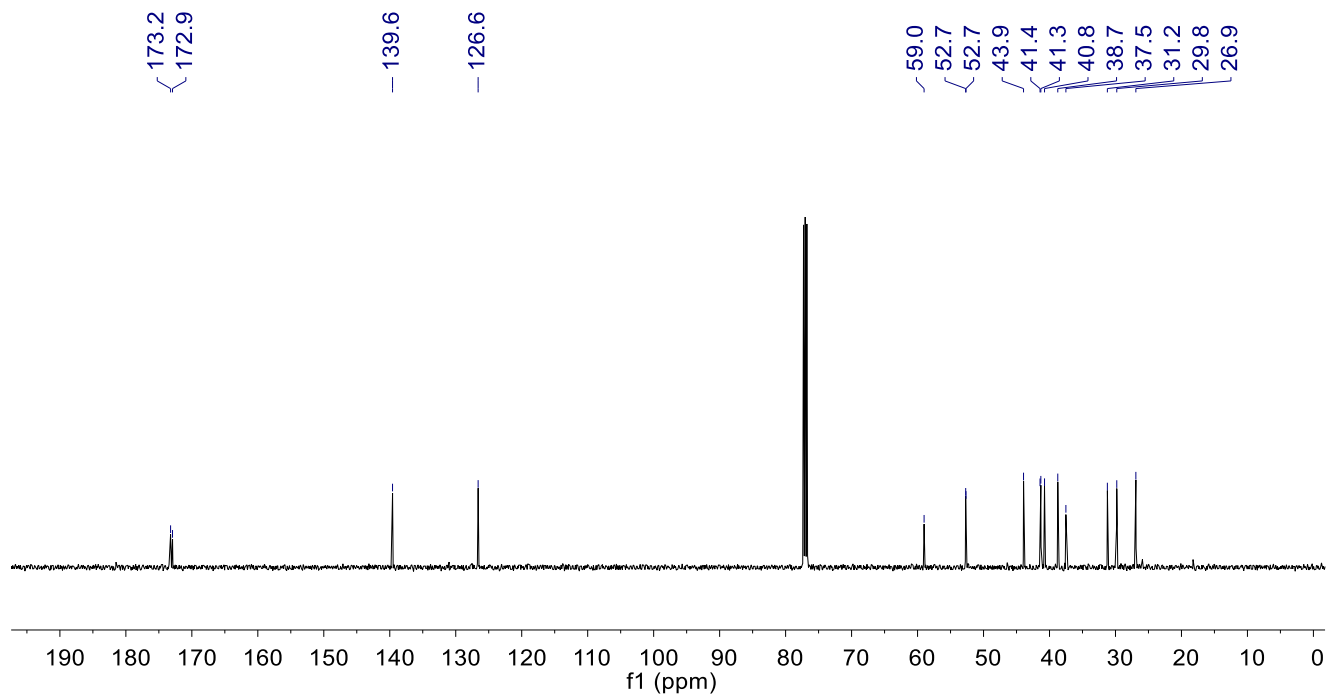
Figure S43: ^{13}C{^{1}H} NMR spectrum for **29** (CDCl$_3$, 295 K)
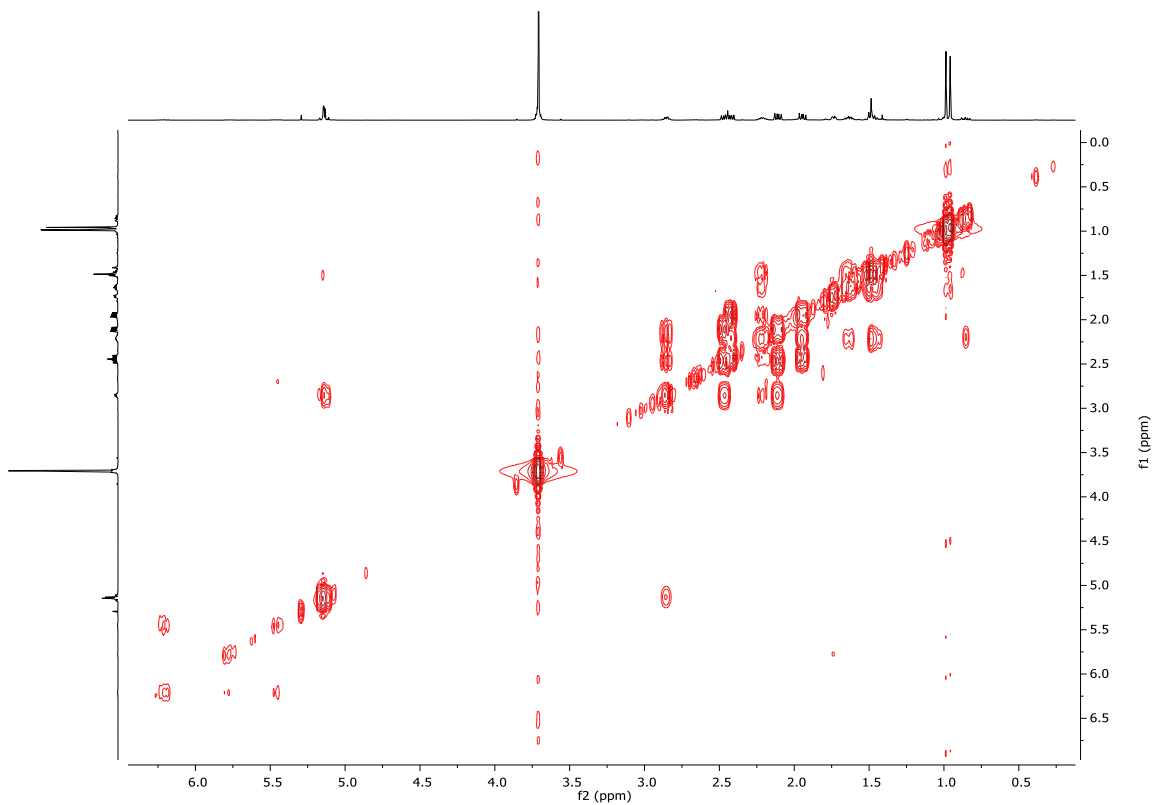
Figure S44: COSY spectrum for **29** (CDCl$_3$, 295 K)
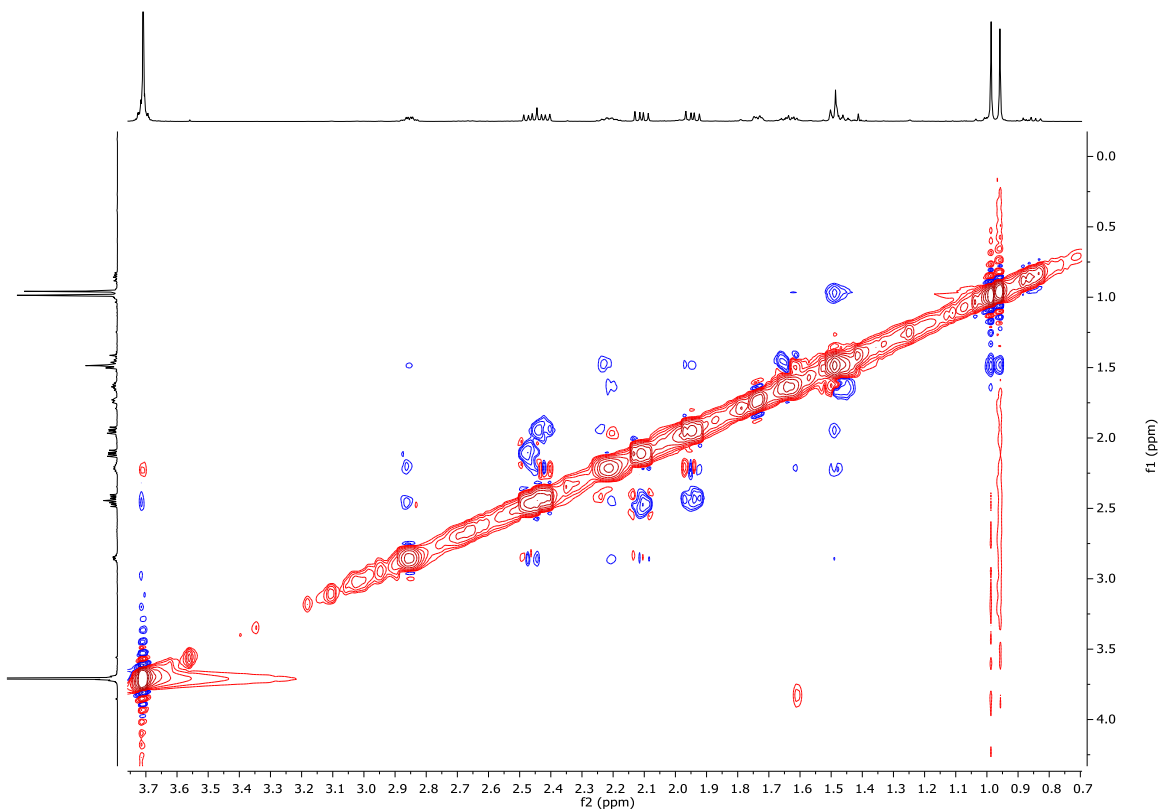
Figure S45: NOESY spectrum for **29** (CDCl$_3$, 295 K)
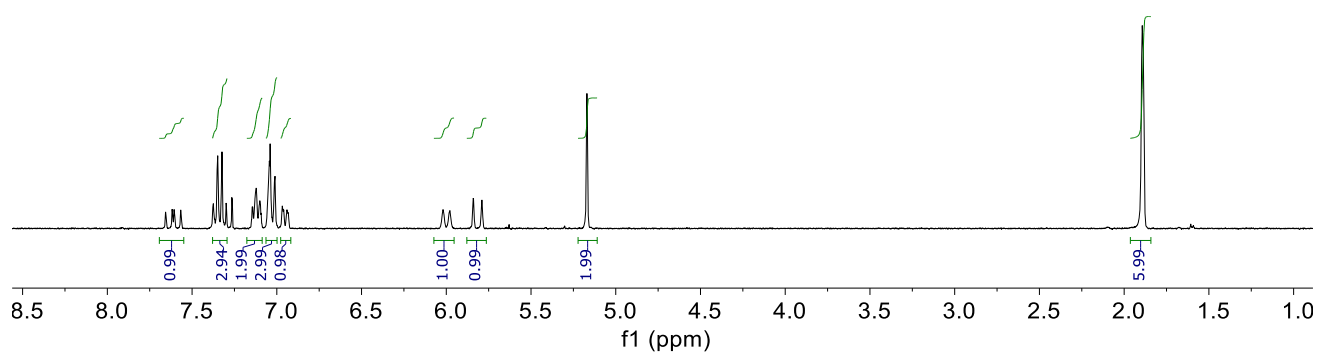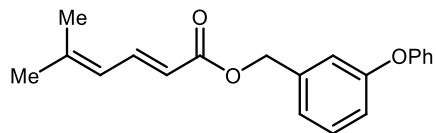
Figure S46: ^{1}H NMR spectrum for **S2** (CDCl$_3$, 295 K)
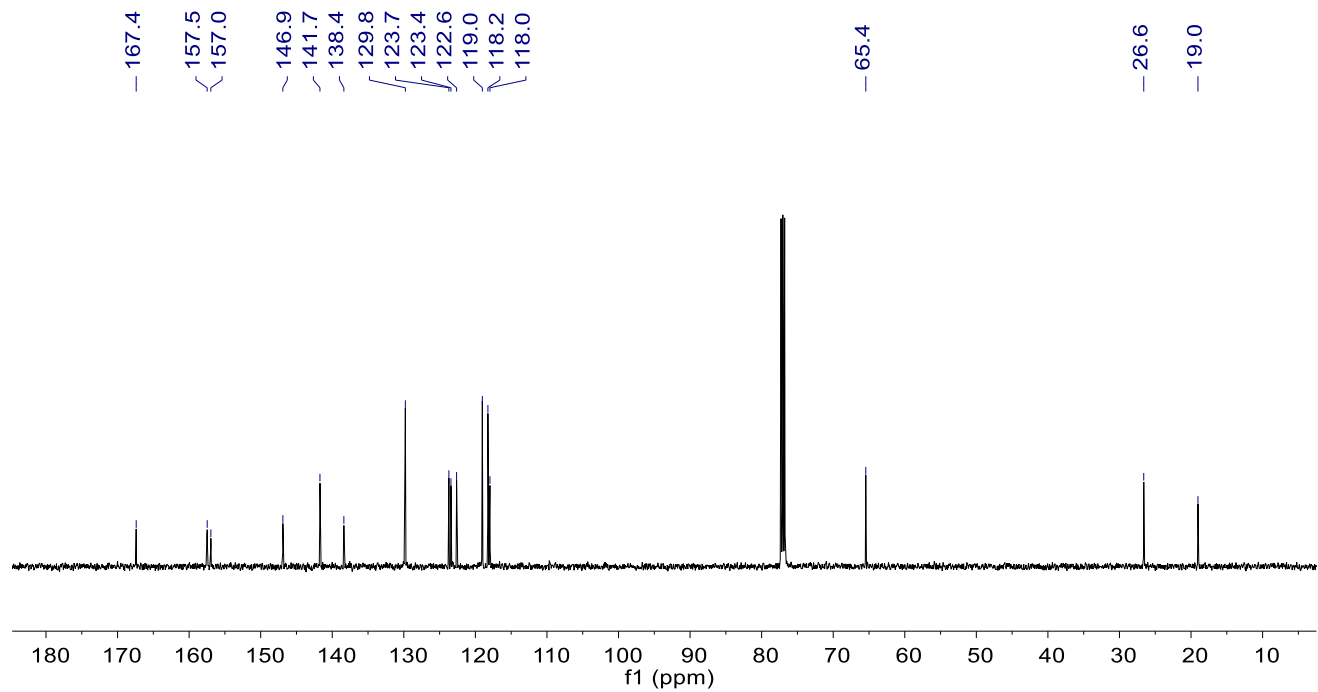
Figure S47: ^{13}C{^{1}H} NMR spectrum for **S2** (CDCl$_3$, 295 K)
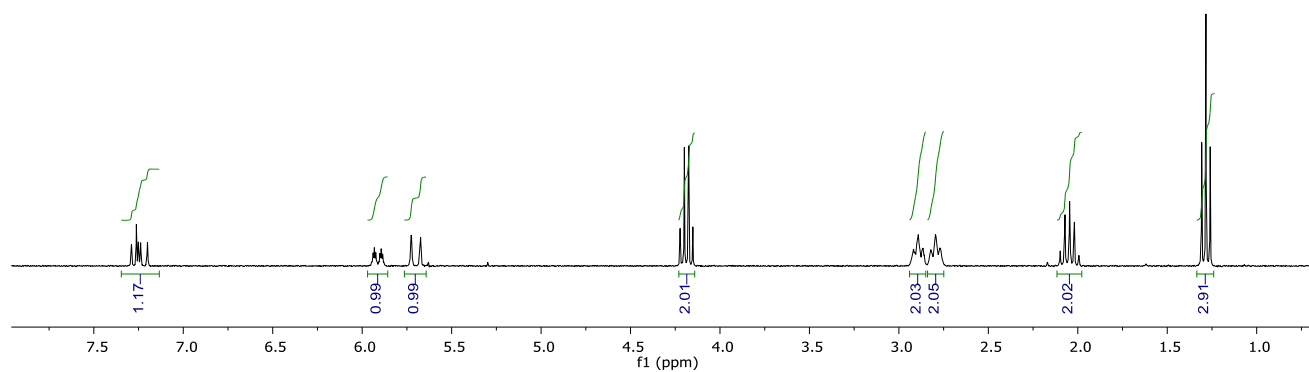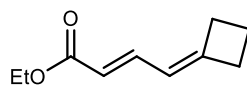
Figure S48: ^{1}H NMR spectrum for **S3** (CDCl$_3$, 295 K)
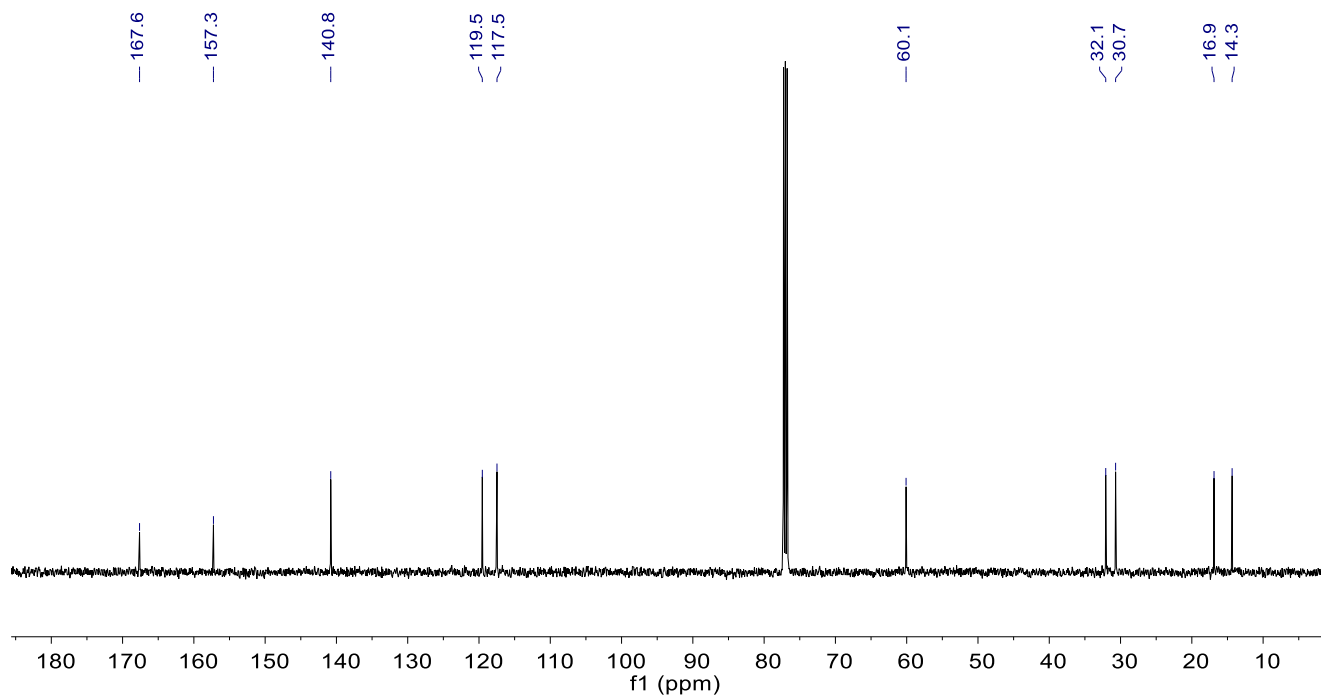
Figure S49: ^{13}C{^{1}H} NMR spectrum for **S3** (CDCl$_3$, 295 K)
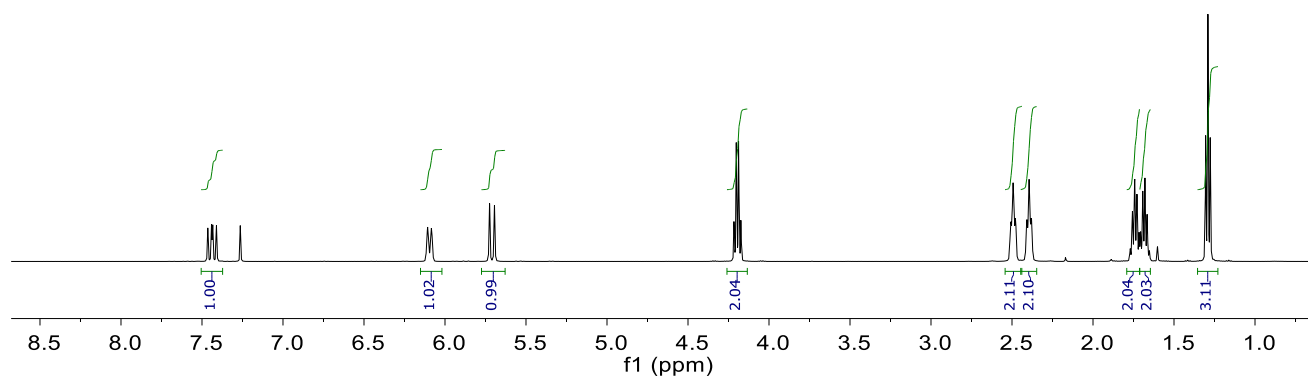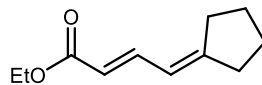
Figure S50: ^{1}H NMR spectrum for **S4** (CDCl$_3$, 295 K)
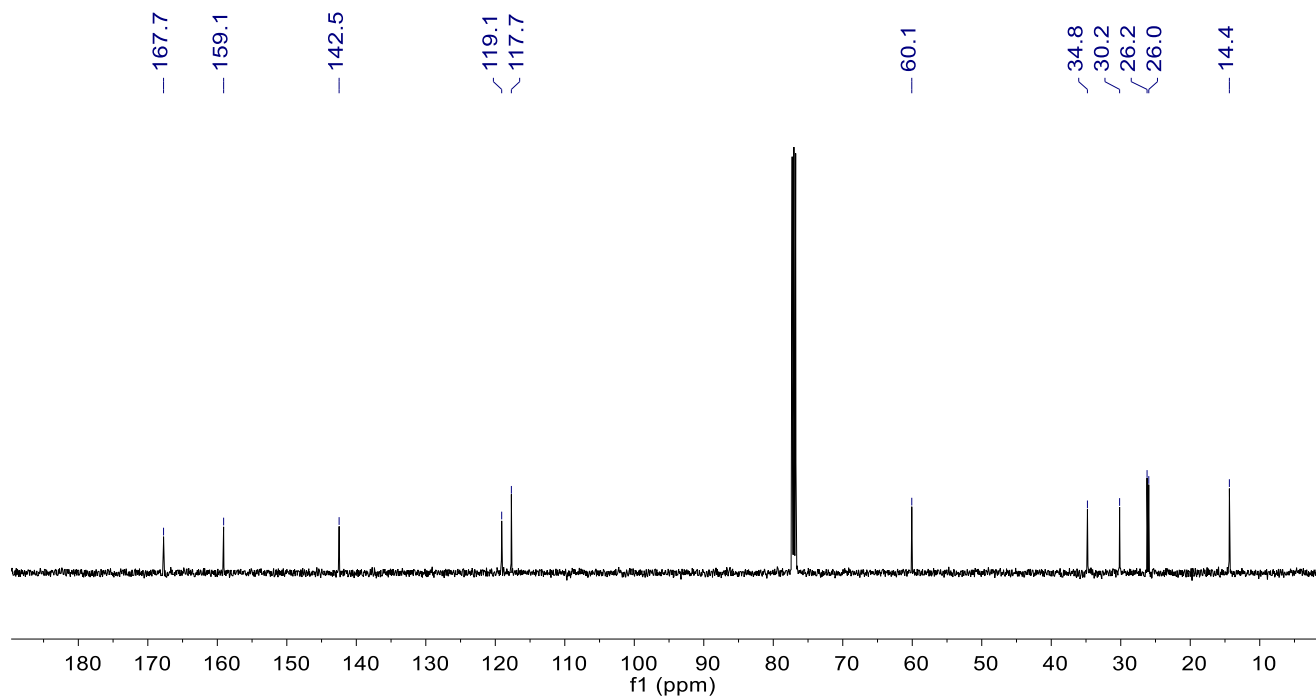
Figure S51: ^{13}C{^{1}H} NMR spectrum for **S4** (CDCl$_3$, 295 K)

Figure S52: ^{1}H NMR spectrum for **S5** (CDCl$_3$, 295 K)

Figure S53: ^{13}C{^{1}H} NMR spectrum for **S5** (CDCl$_3$, 295 K)
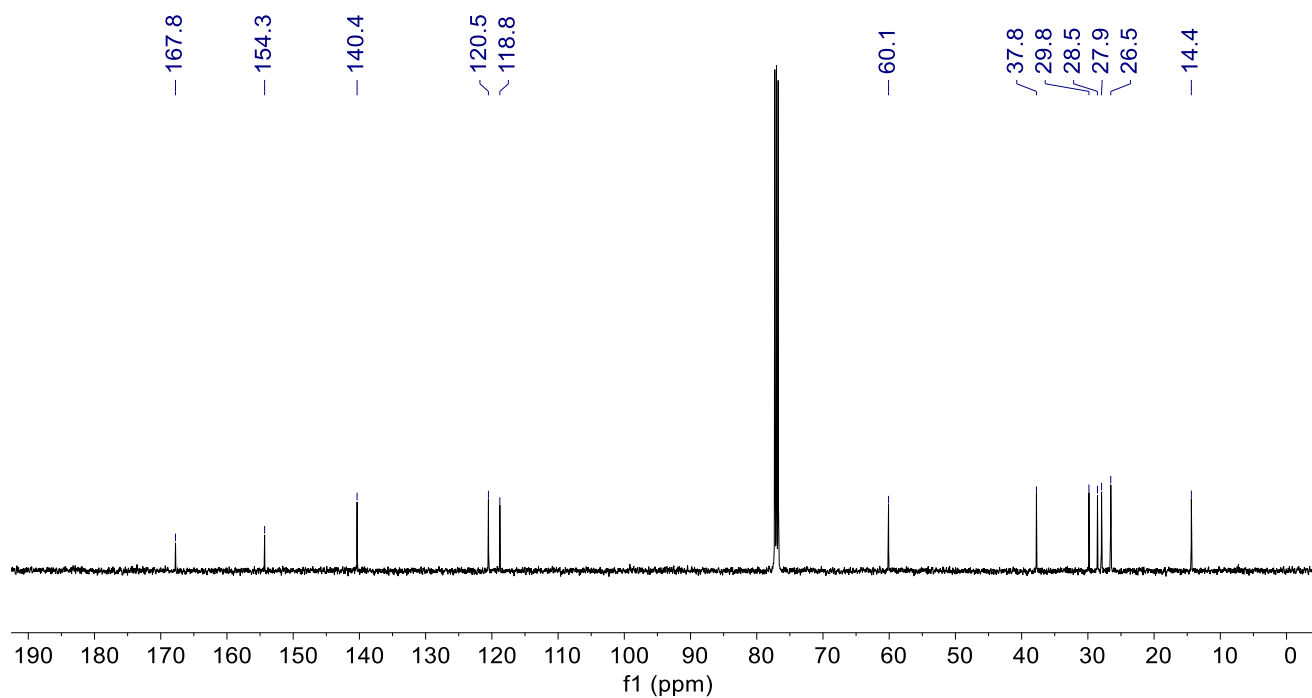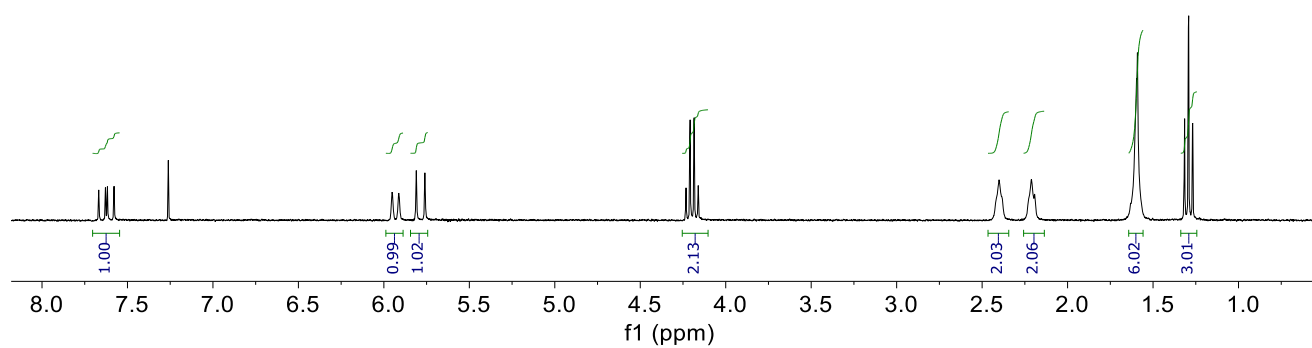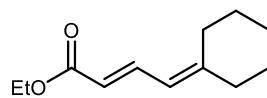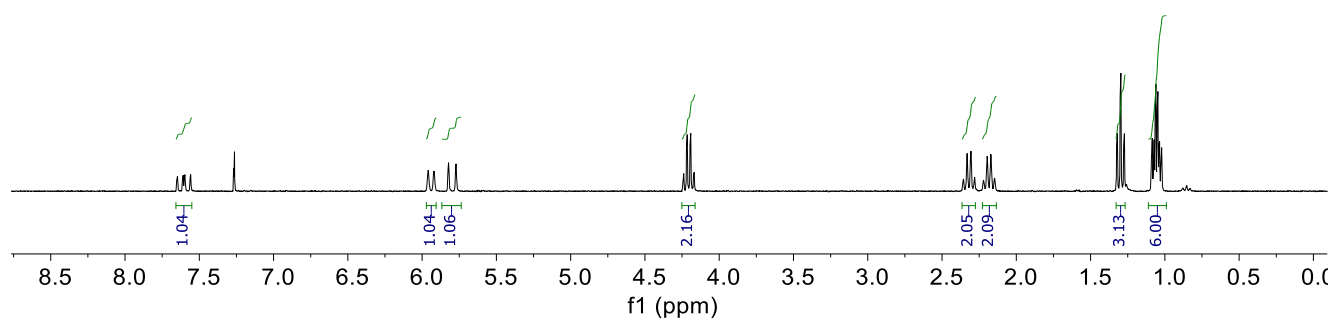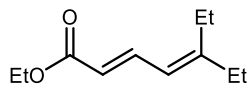
Figure S54: ^{1}H NMR spectrum for **S6** (CDCl$_3$, 295 K)
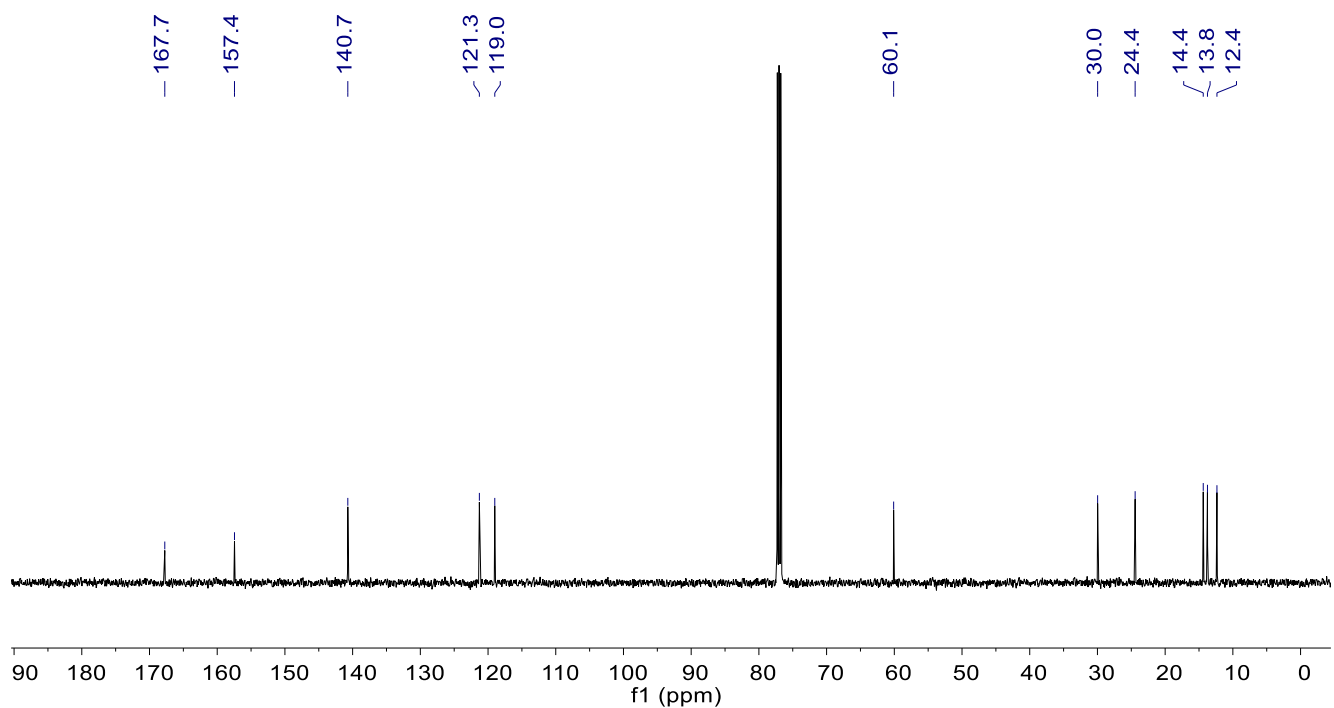
Figure S55: ^{13}C{^{1}H} NMR spectrum for **S6** (CDCl$_3$, 295 K)
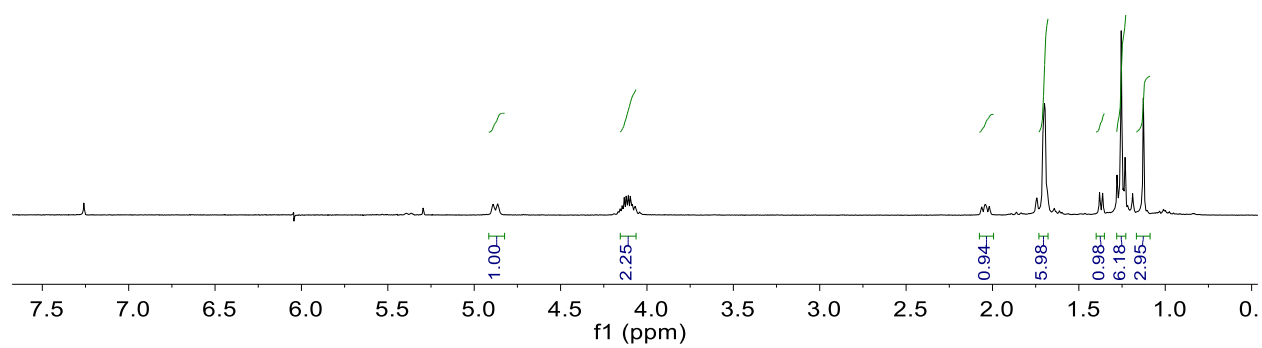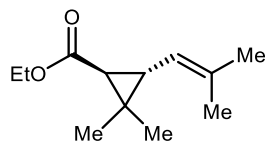
Figure S56: ^{1}H NMR spectrum for **19** (CDCl$_3$, 295 K)
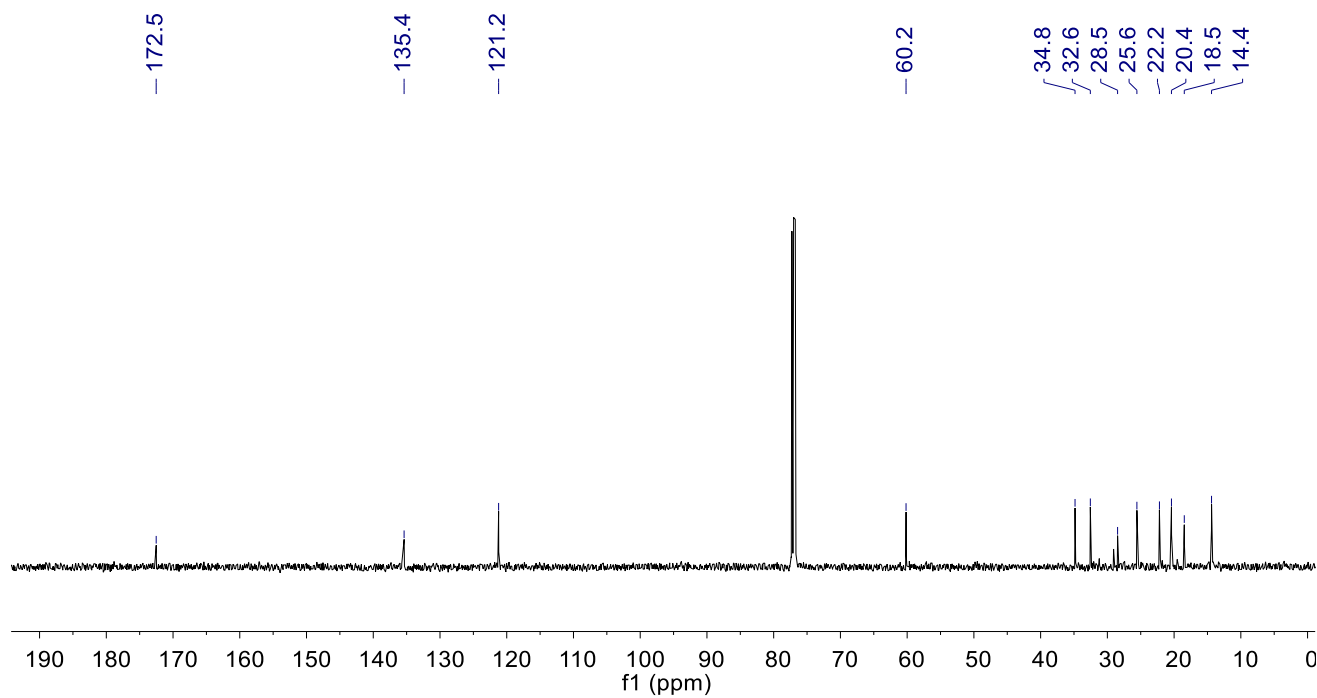
Figure S57: ^{13}C{^{1}H} NMR spectrum for **19** (CDCl$_3$, 295 K)
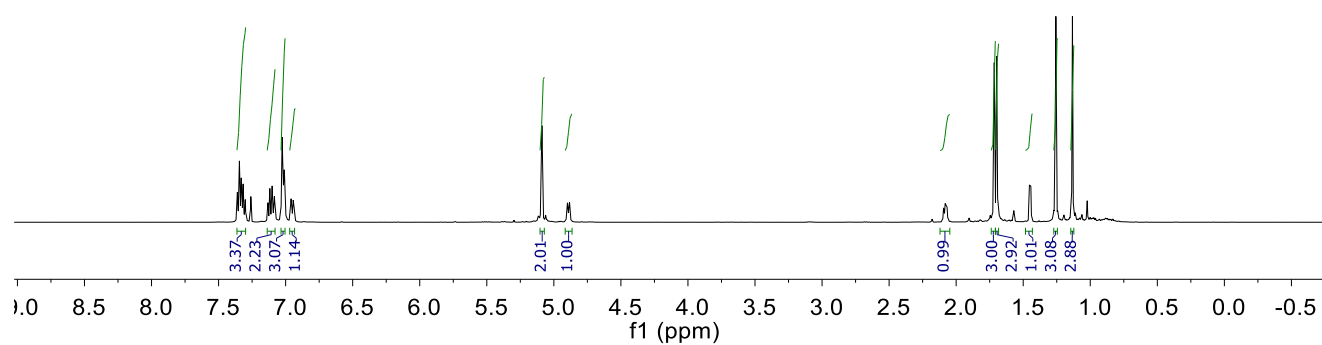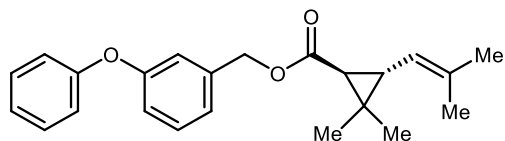
Figure S58: ^{1}H NMR spectrum for **20** (CDCl$_3$, 295 K)
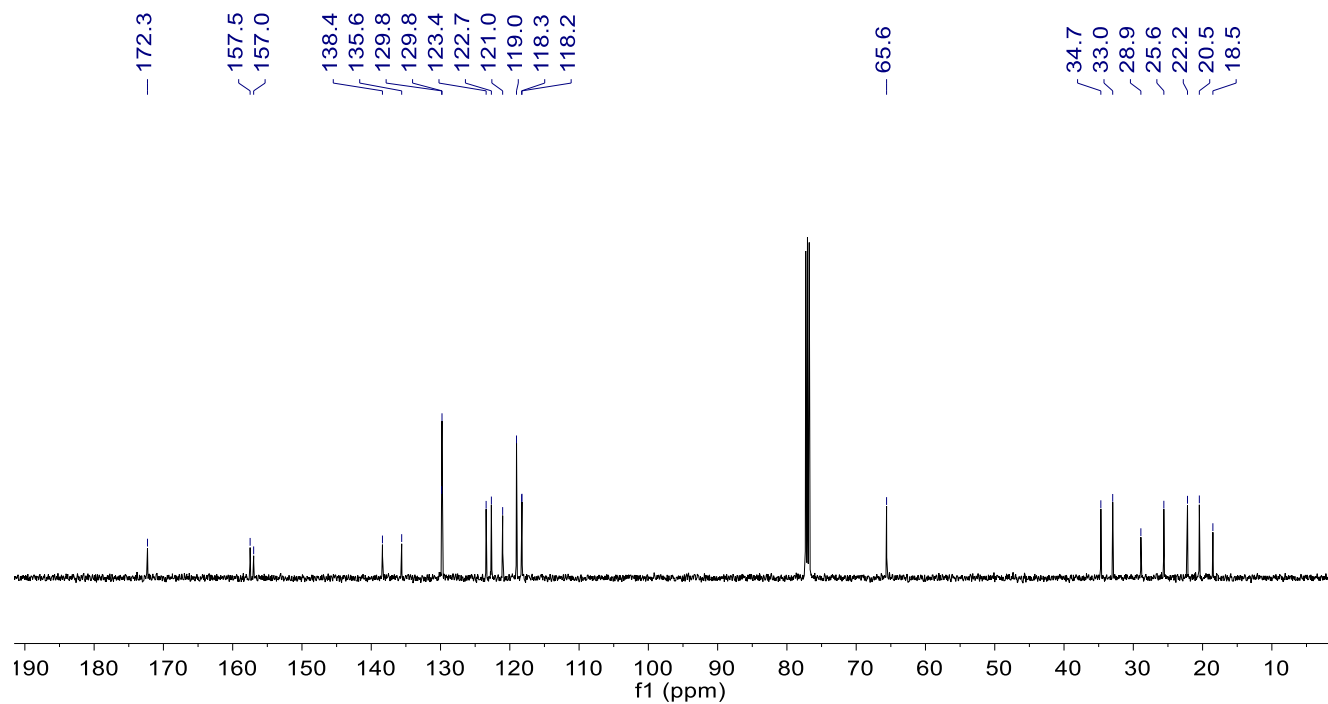
Figure S59: ^{13}C{^{1}H} NMR spectrum for **20** (CDCl$_3$, 295 K)

1:9 (cis/trans)
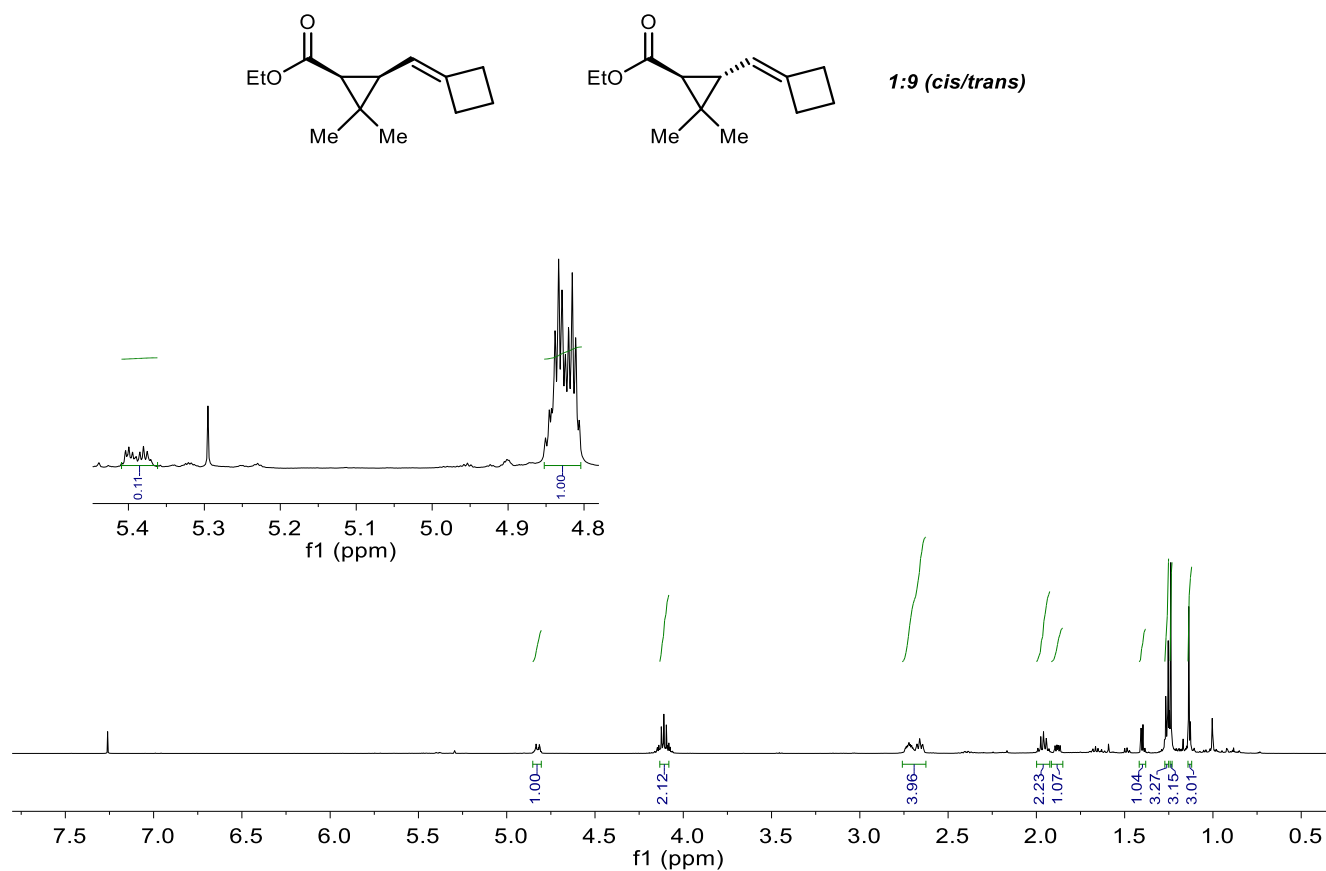
Figure S60: ¹H NMR spectrum for **21** (CDCl₃, 295 K)
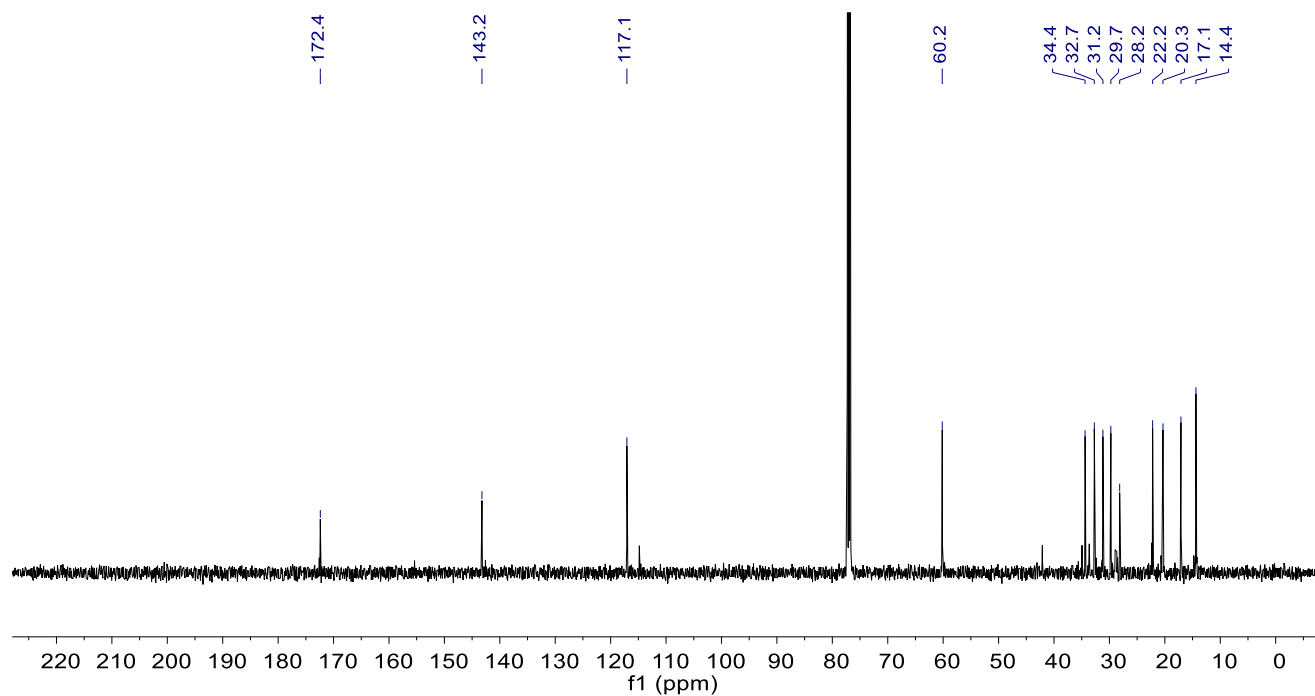
Figure S61: ¹³C{¹H} NMR spectrum for **21** (CDCl₃, 295 K

1:13 (cis/trans)
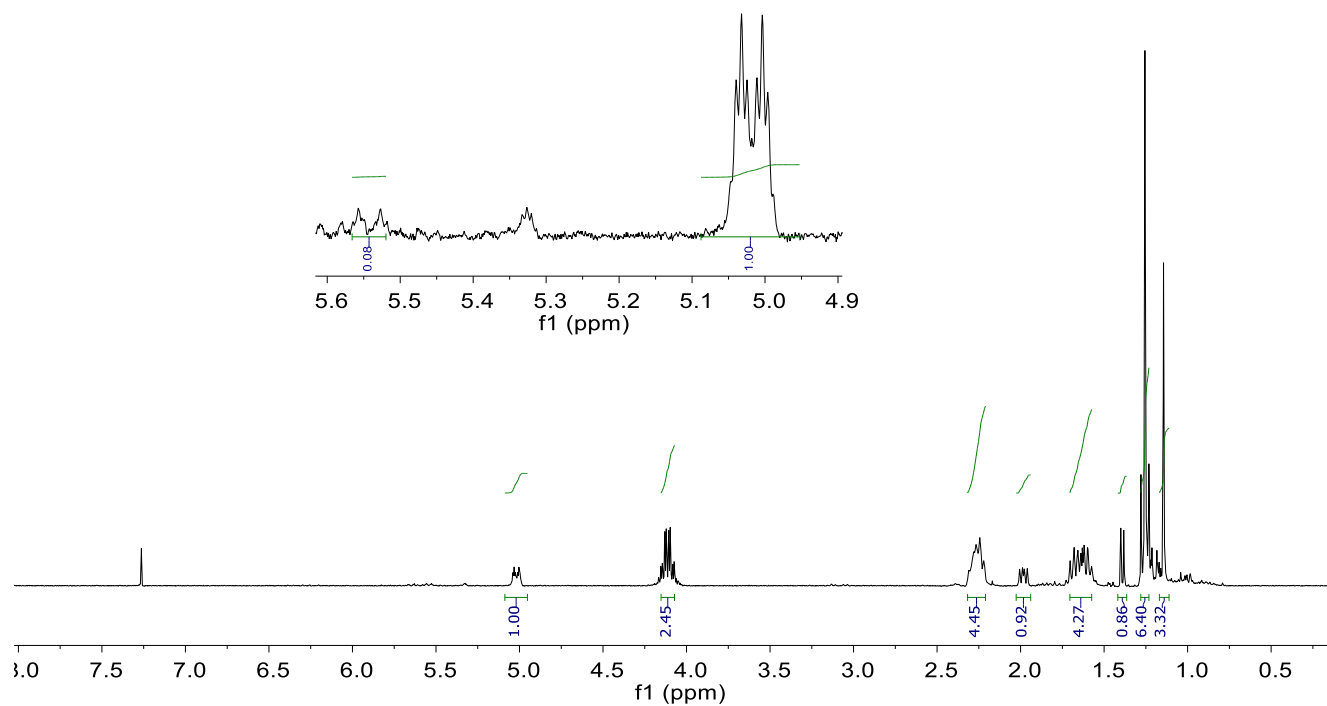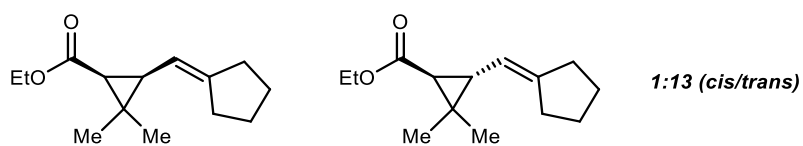
Figure S62: ^{1}H NMR spectrum for **22** (CDCl$_3$, 295 K)
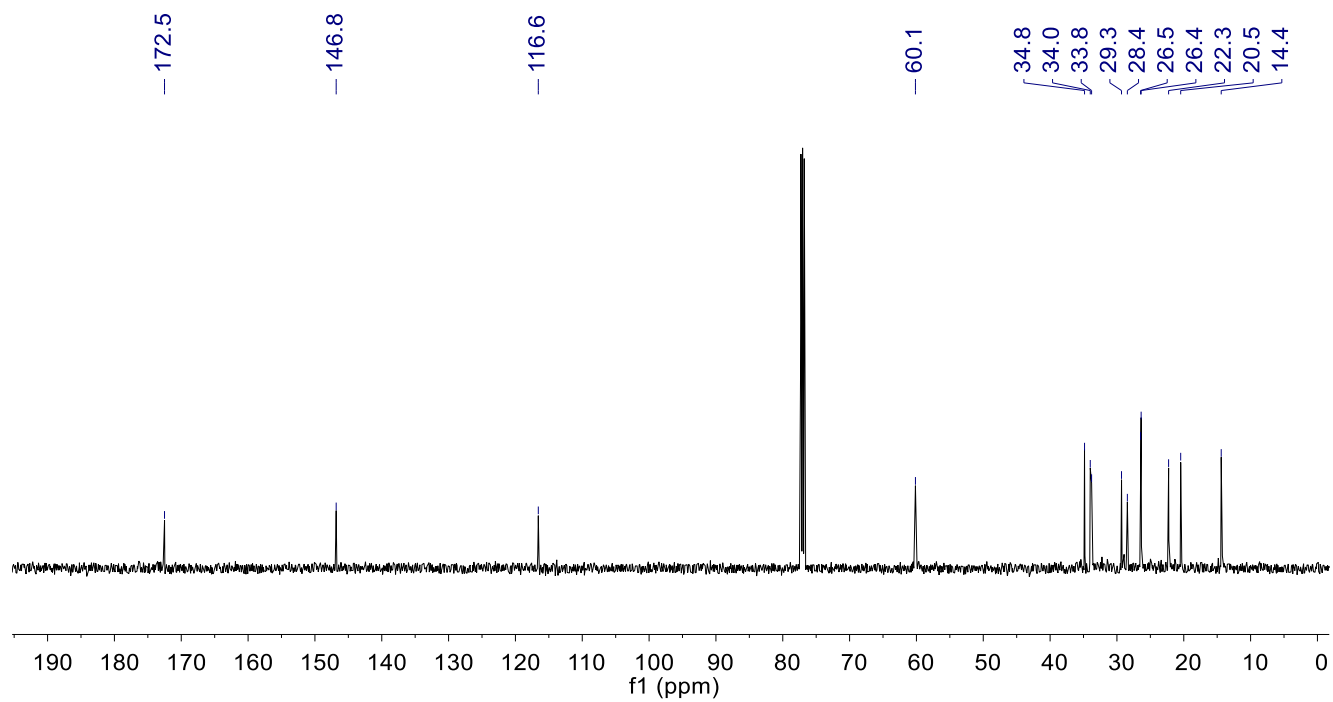
Figure S63: $^{13}C\{^1H\}$ NMR spectrum for **22** (CDCl$_3$, 295 K)

1:13 (cis/trans)
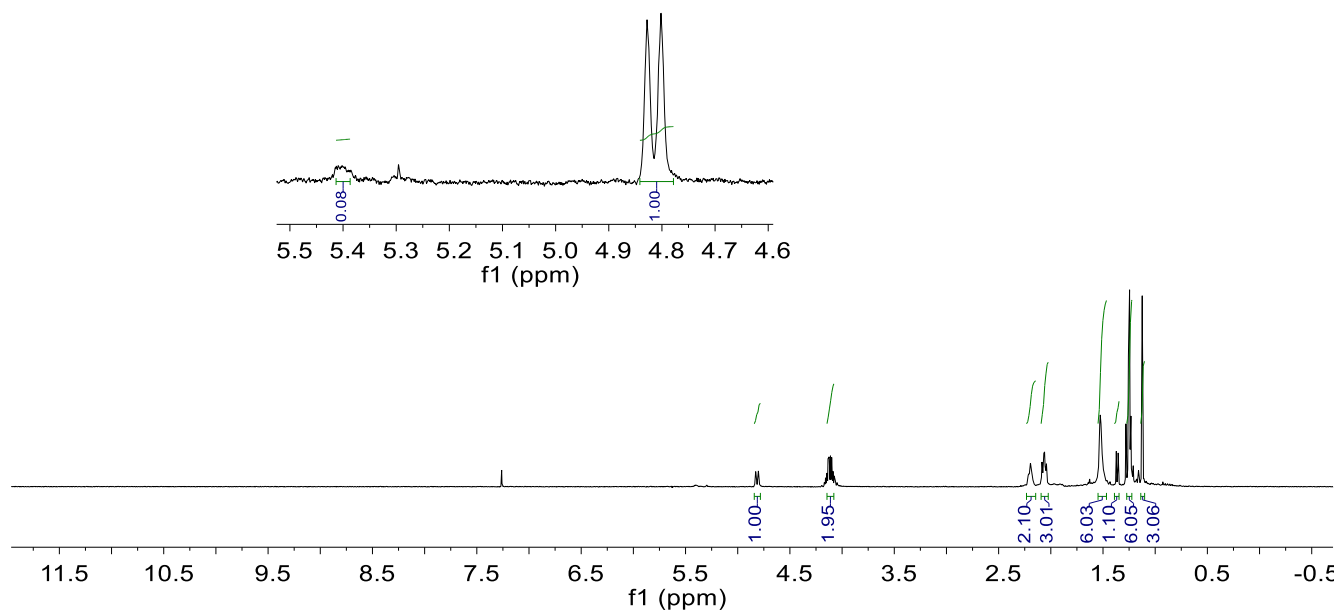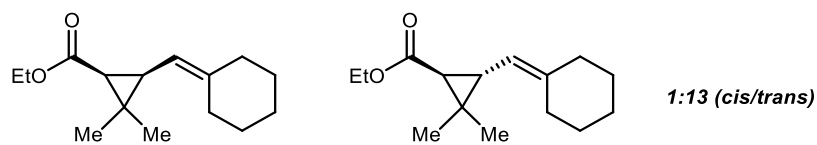
Figure S64: ^{1}H NMR spectrum for **23** (CDCl$_3$, 295 K)
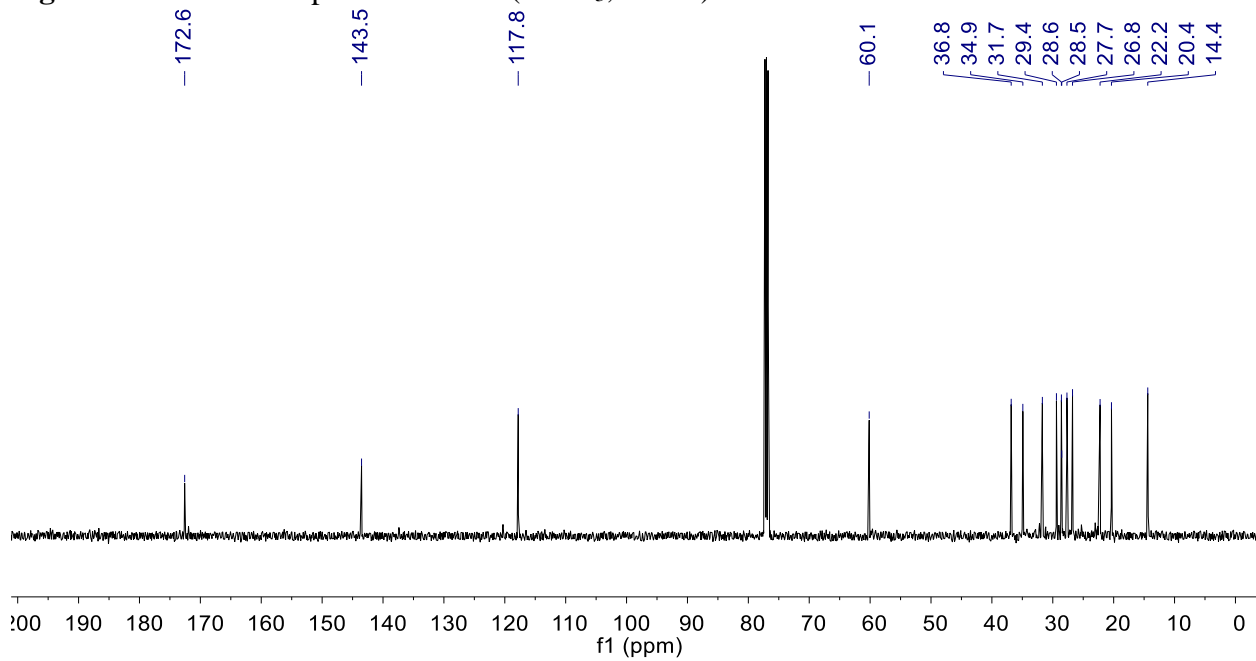
Figure S65: ^{13}C{^{1}H} NMR spectrum for **23** (CDCl$_3$, 295 K)
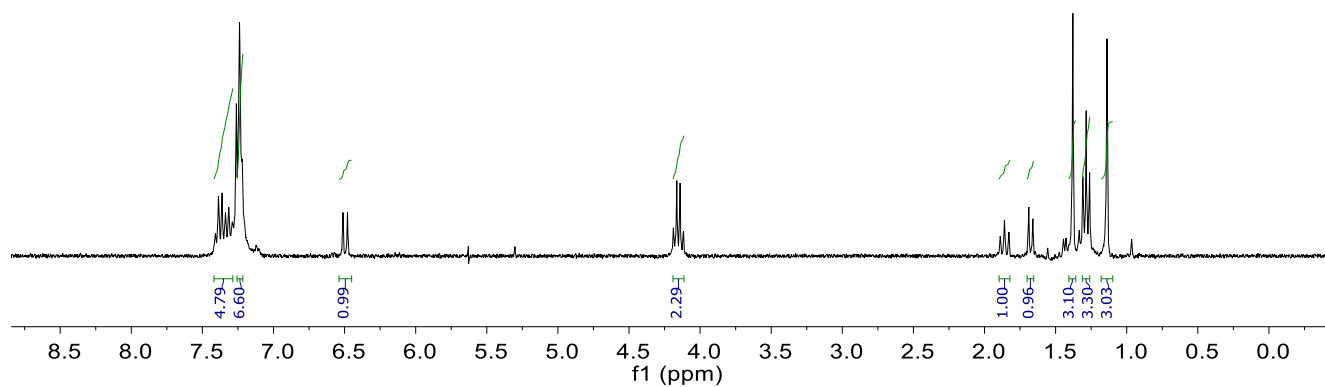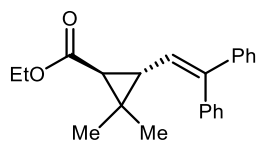
Figure S66: ^{1}H NMR spectrum for **24** (CDCl$_3$, 295 K)
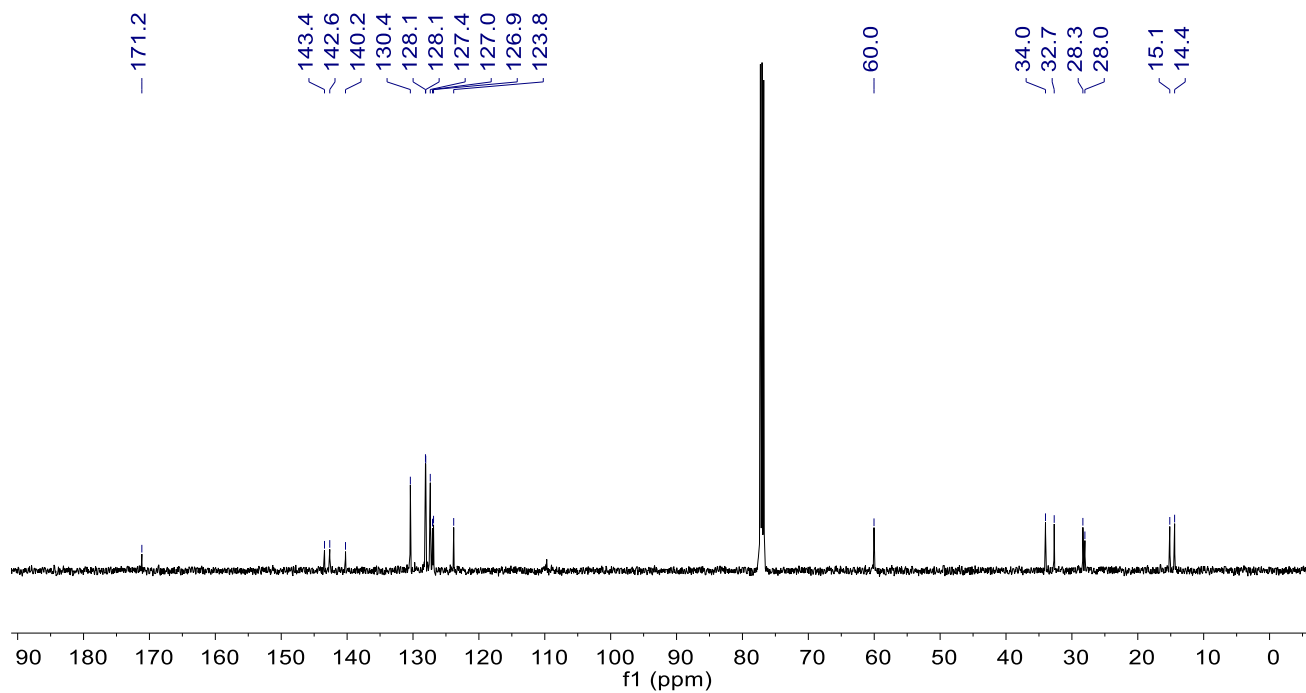
Figure S67: ^{13}C{^{1}H} NMR spectrum for **24** (CDCl$_3$, 295 K)
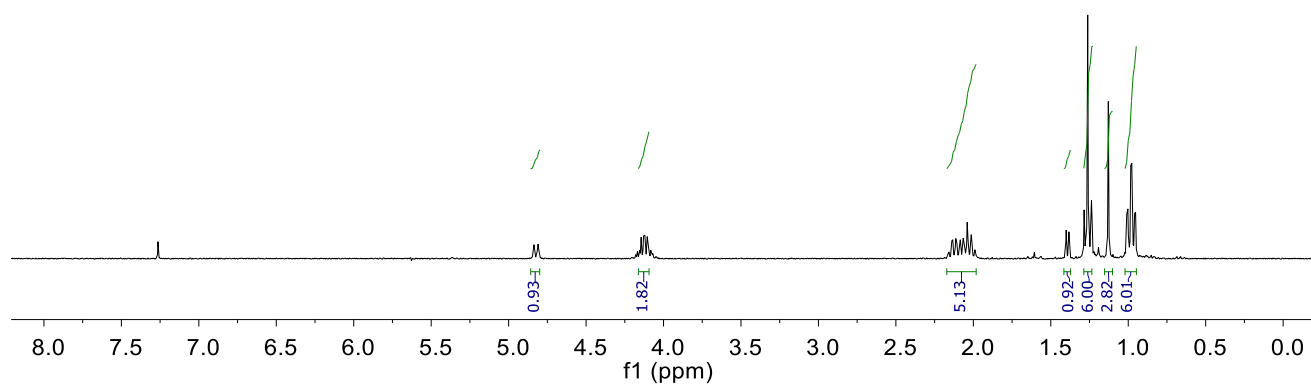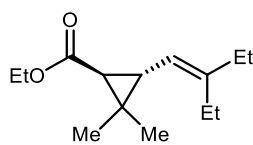
Figure S68: ¹H NMR spectrum for **25** (CDCl₃, 295 K)
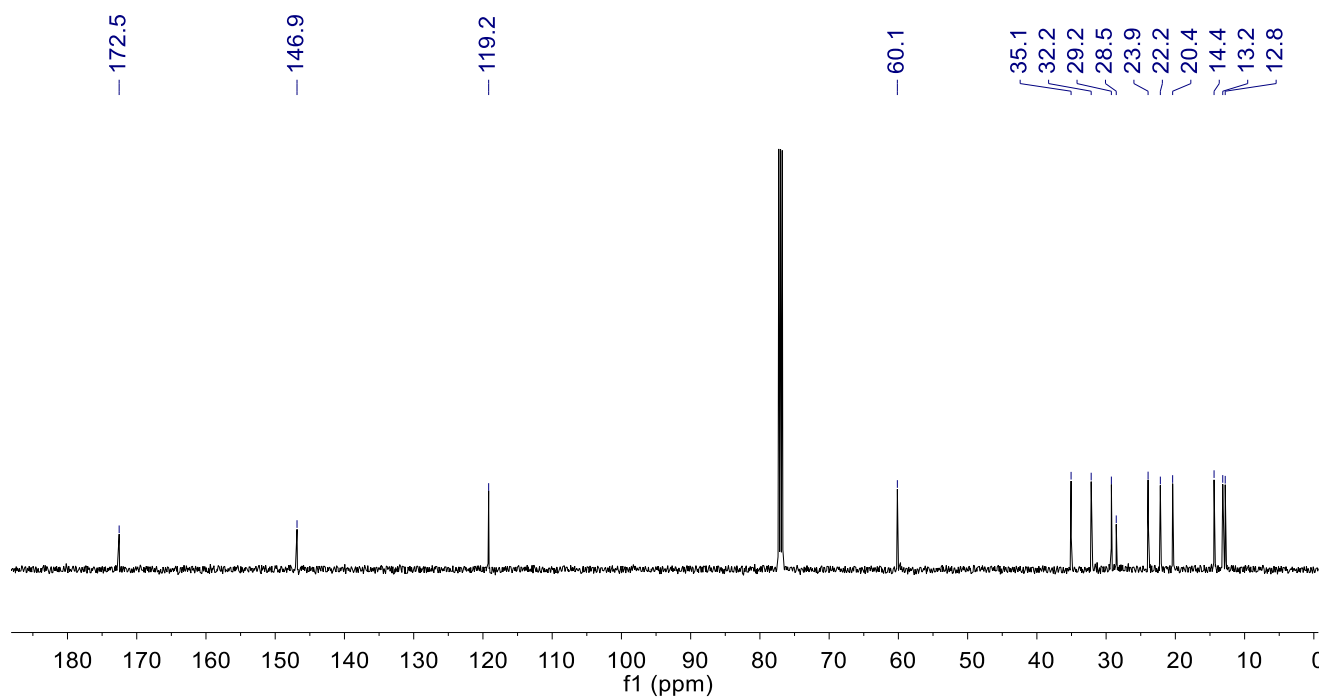
Figure S69: ¹³C{¹H} NMR spectrum for **25** (CDCl₃, 295 K)
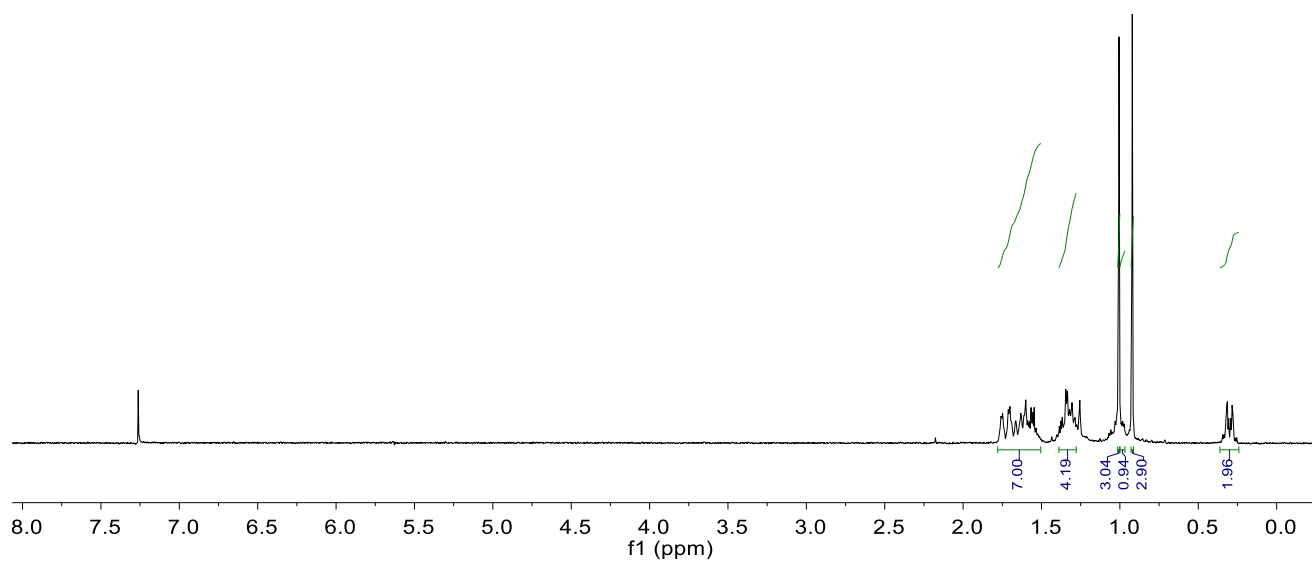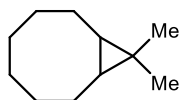
Figure S70: ^{1}H NMR spectrum for **31** (CDCl$_3$, 295 K)
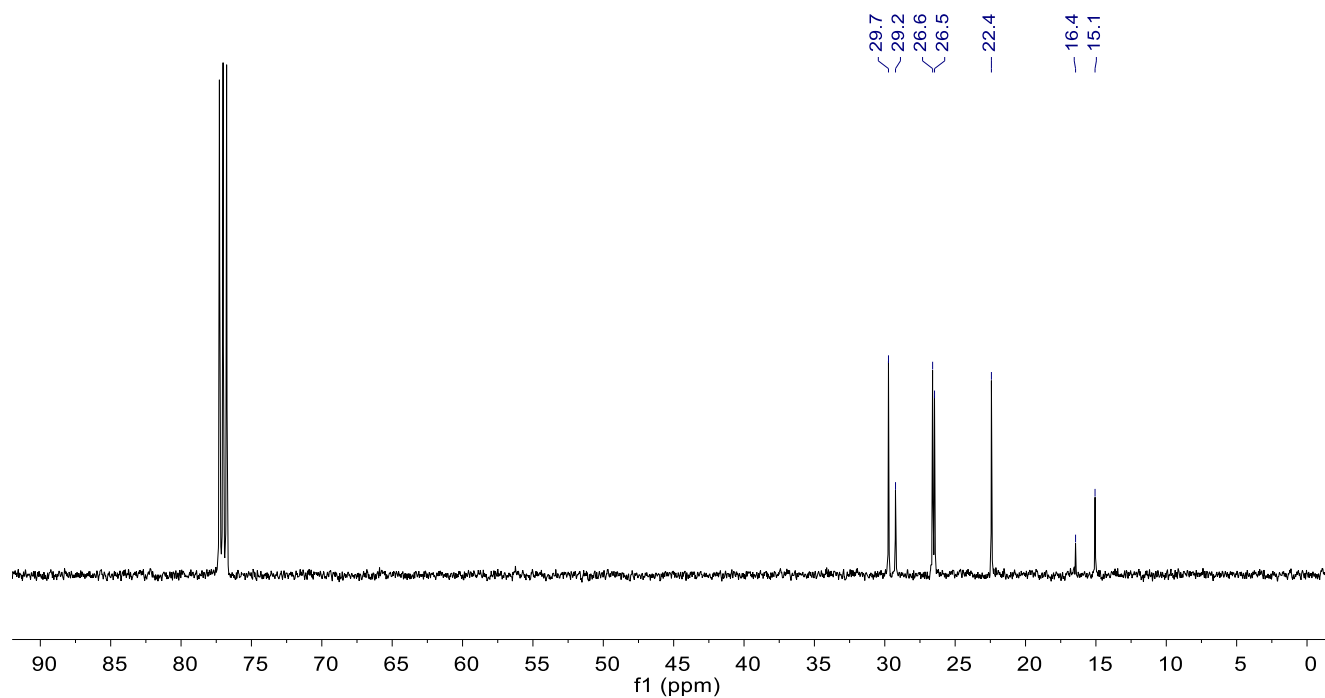
Figure S71: ^{13}C{^{1}H} NMR spectrum for **31** (CDCl$_3$, 295 K)
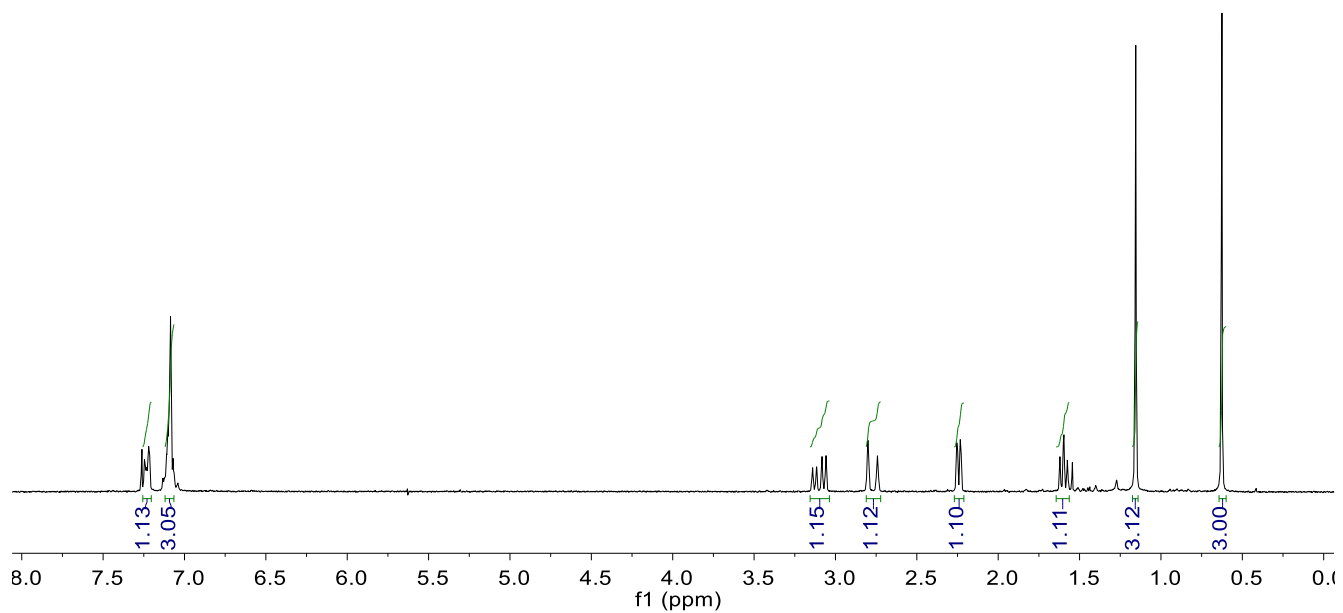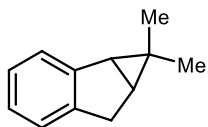
Figure S72: ^{1}H NMR spectrum for **32** (CDCl$_3$, 295 K)
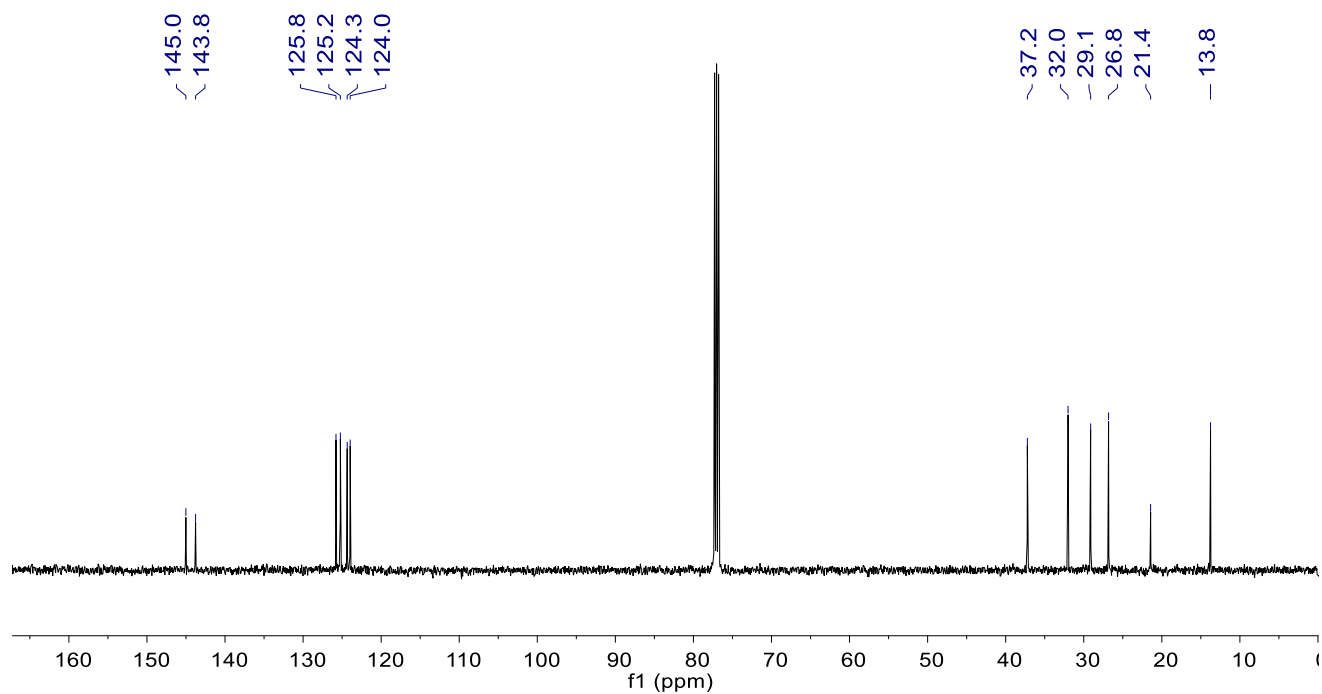
Figure S73: ^{13}C{^{1}H} NMR spectrum for **32** (CDCl$_3$, 295 K)
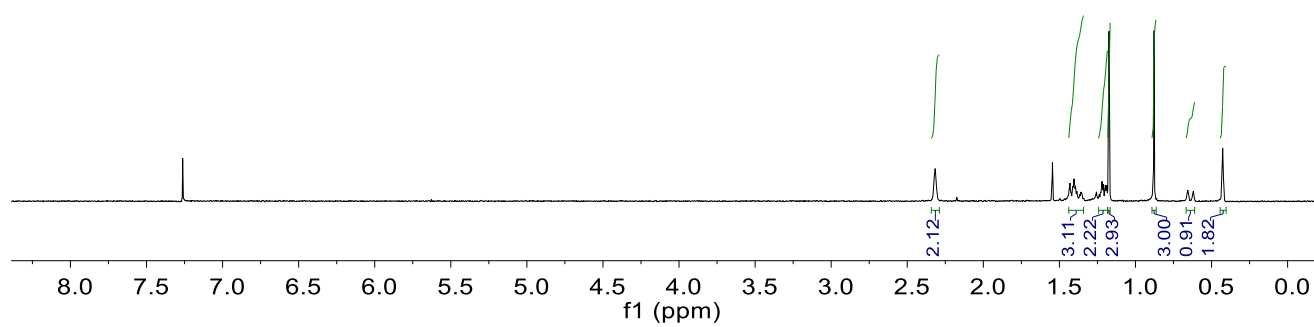
Figure S74: ¹H NMR spectrum for **33** (CDCl₃, 295 K)
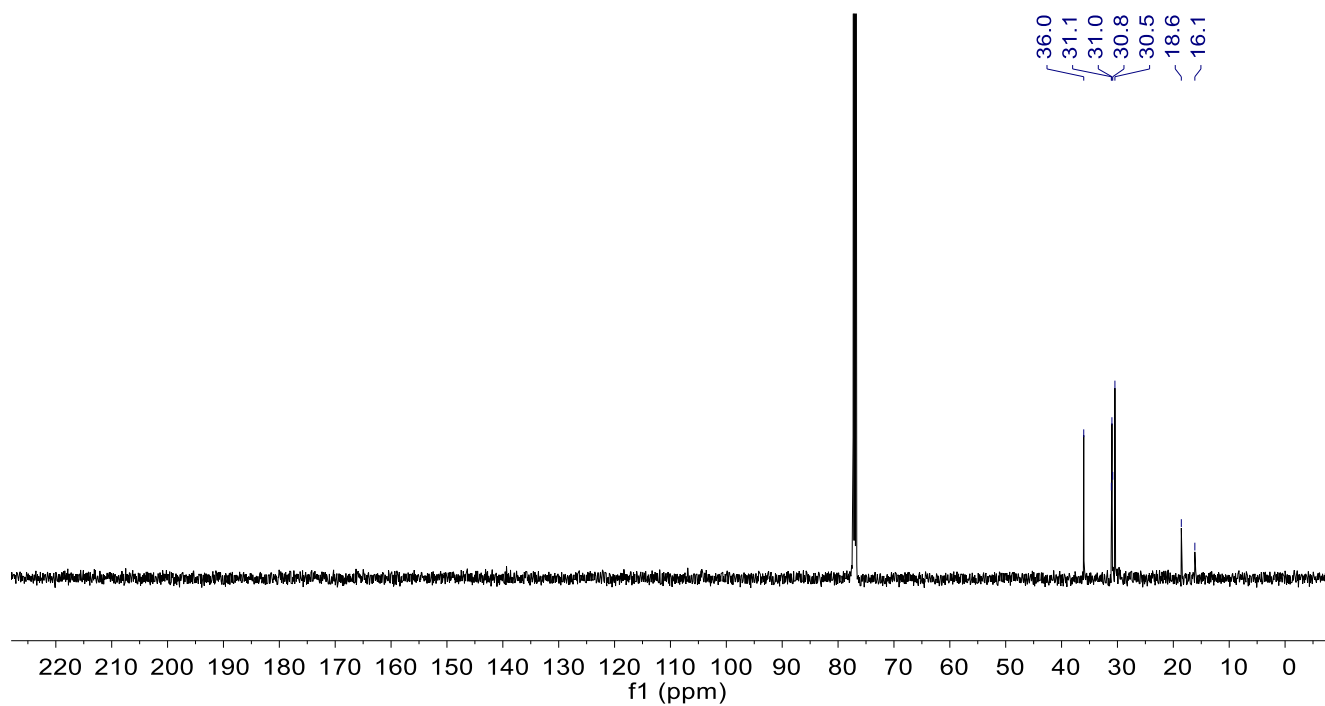
Figure S75: ¹³C{¹H} NMR spectrum for **33** (CDCl₃, 295 K)
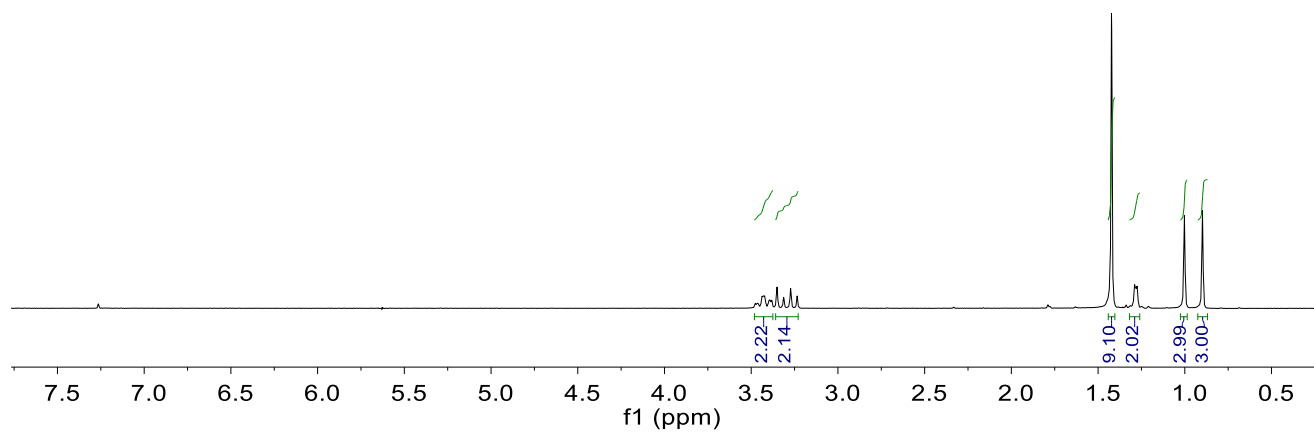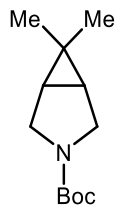
Figure S76: ^{1}H NMR spectrum for **35** (CDCl$_3$, 295 K)
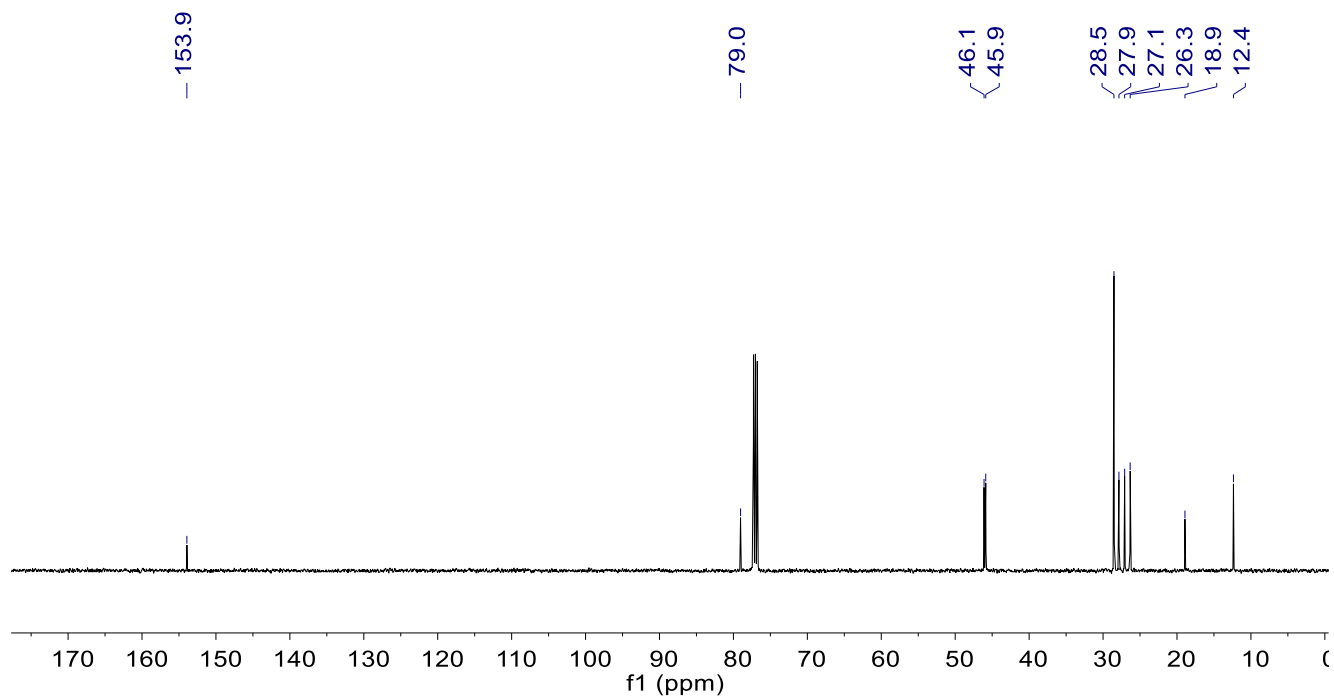
**Figure S77**: ^{13}C{^{1}H} NMR spectrum for **35** (CDCl$_3$, 295 K)
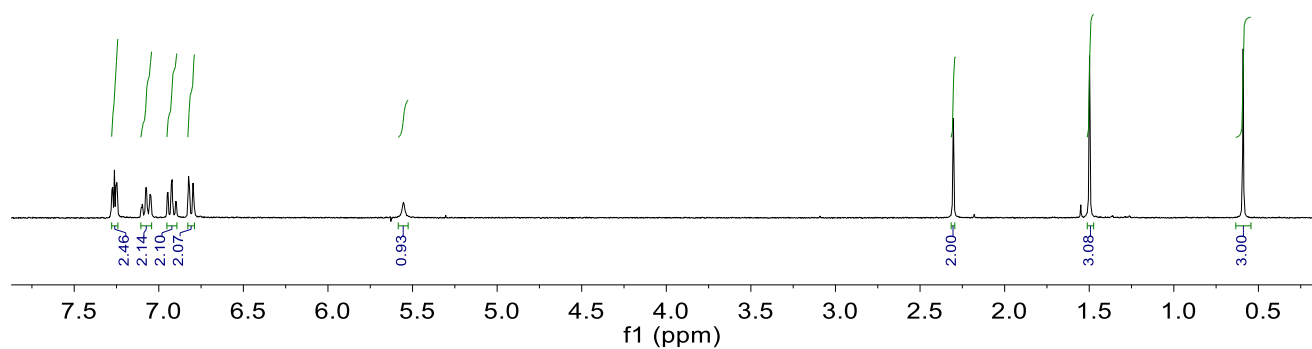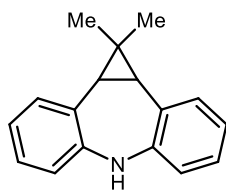
Figure S78: ^{1}H NMR spectrum for **37** (CDCl$_3$, 295 K)
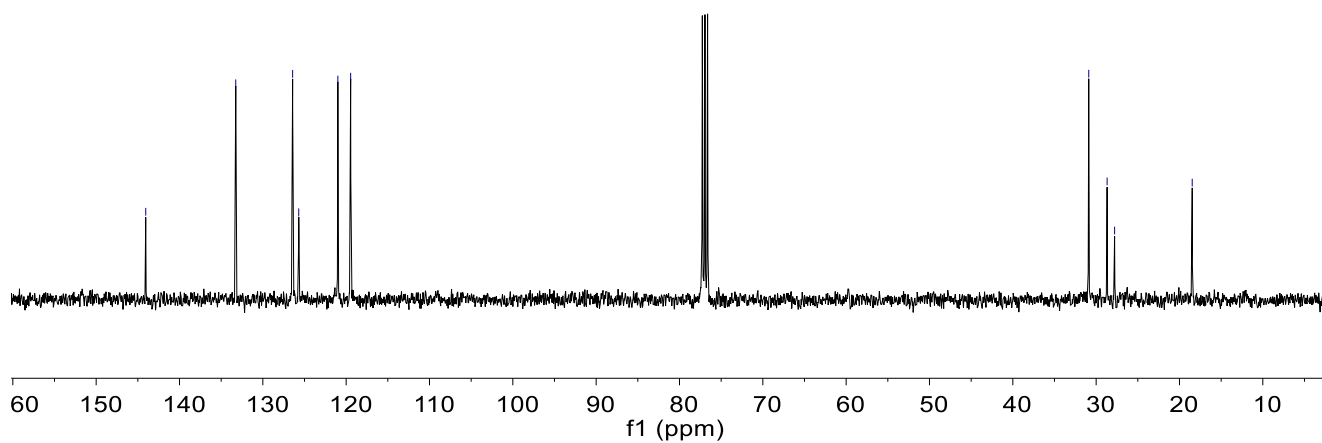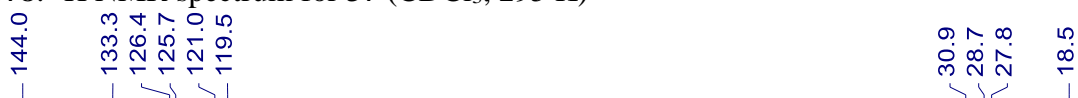
**Figure S79**: ^{13}C{^{1}H} NMR spectrum for **37** (CDCl$_3$, 295 K)
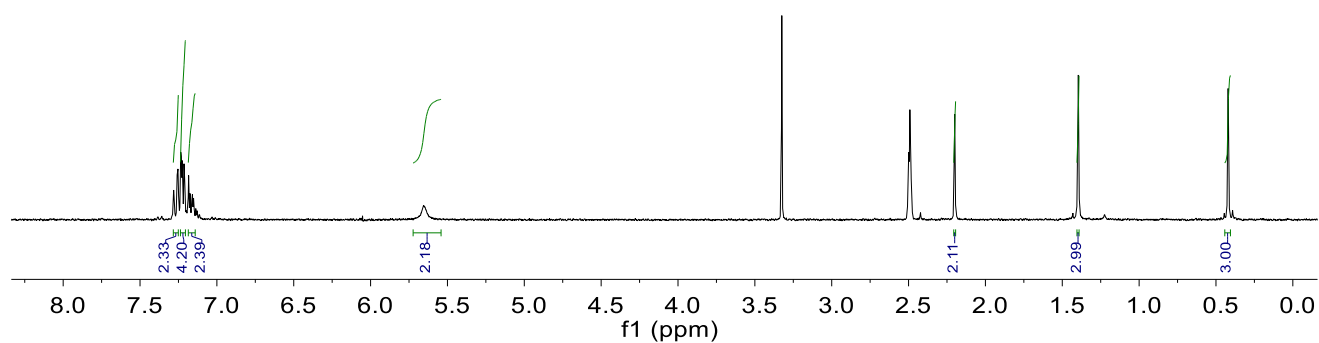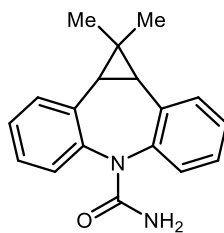
Figure S80: ^{1}H NMR spectrum for **38** (DMSO-d$_6$, 295 K)
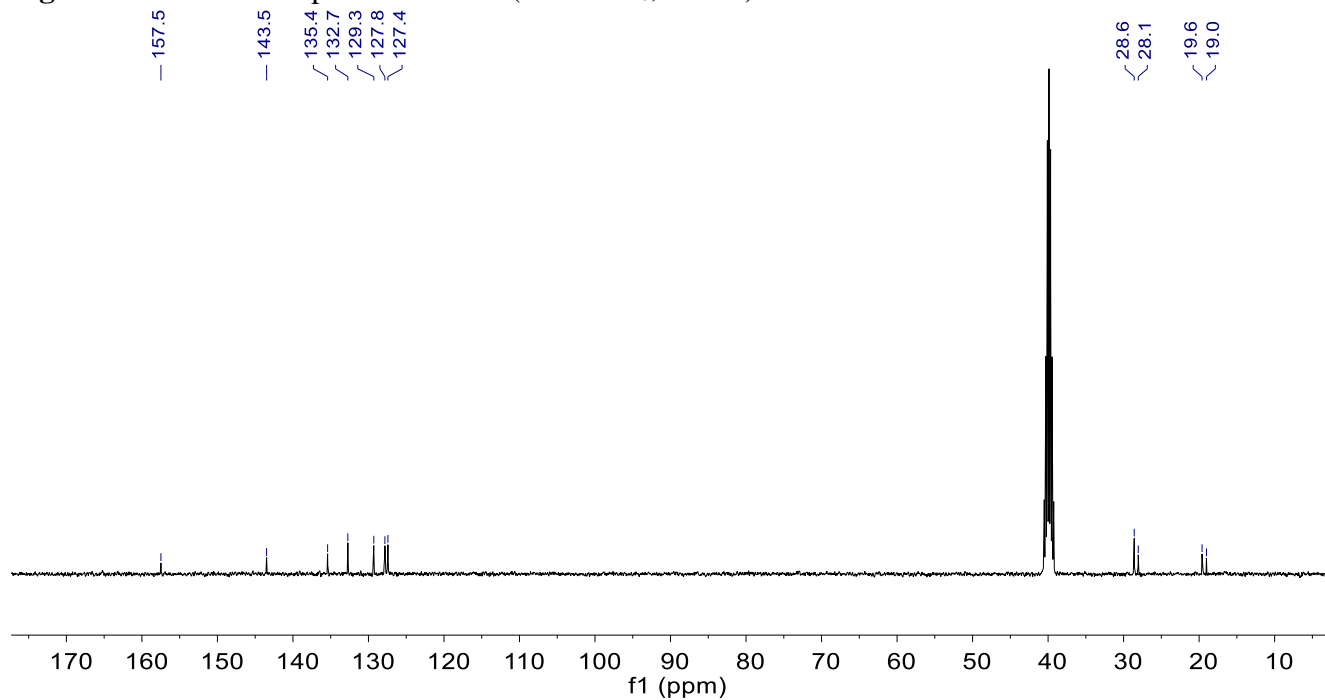
Figure S81: ^{13}C{^{1}H} NMR spectrum for **38** (DMSO-d$_6$, 295 K)

9. IR Spectra
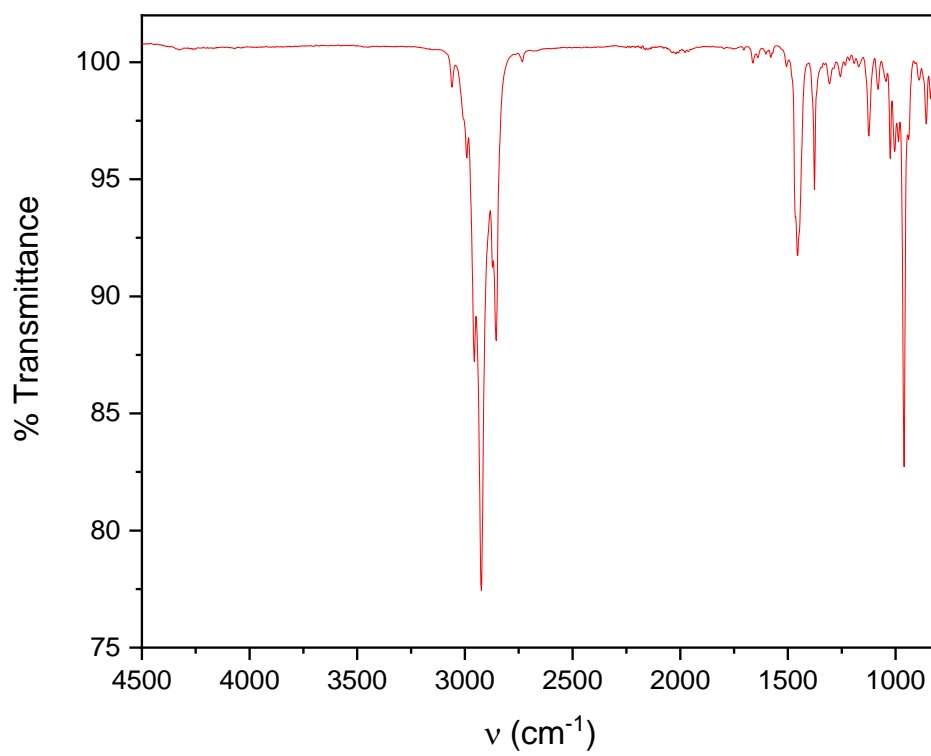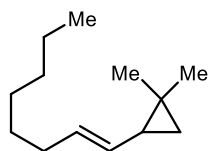
Figure S82: ATR-IR spectrum for **2**
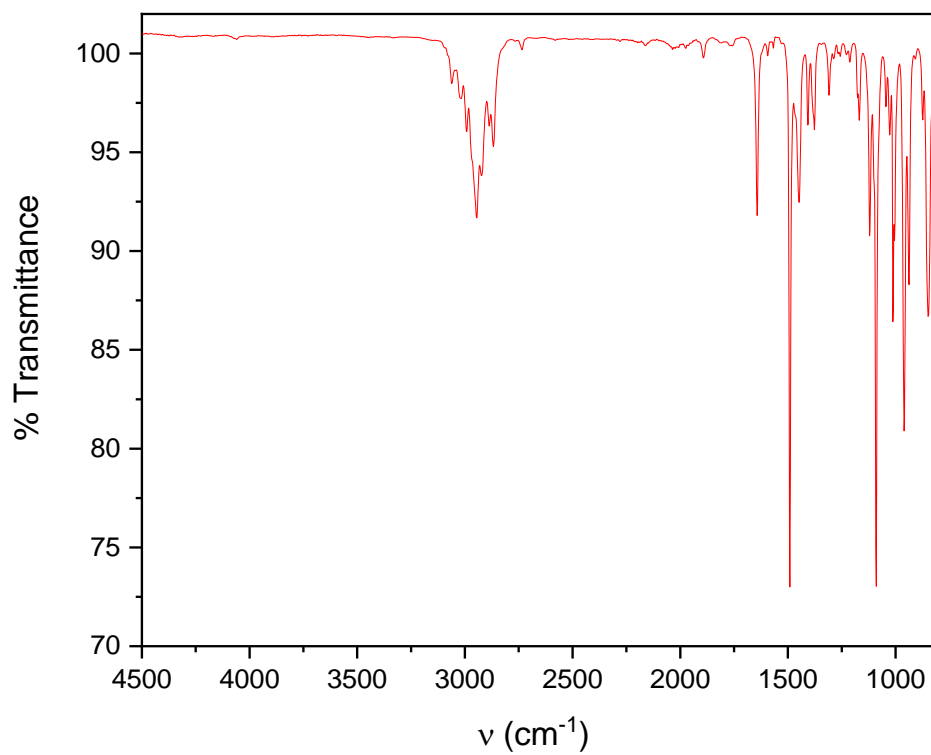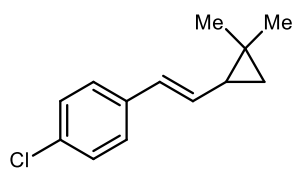
Figure S83: ATR-IR spectrum for **4**
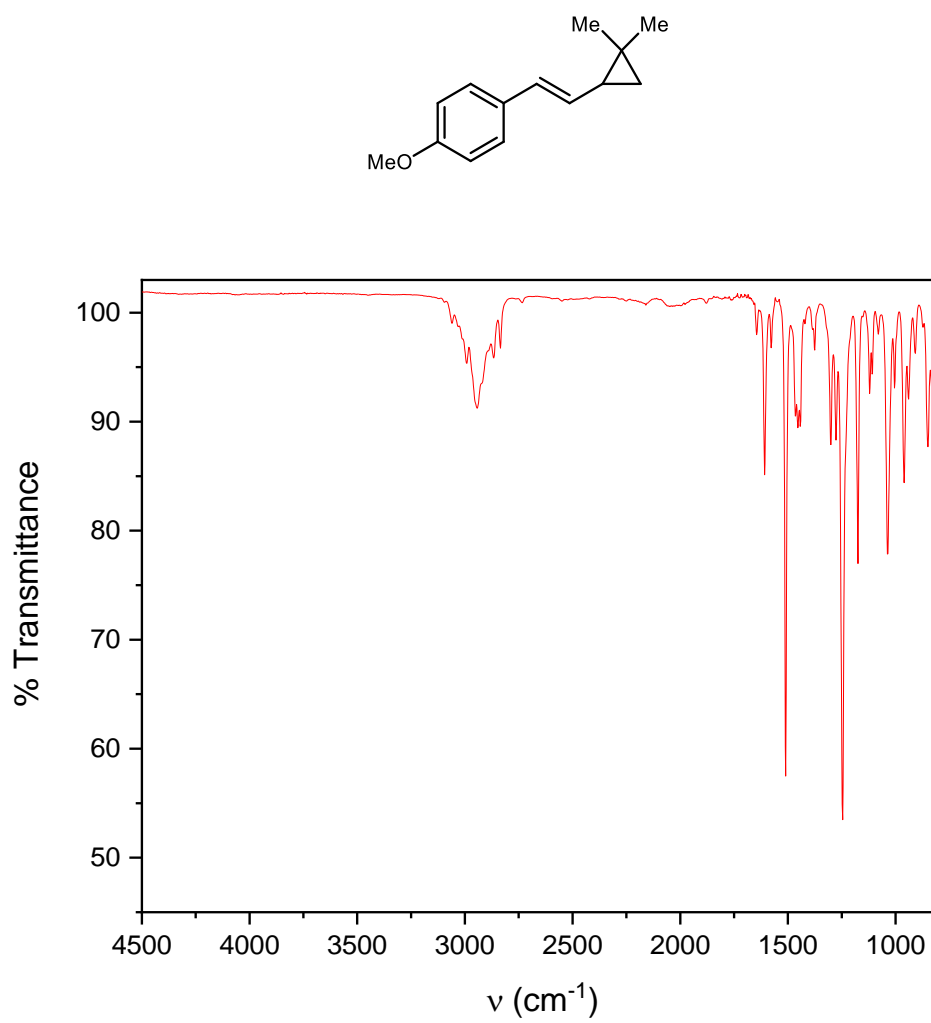
Figure S84: ATR-IR spectrum for **5**
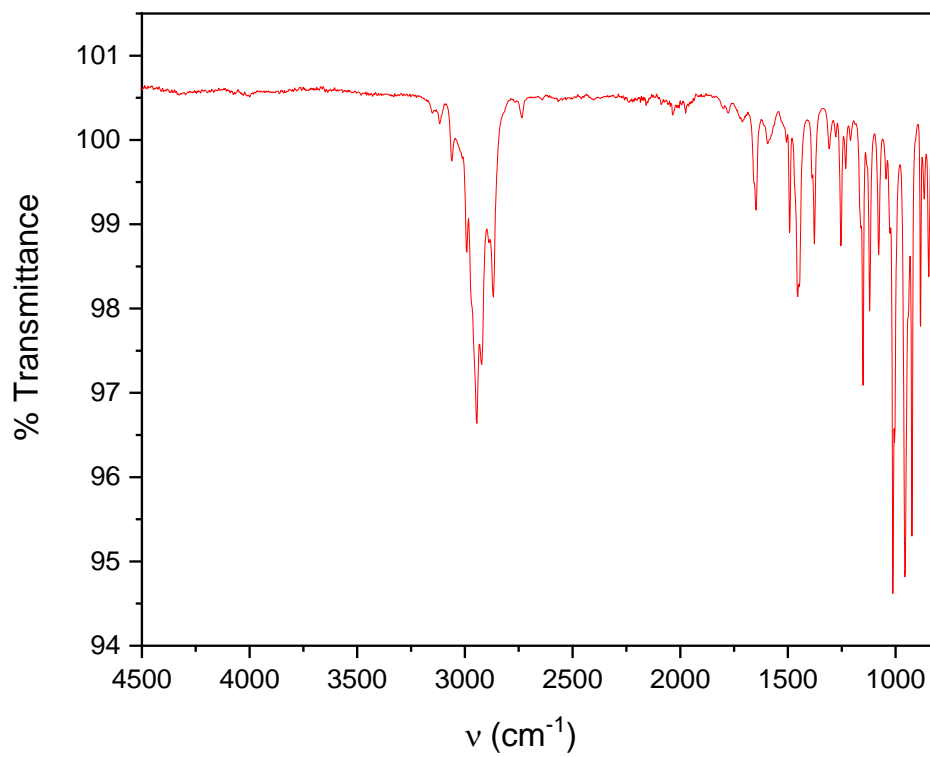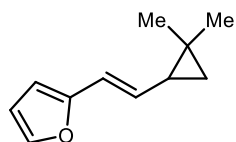
Figure S85: ATR-IR spectrum for **6**
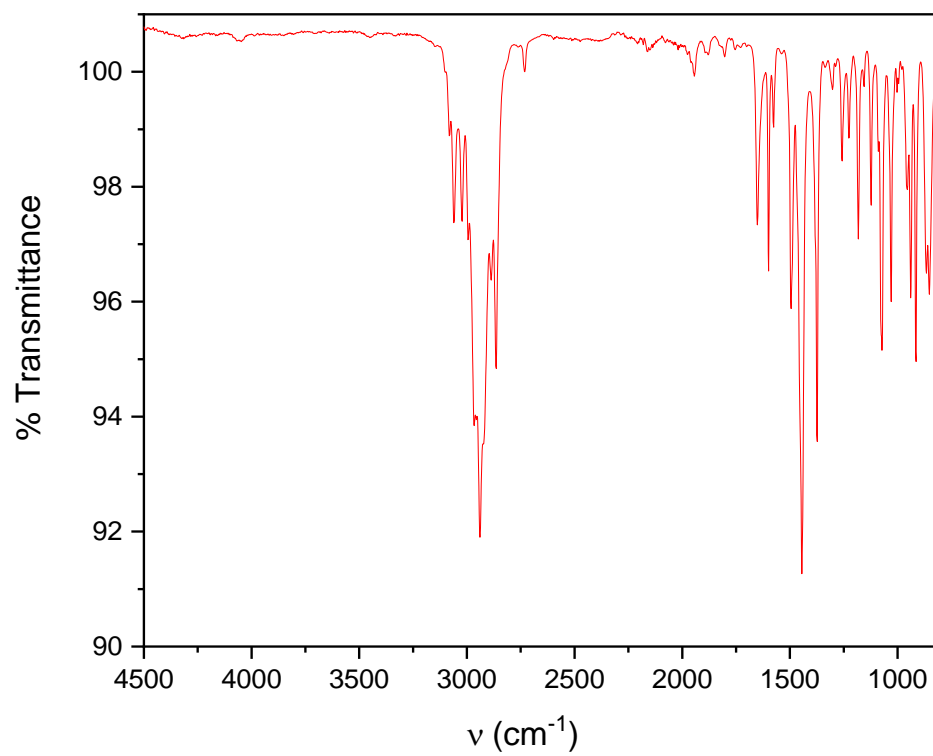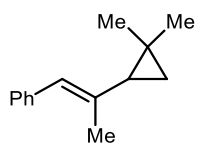
Figure S86: ATR-IR spectrum for **7**
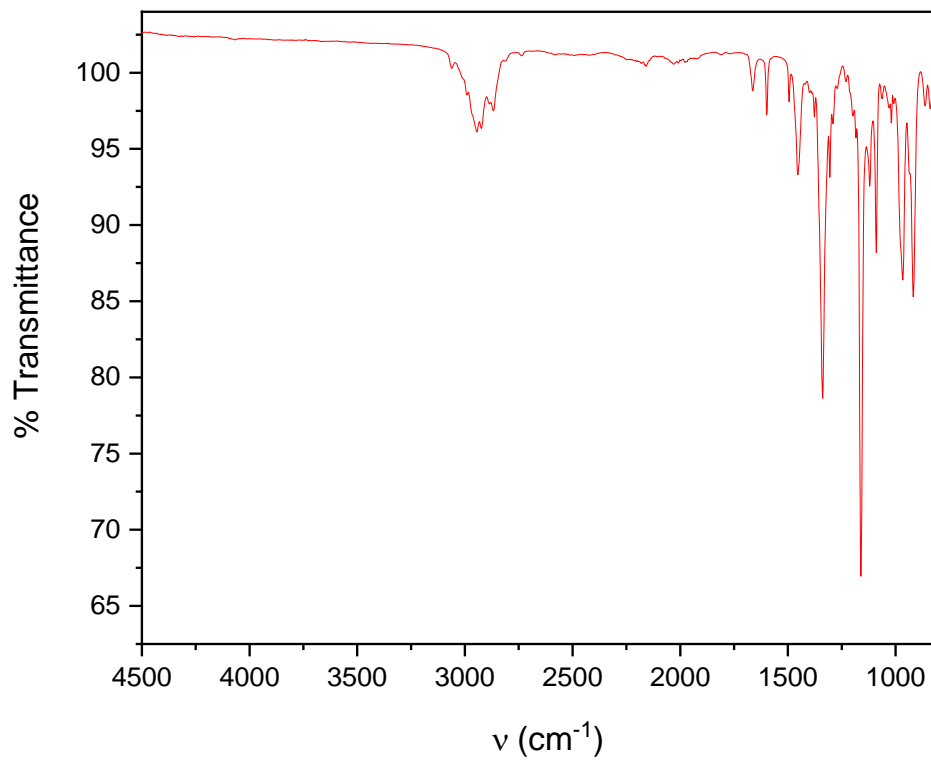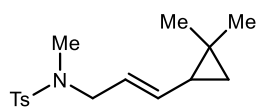
Figure S87: ATR-IR spectrum for **8**
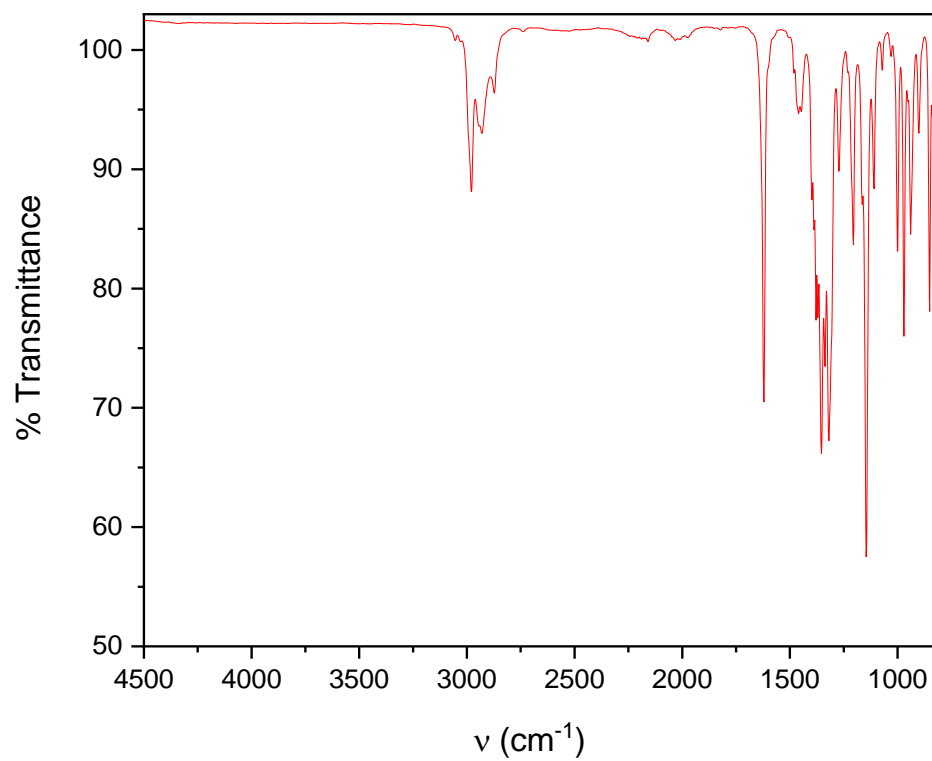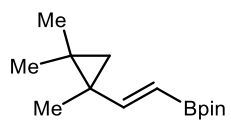
Figure S88: ATR-IR spectrum for **9**
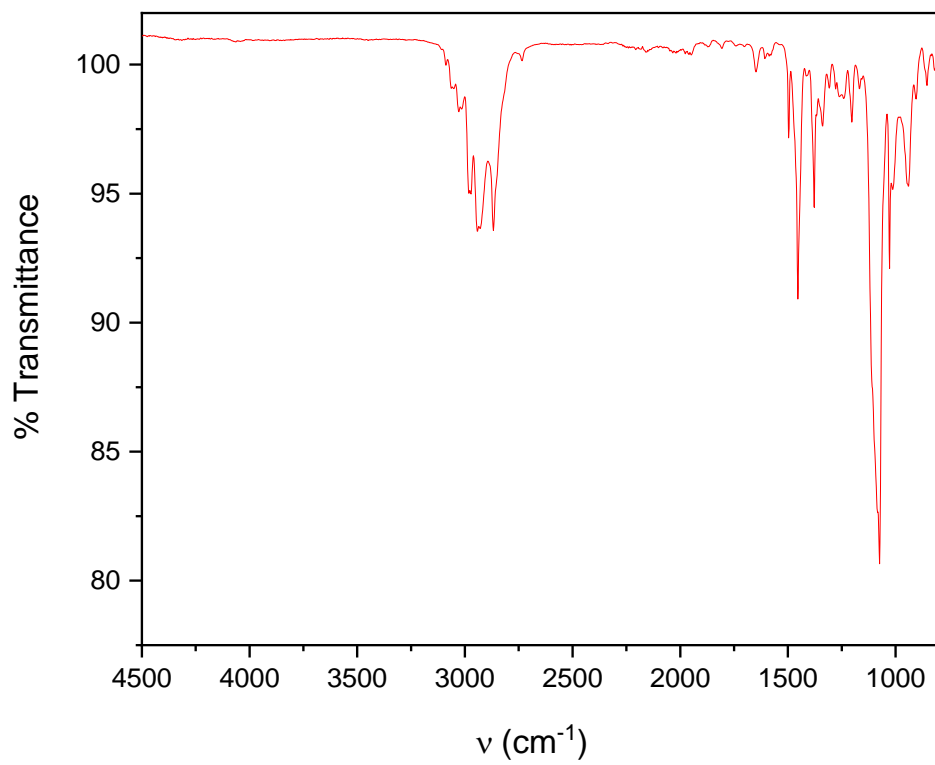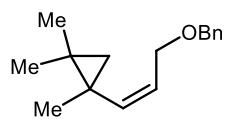
Figure S89: ATR-IR spectrum for **10**
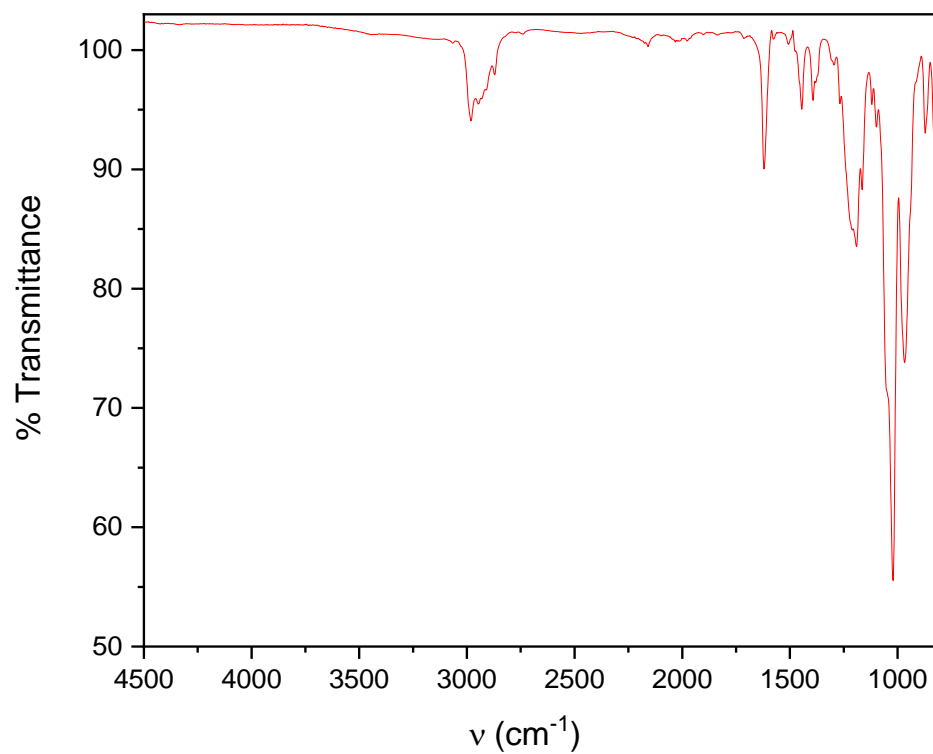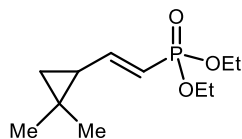
Figure S90: ATR-IR spectrum for **11**
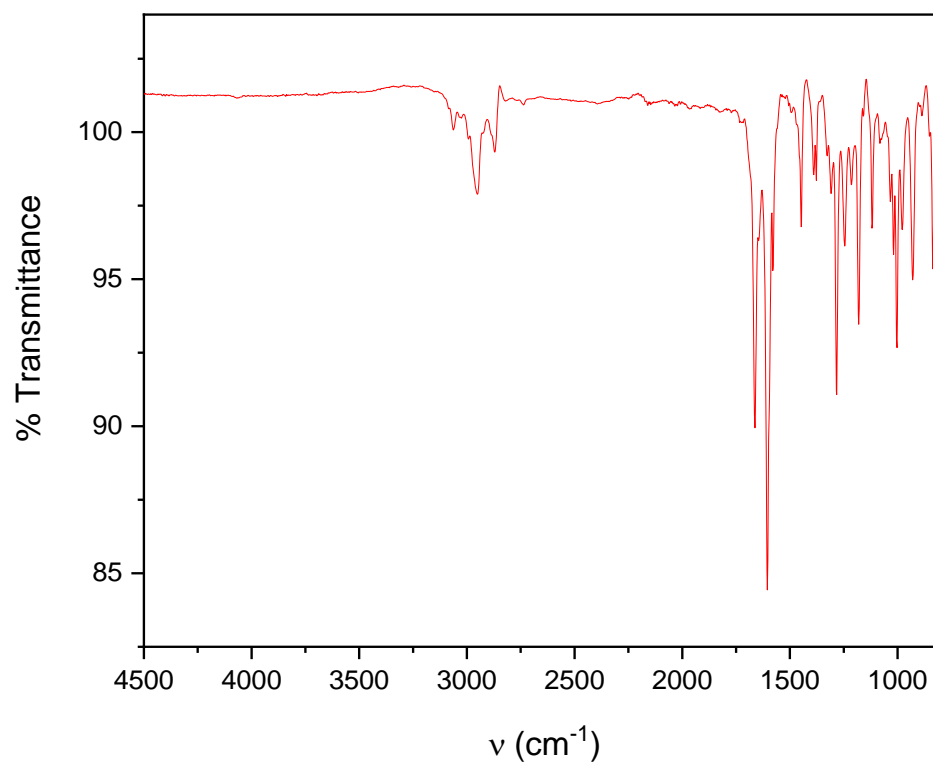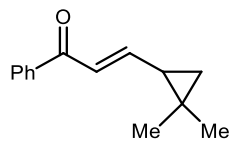
Figure S91: ATR-IR spectrum for **12**
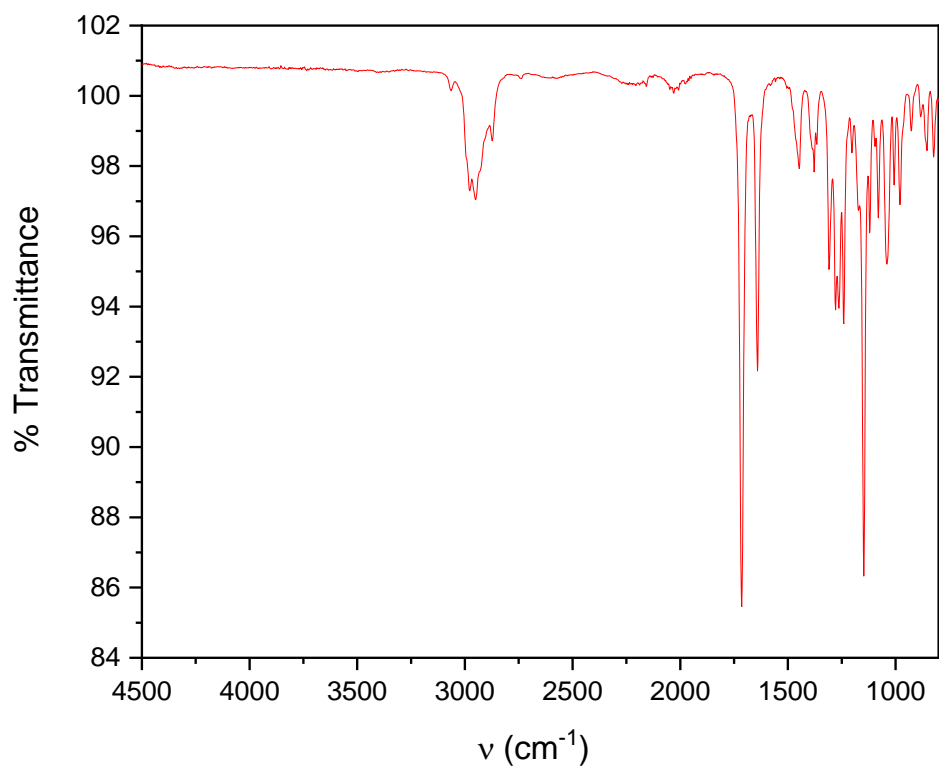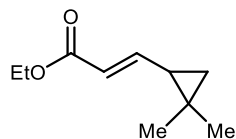
Figure S92: ATR-IR spectrum for **13**
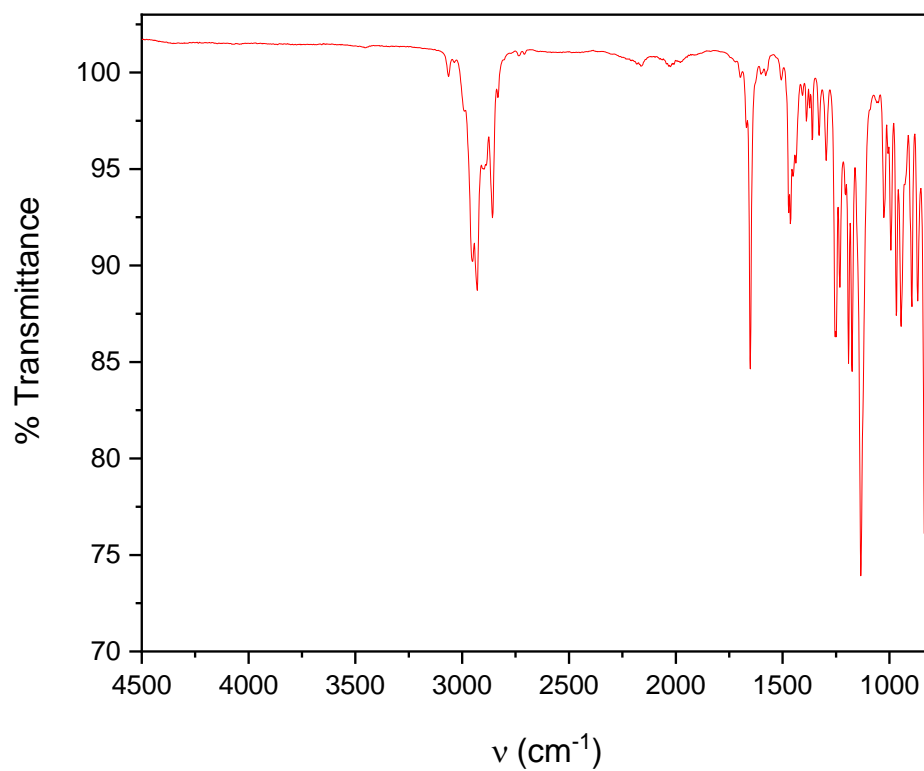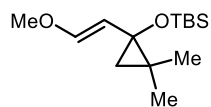
Figure S93: ATR-IR spectrum for **14**
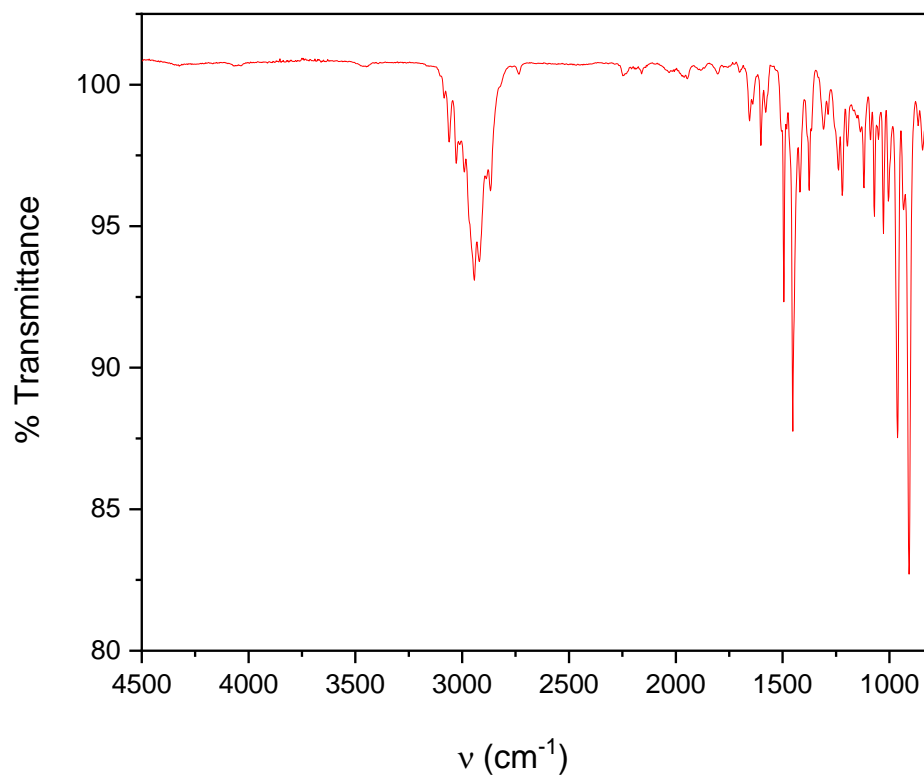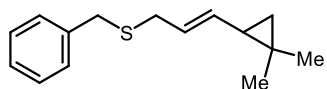
Figure S94: ATR-IR spectrum for **15**
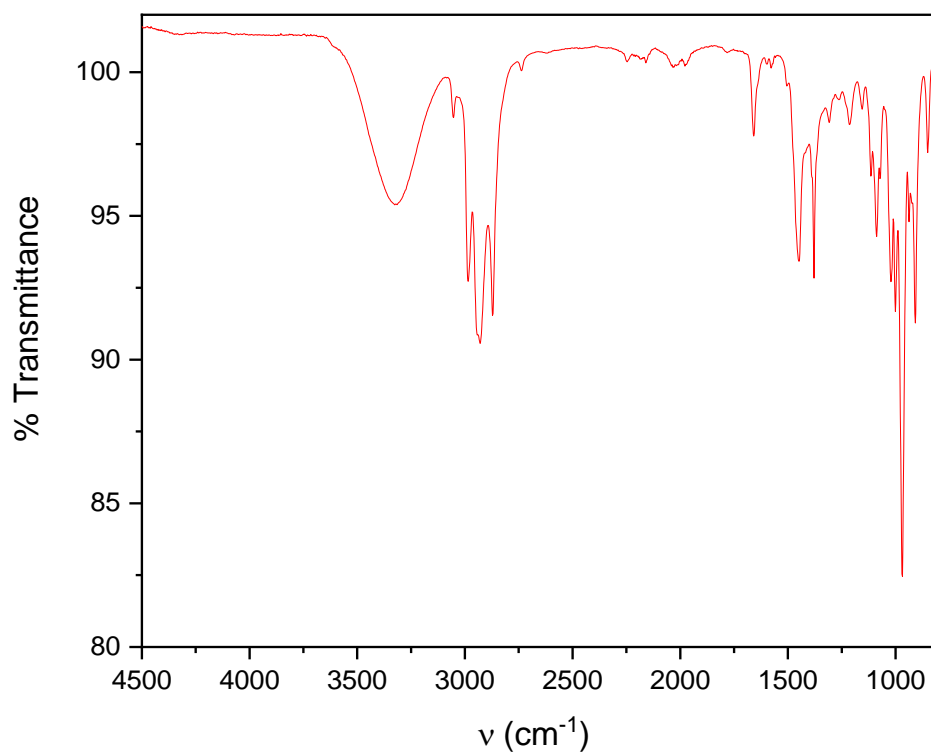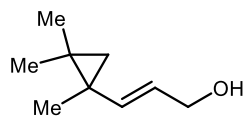
Figure S95: ATR-IR spectrum for **18**
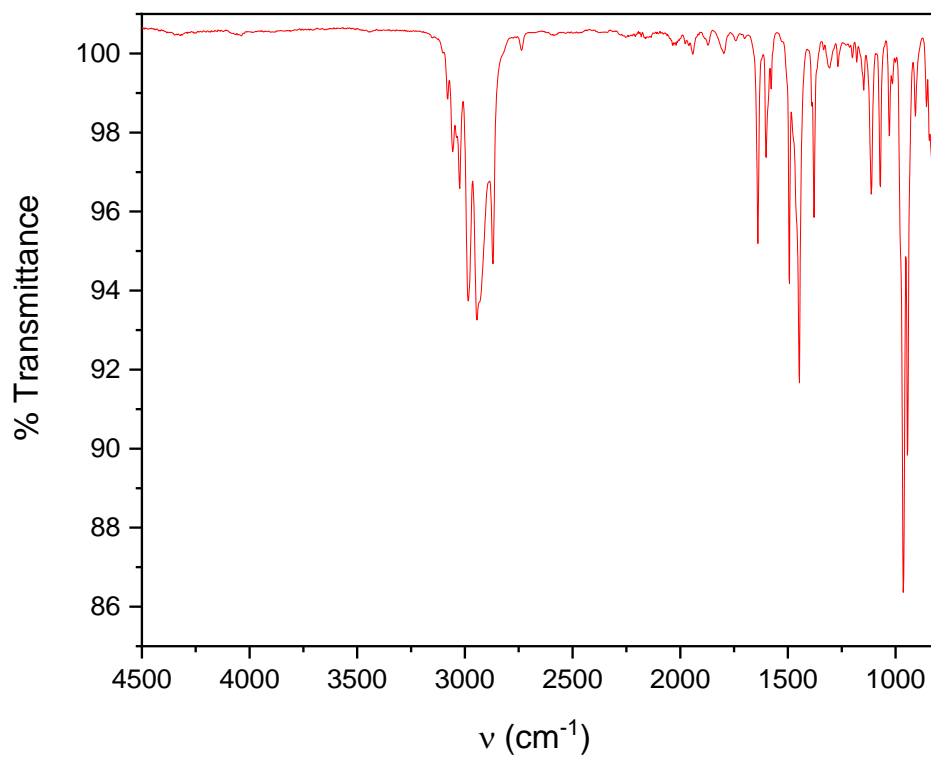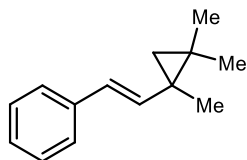
Figure S96: ATR-IR spectrum for **26**
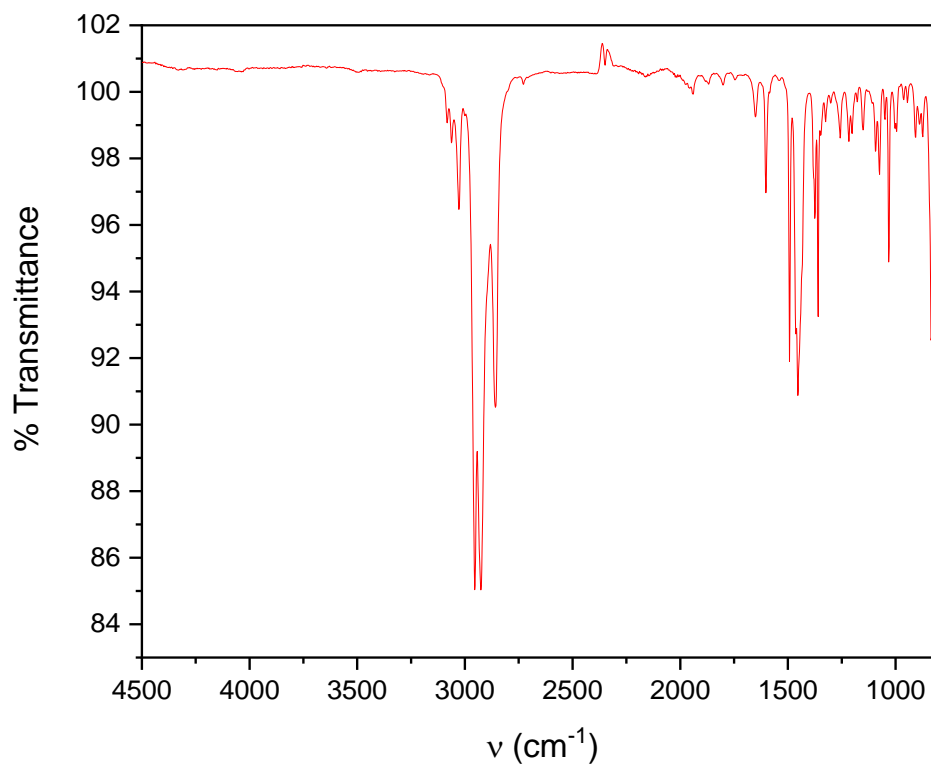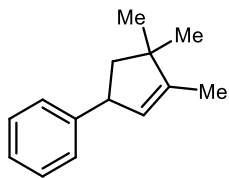
Figure S97: ATR-IR spectrum for **27**
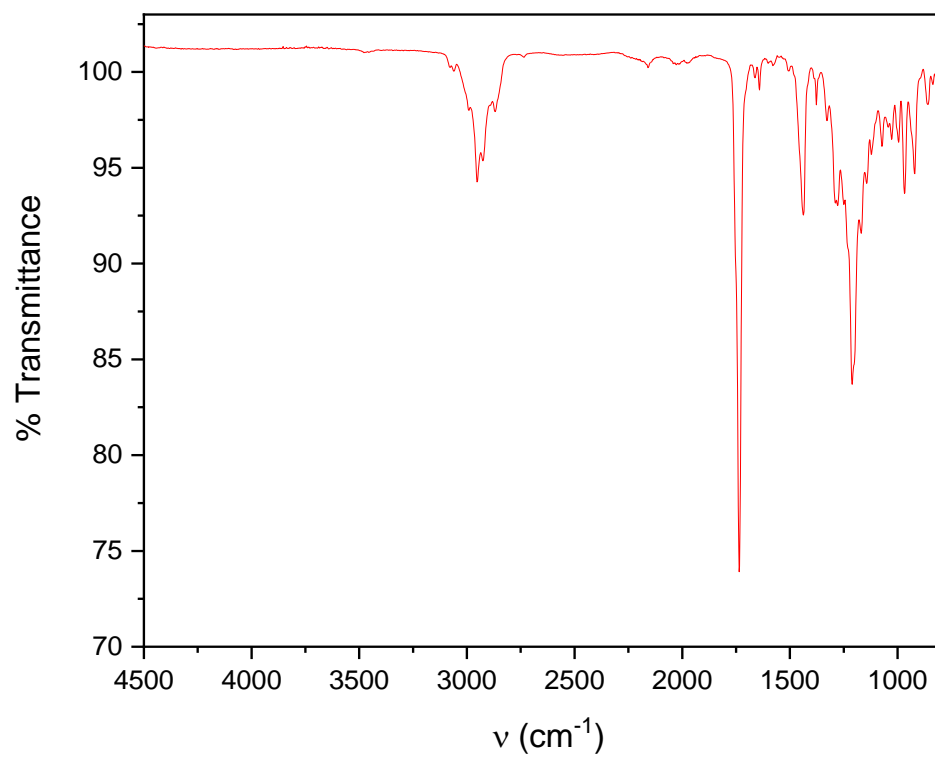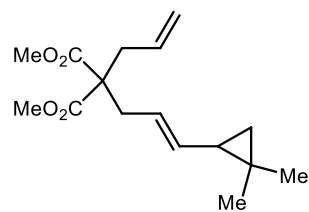
Figure S98: ATR-IR spectrum for **28**
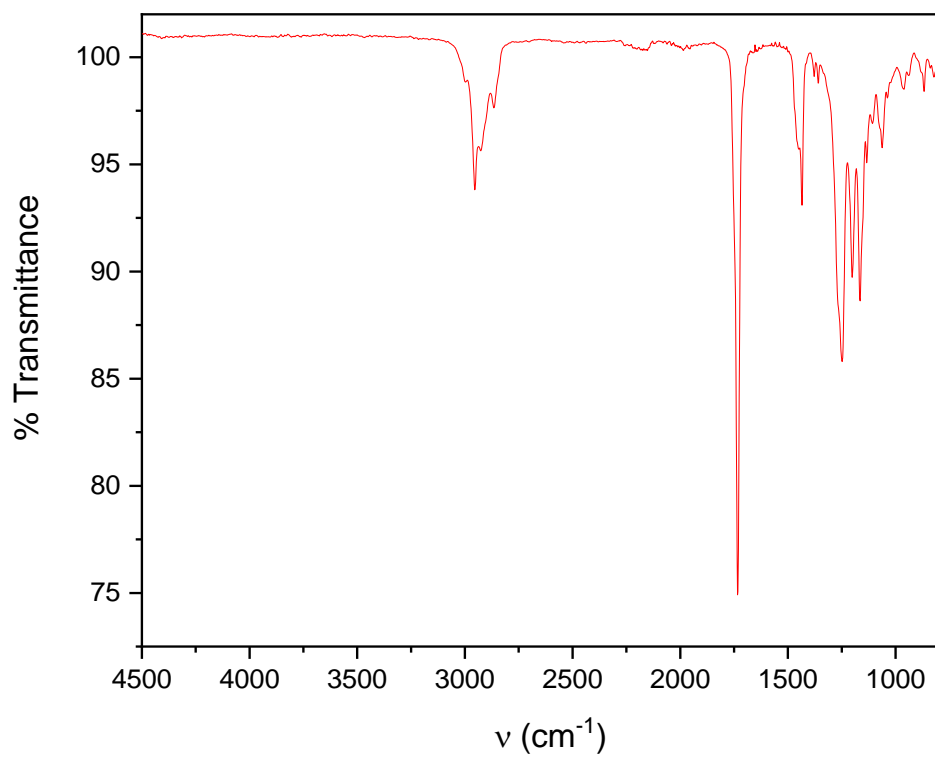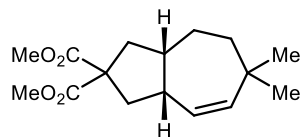
Figure S99: ATR-IR spectrum for **29**
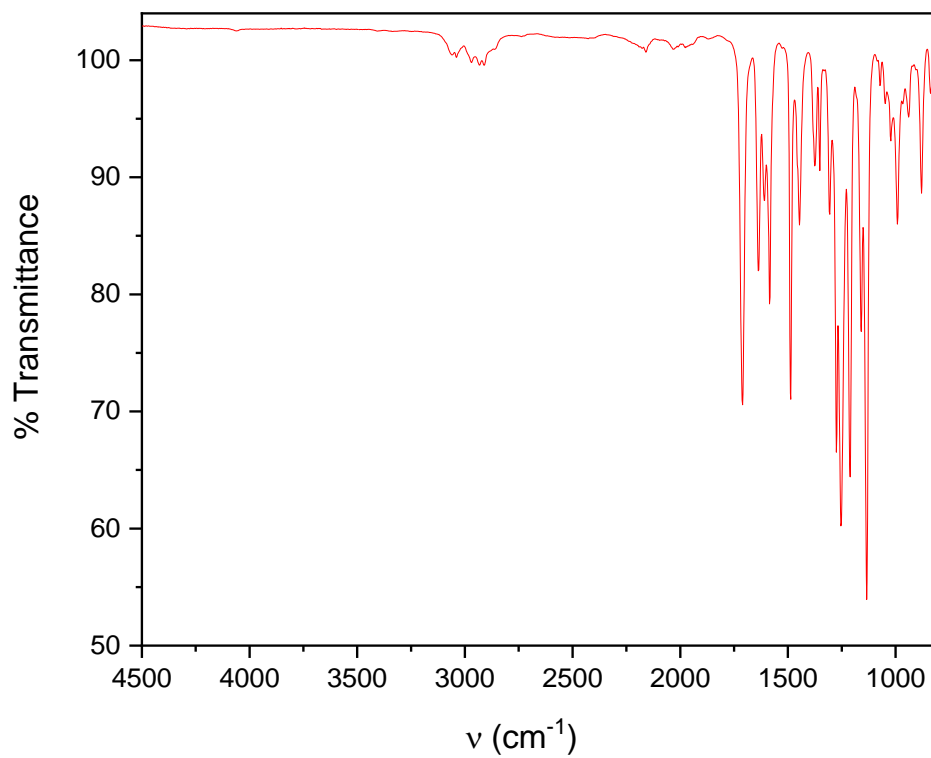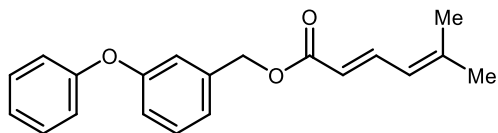
Figure S100: ATR-IR spectrum for **S2**
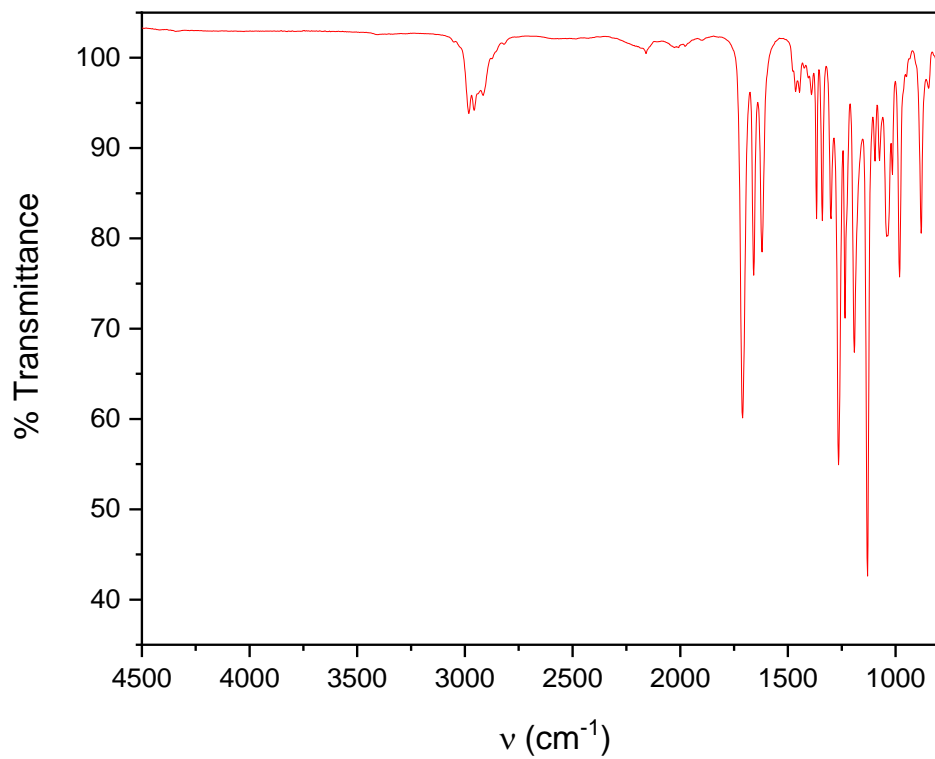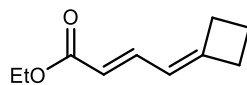
Figure S101: ATR-IR spectrum for **S3**
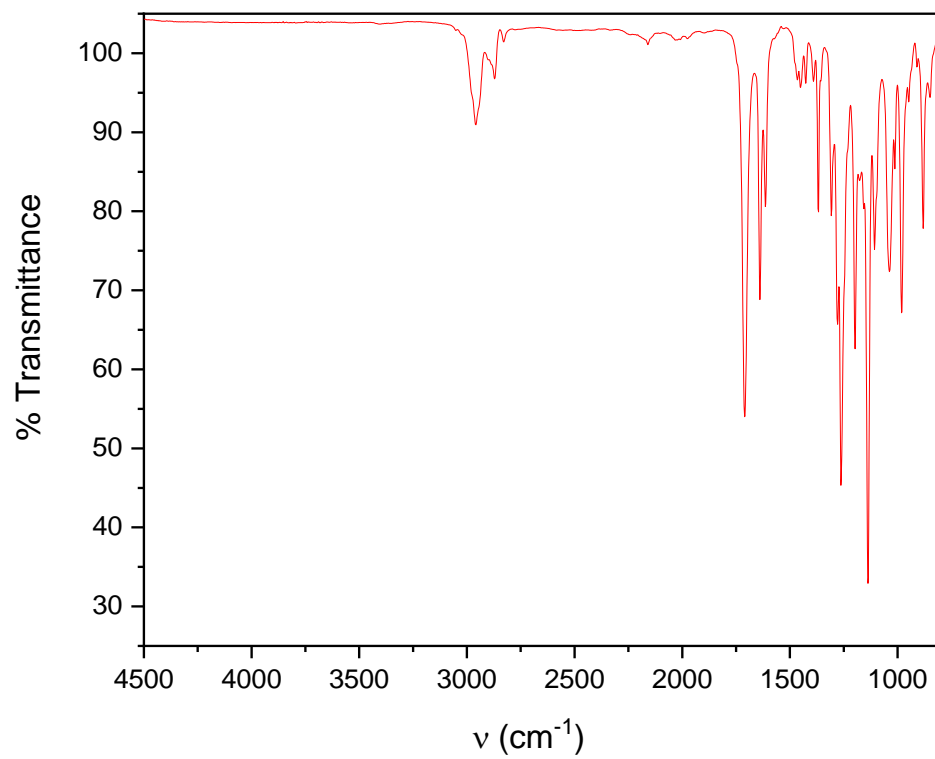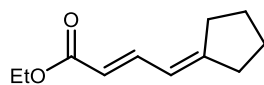
Figure S102: ATR-IR spectrum for **S4**
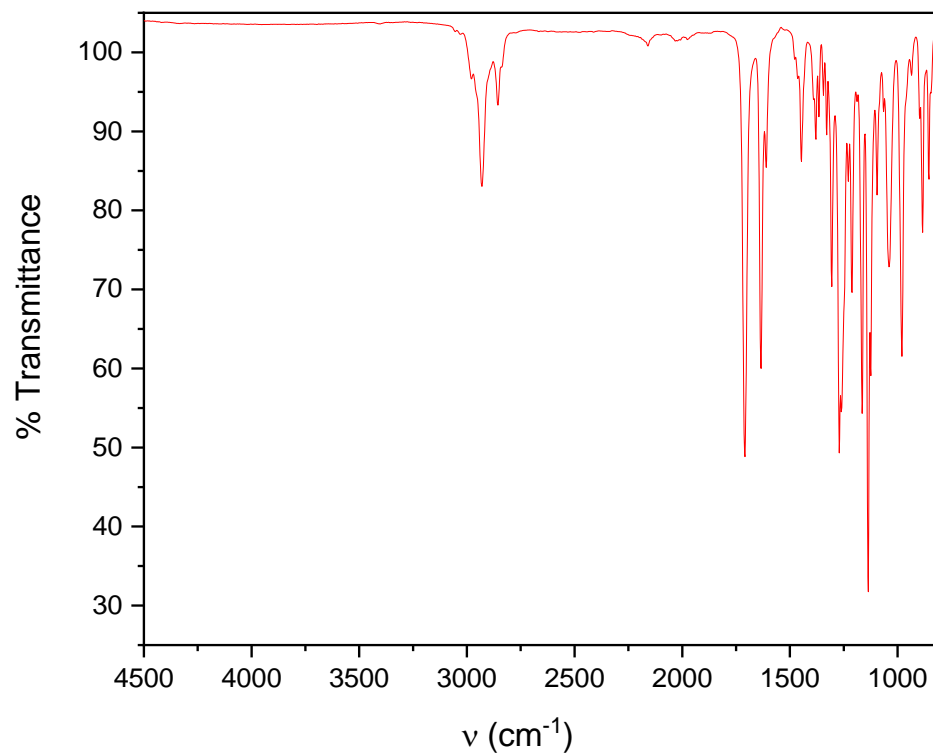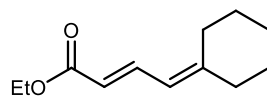
Figure S103: ATR-IR spectrum for **S5**
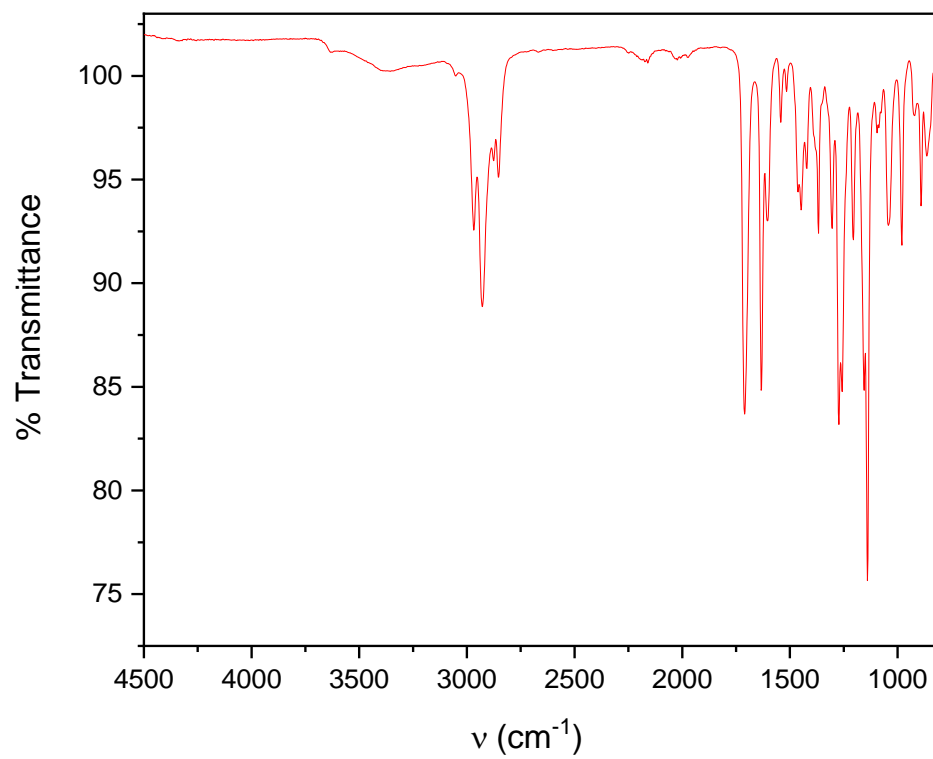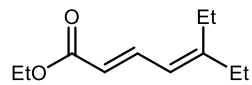
Figure S104: ATR-IR spectrum for **S6**
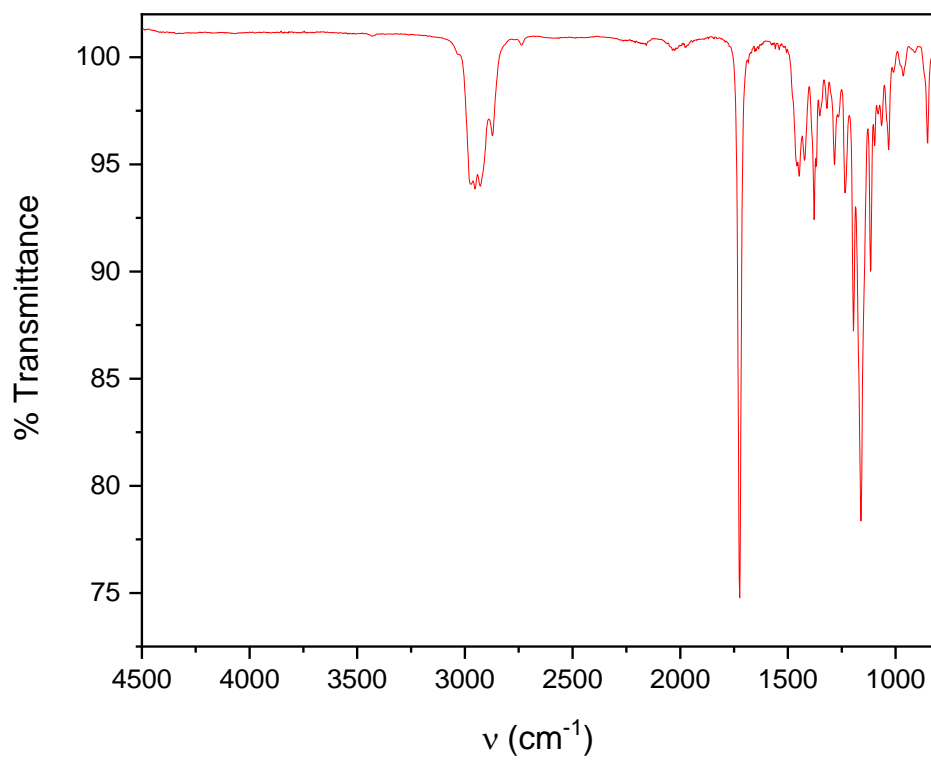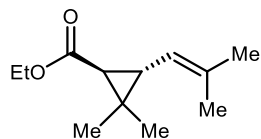
Figure S105: ATR-IR spectrum for **19**
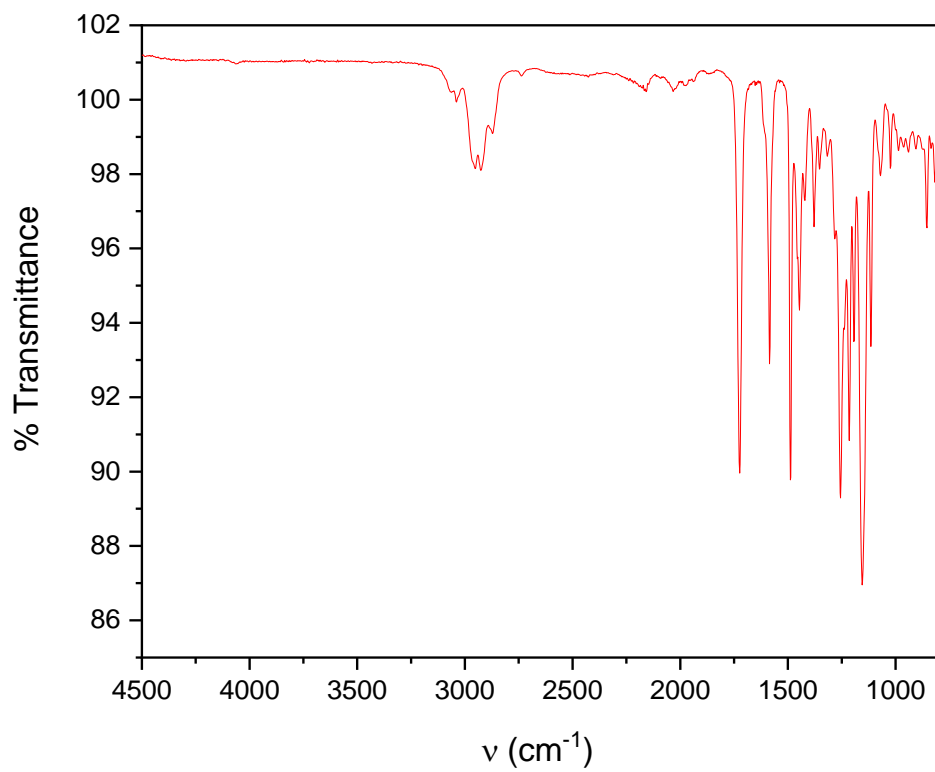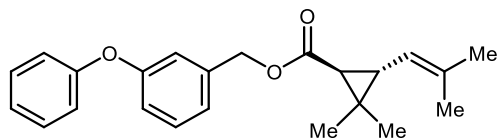
Figure S106: ATR-IR spectrum for **20**
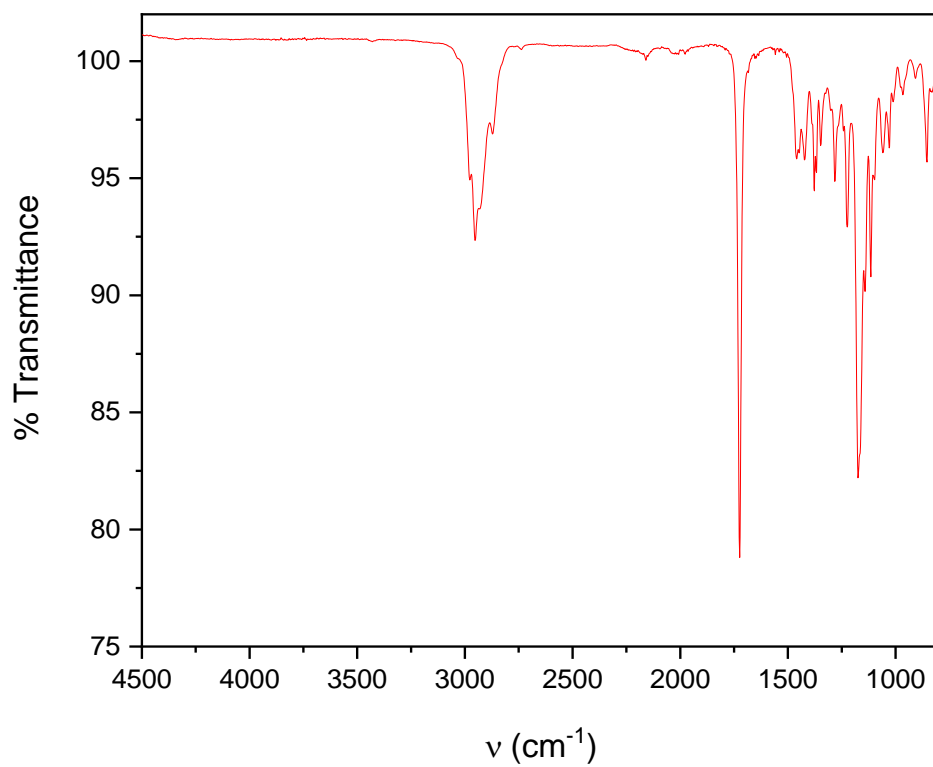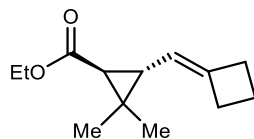
Figure S107: ATR-IR spectrum for **21**
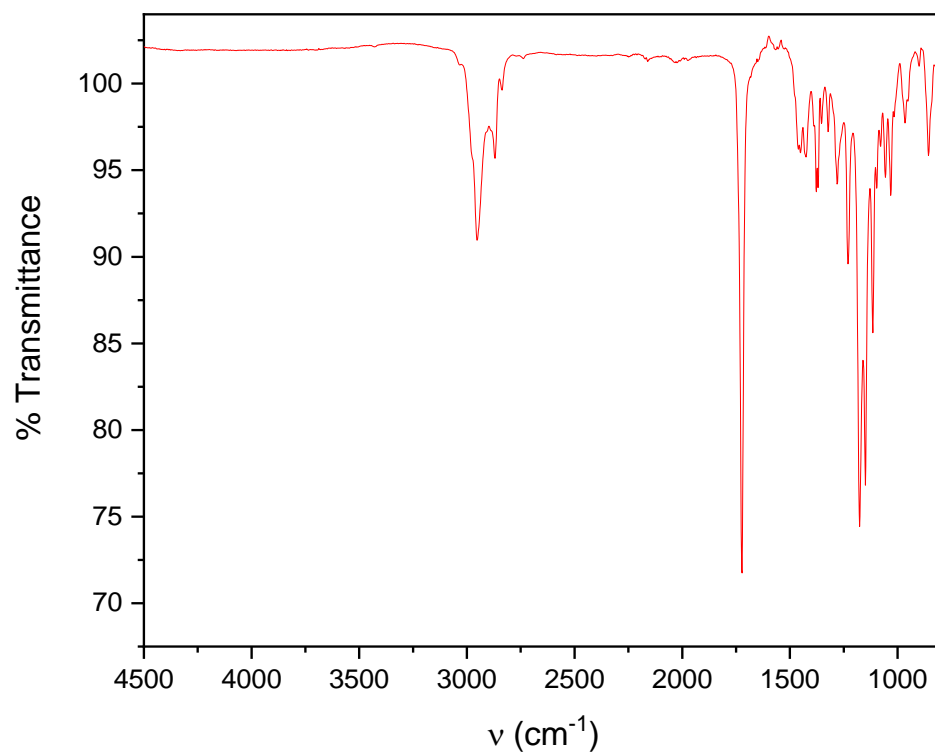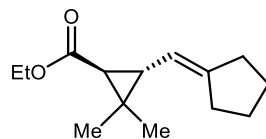
Figure S108: ATR-IR spectrum for **22**
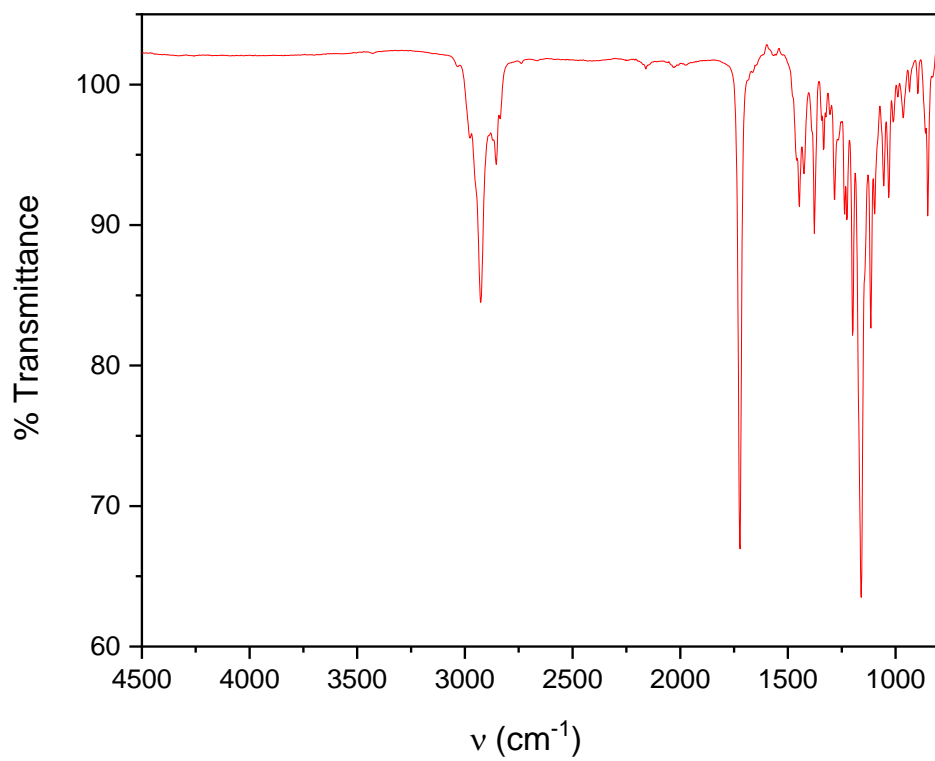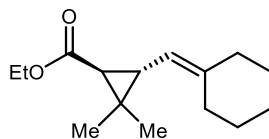
Figure S109: ATR-IR spectrum for **23**
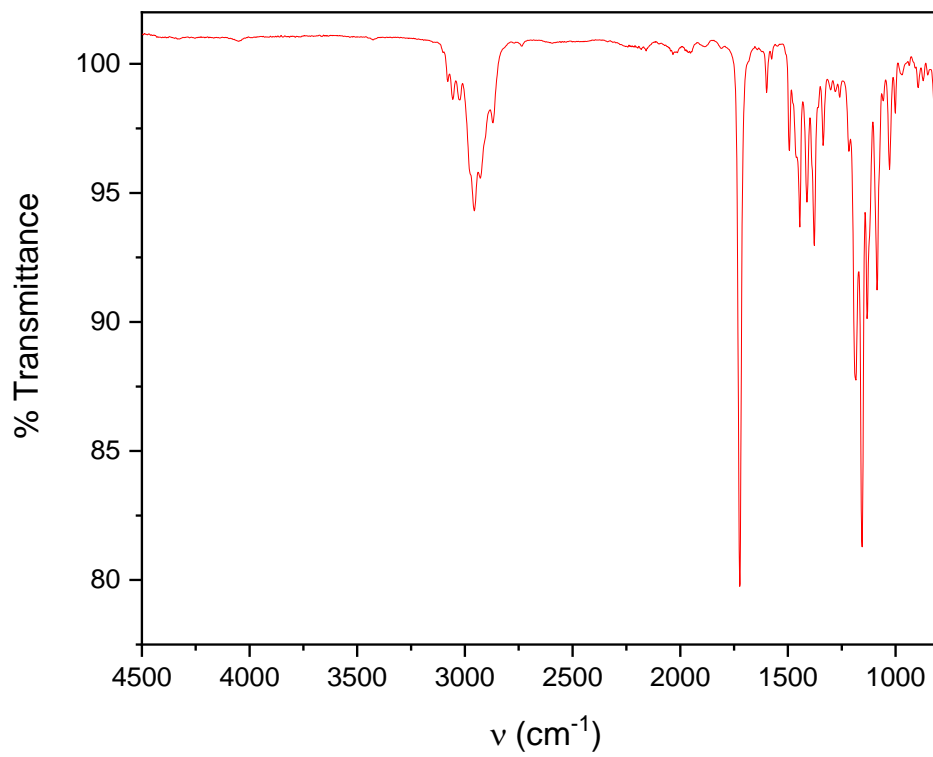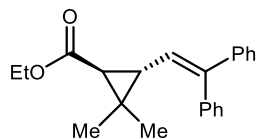
Figure S110: ATR-IR spectrum for **24**
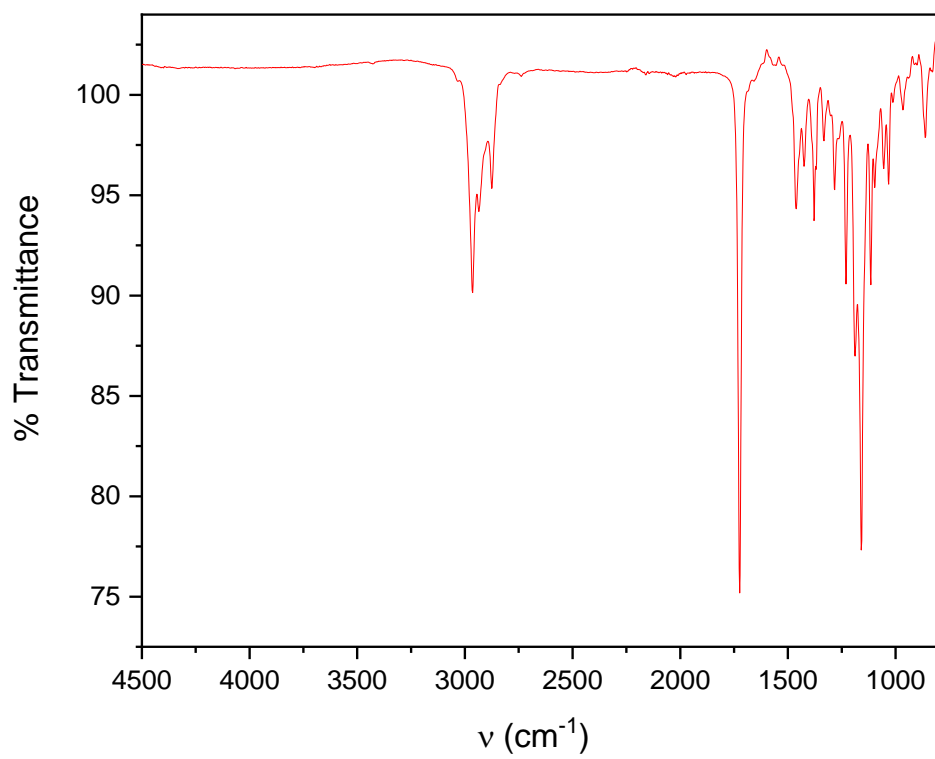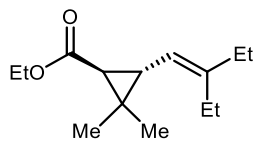
Figure S111: ATR-IR spectrum for **25**
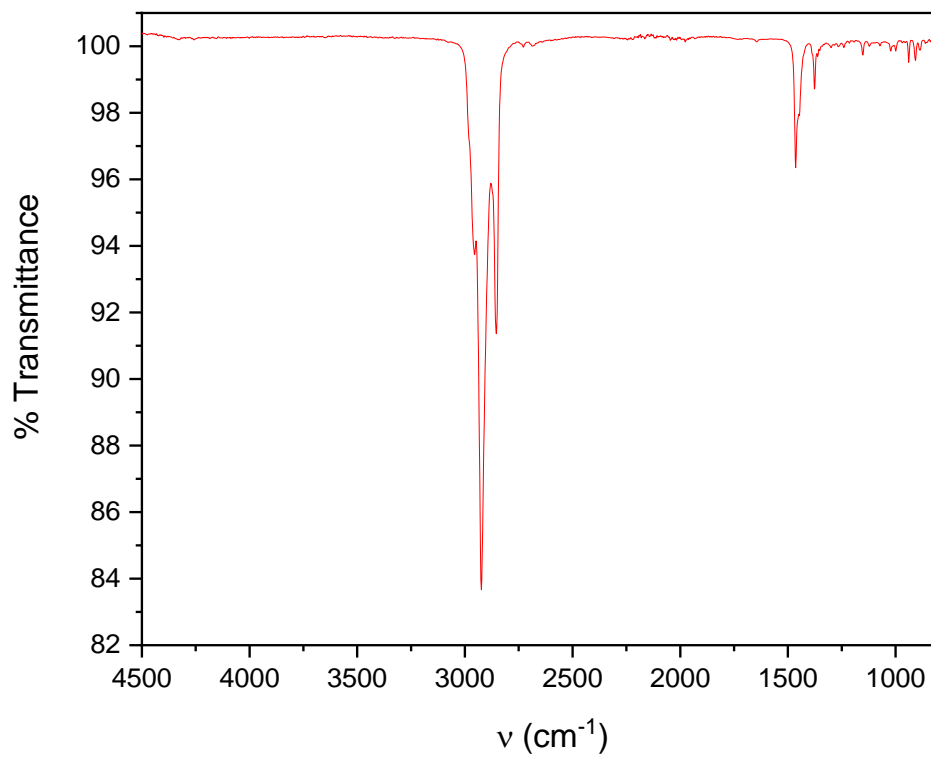
Figure S112: ATR-IR spectrum for **31**
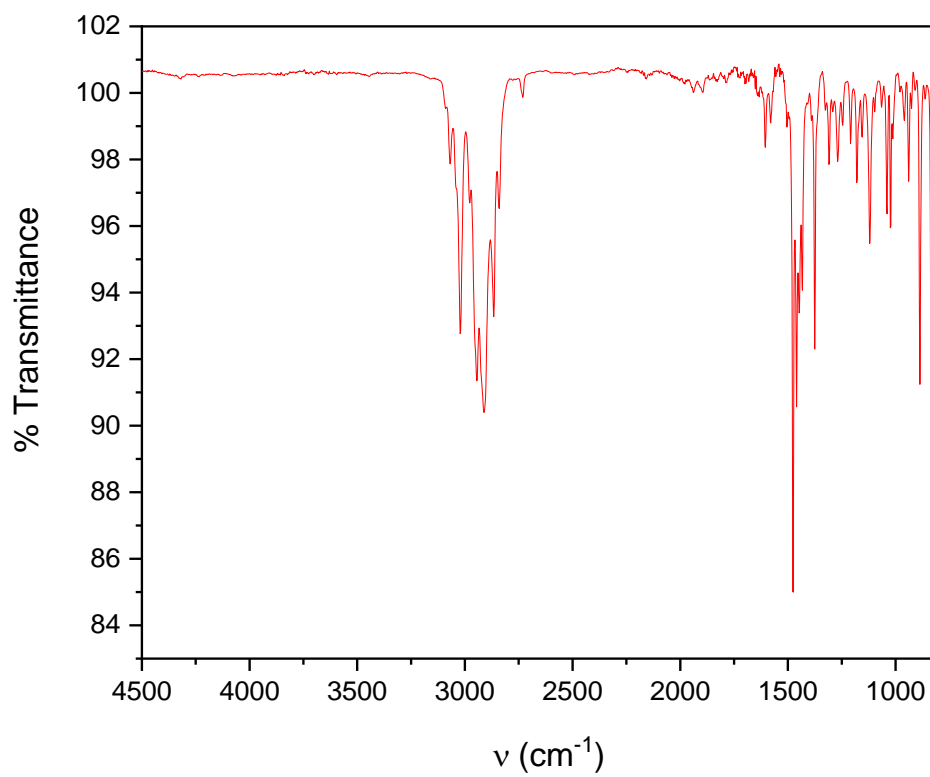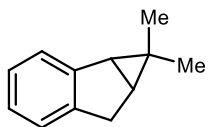
Figure S113: ATR-IR spectrum for **32**
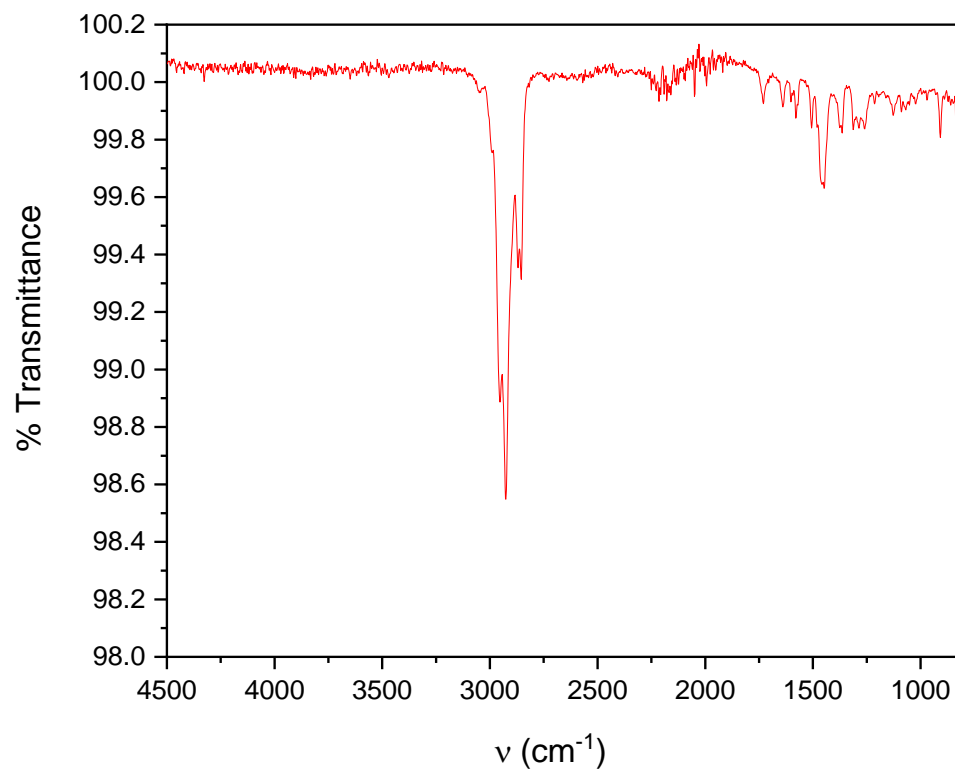
Figure S114: ATR-IR spectrum for **33**
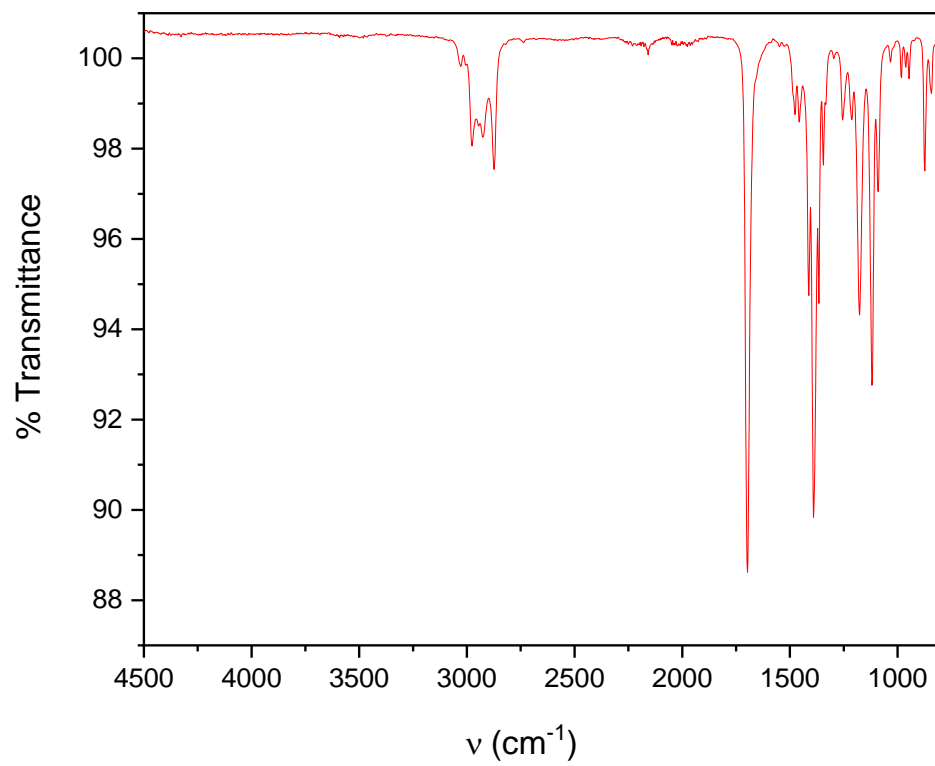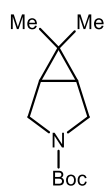
Figure S115: ATR-IR spectrum for **35**
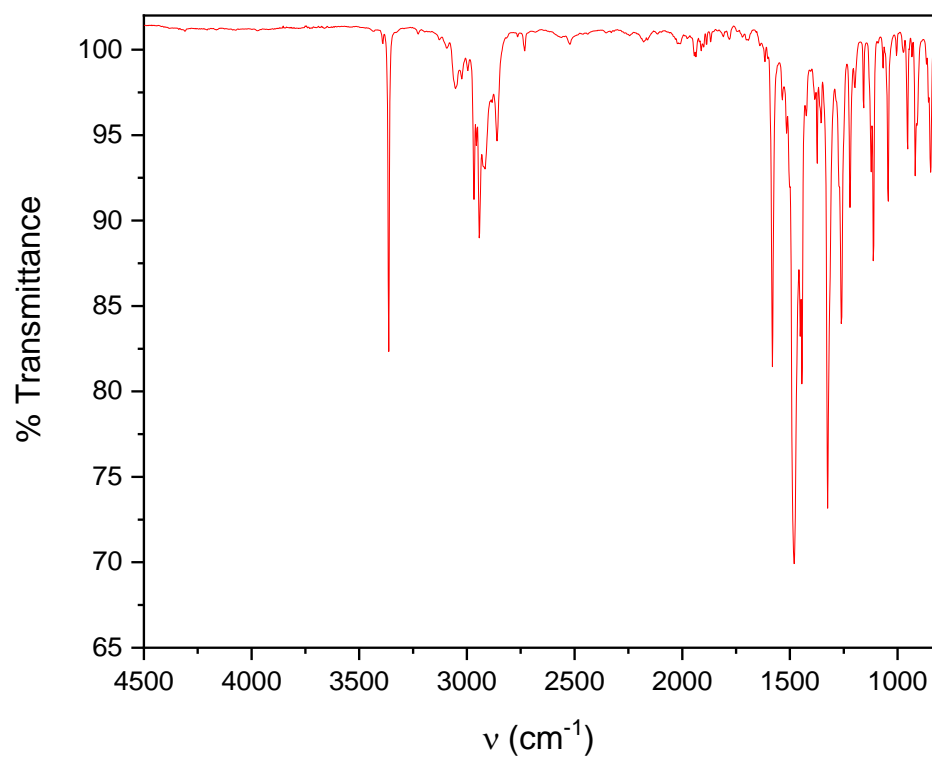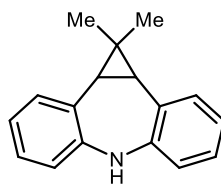
Figure S116: ATR-IR spectrum for **37**
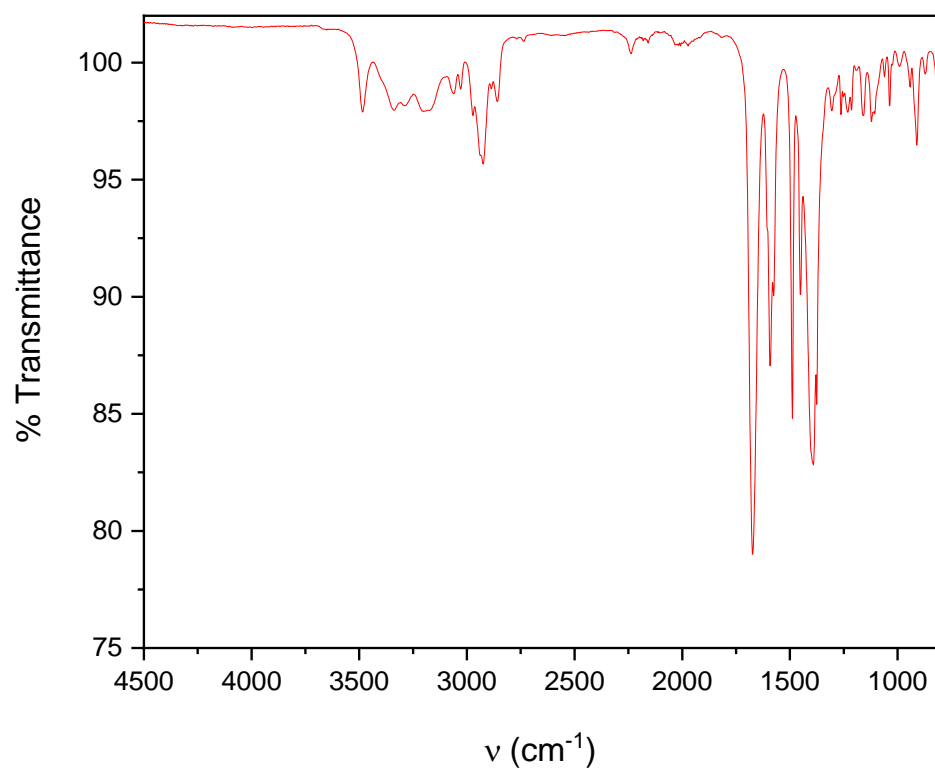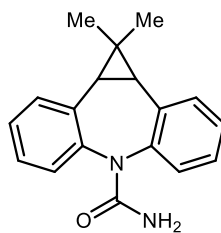
Figure S117: ATR-IR spectrum for **38**

10.References

[1] Wei, L.; Yang, Y.; Fan, R.; Wang, P.; Li, L.; Yu, J.; Yang, B.; Cao, W. RSC Adv. 2013. 3, 25908-25916.

[2] A. M. A. Bennett (DuPont), WO Pat., 98/27124, 1998.

[3] Charette, A. B.; Wilb, N.; Synlett, 2002, 1, 0176-0178.

[4] Redies, K. M.; Fallon, T.; Oestreich, M. Organometallics, 2014, 33, 3235-3238.

[5] Britovsek, G.J.P.; Bruce, M.; Gibson, V.C.; Kimberley, B.S.; Maddox, P.J.; MastroIannni, S.; McTavish, S.J.; Redshaw, C.; Solan, G.A.; Stromberg, S.; White, A.J.P.; Williams, D.J. J. Am. Chem. Soc. 1999, 121, 8728-8740.

[6] Ardolino, M.J.; Morken, J.P. J. Am. Chem. Soc. 2012, 134, 8770-8773.

[7] Marcum, J.S.; Roberts, C.; Manan, R.S.; Cervarich, T.N.; Meek, S.M. J. Am. Chem. Soc. 2017, 139, 15580- 15583.

[8] Sun, X.; Li, X.; Song, S.; Zhu, Y.; Lilang, Y.; Jiao, N. J. Am. Chem. Soc. 2015, 137, 6059-6066.

[9] Sargent, B.T.; Alexanian, E.J.; J. Am. Chem. Soc. 2017, 139, 12438-12440.

[10] Sarrdini, S.R.; Brown, K. J. Am. Chem. Soc. 2017, 139, 9823-9826.

[11] Kimura, M.; Ezoe, A.; Mori, M.; Tamaru, T. J. Am. Chem. Soc. 2005, 127, 201-209.

[12] Cannillo, A.; Norsikian, S.; Retailleau, P.; Dau, M. E.; Iorga, B. I.; Beau, J.M. Chem. Eur. J. 2013, 19, 9127- 9131

[13] Yu, Y.; Lin, R.; Zhang, Y. Tetrahedron, Lett. 1993, 34, 4547-4550.

[14] Zhao, D.; Lied, F.; Glorius, F. Chem. Sci. 2014, 5, 2869-2873.

[15] Turos, E.; Parvez, M.; Garigipati, R.S.; Weinreb, S. M. J. Org. Chem. 1988, 53, 1116-1118.

[16] Stevenson, S. M.; Higgins, R. F.; Shores, M. P.; Ferreira, E. M. Chem. Sci. 2017, 8, 654-660.

[17] Wender, P. A.; Christy, J.P. J. Am. Chem. Soc. 2006, 128, 5354-5355.

[18] Zuo, G.; Louie, J. Angew. Chem. Int. Ed. 2004, 43, 2277-2279.

[19] Wender, P. A.; Husfeld, C. O.; Langkopf, E.; Love, J.A. J. Am. Chem. Soc. 1998, 120, 1940-1941.

[20] Pohjala, L.; Alakurtti, S.; Ahola, T.; Yli-Kauhaluoma, J.; Tamella, P. J. Nat. Prod. 2009. 72, 1917-1926.

[21] Hatch, C.E.; Baum, J.S.; Takashima, T.; Kondo, K. J. Org. Chem. 1980, 45, 3281-3285.

[22] Abarbri, M.; Parrain, J.; Cintrat, J.; Duchene, ,A. Synthesis. 1996, 1, 82-86.

[23] Jiang, Y.; Thomson, R.J.; Schaus, S.E. Angew. Chem. Int. Ed. 2017, 56, 16631-16635.

[24] Wickham, G.; Wells, G.J.; Waykole, L.; Paquette, L.A. J. Org. Chem. 1985, 50, 3485-3489

[25] Pettigrew, J.D.; Cadieux, J.A.; So, S.S.S.; Wilson, P.D. Org. Lett. 2005, 7, 467-470.

[26] Chuit, C.; Foulon, J.P.; Normant, J.F. Tetrahedron. 1980, 36, 2305-2310.

[27] Garayalde, D.; Gomez-Bengoa, E.; Huang, X.; Goeke, A.; Nevado, C. J. Am. Chem. Soc. 2010, 132, 4720- 4730.

[28] Wint, L. T.; McCarthyl, P.A. J. Label. Compd. Radiopharm. 1988, 25, 1289-1297.

[29] Ravinder, B.; Reddy, S.R.; Sridhar, M.; Mohan, M.M.; Srinivas, K.; Reddy, A.P.; Bandichhor, R. Tetrahedron Lett. 2013, 54, 2841-2844.

Dehydrogenative Transformations of Imines Using a Heterogeneous Photocatalyst

Colby M. Adolph,[†] Jacob Werth,[†] Ramajeyam Selvaraj, Evan C. Wegener, and Christopher Uyeda*[ID]

Department of Chemistry, Purdue University, West Lafayette, Indiana 47907, United States

S Supporting Information

ABSTRACT: Heterogeneous semiconductors are underexploited as photoredox catalysts in organic synthesis relative to their homogeneous, molecular counterparts. Here, we report the use of metal/TiO_2 particles as catalysts for light-induced dehydrogenative imine transformations. The highly oxophilic nature of the TiO_2 surface promotes the selective binding and dehydrogenation of alcohols in the presence of other oxidizable and Lewis basic functional groups. This feature enables the clean photogeneration of aldehyde equivalents that can be utilized in multicomponent couplings.
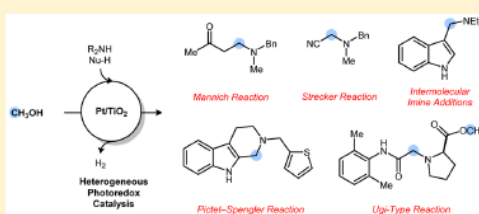
Photoredox catalysis has emerged as a powerful platform for introducing kinetically facile single-electron pathways into a broad range of organic transformations.[1] The most common photosensitizers being used in current methods are molecular transition-metal complexes or organic dyes that act as single-electron donors or acceptors in their excited state. Because these photosensitizers generally function by outersphere electron transfer,[2] designing a viable catalytic process requires carefully balancing the redox potentials of each starting material, reaction intermediate, and product. In comparison to their molecular counterparts, heterogeneous semiconductors, extensively studied in energy catalysis,[3] have seen significantly less use in organic synthesis. In principle, the ability to exploit specific interactions between surface sites and organic substrates may provide complementary tools to build selectivity into photoredox reactions.

TiO_2 is a large band gap semiconducting material. Upon excitation with UV light, TiO_2 is capable of delivering oxidizing equivalents at 3.0 V vs NHE, a potential that is sufficiently oxidizing to generate hydroxyl radicals from water.[4] Because of its potent oxidizing power, TiO_2 has garnered interest as a photocatalyst for water or air purification, where the complete degradation of all organic contaminants to CO_2 is desired.[5] Recently, the oxophilic nature of the TiO_2 surface has been exploited to bind alcohol substrates and enable their mild dehydrogenation under less energetic visible/near-UV light illumination.[6] When coupled with an efficient proton reduction catalyst, such as Pt metal, the reaction can be conducted under strictly anaerobic conditions, generating H_2 as the sole stoichiometric byproduct.[7] This approach presents an attractive alternative to dark transition-metal catalyzed alcohol dehydrogenation methods, which often require high temperatures and/or the use of stoichiometric oxidants.[8,9]

Metal/TiO_2-mediated alcohol dehydrogenations have been predominantly studied from the perspective of renewable H_2 generation;[3,7] however, there is significant underexplored potential for their application in more complex organic transformations.[10] Realizing this goal would require establishing the compatibility of these large band gap semiconductors with redox-sensitive functional groups. Here, we report our initial efforts to explore these concepts in a series of multicomponent imine transformations (Figure 1). Light-induced, dehydrogenative variants of the Pictet–Spengler cyclization, the Strecker reaction, the Mannich reaction, and Ugi-type couplings are described.

Figure 1. A photocatalytic scheme for dehydrogenative imine transformations using a Pt/TiO_2 catalyst.

We initiated our studies by preparing known platinized TiO_2 materials by photodepositing H_2PtCl_6 (0.5 wt % Pt) onto P25 TiO_2 using i-PrOH as a sacrificial reductant.[11] This relatively straightforward catalyst preparation avoids the need for high-temperature calcination, which is a commonly employed alternative procedure described in the literature.[12] The Pictet–Spengler cyclization of tryptamine substrate 1 served as an appropriate venue to test the compatibility of photocatalytic alcohol dehydrogenation with oxidizable functional groups, including a secondary amine and an electron-rich

heterocycle. It is noteworthy in this context that **1** undergoes electrochemical degradation at 1.2 V vs NHE (see Supporting Information for CV data), which is significantly less positive than the valence band potential of TiO_2. Consequently, when solutions of **1** in MeOH were combined with Pt/TiO_2 and irradiated under a high-energy, 254 nm light source, rapid decomposition was observed, forming an intractable mixture of products (Figure 2a).
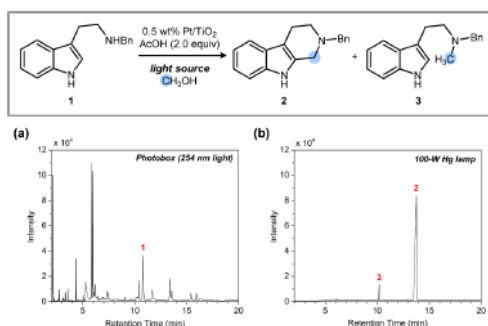
Figure 2. Gas chromatography data for photocatalytic dehydrogenative Pictet−Spengler cyclizations conducted using (a) a 254 nm light source in a photobox or (b) a 100-W Hg lamp.

Aliphatic alcohols, such as MeOH, coordinate to the Lewis acidic TiO_2 surface, creating higher energy donor levels that can be excited using less energetic photons. Accordingly, when the same reaction shown in Figure 2 is illuminated with a 100-W Hg lamp (Figure 2b), MeOH dehydrogenation proceeds cleanly to form formaldehyde equivalents that are incorporated into the tetrahydro-β-carboline product **2** (90% isolated yield). The *N*-methylated product **3** is observed as a minor side product (6% yield). The formation of H_2 as a stoichiometric byproduct was confirmed by mass analysis of the headspace gas. Additionally, when CD_3OD was used in place of CH_3OH, deuterium was incorporated into product **2**, and D_2 gas was evolved.

Key control experiments conducted during our optimization studies are collected in Table 1. No conversion of starting material is observed when the reaction is conducted in the dark (entry 2), when a 500 nm cutoff filter is applied to the light source (entry 3), or when the TiO_2 photocatalyst is omitted (entries 4 or 5). The use of quartz over standard borosilicate glassware resulted in a modest decrease in the yield of **2**, consistent with a beneficial effect associated with filtering out <300 nm light (entry 6). Under aerobic conditions, significant product formation is observed but the yield is diminished due to competing degradation processes (entry 7). The presence of AcOH positively impacts yield (entry 8), and the use of a stronger acid, such as HCl, causes a precipitous decrease in the formation of **2** (entry 9). Bare TiO_2 without Pt deposition is a significantly less effective catalyst (entry 10). Finally, attempts to platinize TiO_2 *in situ* under the standard reaction conditions led to a decrease in the yield of the desired product (entry 11).

With a set of optimized conditions in hand, we next evaluated modifications to the catalyst by photodepositing other noble metals onto TiO_2. The metal dopants shown in Table 2 were selected based on their prior use in related alcohol oxidation[6a,13] and water splitting reactions.[14] TiO_2 deposited

Table 1. Reaction Optimization Studies and Control Experiments

entry	modifications from standard conditions	conversion (%)	yield 2 (%)
1	none[a]	>99	90
2	in the dark	0	0
3	100-W Hg lamp with a 500 nm cutoff filter	0	0
4	no Pt/TiO_2	0	0
5	H_2PtCl_6 instead of Pt/TiO_2	0	0
6	quartz instead of borosilicate glassware	>99	74
7	under air instead of an N_2 atmosphere	>99	52
8	no AcOH	92	44
9	HCl instead of AcOH	70	3
10	nonplatinized TiO_2	94	39
11	H_2PtCl_6 + TiO_2 (*in situ* platinization)	>99	66

[a]Reactions were conducted on a 0.2 mmol scale of **1** using AcOH (2.0 equiv) and 0.5 wt % Pt/TiO_2 (5.0 mg) in MeOH (3 mL). Reactions were run in borosilicate glassware under an N_2 atmosphere for 15 h at room temperature under a 100-W Hg lamp.

Table 2. Screen of Metal Dopants[a]

entry	metal dopant	conversion (%)	yield 2 (%)	yield 3 (%)
1	Pt	>99	90	6
2	Au	38	33	1
3	Ag	64	51	4
4	Pd	>99	48	45
5	Pd[b]	>99	56	40

[a]Reactions were conducted under the standard conditions shown in Table 1. [b]Using CD_3OD instead of CH_3OH.

with Ag or Au nanoparticles (entries 2 and 3) proved to be selective catalysts but afforded slower rates than the Pt analogue. Interestingly, the Pd/TiO_2 catalyst effected the rapid consumption of starting material but formed increased amounts of the *N*-methylated side product **3** (entry 4).[15] We reasoned that the deposited Pd nanoparticles may be more effective at hydrogenating the putative iminium ion intermediate prior to cyclization. Using CD_3OD, the *N*-Me group is fully deuterated, confirming the source of the H atom equivalents. Additionally, a decrease in the fraction of the *N*-Me product **3** is observed with CD_3OD, suggesting that there is a significant primary KIE associated with the selectivity-determining step (entry 5).

The substrate scope (Figure 3) for the dehydrogenative Pictet−Spengler cyclization was explored under the optimized conditions shown in Table 1. A variety of common functional groups were found to be tolerated, including halides, alkenes, ethers, alcohols, esters, and trifluoromethyl substituents. Additionally, both electron-deficient (**7** and **9**) and electron-rich (**8**) ring systems were unaffected by the photocatalyst. Of particular note, *N*-PMB groups (**5**), which are typically deprotected under oxidative conditions, remained intact during the reaction. Due to the large excess of MeOH, which is being

The Journal of Organic Chemistry
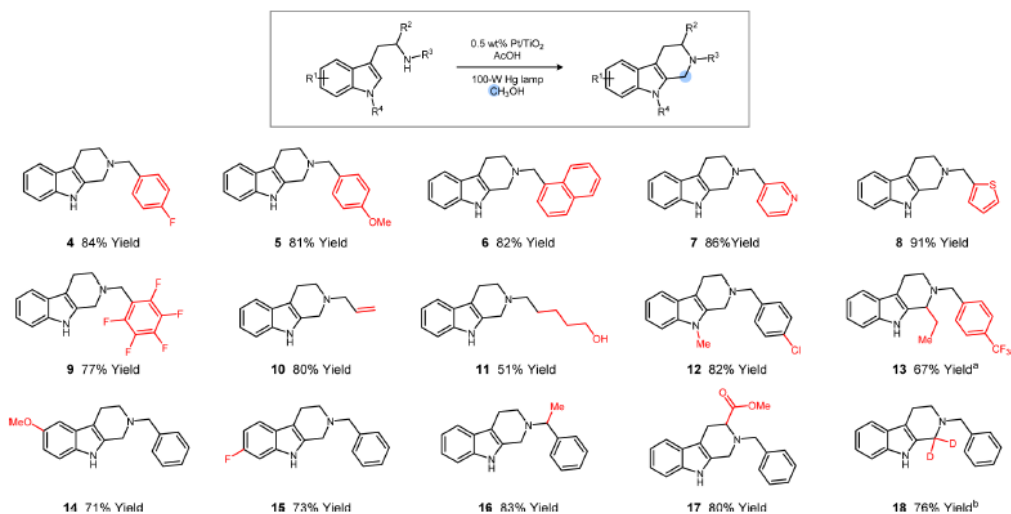
Figure 3. Substrate scope for the photocatalytic dehydrogenative Pictet−Spenger cyclization. Variations from the model substrate (1) are highlighted in red. [a] Using n-PrOH in the place of CH_3OH. [b] Using CD_3OD in the place of CH_3OH.

used as a solvent in these reactions, unprotected alcohols incorporated into the substrate (11) do not suffer from competing oxidation under the photocatalytic conditions. CD_3OD provided a commercially available source of D_2CO equivalents that afford access to deuterium labeled products (18) in high yield. Finally, the use of other aliphatic alcohols, such as n-PrOH, provided good yields of the cyclized product (13).

The photocatalytic dehydrogenation was extended to other transformations involving imine intermediates (Figure 4). For example, the intermolecular aminomethylation of unprotected indole proceeds with the expected C3-selectivity to form 19 in 68% yield. This reaction also tolerates the use of tetrahydro-isoquinoline, which is susceptible to dehydrogenation under a closely related set of photocatalytic conditions.[10c] Strecker reactions can be carried out using TMSCN as a cyanide source. Three-component Mannich reactions employing an excess of acetone yield the β-aminoketone product 23 in 57% yield. Finally, the combination of a secondary amine and an isonitrile generates an interrupted Ugi-type product (24) in 82% yield.[16] Notably, when unprotected proline was used as a coupling partner, the reaction was accompanied by methyl ester formation (25). A proposed mechanism is described in the Supporting Information and involves capture of the putative nitrilium intermediate by the pendant carboxylic acid.

In summary, metal/TiO_2 catalysts under visible/near-UV light irradiation promote the mild dehydrogenation of simple aliphatic alcohols. This process is compatible with a broad range of organic functional groups such that the aldehyde equivalents being generated can be productively utilized in multicomponent reactions involving imine intermediates. Collectively, these studies demonstrate the utility of oxophilic semiconducting materials in promoting photoredox reactions that are not strictly governed by outersphere electron transfer processes.

■ EXPERIMENTAL SECTION

General Information. All reactions were carried out using standard Schlenk techniques under an atmosphere of N_2. Reagents and solvents were purchased from commercial sources and used without further purification unless otherwise noted. TiO_2 (P-25, Aeroxide) was obtained from Sigma-Aldrich, and H_2PtCl_6 was obtained from Strem Chemical. ^1H and $^{13}C\{^1H\}$ NMR spectra are reported in parts per million relative to tetramethylsilane using the residual solvent resonances as an internal standard. High-resolution mass data were obtained using an Agilent 6320 Ion Trap MS system. ICP-MS data were obtained using a ThermoFinnigan Element2 instrument. XRD patterns were measured on a Panalytical Empyrean Powder X-ray diffractometer.

Residual Gas Analyzer. Gas evolution was analyzed using a residual gas analysis (RGA) mass spectrometer designed and built by the Amy Facility for Chemical Instrumentation at Purdue University. The headspace of the reaction mixture was collected with a gastight syringe and injected into the custom-made glass RGA cell. Argon was used as a carrier gas, and the gas mixture was drawn by a Varian model SH 100 vacuum pump into a Stanford Research Systems RGA 100 mass spectrometer equipped with an Alcatel ATH31 Series turbopump.

Preparation of Pt/TiO_2 (0.5 wt % Pt) Photocatalyst. A 20 mL microwave vial was charged with a magnetic stir bar, TiO_2 (P25, Aldrich, 1.0 g), i-PrOH (9.0 mL), and distilled water (7.0 mL). H_2PtCl_6 (0.5 wt % Pt relative to TiO_2, 13.3 mg) was added as a solution in distilled water (2.0 mL). The vial was sealed with a 14/20 rubber septum, and the mixture was sonicated for 30 min and then sparged with N_2 for 45 min. The reaction vessel was placed into a reflective dewar containing water at ambient temperature. The mixture was stirred under irradiation with a 100-W Hg lamp (UVP-Blak-Ray B-100YP). After 30 min, the reaction mixture was transferred to a centrifuge tube and spun down to a solid pellet. The liquid phase was decanted, and the solid was resuspended in distilled water before being spun down again. After the rinse was repeated twice, the gray solid was isolated and allowed to dry in a 125 °C oven overnight. ICP-MS analysis determined the amount of deposited platinum to be approximately 0.489%.

Preparation of Pd/TiO_2 (0.5 wt % Pd) Photocatalyst. A 20 mL microwave vial was charged with a magnetic stir bar, TiO_2 (P25, Aldrich, 1.0 g), i-PrOH (9.0 mL), and distilled water (7.0 mL).

The Journal of Organic Chemistry
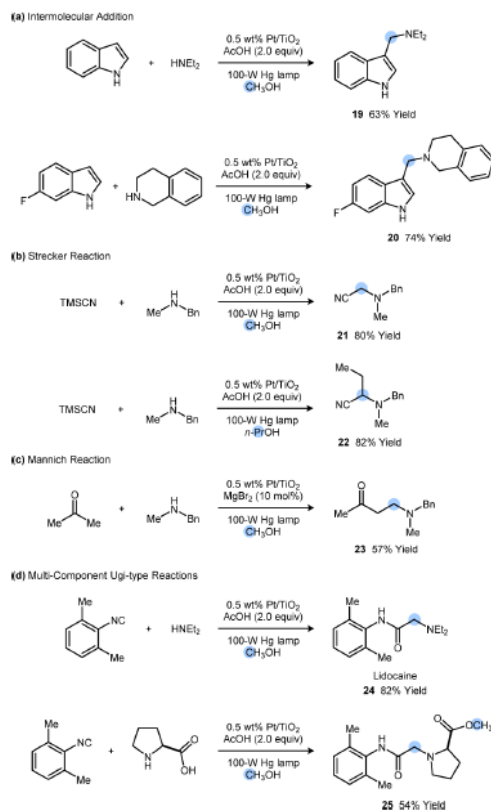
Figure 4. Multicomponent imine transformations enabled by the photocatalytic dehydrogenation of MeOH.

Pd(NO$_3$)$_2$ (0.5 wt % Pd relative to TiO$_2$, 26.0 mg) was added as a solution in distilled water (2.0 mL). The vial was sealed with a 14/20 rubber septum, and the mixture was sonicated for 30 min and then sparged with N$_2$ for 45 min. The reaction vessel was placed into a reflective dewar containing water at ambient temperature. The mixture was stirred under irradiation with a 100-W Hg lamp (UVP-Blak-Ray B-100YP). After 30 min, the reaction mixture was transferred to a centrifuge tube and spun down to a solid pellet. The liquid phase was decanted, and the solid was resuspended in distilled water before being spun down again. After the rinse was repeated twice, the gray solid was isolated and allowed to dry in a 125 °C oven overnight.

Preparation of Au/TiO$_2$ (0.5 wt % Au) Photocatalyst. A 20 mL microwave vial was charged with a magnetic stir bar, TiO$_2$ (P25, Aldrich, 1.0 g), i-PrOH (9.0 mL), and distilled water (7.0 mL). HAuCl$_4$·H$_2$O (0.5 wt % Au relative to TiO$_2$, 9.0 mg) was added as a solution in distilled water (2.0 mL). The vial was sealed with a 14/20 rubber septum, and the mixture was sonicated for 30 min and then sparged with N$_2$ for 45 min. The reaction vessel was placed into a reflective dewar containing water at ambient temperature. The mixture was stirred under irradiation with a 100-W Hg lamp (UVP-Blak-Ray B-100YP). After 30 min, the reaction mixture was transferred to a centrifuge tube and spun down to a solid pellet. The liquid phase was decanted, and the solid was resuspended in distilled water before being spun down again. After the rinse was repeated twice, the purple solid was isolated and allowed to dry in a 125 °C oven overnight.

Preparation of Ag/TiO$_2$ (0.5 wt % Ag) Photocatalyst. A 20 mL microwave vial was charged with a magnetic stir bar, TiO$_2$ (P25, Aldrich, 1.0 g), i-PrOH (9.0 mL), and distilled water (7.0 mL). AgNO$_3$ (0.5 wt % Ag relative to TiO$_2$, 8.0 mg) was added as a solution in distilled water (2.0 mL). The vial was sealed with a 14/20 rubber septum, and the mixture was sonicated for 30 min and then sparged with N$_2$ for 45 min. The reaction vessel was placed into a reflective dewar containing water at ambient temperature. The mixture was stirred under irradiation with a 100-W Hg lamp (UVP-Blak-Ray B-100YP). After 30 min, the reaction mixture was transferred to a centrifuge tube and spun down to a solid pellet. The liquid phase was decanted, and the solid was resuspended in distilled water before being spun down again. After the rinse was repeated twice, the red solid was isolated and allowed to dry in a 125 °C oven overnight.

General Procedure for Tetrahydro-β-carboline Synthesis. A 50 mL Schlenk tube was charged with a magnetic stir bar, the tryptamine substrate (0.2 mmol), the Pt/TiO$_2$ catalyst (5 mg/0.2 mmol of substrate), AcOH (0.4 mmol), and MeOH (3.0 mL). The reaction vessel was sealed and degassed by the freeze–pump–thaw procedure. Reactions were stirred under irradiation by a 100-W Hg lamp (UVP-Blak-Ray B-100YP). After 15 h, the reaction mixture was quenched with aqueous sodium hydroxide (1.0 M, 10 mL), and the product was extracted using CH$_2$Cl$_2$ (3 × 5 mL). The combined organic phases were dried over MgSO$_4$, filtered, and concentrated to dryness under reduced pressure. Products were isolated following purification by column chromatography. All reactions were run in duplicate.

2-Benzyl-2,3,4,9-tetrahydro-1H-pyrido[3,4-b]indole (2).[17] Isolated yields were determined following purification by column chromatography (SiO$_2$, 0–5% MeOH in CH$_2$Cl$_2$). Run 1: 43 mg, 83% Run 2: 51 mg, 97%. ^{1}H NMR (300 MHz, CDCl3) δ 7.66 (s, 1H), 7.51–7.32 (m, 6H), 7.27–7.24 (m, 1H), 7.17–7.08 (m, 2H), 3.78 (s, 2H), 3.59 (s, 2H), 2.95–2.91 (m, 2H), 2.86–2.82 (m, 2H). ^{13}C{^{1}H} NMR (126 MHz, CDCl3) δ 138.5, 136.1, 131.9, 129.2, 128.5, 127.3, 121.3, 119.4, 118.1, 110.8, 108.4, 62.1, 51.0, 50.2, 21.3.

2-(4-Fluorobenzyl)-2,3,4,9-tetrahydro-1H-pyrido[3,4-b]-indole (4). Isolated yields were determined following purification by column chromatography (SiO$_2$, 0–5% MeOH in CH$_2$Cl$_2$). Run 1: 45 mg, 80% Run 2: 49 mg, 87%. ^{1}H NMR (300 MHz, CDCl$_3$) δ 7.68 (s, 1H), 7.49 (d, J = 6.9 Hz, 1H), 7.40–7.35 (m, 2H), 7.29–7.26 (m, 1H), 7.17–7.10 (m, 2H), 7.05 (t, J = 8.7 Hz, 2H), 3.73 (s, 2H), 3.60 (s, 2H), 2.93–2.89 (m, 2H), 2.84 (d, J = 5.3 Hz, 2H). ^{13}C{^{1}H} NMR (126 MHz, CDCl$_3$) δ 162.2 (d, [1]J_{C-F} = 245.2 Hz), 136.1, 134.2, 131.8, 130.7 (d, [2]J_{C-F} = 7.8 Hz), 127.3, 121.5, 119.5, 118.1, 115.3 (d, [3]J_{C-F} = 21.1 Hz), 110.8, 108.5, 61.3, 50.9, 50.2, 21.3. HRMS (ESI, m/z): [M + H]$^+$ calcd for C$_{18}$H$_{18}$FN$_2$, 281.1454; found, 281.1447.

2-(4-Methoxybenzyl)-2,3,4,9-tetrahydro-1H-pyrido[3,4-b]-indole (5). Isolated yields were determined following purification by column chromatography (SiO$_2$, 0–5% MeOH in CH$_2$Cl$_2$). Run 1: 46 mg, 78% Run 2: 49 mg, 84%. ^{1}H NMR (300 MHz, CDCl$_3$) δ 7.72 (s, 1H), 7.47 (d, J = 6.7 Hz, 1H), 7.33–7.27 (m, 3H), 7.11 (qd, J = 7.1 Hz, 1.5 Hz, 2H), 6.91–6.87 (m, 2H), 3.82 (s, 3H), 3.73 (s, 2H), 3.65 (s, 2H), 2.93–2.90 (m, 2H), 2.84–2.80 (m, 2H). ^{13}C{^{1}H} NMR (126 MHz, CDCl$_3$) δ 159.0, 136.1, 131.9, 130.5, 127.4, 121.4, 119.5, 118.1, 113.8, 110.8, 108.5, 61.4, 55.4, 50.8, 50.1, 21.2. HRMS (ESI, m/z): [M + H]$^+$ calcd for C$_{19}$H$_{21}$N$_2$O, 293.1654; found, 293.1645.

2-(Naphthalen-1-ylmethyl)-2,3,4,9-tetrahydro-1H-pyrido-[3,4-b]indole (6). Isolated yields were determined following purification by column chromatography (SiO$_2$, 0–5% MeOH in CH$_2$Cl$_2$). Run 1: 49 mg, 79% Run 2: 52 mg, 84%. ^{1}H NMR (300 MHz, CDCl$_3$) δ 8.38–8.35 (m, 1H), 7.88–7.85 (m, 1H), 7.82 (d, J = 8.5 Hz, 1H), 7.61 (s, 1H), 7.55–7.44 (m, 5H), 7.29–7.28 (m, 1H), 7.15–7.06 (m, 2H), 4.20 (s, 2H), 3.71 (s, 2H), 3.03 (t, J = 5.9 Hz, 2H), 2.85 (t, J = 5.5 Hz, 2H). ^{13}C{^{1}H} NMR (126 MHz, CDCl$_3$) δ 136.1, 134.0, 132.7, 128.6, 128.3, 127.6, 127.4, 126.1, 125.9, 125.3, 124.8, 121.5, 119.5, 118.1, 110.8, 108.6, 60.0, 51.3, 50.3, 21.3. HRMS (ESI, m/z): [M + H]$^+$ calcd for C$_{22}$H$_{21}$N$_2$, 313.1705; found, 312.1696.

2-(Pyridin-3-ylmethyl)-2,3,4,9-tetrahydro-1H-pyrido[3,4-b]-indole (7). Isolated yields were determined following purification by column chromatography (SiO$_2$, 0–5% MeOH in CH$_2$Cl$_2$). Run 1: 43

mg, 82% Run 2: 47 mg, 90%. ^{1}H NMR (300 MHz, DMSO-d_6) δ 10.67 (s, 1H), 8.57 (d, J = 1.5 Hz, 1H), 8.49 (dd, J = 1.7 Hz, 4.8 Hz, 1H), 7.78 (dt, J = 1.8 Hz, 7.8 Hz, 1H), 7.39–7.33 (m, 2H), 7.26 (d, J = 7.9 Hz, 1H), 7.02–6.90 (m, 2H), 3.75 (s, 2H), 3.57 (s, 2H), 2.78 (d, J = 5.0 Hz, 1H), 2.69 (d, J = 5.0 Hz, 2H). ^{13}C{^{1}H} NMR (126 MHz, DMSO-d_6) δ 150.0, 148.4, 136.5, 135.8, 134.1, 132.6, 126.7, 123.5, 120.3, 118.3, 117.4, 110.9, 106.3, 58.4, 50.5, 49.8, 21.1. HRMS (ESI, m/z): [M + H]+ calcd for C$_{12}$H$_{18}$N$_3$, 264.1501; found, 264.1505.

2-(Thiophen-2-ylmethyl)-2,3,4,9-tetrahydro-1H-pyrido[3,4-b]indole (8). Isolated yields were determined following purification by column chromatography (SiO$_2$, 0–5% MeOH in CH$_2$Cl$_2$). Run 1: 51 mg, 95% Run 2: 47 mg, 87%. ^{1}H NMR (300 MHz, CDCl$_3$) δ 7.67 (s, 1H), 7.47 (d, J = 7.8 Hz, 1H), 7.31–7.28 (m, 2H), 7.11 (qd, J = 1.6 Hz, 7.1 Hz, 2H), 7.00–6.97 (m, 2H), 4.01 (s, 2H), 3.76 (s, 2H), 2.98 (t, J = 6.2 Hz, 2H), 2.84 (t, J = 5.4 Hz, 2H). ^{13}C{^{1}H} NMR (126 MHz, CDCl$_3$) δ 141.9, 136.2, 131.6, 127.4, 126.7, 126.3, 125.4, 121.5, 119.5, 118.1, 110.8, 108.5, 56.0, 50.6, 49.9, 21.1. HRMS (ESI): [M + H]$^+$ calcd for C$_{16}$H$_{17}$N$_2$S, 269.1113; found, 269.1106.

2-((Perfluorophenyl)methyl)-2,3,4,9-tetrahydro-1H-pyrido-[3,4-b]indole (9). The reaction was run with the following modifications from the general procedure: 10 mg of Pt/TiO$_2$, 10 equiv of AcOH, and a 24-h reaction time. Isolated yields were determined following purification by column chromatography (SiO$_2$, 0–5% MeOH in CH$_2$Cl$_2$). Run 1: 54 mg, 76% Run 2: 55 mg, 78%. ^{1}H NMR (300 MHz, CDCl$_3$) δ 7.73 (s, 1H), 7.46 (d, J = 7.4 Hz, 1H), 7.29 (d, J = 7.3 Hz, 1H), 7.15–7.05 (m, 2H), 3.97 (s, 2H), 3.74 (s, 2H), 2.96 (t, J = 5.7 Hz, 2H), 2.84 (t, J = 5.4 Hz, 2H). ^{13}C{^{1}H} NMR (126 MHz, CDCl$_3$) δ 136.2, 131.1, 127.3, 121.7, 119.6, 118.1, 110.9, 108.3, 50.6, 49.5, 48.0, 21.4. ^{19}F NMR (282 MHz, CDCl$_3$) δ −143.0, −156.1, −163.5. HRMS (ESI, m/z): [M + H]$^+$ calcd for C$_{18}$H$_{14}$F$_5$N$_2$, 353.1077; found, 353.1070.

2-Allyl-2,3,4,9-tetrahydro-1H-pyrido[3,4-b]indole (10).[17] Isolated yields were determined following purification by column chromatography (SiO$_2$, 0–5% MeOH in CH$_2$Cl$_2$). Run 1: 33 mg, 77% Run 2: 35 mg, 83%. ^{1}H NMR (300 MHz, CDCl$_3$) δ 7.72 (s, 1H), 7.48 (d, J = 7.6 Hz, 1H), 7.30 (d, J = 7.2 Hz, 1H), 7.11 (qd, J = 1.5, 7.2 Hz, 2H), 6.04–5.92 (m, 1H), 5.30–5.20 (m, 2H), 3.71 (s, 2H), 3.29 (d, J = 6.5 Hz, 2H), 2.93–2.81 (m, 4H). ^{13}C{^{1}H} NMR (126 MHz, CDCl$_3$) δ 136.2, 135.2, 131.8, 127.3, 121.4, 119.4, 118.4, 118.1, 110.9, 108.4, 60.8, 50.8, 50.2, 21.3.

5-(1,3,4,9-Tetrahydro-2H-pyrido[3,4-b]indol-2-yl)pentan-1-ol (11). The reaction was run with the following modifications from the general procedure: 10 mg of Pt/TiO$_2$, 10 equiv of AcOH, and a 24-h reaction time. Isolated yields were determined following purification by column chromatography on (SiO$_2$, 0–5% MeOH in CH$_2$Cl$_2$). Run 1: 21 mg, 40% Run 2: 32 mg, 62%. ^{1}H NMR (300 MHz, CDCl$_3$) δ 8.61 (s, 1H), 7.43 (d, J = 7.1 Hz, 1H), 7.28 (d, J = 7.3 Hz, 1H), 7.09 (qd, J = 1.2, 7.8 Hz, 2H), 3.68 (s, 2H), 3.60 (t, J = 6.3 Hz, 2H), 3.32 (s, 1H), 2.89–2.83 (m, 4H), 2.59 (t, J = 7.4 Hz, 2H), 1.66–1.51 (m, 4H), 1.39 (q, J = 6.9 Hz, 2H). ^{13}C{^{1}H} NMR (126 MHz, CDCl$_3$) δ 136.4, 130.3, 127.0, 121.7, 119.5, 118.1, 111.1, 107.7, 62.5, 57.1, 51.0, 50.1, 32.3, 26.3, 23.5, 20.6. HRMS (ESI): [M + H]$^+$ calcd for C$_{16}$H$_{23}$N$_2$O, 259.1811; found, 259.1808.

2-(4-Chlorobenzyl)-9-methyl-2,3,4,9-tetrahydro-1H-pyrido-[3,4-b]indole (12). Isolated yields were determined following purification by column chromatography (SiO$_2$, 0–5% MeOH in CH$_2$Cl$_2$). Run 1: 52 mg, 83% Run 2: 50 mg, 81%. ^{1}H NMR (300 MHz, CDCl$_3$) δ 7.51 (d, J = 7.7 Hz, 1H), 7.40–7.33 (m, 4H), 7.29–7.27 (m, 1H), 7.20 (td, J = 6.9 Hz, 1.2 Hz, 1H), 7.11 (td, J = 7.8 Hz, 1.2 Hz, 1H), 3.79 (s, 2H), 3.69 (s, 2H), 3.56 (s, 3H), 2.92–2.84 (m, 4H). ^{13}C{^{1}H} NMR (126 MHz, CDCl$_3$) δ 137.2, 137.1, 133.1, 133.3, 133.0, 130.4, 128.7, 126.8, 121.0, 119.0, 118.1, 108.8, 107.3, 61.5, 50.9, 49.5, 29.3, 21.5. HRMS (ESI): [M + H]$^+$ calcd for C$_{19}$H$_{20}$ClN$_2$, 311.1315; found, 311.1307.

1-Ethyl-2-(4-trifluoromethylbenzyl)-2,3,4,9-tetrahydro-1H-pyrido[3,4-b]indole (13). The reaction was run with the following modifications from the general procedure: 10 mg of Pt/TiO$_2$, 10 equiv of AcOH, n-PrOH solvent, and a 24-h reaction time. Isolated yields were determined following purification by column chromatography (SiO$_2$, 1:10 acetone/petroleum ether). Run 1: 48 mg, 67% Run 2: 48

mg, 67%. ^{1}H NMR (300 MHz, CDCl$_3$) δ 7.64 (s, 1H), 7.61 (d, J = 8.2 Hz, 2H), 7.53 (d, J = 6.7 Hz, 3H), 7.34 (d, J = 7.2 Hz, 1H), 7.21–7.11 (m, 2H), 3.83 (q, J = 14.0 Hz, 2H), 3.55 (t, J = 6.4 Hz, 1H), 3.29–3.20 (m, 1H), 2.96–2.84 (m, 2H), 2.67–2.59 (m, 1H), 1.84 (q, J = 7.6 Hz, 2H), 1.01 (t, J = 7.3 Hz, 3H). ^{13}C{^{1}H} NMR (126 MHz, CDCl$_3$) δ 144.4, 136.0, 135.2, 129.4 (q, $^2J_{C-F}$ = 32.2 Hz) 129.1, 127.4, 126.5 (q, $^1J_{C-F}$ = 233.9 Hz) 125.3 (d, $^3J_{C-F}$ = 3.5 Hz) 121.7, 119.5, 118.2, 110.8, 108.2, 58.5, 57.1, 45.2, 27.5, 18.3, 10.9. ^{19}F NMR (282 MHz, CDCl$_3$) δ −63.8. HRMS (ESI, m/z): [M + H]$^+$ calcd for C$_{21}$H$_{22}$F$_3$N$_2$, 359.1735; found, 359.1732.

2-Benzyl-6-methoxy-2,3,4,9-tetrahydro-1H-pyrido[3,4-b]-indole (14). Isolated yields were determined following purification by column chromatography (SiO$_2$, 0–5% MeOH in CH$_2$Cl$_2$). Run 1: 43 mg, 74% Run 2: 40 mg, 68%. ^{1}H NMR (300 MHz, CDCl$_3$) δ 7.58 (s, 1H), 7.43–7.30 (m, 5H), 7.15 (d, J = 8.4 Hz, 1H), 6.94 (d, J = 2.5 Hz, 1H), 6.78 (dd, J = 2.5, 8.7, 1H), 3.86 (s, 3H), 3.77 (s, 2H), 3.60 (s, 2H), 2.91 (t, J = 6.0 Hz, 2H), 2.80 (t, J = 5.3 Hz, 2H). ^{13}C{^{1}H} NMR (126 MHz, CDCl$_3$) δ 154.1, 138.4, 132.8, 131.2, 129.3, 128.5, 127.8, 127.4, 111.5, 111.0, 108.3, 100.4, 62.1, 56.0, 51.0, 50.4, 21.3. HRMS (ESI, m/z): [M + H]$^+$ calcd for C$_{19}$H$_{21}$N$_2$O, 293.1654; found, 293.1647.

2-Benzyl-7-fluoro-2,3,4,9-tetrahydro-1H-pyrido[3,4-b]indole (15). Isolated yields were determined following purification by column chromatography (SiO$_2$, 0–5% MeOH in CH$_2$Cl$_2$). Run 1: 48 mg, 85% Run 2: 34 mg, 60%. ^{1}H NMR (300 MHz, CD$_3$OD) δ 7.42–7.29 (m, 7H), 6.95 (dd, J = 2.3 Hz, 10 Hz, 1H), 6.77–6.71 (m, 1H), 3.77 (s, 3H), 3.63 (s, 3H), 2.90–2.86 (m, 2H), 2.80–2.76 (m, 2H). ^{13}C{^{1}H} NMR (126 MHz, CD$_3$OD) δ 151.4 (d, $^1J_{C-F}$ = 234.2 Hz), 129.0, 128.4 (d, $^3J_{C-F}$ = 12.6 Hz), 121.3, 120.6, 120.0, 119.7, 119.1, 109.7 (d, $^3J_{C-F}$ = 10.1 Hz), 98.6, 98.3 (d, $^2J_{C-F}$ = 24.6 Hz), 88.5 (d, $^2J_{C-F}$ = 26.1 Hz), 53.7, 42.4, 41.7, 12.5. ^{19}F NMR (282 MHz, CD$_3$OD) δ −123.6. HRMS (ESI, m/z): [M + H]$^+$ calcd for C$_{18}$H$_{18}$FN$_2$, 281.1454; found, 281.1451.

2-(1-Phenylethyl)-2,3,4,9-tetrahydro-1H-pyrido[3,4-b]indole (16). Isolated yields were determined following purification by column chromatography (SiO$_2$, 0–5% MeOH in CH$_2$Cl$_2$). Run 1: 43 mg, 78% Run 2: 49 mg, 88%. ^{1}H NMR (300 MHz, CDCl$_3$) δ 7.64 (s, 1H), 7.47 (d, J = 7.2 Hz, 1H), 7.42–7.28 (m, 6H), 7.10 (qd, J = 7.0 Hz, 1.4 Hz, 2H), 3.80–3.61 (m, 3H), 3.00–2.92 (m, 1H), 2.87–2.75 (m, 3H), 1.50 (d, J = 6.7 Hz, 3H). ^{13}C{^{1}H} NMR (126 MHz, CDCl$_3$) δ 144.5, 136.1, 132.3, 128.6, 127.7, 127.4, 127.2, 121.4, 119.4, 118.1, 110.8, 108.7, 63.9, 48.4, 48.2, 21.5, 20.6. HRMS (ESI, m/z): [M + H]$^+$ calcd for C$_{19}$H$_{21}$N$_2$, 277.1705; found, 277.1701.

Methyl 2-Benzyl-2,3,4,9-tetrahydro-1H-pyrido[3,4-b]indole-3-carboxylate (17).[18] Isolated yields were determined following purification by column chromatography (SiO$_2$, 0–5% MeOH in CH$_2$Cl$_2$). Run 1: 53 mg, 83% Run 2: 49 mg, 76%. ^{1}H NMR (300 MHz, CD$_3$OD) δ 7.41–7.23 (m, 8H), 7.06–6.94 (m, 2H), 4.14 (d, J = 15.2 Hz, 1H), 3.99 (s, 2H), 3.80–3.97 (m, 1H), 3.82 (d, J = 15.0 Hz, 1H), 3.65 (s, 3H), 3.19–3.03 (m, 2H). ^{13}C{^{1}H} NMR (126 MHz, CD$_3$OD) δ 165.2, 130.1, 128.5, 123.3, 120.8, 120.0, 119.0, 118.8, 112.4, 110.2, 108.8, 102.3, 96.5, 51.0, 50.2, 42.5, 37.8, 15.6.

2-Benzyl-2,3,4,9-tetrahydro-1H-pyrido[3,4-b]indole-1,1-d_2 (18). Isolated yield was determined following purification by column chromatography (SiO$_2$, 0–5% MeOH in CH$_2$Cl$_2$) (40 mg, 76% Yield). ^{1}H NMR (300 MHz, CD$_3$OD) δ 7.72 (s, 1H), 7.50–7.23 (m, 7H), 7.11–7.07 (m, 2H), 3.77 (s, 2H), 2.96–2.82 (m, 4H).

Intermolecular Addition: N-((1H-Indol-3-yl)methyl)-N-ethyl-ethanamine (19).[19] A 50 mL Schlenk tube was charged with a magnetic stir bar, the Pt/TiO$_2$ catalyst (5.0 mg), indole (23.4 mg, 0.2 mmol, 1.0 equiv), Et$_2$NH (41.3 μL, 0.4 mmol, 2.0 equiv), AcOH (22.9 μL, 0.4 mmol, 2.0 equiv), and MeOH (2.0 mL). The reaction vessel was sealed and degassed by the freeze–pump–thaw procedure. Reactions were stirred under irradiation by a 100-W Hg lamp. After 15 h, the reaction mixture was quenched with aqueous sodium hydroxide (1.0 M, 10 mL), and the product was extracted using CH$_2$Cl$_2$ (3 × 5 mL). The combined organic phases were dried over MgSO$_4$, filtered, and concentrated to dryness under reduced pressure. Products were isolated following purification by column chromatography (SiO$_2$, 0–5% MeOH in CH$_2$Cl$_2$). Run 1: 23 mg, 58% Run 2: 27 mg, 68%. ^{1}H

The Journal of Organic Chemistry

NMR (300 MHz, CDCl$_3$) δ 8.10 (s, 1H), 7.73 (d, J = 8.3 Hz, 1H), 7.36 (d, J = 7.8 Hz, 1H), 7.15 (ds, J = 1.1 Hz, 7.0 Hz, 3H), 3.82 (s, 2H), 2.59 (q, J = 7.2 Hz, 4H), 1.11 (t, J = 7.1 Hz, 6H). ^{13}C{^{1}H} NMR (126 MHz, CDCl$_3$) δ 136.3, 128.2, 123.7, 122.1, 119.58, 111.1, 48.0, 46.7, 12.0.

Intermolecular Addition: 2-((6-Fluoro-1H-indol-3-yl)methyl)-1,2,3,4-tetrahydroisoquinoline (20). The reaction was run according to the general procedure described for compound 19. Isolated yields were determined following purification by column chromatography (SiO$_2$, 0−2% MeOH in CH$_2$Cl$_2$). Run 1: 38 mg, 82% Run 2: 30 mg, 65%. ^{1}H NMR (300 MHz, CDCl$_3$) δ 8.19 (s, 1H), 7.69 (dd, J = 8.7, 5.4 Hz, 1H), 7.19−6.93 (m, 6H), 6.88 (td, 1H), 3.88 (s, 2H), 3.72 (s, 2H), 2.95−2.76 (m, 4H). ^{13}C{^{1}H} NMR (126 MHz, CDCl$_3$) δ 160.1 (d, $^{1}J_{C-F}$ = 237.2 Hz), 136.4, 135.1, 134.6, 128.8, 126.8, 126.2, 125.7, 124.6, 123.9 (d, $^{3}J_{C-F}$ = 3.6 Hz), (d, $^{3}J_{C-F}$ = 10.1 Hz), 113.0, 108.4 (d, $^{2}J_{C-F}$ = 24.3 Hz), 97.4 (d, $^{2}J_{C-F}$ = 26.1 Hz), 56.2, 53.5, 50.6, 29.9, 29.3. ^{19}F NMR (282 MHz, CDCl$_3$) δ −122.84. HRMS (ESI, m/z): [M + H]$^{+}$ calcd for C$_{18}$H$_{17}$FN$_2$, 281.1454; found, 281.1447.

Strecker Reaction: 2-(Benzyl(methyl)amino)acetonitrile (21).[20] A 50 mL Schlenk tube was charged with a magnetic stir bar, the Pt/TiO$_2$ catalyst (5.0 mg), N-benzylmethylamine (24.2 mg, 0.2 mmol, 1.0 equiv), TMSCN (27.5 μL, 0.22 mmol, 1.1 equiv), AcOH (22.9 μL, 0.4 mmol, 2.0 equiv), and MeOH (2.0 mL). The reaction vessel was sealed and degassed by the freeze−pump−thaw procedure. Reactions were stirred under irradiation by a 100-W Hg lamp. After 24 h, the reaction mixture was quenched with aqueous sodium hydroxide (1.0 M, 10 mL), and the product was extracted using CH$_2$Cl$_2$ (3 × 5 mL). The combined organic phases were dried over MgSO4, filtered, and concentrated to dryness under reduced pressure. Run 1: 28 mg, 86% Run 2: 23 mg, 73%. ^{1}H NMR (300 MHz, CDCl$_3$) δ 7.36−7.31 (m, 5H), 3.61 (s, 2H), 3.45 (s, 2H), 2.44 (s, 3H). ^{13}C{^{1}H} NMR (126 MHz, CDCl$_3$) δ 137.0, 129.0, 128.6, 127.8, 114.5, 60.1, 44.1, 42.3.

Strecker Reaction: 2-(Benzyl(methyl)amino)butanenitrile (22).[21] A 50 mL Schlenk tube was charged with a magnetic stir bar, the Pt/TiO$_2$ catalyst (5.0 mg), N-benzylmethylamine (24.2 mg, 0.2 mmol, 1.0 equiv), TMSCN (27.5 μL, 0.22 mmol, 1.1 equiv), AcOH (22.9 μL, 0.4 mmol, 2.0 equiv), and PrOH (3.0 mL). The reaction vessel was sealed and degassed by the freeze−pump−thaw procedure. Reactions were stirred under irradiation by a 100-W Hg lamp. After 24 h, the reaction mixture was quenched with aqueous sodium hydroxide (1.0 M, 10 mL), and the product was extracted using CH$_2$Cl$_2$ (3 × 5 mL). The combined organic phases were dried over MgSO$_4$, filtered, and concentrated to dryness under reduced pressure. Run 1: 32 mg, 84% Run 2: 30 mg, 80%. ^{1}H NMR (300 MHz, CDCl$_3$) δ 7.34−7.28 (m, 5H), 3.77 (d, J = 13.3 Hz, 1H), 3.49−3.42 (m, 2H), 2.30 (s, 3H), 1.84−1.78 (m, 2H), 1.03 (t, J = 7.4 Hz, 3H). ^{13}C{^{1}H} NMR (126 MHz, CDCl$_3$) δ 137.6, 128.8, 128.5, 127.6, 117.1, 59.8, 57.8, 38.0, 24.9, 10.6.

Mannich Reaction: 4-(Benzyl(methyl)amino)butan-2-one (23).[22] A 50 mL Schlenk tube was charged with a magnetic stir bar, the Pt/TiO$_2$ catalyst (10.0 mg), N-benzylmethylamine (24.2 mg, 0.2 mmol, 1.0 equiv), MgBr$_2$ (3.68 mg, 10 mol %), acetone (0.1 mL, 1.4 mmol, 7 equiv), and MeOH (2.0 mL). The reaction vessel was sealed and degassed by the freeze−pump−thaw procedure. Reactions were stirred under irradiation by a 100-W Hg lamp. After 24 h, the reaction mixture was quenched with aqueous sodium hydroxide (1.0 M, 10 mL), and the product was extracted using CH$_2$Cl$_2$ (3 × 5 mL). The combined organic phases were dried over MgSO$_4$, filtered, and concentrated to dryness under reduced pressure. Products were isolated following purification by column chromatography (SiO$_2$, 0−5% MeOH in CH$_2$Cl$_2$). Run 1: 21 mg, 55% Run 2: 23 mg, 59%. ^{1}H NMR (300 MHz, CDCl$_3$) δ 7.33−7.23 (m, 5H), 3.50 (s, 2H), 2.73−2.70 (m, 2H), 2.65−2.62 (m, 2H), 2.19 (s, 3H), 2.14 (s, 3H). ^{13}C{^{1}H} NMR (126 MHz, CDCl$_3$) δ 208.3, 138.7, 129.2, 128.4, 127.3, 62.5, 52.1, 42.1, 30.1.

Ugi-Type Reaction: Lidocaine (24).[23] A 50 mL Schlenk tube was charged with a magnetic stir bar, the Pt/TiO$_2$ catalyst (5.0 mg), Et$_2$NH (20.7 μL, 0.2 mmol, 2.0 equiv), 2,6-dimethylphenylisonitrile (13.1 mg, 0.1 mmol, 1.0 equiv), AcOH (11.5 μL, 0.2 mmol, 2.0 equiv), and MeOH (2.0 mL). The reaction vessel was sealed and degassed by the freeze−pump−thaw procedure. Reactions were stirred under irradiation by a 100-W Hg lamp. After 24 h, the reaction mixture was quenched with aqueous sodium hydroxide (1.0 M, 10 mL), and the product was extracted using CH$_2$Cl$_2$ (3 × 5 mL). The combined organic phases were dried over MgSO$_4$, filtered, and concentrated to dryness under reduced pressure. Products were isolated following purification by column chromatography (SiO$_2$, 1:1 EtOAc/hexane). Run 1: 37 mg, 79% Run 2: 40 mg, 85%. ^{1}H NMR (300 MHz, CDCl$_3$) δ 8.91 (s, 1H), 7.09 (s, 3H), 3.22 (s, 2H), 2.69 (q, J = 7.1 Hz, 4H), 2.24 (s, 6H), 1.14 (t, J = 7.1 Hz, 6H). ^{13}C{^{1}H} NMR (126 MHz, CDCl$_3$) δ 170.4, 135.2, 134.1, 128.4, 127.2, 57.7, 49.1, 18.7, 12.8.

Ugi-Type Reaction: Methyl (2-((2,6-Dimethylphenyl)amino)-2-oxoethyl)prolinate (25).[24] A 50 mL Schlenk tube was charged with a magnetic stir bar, the Pt/TiO$_2$ catalyst (5.0 mg), L-proline (23.0 mg, 0.2 mmol, 2.0 equiv), 2,6-dimethylphenylisonitrile (13.1 mg, 0.1 mmol, 1.0 equiv), AcOH (11.5 μL, 0.2 mmol, 2.0 equiv), and MeOH (2.0 mL). The reaction vessel was sealed and degassed by the freeze−pump−thaw procedure. Reactions were stirred under irradiation by a 100-W Hg lamp. After 24 h, the reaction mixture was quenched with aqueous sodium hydroxide (1.0 M, 10 mL), and the product was extracted using CH$_2$Cl$_2$ (3 × 5 mL). The combined organic phases were dried over MgSO$_4$, filtered, and concentrated to dryness under reduced pressure. Products were isolated following purification by column chromatography (SiO$_2$, 1:1 EtOAc/hexane). Run 1: 28 mg, 48% Run 2: 35 mg, 60%. ^{1}H NMR (300 MHz, CDCl$_3$) δ 8.99 (s, 1H), 7.09 (s, 3H), 3.74 (s, 3H), 3.65−3.53 (m, 2H), 3.39−3.30 (m, 2H), 2.66 (q, J = 7.8 Hz, 1H), 2.25 (s, 6H), 2.09−1.89 (m, 4H). ^{13}C{^{1}H} NMR (126 MHz, CDCl$_3$) δ 174.8, 169.6, 135.4, 134.1, 128.3, 127.2, 66.0, 58.8, 55.1, 52.2, 30.0, 24.5, 18.6.

■ ASSOCIATED CONTENT

$\ominus$ Supporting Information

The Supporting Information is available free of charge on the ACS Publications website at DOI: 10.1021/acs.joc.7b00617.

> Additional experimental details, cyclic voltammetry data, NMR spectra, and IR spectra (PDF)

■ AUTHOR INFORMATION

Corresponding Author

*E-mail: cuyeda@purdue.edu.

ORCID

Christopher Uyeda: 0000-0001-9396-915X

Author Contributions

†C.M.A. and J.W. contributed equally.

Notes

The authors declare no competing financial interest.

■ REFERENCES

(1) (a) Narayanam, J. M. R.; Stephenson, C. R. J. *Chem. Soc. Rev.* **2011**, *40*, 102−113. (b) Prier, C. K.; Rankic, D. A.; MacMillan, D. W. C. *Chem. Rev.* **2013**, *113*, 5322−5363. (c) Xi, Y.; Yi, H.; Lei, A. *Org. Biomol. Chem.* **2013**, *11*, 2387−2403. (d) Schultz, D. M.; Yoon, T. P. *Science* **2014**, *343*, 1239176. (e) Romero, N. A.; Nicewicz, D. A. *Chem. Rev.* **2016**, *116*, 10075−10166. (f) Tellis, J. C.; Kelly, C. B.; Primer, D. N.; Jouffroy, M.; Patel, N. R.; Molander, G. A. *Acc. Chem. Res.* **2016**, *49*, 1429−1439.

(2) Huo, H.; Shen, X.; Wang, C.; Zhang, L.; Rose, P.; Chen, L.-A.; Harms, K.; Marsch, M.; Hilt, G.; Meggers, E. *Nature* **2014**, *515*, 100–103.

(3) (a) Ni, M.; Leung, M. K. H.; Leung, D. Y. C.; Sumathy, K. *Renewable Sustainable Energy Rev.* **2007**, *11*, 401–425. (b) Chen, X.; Shen, S.; Guo, L.; Mao, S. S. *Chem. Rev.* **2010**, *110*, 6503–6570. (c) Tran, P. D.; Wong, L. H.; Barber, J.; Loo, J. S. C. *Energy Environ. Sci.* **2012**, *5*, 5902–5918.

(4) (a) Linsebigler, A. L.; Lu, G.; Yates, J. T. *Chem. Rev.* **1995**, *95*, 735–758. (b) Carp, O.; Huisman, C. L.; Reller, A. *Prog. Solid State Chem.* **2004**, *32*, 33–177.

(5) (a) Bhatkhande, D. S.; Pangarkar, V. G.; Beenackers, A. A. C. M. *J. Chem. Technol. Biotechnol.* **2002**, *77*, 102–116. (b) Gaya, U. I.; Abdullah, A. H. *J. Photochem. Photobiol., C* **2008**, *9*, 1–12. (c) Malato, S.; Fernández-Ibáñez, P.; Maldonado, M. I.; Blanco, J.; Gernjak, W. *Catal. Today* **2009**, *147*, 1–59.

(6) (a) Enache, D. I.; Edwards, J. K.; Landon, P.; Solsona-Espriu, B.; Carley, A. F.; Herzing, A. A.; Watanabe, M.; Kiely, C. J.; Knight, D. W.; Hutchings, G. J. *Science* **2006**, *311*, 362–365. (b) Zhang, M.; Chen, C.; Ma, W.; Zhao, J. *Angew. Chem., Int. Ed.* **2008**, *47*, 9730–9733.

(7) (a) Fan, W.; Lai, Q.; Zhang, Q.; Wang, Y. *J. Phys. Chem. C* **2011**, *115*, 10694–10701. (b) Gärtner, F.; Losse, S.; Boddien, A.; Pohl, M.-M.; Denurra, S.; Junge, H.; Beller, M. *ChemSusChem* **2012**, *5*, 530–533. (c) Ruberu, T. P. A.; Nelson, N. C.; Slowing, I. I.; Vela, J. *J. Phys. Chem. Lett.* **2012**, *3*, 2798–2802. (d) Schneider, J.; Matsuoka, M.; Takeuchi, M.; Zhang, J.; Horiuchi, Y.; Anpo, M.; Bahnemann, D. W. *Chem. Rev.* **2014**, *114*, 9919–9986. (e) Song, W.; Vannucci, A. K.; Farnum, B. H.; Lapides, A. M.; Brennaman, M. K.; Kalanyan, B.; Alibabaei, L.; Concepcion, J. J.; Losego, M. D.; Parsons, G. N.; Meyer, T. J. *J. Am. Chem. Soc.* **2014**, *136*, 9773–9779. (f) Hou, H.; Shang, M.; Gao, F.; Wang, L.; Liu, Q.; Zheng, J.; Yang, Z.; Yang, W. *ACS Appl. Mater. Interfaces* **2016**, *8*, 20128–20137.

(8) (a) Mallat, T.; Baiker, A. *Chem. Rev.* **2004**, *104*, 3037–3058. (b) Stahl, S. S. *Angew. Chem., Int. Ed.* **2004**, *43*, 3400–3420. (c) Schultz, M. J.; Sigman, M. S. *Tetrahedron* **2006**, *62*, 8227–8241. (d) Dobereiner, G. E.; Crabtree, R. H. *Chem. Rev.* **2010**, *110*, 681–703. (e) Gunanathan, C.; Milstein, D. *Science* **2013**, *341*, 1229712.

(9) (a) Sun, C.; Zou, X.; Li, F. *Chem. - Eur. J.* **2013**, *19*, 14030–14033. (b) Kim, S. H.; Hong, S. H. *Org. Lett.* **2016**, *18*, 212–215. (c) Kang, B.; Hong, S. H. *Adv. Synth. Catal.* **2015**, *357*, 834–840. (d) Li, F.; Lu, L.; Liu, P. *Org. Lett.* **2016**, *18*, 2580–2583.

(10) (a) Shiraishi, Y.; Sugano, Y.; Tanaka, S.; Hirai, T. *Angew. Chem., Int. Ed.* **2010**, *49*, 1656–1660. (b) Lang, X.; Ji, H.; Chen, C.; Ma, W.; Zhao, J. *Angew. Chem., Int. Ed.* **2011**, *50*, 3934–3937. (c) Lang, X.; Chen, X.; Zhao, J. *Chem. Soc. Rev.* **2014**, *43*, 473–486. (d) Shiraishi, Y.; Ikeda, M.; Tsukamoto, D.; Tanaka, S.; Hirai, T. *Chem. Commun.* **2011**, *47*, 4811–4813.

(11) Hermann, J. M.; Disdier, J.; Pichat, P. *J. Phys. Chem.* **1986**, *90*, 6028–6034.

(12) Wenderich, K.; Mul, G. *Chem. Rev.* **2016**, *116*, 14587–14619.

(13) Deshmane, V. G.; Owen, S. L.; Abrokwah, R. Y.; Kuila, D. *J. Mol. Catal. A: Chem.* **2015**, *408*, 202–213.

(14) Patra, K. K.; Gopinath, C. S. *ChemCatChem* **2016**, *8*, 3294–3311.

(15) Shiraishi, Y.; Fujiwara, K.; Sugano, Y.; Ichikawa, S.; Hirai, T. *ACS Catal.* **2013**, *3*, 312–320.

(16) Tron, G. C. *Eur. J. Org. Chem.* **2013**, *2013*, 1849–1859.

(17) Pumphrey, A. L.; Dong, H.; Driver, T. G. *Angew. Chem., Int. Ed.* **2012**, *51*, 5920–5923.

(18) Wu, N.; Song, F.; Yan, L.; Li, J.; You, J. *Chem. - Eur. J.* **2014**, *20*, 3408–3414.

(19) Pierce, L. T.; Cahill, M. M.; McCarthy, F. O. *Tetrahedron* **2011**, *67*, 4601–4611.

(20) Padwa, A.; Eisenbarth, P.; Venkatramanan, M. K.; Wong, G. S. K. *J. Org. Chem.* **1987**, *52*, 2427–2432.

(21) Couty, F.; David, O.; Durrat, F. *Tetrahedron Lett.* **2007**, *48*, 1027–1031.

(22) Collina, S.; Loddo, G.; Urbano, M.; Linati, L.; Callegari, A.; Ortuso, F.; Alcaro, S.; Laggner, C.; Langer, T.; Prezzavento, O.; Ronsisvalle, G.; Azzolina, O. *Bioorg. Med. Chem.* **2007**, *15*, 771–783.

(23) Britton, J.; Chalker, J. M.; Raston, C. L. *Chem. - Eur. J.* **2015**, *21*, 10660–10665.

(24) Ren, X.; O'Hanlon, J. A.; Morris, M.; Robertson, J.; Wong, L. L. *ACS Catal.* **2016**, *6*, 6833–6837.

Chemical Science

Check for updates

Regioselective Simmons–Smith-type cyclopropanations of polyalkenes enabled by transition metal catalysis†

Jacob Werth and Christopher Uyeda *

A [$^{i-Pr}$PDI]CoBr$_2$ complex (PDI = pyridine-diimine) catalyzes Simmons–Smith-type reductive cyclopropanation reactions using CH$_2$Br$_2$ in combination with Zn. In contrast to its non-catalytic variant, the cobalt-catalyzed cyclopropanation is capable of discriminating between alkenes of similar electronic properties based on their substitution patterns: monosubstituted > 1,1-disubstituted > (Z)-1,2-disubstituted > (E)-1,2-disubstituted > trisubstituted. This property enables synthetically useful yields to be achieved for the monocyclopropanation of polyalkene substrates, including terpene derivatives and conjugated 1,3-dienes. Mechanistic studies implicate a carbenoid species containing both Co and Zn as the catalytically relevant methylene transfer agent.

Introduction

Cyclopropanes are common structural elements in synthetic and natural biologically active compounds.[1] The Simmons–Smith cyclopropanation reaction was first reported over half a century ago but remains today one of the most useful methods for converting an alkene into a cyclopropane.[2] As compared to diazomethane, which is shock sensitive and must be prepared from complex precursors, CH$_2$I$_2$ is both stable and readily available, making it an attractive methylene source. Additionally, the stereospecificity of the Simmons–Smith reaction allows diastereomeric relationships in cyclopropanes to be established with a high degree of predictability. Several advances have addressed many of the limitations of the initial Simmons–Smith protocol. For example, Et$_2$Zn can be used in the place of Zn to more reliably and quantitatively generate the active carbenoid reagent.[3] Acidic additives, such as CF$_3$CO$_2$H[4] and substituted phenols,[5] have been found to accelerate the cyclopropanation of challenging substrates. Finally, Zn carbenoids bearing dialkylphosphate anions[6] or bipyridine ligands[7] are sufficiently stable to be stored in solution at low temperatures (Fig. 1).

Despite the many notable contributions in Zn carbenoid chemistry, a persistent limitation of Simmons–Smith-type cyclopropanations is their poor selectivity when attempting to discriminate between multiple alkenes of similar electronic properties. For example, the terpene natural product limonene

possesses a 1,1-disubstituted and a trisubstituted alkene. Friedrich reported that, under a variety of Zn carbenoid conditions, the two alkenes are cyclopropanated with similar rates, resulting in mixtures of monocyclopropanated (up to a 5 : 1 ratio of regioisomers) and dicyclopropanated products.[8] This issue is exacerbated by the challenge associated with separating the two monocyclopropane regioisomers, which only differ in the position of a non-polar CH$_2$ group. In general, synthetically useful regioselectivities in Simmons–Smith reactions are only observed for substrates containing directing groups.[9]

In principle, catalysis may provide an avenue to address selectivity challenges in Simmons–Smith-type cyclopropanations; however, unlike diazoalkane transfer reactions,
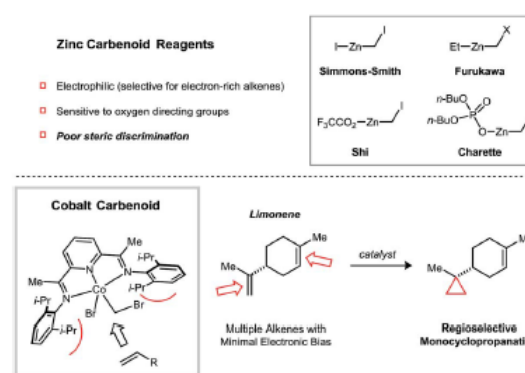
Fig. 1 Factors governing alkene selectivity in Zn carbenoid-mediated cyclopropanation reactions. Cobalt-catalyzed reductive cyclopropanation exhibiting high regioselectivities in polyalkene substrates based on alkene substitution patterns.

Department of Chemistry, Purdue University, West Lafayette, IN 47907, USA. E-mail: cuyeda@purdue.edu

which are catalyzed by a broad range of transition metal complexes,[9b,10] there has been comparatively little progress toward the development of robust catalytic strategies for reductive cyclopropanations.[11] Lewis acids in substoichiometric loadings have been observed to accelerate the Simmons–Smith reaction, but in many cases, this rate effect is restricted to allylic alcohol substrates.[12,13]

Recently, our group described an alternative approach to catalyzing reductive cyclopropanation reactions using a transition metal complex that is capable of activating the dihaloalkane reagent by C–X oxidative addition. A dinickel catalyst was shown to promote methylene[14] and vinylidene[15] transfer using CH_2Cl_2 and 1,1-dichloroalkenes in combination with Zn as a stoichiometric reductant. Here, we describe a mononuclear [PDI]Co (PDI = pyridine-diimine) catalyst[16] that imparts a high degree of steric selectivity in the cyclopropanation of polyalkene substrates. Mechanistic studies suggest that the key intermediate responsible for methylene transfer is a heterobimetallic conjugate of Co and Zn.

Results and discussion

4-Vinyl-1-cyclohexene contains a terminal and an internal alkene of minimal electronic differentiation and thus provided a suitable model substrate to initiate our studies (Table 1).[8,17] Under standard CH_2I_2/Et_2Zn conditions (entry 1), there is a modest preference for cyclopropanation of the more electron-rich disubstituted alkene (rr = 1 : 6.7) with increasing amounts of competing dicyclopropanation being observed at higher conversions (entries 2 and 3). Other modifications to the conditions, including the use of a Brønsted acid[4] (entry 4) or a Lewis acid additive[12b,18] (entry 5), did not yield any improvements in selectivity. Likewise, an Al carbenoid generated using CH_2I_2 and $AlEt_3$ afforded a similar preference for cyclopropanation of the endocyclic alkene (entry 6).[19]

In a survey of transition metal catalysts, the $[^{i-Pr}PDI]CoBr_2$ complex 1 was identified as a highly regioselective catalyst for the cyclopropanation of 4-vinyl-1-cyclohexene, targeting the less hindered terminal alkene (Table 2). CH_2Br_2 and Zn alone do not afford any background levels of cyclopropanation (entry 1); however, the addition of 6 mol% $[^{i-Pr}PDI]CoBr_2$ (1) provided monocyclopropane 3 (81% yield) with a >50 : 1 rr and <1% of the dicyclopropane product (entry 5). The steric profile of the catalyst appears to be critically important for yield. For example, the mesityl- (entry 6) and phenyl-substituted variants (entry 7) of the ligand provided only 58% and 4% yield respectively under the same reaction conditions. Related N-donor ligands similarly afforded low levels of conversion (entries 8–12) as did the use of other first-row transition metals, including Fe (entry 14) and Ni (entry 15), in the place of Co.

In order to define the selectivity properties of catalyst 1, we next conducted competition experiments using alkenes bearing different patterns of substitution (Fig. 2). Reactions were carried out using an equimolar amount of each alkene and run to full conversion of the limiting CH_2Br_2 reagent (1.0 equiv.). Monosubstituted alkenes are the most reactive class of substrates using 1 but are not adequately differentiated from 1,1-disubstituted alkenes (3 : 1). By contrast, terminal alkenes are significantly more reactive than internal alkenes, providing synthetically useful selectivities (≥31 : 1). Furthermore, a model Z-alkene was cyclopropanated in preference to its E-alkene congener in a 33 : 1 ratio. Using catalyst 1, trisubstituted alkenes are poorly reactive, and no conversion is observed for tetrasubstituted alkenes.

The synthetic applications of the catalytic regioselective cyclopropanation were examined using the terpene natural products and derivatives shown in Fig. 3. In all cases, the selectivity properties follow the trends established in the competition experiments. Substrates containing ether or free alcohol functionalities (e.g., 7, 10, and 11) exhibit a strong directing group effect under classical Simmons–Smith conditions; however, catalyst 1 overrides this preference and targets the less hindered alkene. Additionally, the presence of electron-deficient α,β-unsaturated carbonyl systems (e.g., 9, 13, and 14) do not perturb the expected steric selectivity.

Table 1 Regioselectivity studies using Zn and Al carbenoid reagents[a]

Entry	Reaction conditions	Yield (3 + 4)	rr (3 : 4)	Yield 5
1	CH_2I_2 (1.0 equiv.), Et_2Zn (0.5 equiv.)	28%	1 : 6.7	3%
2	CH_2I_2 (1.0 equiv.), Et_2Zn (1.0 equiv.)	33%	1 : 4.6	5%
3	CH_2I_2 (2.0 equiv.), Et_2Zn (2.0 equiv.)	53%	1 : 6.5	16%
4	CH_2I_2 (1.0 equiv.), Et_2Zn (1.0 equiv.), 3,5-difluorobenzoic acid (2.0 equiv.)	28%	1 : 3.5	19%
5	CH_2I_2 (2.0 equiv.), Et_2Zn (2.0 equiv.), $TiCl_4$ (0.2 equiv.)	13%	1 : 4.6	1%
6	CH_2I_2 (1.2 equiv.), $AlEt_3$ (1.2 equiv.)	38%	1 : 3.1	9%

[a] Reaction conditions: 4-vinylcyclohexene (0.14 mmol), CH_2Cl_2 (1.0 mL), 24 h, 22 °C. Yields and ratios of regioisomers were determined by GC analysis against an internal standard.

Chemical Science

Table 2 Catalyst structure–activity relationship studies[a]

Entry	Metal source	Ligand	Yield (3 + 4)	rr (3 : 4)	Yield 5
1	—	—	<1%	—	<1%
2	CoBr$_2$	—	<1%	—	<1%
3	Co(DME)Br$_2$	—	<1%	—	<1%
4	—	$^{i-Pr}$PDI	<1%	—	<1%
5	CoBr$_2$	$^{i-Pr}$PDI	81%	>50 : 1	<1%
6	CoBr$_2$	^{Me}PDI	58%	>50 : 1	<1%
7	CoBr$_2$	^{Ph}PDI	4%	—	<1%
8	CoBr$_2$	$^{i-Pr}$DAD	<1%	—	<1%
9	CoBr$_2$	$^{i-Pr}$IP	2%	—	<1%
10	CoBr$_2$	Terpy	4%	—	<1%
11	CoBr$_2$	$^{t-Bu}$PyBOX	<1%	—	<1%
12	CoBr$_2$	^{Ph}PyBOX	<1%	—	<1%
13	CoBr$_2$	PPh$_3$ (12 mol%)	<1%	—	0%
14	FeBr$_2$	$^{i-Pr}$PDI	3%	—	<1%
15	NiBr$_2$	$^{i-Pr}$PDI	<1%	—	<1%

[a] Reaction conditions: 4-vinylcyclohexene (0.14 mmol), THF (1.0 mL), 24 h, 22 °C. Yields and ratios of regioisomers were determined by GC analysis against an internal standard.

Vinylcyclopropanes are a valuable class of synthetic intermediates that engage in catalytic strain-induced ring-opening reactions.[20] The monocyclopropanation of a diene represents an attractive approach to their synthesis but would require a catalyst that is capable of imparting a high degree of regioselectivity and avoiding secondary additions to form dicyclopropane products.[21] These challenges are addressed for a variety of diene classes using catalyst 1 (Fig. 4). Over the substrates that we have examined, the selectivities for cyclopropanation of the terminal over the internal double bond of the diene system are uniformly high. Additionally, the catalyst is tolerant of vinyl bromide (15) and vinyl boronate (23) functional groups, which are commonly used in cross-coupling reactions.

Like the non-catalytic Simmons–Smith reaction,[2c] the cyclopropanation using 1 is stereospecific within the limit of detection, implying a mechanism in which the two C–C σ-bonds are either formed in a concerted fashion or by a stepwise process that does not allow for single bond rotation. For example,
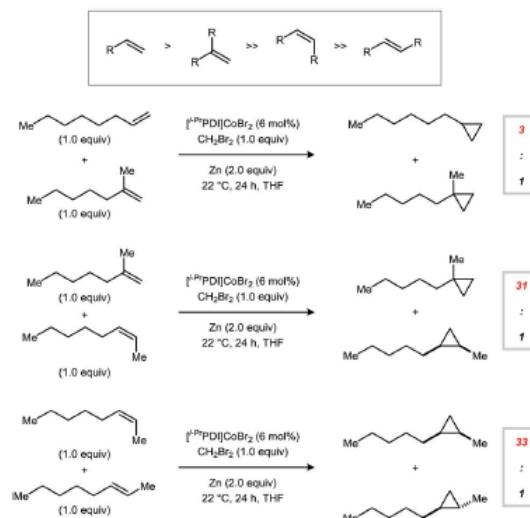
Fig. 2 Intermolecular competition experiments probing selectivity based on alkene substitution patterns. Reactions were conducted using a 1 : 1 : 1 molar ratio of the two alkene starting materials and CH$_2$Br$_2$.
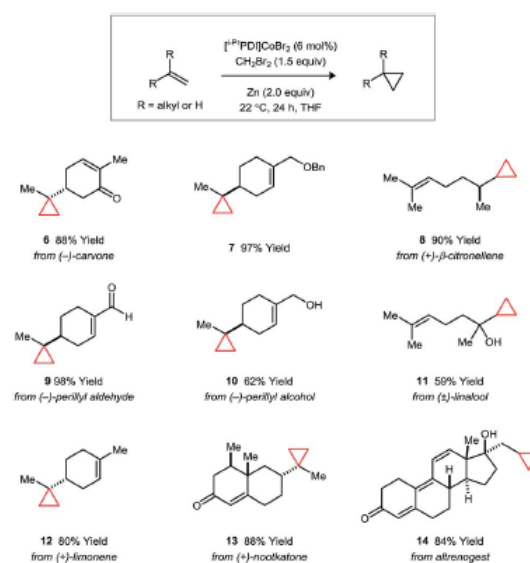
Fig. 3 Catalytic regioselective monocyclopropanations of terpene natural products and derivatives. Isolated yields following purification are averaged over two runs.

cyclopropanation of the Z-alkene 24 affords the cis-disubstituted cyclopropane 25 in 95% yield as a single diastereomer (Fig. 5a). Furthermore, the vinylcyclopropane substrates 26 and 28, commonly used as tests for cyclopropylcarbinyl radical intermediates, react without ring-opening to afford products 27 and 29 (Fig. 5b).
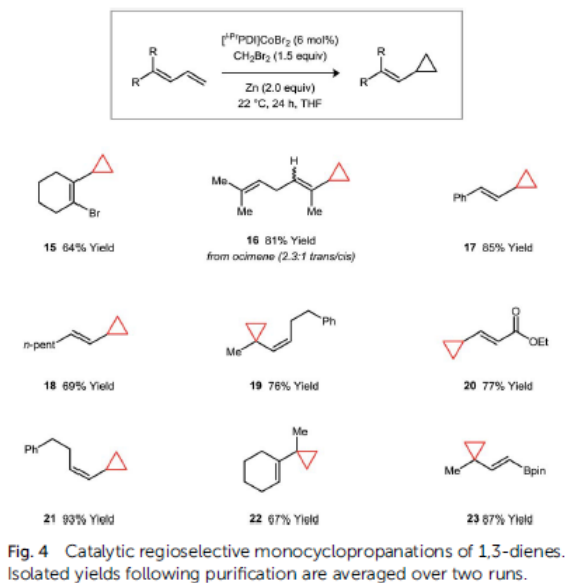
Fig. 4 Catalytic regioselective monocyclopropanations of 1,3-dienes. Isolated yields following purification are averaged over two runs.

Under standard catalytic conditions, the reaction mixtures using **1** adopt a deep violet color, which persists until complete consumption of the alkene. The UV-vis spectrum of the catalytic mixture at partial conversion is consistent with a Co(I) resting state (Fig. 6a). The authentic [$^{i-Pr}$PDI]CoBr complex (**30**) can be prepared by stirring the [$^{i-Pr}$PDI]CoBr$_2$ complex **1** over excess Zn metal.[22] Cyclic voltammetry data (Fig. 6b) indicates an $E_{1/2}$ for the Co(II)/Co(I) redox couple of -1.00 V *vs.* Fc/Fc$^+$. The large peak-to-peak separation (0.96 V in 0.3 M [n-Bu$_4$N][PF$_6$]/THF) is characteristic of a slow bromide dissociation step following electron transfer. The second Co(I)/Co(0) reduction event is significantly more cathodic at -1.93 V and is inaccessible using Zn.

In order to decouple the cyclopropanation steps of the mechanism from catalyst turnover, we conducted stoichiometric reactions with the isolated [$^{i-Pr}$PDI]CoBr complex in the
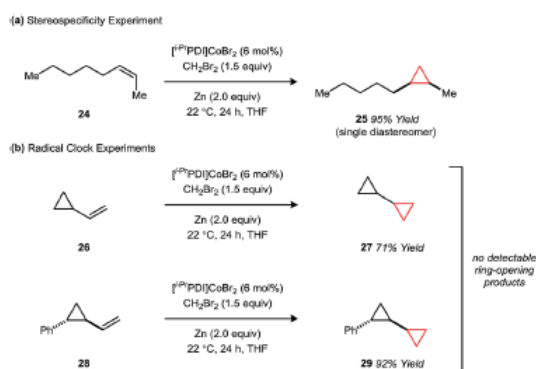
Fig. 5 Mechanistic studies probing the concertedness of cyclopropane formation.

Fig. 6 Mechanistic studies probing the nature of the active carbenoid intermediate. (a) Identification of the catalyst resting state. (b) Cyclic voltammetry data for the [$^{i-Pr}$PDI]CoBr$_2$ complex. (c) Stoichiometric cyclopropanation reactions using the [$^{i-Pr}$PDI]CoBr$_2$ complex in the absence and presence of ZnBr$_2$. (d) A proposed Co/Zn carbenoid species. (e) Proposed dinuclear mechanism for the Lewis acid-accelerated Simmons–Smith reaction. (f) Solid-state structure for the [$^{i-Pr}$PDI]CoBr$_2$Zn(THF/Et$_2$O)Br$_2$ complex (**31**). The solvent molecule bound to Zn is disordered between Et$_2$O and THF. Only the THF-bound structure is shown for clarity.

absence of Zn (Fig. 6c). The reaction of **30** with 4-vinylcyclohexene and CH$_2$Br$_2$ generates the [$^{i-Pr}$PDI]CoBr$_2$ complex **1** within 24 h at room temperature but forms cyclopropanated products in a relatively low combined yield of 26%, which is not commensurate with the efficiency of the catalytic process. Furthermore, the regioselectivity is only 3 : 1, whereas the catalytic cyclopropanation achieves a >50 : 1 selectivity for this substrate. When the same stoichiometric reaction is conducted in the presence of ZnBr$_2$, the yield and selectivity of the catalytic process is fully restored.

The Co-containing product (**31**) of the stoichiometric reaction in the presence of ZnBr$_2$ is green, which is notably distinct

from the tan color of the $[^{i-Pr}PDI]CoBr_2$ complex **1**. This green species is NMR silent but may be crystallized from saturated solutions in Et_2O to afford **31** (Fig. 6f). The solid-state structure reveals the expected $[^{i-Pr}PDI]CoBr_2$ fragment in a distorted square pyramidal geometry ($\tau_5 = 0.36$) with a $Zn(THF/Et_2O)Br_2$ Lewis acid coordinated to one of the Br ligands. This interaction induces an asymmetry in the structure, causing the Co–Br1 distance (2.557(1) Å) to be elongated relative to the Co–Br2 distance (2.358(2) Å).

Collectively, these studies suggest that both Co and Zn are present in the reactive carbenoid intermediate, and that $ZnBr_2$ may interact with the $[^{i-Pr}PDI]Co$ complex through Lewis acid–base interactions. There is a notable similarity between the observed Co/Zn effect and previous studies of Lewis acid acceleration in the Simmons–Smith cyclopropanation. For example, Zn carbenoid reactions are known to be accelerated by the presence of ZnX_2,[12c] which is generated as a byproduct of the reaction. DFT calculations conducted by Nakamura have suggested that the origin of this rate acceleration may be due to the accessibility of a five-membered ring transition state, which requires the presence of an additional Zn equivalent to function as a halide shuttle.[23]

Conclusions

In summary, transition metal catalysis provides a pathway to accessing unique selectivity in reductive carbenoid transfer reactions. A $[^{i-Pr}PDI]CoBr_2$ complex functions as a robust catalyst for Simmons–Smith type cyclopropanation using a CH_2Br_2/Zn reagent mixture. This system exhibits the highest regioselectivities that have been observed in reductive cyclopropanations based solely on the steric properties of the alkene substrate. Accordingly, a range of terpenes and conjugated dienes may be converted to a single monocyclopropanated product. Ongoing studies are directed at exploring the applications of transition metal catalysts to other classes of carbenoid transfer reactions.

Conflicts of interest

There are no conflicts to declare.

Acknowledgements

Notes and references

1 (a) J. Salaun and M. Baird, *Curr. Med. Chem.*, 1995, **2**, 511–542; (b) W. A. Donaldson, *Tetrahedron*, 2001, **57**, 8589–8627; (c) L. A. Wessjohann, W. Brandt and T. Thiemann, *Chem. Rev.*, 2003, **103**, 1625–1648; (d) N. A. Meanwell, *J.*

2 (a) H. E. Simmons and R. D. Smith, *J. Am. Chem. Soc.*, 1958, **80**, 5323–5324; (b) H. E. Simmons and R. D. Smith, *J. Am. Chem. Soc.*, 1959, **81**, 4256–4264; (c) A. B. Charette and A. Beauchemin, *Org. React.*, 2001, **58**, 1–415.

3 (a) J. Furukawa, N. Kawabata and J. Nishimura, *Tetrahedron Lett.*, 1966, **7**, 3353–3354; (b) J. Furukawa, N. Kawabata and J. Nishimura, *Tetrahedron*, 1968, **24**, 53–58.

4 (a) Z. Yang, J. C. Lorenz and Y. Shi, *Tetrahedron Lett.*, 1998, **39**, 8621–8624; (b) J. C. Lorenz, J. Long, Z. Yang, S. Xue, Y. Xie and Y. Shi, *J. Org. Chem.*, 2004, **69**, 327–334.

5 A. B. Charette, S. Francoeur, J. Martel and N. Wilb, *Angew. Chem., Int. Ed.*, 2000, **39**, 4539–4542.

6 A. Voituriez, L. E. Zimmer and A. B. Charette, *J. Org. Chem.*, 2010, **75**, 1244–1250.

7 A. B. Charette, J.-F. Marcoux, C. Molinaro, A. Beauchemin, C. Brochu and É. Isabel, *J. Am. Chem. Soc.*, 2000, **122**, 4508–4509.

8 There is some conflicting data in the literature regarding the regioselectivity of Zn carbenoid addition to limonene; however, the most recent and comprehensive studies have found that mixtures of regioisomers are formed and that the product ratios depend on the reaction conditions: (a) S. D. Koch, R. M. Kliss, D. V. Lopiekes and R. J. Wineman, *J. Org. Chem.*, 1961, **26**, 3122–3125; (b) H. E. Simmons, E. P. Blanchard and R. D. Smith, *J. Am. Chem. Soc.*, 1964, **86**, 1347–1356; (c) E. C. Friedrich and F. Niyati-Shirkhodaee, *J. Org. Chem.*, 1991, **56**, 2202–2205.

9 (a) A. H. Hoveyda, D. A. Evans and G. C. Fu, *Chem. Rev.*, 1993, **93**, 1307–1370; (b) H. Lebel, J.-F. Marcoux, C. Molinaro and A. B. Charette, *Chem. Rev.*, 2003, **103**, 977–1050.

10 (a) H. Nozaki, S. Moriuti, M. Yamabe and R. Noyori, *Tetrahedron Lett.*, 1966, **7**, 59–63; (b) M. P. Doyle, *Chem. Rev.*, 1986, **86**, 919–939; (c) M. P. Doyle, M. A. McKervey and T. Ye, *Modern catalytic methods for organic synthesis with diazo compounds*, Wiley, 1998; (d) H. Pellissier, *Tetrahedron*, 2008, **64**, 7041–7095.

11 Photoredox catalysts for reductive cyclopropanation reactions: (a) A. M. del Hoyo, A. G. Herraiz and M. G. Suero, *Angew. Chem., Int. Ed.*, 2017, **56**, 1610–1613; (b) A. M. del Hoyo and M. García Suero, *Eur. J. Org. Chem.*, 2017, **2017**, 2122–2125.

12 (a) H. Takahashi, M. Yoshioka, M. Ohno and S. Kobayashi, *Tetrahedron Lett.*, 1992, **33**, 2575–2578; (b) A. B. Charette and C. Brochu, *J. Am. Chem. Soc.*, 1995, **117**, 11367–11368; (c) S. E. Denmark and S. P. O'Connor, *J. Org. Chem.*, 1997, **62**, 584–594; (d) A. B. Charette, C. Molinaro and C. Brochu, *J. Am. Chem. Soc.*, 2001, **123**, 12168–12175; (e) H. Shitama and T. Katsuki, *Angew. Chem., Int. Ed.*, 2008, **47**, 2450–2453; (f) J. Balsells and P. J. Walsh, *J. Org. Chem.*, 2000, **65**, 5005–5008.

13 J. Long, H. Du, K. Li and Y. Shi, *Tetrahedron Lett.*, 2005, **46**, 2737–2740.

14 Y.-Y. Zhou and C. Uyeda, *Angew. Chem., Int. Ed.*, 2016, **55**, 3171–3175.

Med. Chem., 2011, **54**, 2529–2591; (e) D. Y. K. Chen, R. H. Pouwer and J.-A. Richard, *Chem. Soc. Rev.*, 2012, **41**, 4631–4642.

GDCh

Communications

Angewandte Chemie International Edition

Check for updates

Carbenoids

Cobalt-Catalyzed Reductive Dimethylcyclopropanation of 1,3-Dienes

Jacob Werth and Christopher Uyeda*

Abstract: Dimethylcyclopropanes are valuable synthetic targets that are challenging to access in high yield using Zn carbenoid reagents. Herein, we describe a cobalt-catalyzed variant of the Simmons–Smith reaction that enables the efficient dimethylcyclopropanation of 1,3-dienes using a Me_2CCl_2/Zn reagent mixture. The reactions proceed with high regioselectivity based on the substitution pattern of the 1,3-diene. The products are vinylcyclopropanes, which serve as substrates for transition-metal-catalyzed ring-opening reactions, including 1,3-rearrangement and [5+2] cycloaddition. Preliminary studies indicate that moderately activated monoalkenes are also amenable to dimethylcyclopropanation under the conditions of cobalt catalysis.

Geminal dimethylation is a common substitution pattern in polycyclic terpene natural products (Scheme 1).[1] Medicinal chemists have also explored the installation of dimethyl groups in biologically active compounds as a strategy to improve their potency or to eliminate metabolic liabilities.[2] There are now over 50 clinically approved pharmaceutical compounds that feature this motif. The presence of *gem*-dimethylation in a target compound introduces significant synthetic complexity, as a hindered tetrasubstituted carbon

atom must be generated. The most common routes utilize classical carbonyl chemistry and entail either a double α-alkylation reaction or the double addition of a methyl nucleophile to a carboxylic acid derivative.[3]

It is attractive to consider an alternative approach based on the formation of dimethylcyclopropanes,[4] which are themselves common in biologically active compounds[2, 5] but may also be diversified into other frameworks through strain-induced ring-opening reactions.[6] The Simmons–Smith reaction is potentially well-suited to addressing these structures; however, it is known that the efficiency of zinc-carbenoid-based cyclopropanation reactions decreases significantly when using disubstituted *gem*-dihaloalkanes.[7] For example, the addition of 2,2-diiodopropane under Furukawa conditions has only been demonstrated for two simple substrates, cyclopentene and cyclohexene, which provide yields up to 59% after a reaction time of 5 days.[8] A notable advance in this area was reported by Charette and Wilb, who showed that directing-group effects can be leveraged to achieve a high-yielding dimethylcyclopropanation of allylic alcohols (Scheme 2).[9] Additionally, a Corey–Chaykovsky-type dimethylcyclopropanation of α,β-unsaturated carbonyl compounds has been developed.[10]

We recently found that [PDI]Co (PDI = pyridine–diimine) complexes function as catalysts[11,12] for Simmons–Smith-type cyclopropanation reactions and generate a reactive carbene equivalent with significantly altered selectivity properties as compared to Zn carbenoids.[13] Motivated by this finding, we became interested in using transition-metal catalysis to address the dimethylcyclopropanation reaction. Herein, we report a cobalt-catalyzed dimethylcyclopropanation of 1,3-dienes using Me_2CCl_2/Zn as a source of isopropylidene equivalents.

The $[^{2,6\text{-}i\text{-}Pr}PDI]CoBr_2$ complex was previously shown to be an effective catalyst for cyclopropanation reactions using CH_2Br_2/Zn;[13] however, it afforded negligible yields in the analogous reactions using Me_2CCl_2/Zn (Table 1, entry 7). We reasoned that the more hindered dimethylcarbene fragment may require the steric profile of the PDI ligand to be correspondingly adjusted. Accordingly, a series of ligands **L1–L4** was prepared by varying the size of the flanking aryl substituents. The 2-*t*-BuPh-derived catalyst was identified as optimal (entry 4), and the dimethylcyclopropanation of a model 1,3-diene **1** provided **2** in 93% yield as a single regioisomer. Zn is not capable of directly activating Me_2CCl_2, and in the absence of the Co catalyst, there was no conversion (entry 1). Although $ZnCl_2$ is generated as a stoichiometric by-product, the presence of $ZnBr_2$ at the start of the reaction provided a modest beneficial effect on the yield (entry 14). $ZnBr_2$ accelerates the initial reduction of the yellow Co^{II} complex to a violet Co^{I} species, which is then capable of activating Me_2CCl_2. Finally, other classes of bidentate and
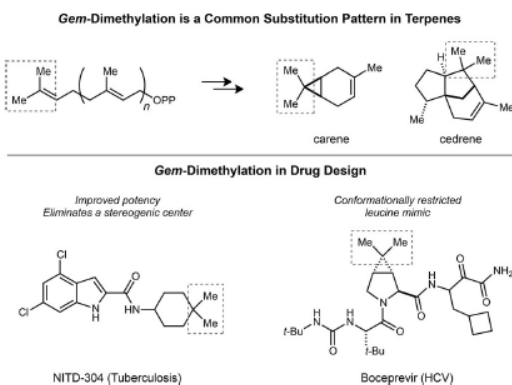
Scheme 1. Rings containing *gem*-dimethyl groups, including dimethylcyclopropanes, are found in biologically active compounds of natural and synthetic origins.

[*] J. Werth, Prof. C. Uyeda
Department of Chemistry, Purdue University
West Lafayette, IN 47907 (USA)
E-mail: cuyeda@purdue.edu

Supporting information and the ORCID identification number(s) for the author(s) of this article can be found under:
https://doi.org/10.1002/anie.201807542.

GDCh

Communications

Angewandte
Chemie
International Edition

(a) Dimethylcyclopropanation Reactions

Charette / *Corey*

allylic alcohols / α,β-unsaturated carbonyl compounds

(b)

Transition Metal Catalysis — Cyclopropanes ⟹ Larger Rings

rearrangement / ring opening / cycloaddition

(c)
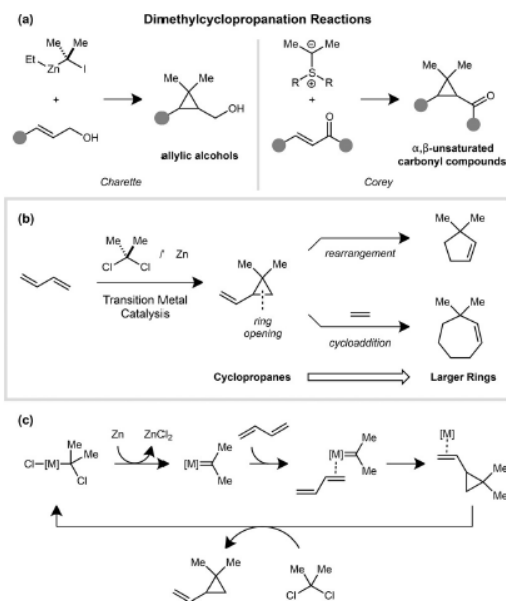
Scheme 2. a) Simmons–Smith-type dimethylcyclopropanation reactions of allylic alcohols and Corey–Chaykovsky dimethylcyclopropanation reactions of α,β-unsaturated carbonyl compounds. b) Transition-metal-catalyzed reductive dimethylcyclopropanation reactions of 1,3-dienes and ring-opening reactions to generate five- and seven-membered rings. c) Proposed mechanism for a transition-metal-catalyzed reductive dimethylcyclopropanation reaction.

Table 1: Catalyst optimization studies.[a]

2-t-BuPDI (**L1**): Ar = 2-(t-Bu)C₆H₄
2,4,6-MePDI (**L2**): Ar = 2,4,6-Me₃C₆H₂
3,5-t-BuPDI (**L3**): Ar = 3,5-(t-Bu)₂C₆H₃
2,6-i-PrPDI (**L4**): Ar = 2,6-(i-Pr)₂C₆H₃

2,6-i-PrIP (**L5**)   2,6-i-PrDAD (**L6**)

bpy (**L7**)   terpy (**L8**)

Entry	Metal source	Ligand	Yield 2 [%]
1	–	–	<1
2	–	2-t-BuPDI (**L1**)	<1
3	CoBr₂	–	<1
4	CoBr₂	2-t-BuPDI (**L1**)	93
5	CoBr₂	2,4,6-MePDI (**L2**)	77
6	CoBr₂	3,5-t-BuPDI (**L3**)	8
7	CoBr₂	2,6-i-PrPDI (**L4**)	2
8	NiBr₂	2-t-BuPDI (**L1**)	5
9	FeBr₂	2-t-BuPDI (**L1**)	4
10	CoBr₂	2,6-i-PrIP (**L5**)	2
11	CoBr₂	2,6-i-PrDAD (**L6**)	<1
12	CoBr₂	bpy (**L7**)	4
13	CoBr₂	terpy (**L8**)	1
14[b]	CoBr₂	2-t-BuPDI (**L1**)	87
15[c]	CoBr₂	2-t-BuPDI (**L1**)	78
16[d]	CoBr₂	2-t-BuPDI (**L1**)	79

[a] Reactions were carried out with 0.14 mmol of the 1,3-diene in THF (1 mL). The yield of **2** was determined by GC analysis against an internal standard. [b] The reaction was carried out without ZnBr₂. [c] The reaction was carried out with 1.1 equivalents of Me₂CCl₂. [d] The reaction was carried out with 2.0 equivalents of Me₂CBr₂.

tridentate ligands containing combinations of pyridine and imine donors were ineffective relative to PDI (entries 10–13). As a point of comparison, the noncatalytic dimethylcyclopropanation of **1** under Furukawa-type Simmons–Smith conditions (I₂CMe₂/Et₂Zn)[9] provided **2** in a moderate yield of 45% along with several inseparable side products (see the Supporting Information for experimental details).

Having optimized the reaction conditions, we next evaluated the scope of the dimethylcyclopropanation reaction (Scheme 3). A variety of 1-substituted, 1,2-disubstituted, and 1,3-disubstituted dienes were viable substrates. In all cases, cyclopropanation occurred at the terminal double bond with high regioselectivity (rr > 19:1). Notably, there was no detectable secondary cyclopropanation of the product alkene despite the presence of excess Me₂CCl₂ and Zn in the reaction mixture. Common functional handles for further synthetic elaboration were tolerated, including a protected amine (product **8**), a BPin group (product **9**), an ester (product **13**), and a free alcohol (product **18**). The activation of Me₂CCl₂ by the Co catalyst is relatively facile, so that aryl chlorides present in the substrate are tolerated (product **4**). The TBS-protected variant of the Danishefsky diene afforded the protected cyclopropanol derivative **14** in high yield.

Unlike the Simmons–Smith reaction, the cobalt-catalyzed process is relatively insensitive to the electronic properties of the diene.[14] For example, the presence of an electron-

withdrawing group, such as a phosphonate ester (product **11**), a ketone (product **12**), or an ester (product **13**), did not significantly decrease the rate of the reaction, nor did it result in poor yields of the product. Additionally, the cobalt catalyst does not appear to interact strongly with alcohol directing groups.[15] The diene **16** was selectively monocyclopropanated at the terminal double bond (rr > 19:1), as expected based solely on steric considerations. By contrast, Furukawa-type conditions using I₂CMe₂/Et₂Zn afford selectivity for the internal double bond, which is proximal to the alcohol.[9]

Synthetic ethyl chrysanthemate (**19**) is prepared on industrial scales by the addition of ethyl diazoacetate to 2,5-dimethyl-2,4-hexadiene.[16] A limitation of this process is that the cyclopropane is formed as a mixture of *cis* and *trans* diastereomers, whereas natural pyrethrins are found only with the *trans* relative configuration. In the cobalt-catalyzed cyclopropanation, ethyl (*E*)-5-methyl-2,4-hexadienoate reacted at the less hindered internal alkene with > 19:1 *trans* selectivity to give **19**. This approach was applied to the synthesis of the commercial pesticide phenothrin (**20**)[17] and

GDCh

Communications

Angewandte Chemie International Edition

(1.0 equiv) + (2.0 equiv) Me Me Cl Cl → [2-t-BuPDI]CoBr₂ **3** (10 mol%) Zn (2.0 equiv) ZnBr₂ (1.0 equiv) THF, 24 h → Me Me (±)

[2-t-BuPDI]CoBr₂ **3**

4 95% yield **5** 95% yield **6** 72% yield **7** 90% yield **8** 54% yield **9** 91% yield **10** 96% yield **11** 92% yield

12 52% yield **13** 90% yield **14** 70% yield **15** 81% yield

Simmons–Smith Reaction[a] ← **16** → Catalytic Conditions

17 35% combined yield 4:1 rr (**17:18**)

18 58% yield 1:>19 rr (**17:18**)

Pyrethroids[b]
Chrysanthemates

ethyl chrysanthemate **19** 62% yield (>19:1 *trans:cis*)

phenothrin **20** 55% yield (>19:1 *trans:cis*)

Novel Pyrethroids

21 (n = 1) 78% yield (9:1 *trans:cis*)
22 (n = 2) 74% yield (13:1 *trans:cis*)
23 (n = 3) 69% yield (13:1 *trans:cis*)

24 21% yield (>19:1 *trans:cis*)

25 52% yield (>19:1 *trans:cis*)

Strain-Induced Ring-Opening Reactions
Vinylcyclopropane Rearrangement (Louie)

ring-opening → Ni(COD)₂ (5 mol%) IPr (10 mol%) 60 °C, 12 h, C₆H₆ →

26 98% yield **27** 65% yield

[5 + 2]-Cycloaddition (Wender)

ring-opening → Rh(PPh₃)₃Cl (5 mol%) AgOTf (5 mol%) 110 °C, 17 h, toluene →

28 90% yield **29** 77% yield

Scheme 3. Studies of the reaction scope. Standard reaction conditions: 1,3-diene (0.14 mmol, 1.0 equiv), Me₂CCl₂ (2.0 equiv), Zn (2.0 equiv), ZnBr₂ (1.0 equiv), [2-t-BuPDI]CoBr₂ (**3**; 10 mol%), THF (1 mL), 22 °C, 24 h. [a] Simmons–Smith reaction conditions: ZnEt₂ (4.0 equiv), I₂CMe₂ (4.0 equiv), CH₂Cl₂ (1.0 mL). [b] Modifications to standard conditions: DCE (1.0 mL) instead of THF, Me₂CBr₂ (2.0 equiv) instead of Me₂CCl₂. Bn = benzyl, COD = 1,5-cyclooctadiene, DCE = 1,2-dichloroethane, IPr = 1,3-bis(2,6-diisopropylphenyl)-2-imidazolidinylidene, pin = pinacolate, TBS = tert-butyldimethylsilyl, Tf = trifluoromethanesulfonyl, Ts = p-toluenesulfonyl.

unnatural pyrethrin analogues that contain other alkyl (product **25**), cycloalkyl (products **21–23**), or aryl substituents (product **24**) in the place of the terminal methyl groups.

We considered the possibility that the vinyl cyclopropane products generated by this method might serve as substrates for transition-metal-catalyzed ring-opening reactions; however, it was unknown at the outset whether the steric hindrance imposed by a *gem*-dimethyl group would be tolerated. Vinyl cyclopropane **26** was prepared from the corresponding 1,3-diene precursor in 98% yield. Heating **26** at 60 °C for 12 h in the presence of a IPr/Ni(COD)₂ catalyst provided the rearranged cyclopentene product **27** in 65% yield.[18] The position of the alkene in **27** indicates that only the less hindered C–C bond is activated by the catalyst.

A substrate containing both a 1,3-diene and an isolated alkene was cyclopropanated under the cobalt-catalyzed conditions to yield a single regioisomer of the monocyclopropane product **28**. When **28** was subjected to the rhodium-catalyzed [5+2] cycloaddition conditions developed by Wender et al.,[19]

the bicyclic product **29** was formed in 77% yield. Like the 1,3-rearrangement reaction, the ring-opening proceeded with high regioselectivity to furnish a single isomer of the product.

Finally, it was of interest to test whether the catalytic conditions developed for the dimethylcyclopropanation of 1,3-dienes could be applied to isolated alkenes. Simple, unactivated alkenes, such as 1-octene or cyclohexene, were unreactive (<2% yield); however, substrates possessing a moderate degree of strain proved to be viable. For example, cyclopentene was cyclopropanated in 87% yield under the standard optimized conditions to give **30** (Scheme 4). This result represents a significant improvement in yield and reaction time over the only previously reported attempt to carry out this transformation (45% yield after 5 days using I₂CMe₂/Et₂Zn).[8] Additionally, cyclooctene, indene, and norbornene reacted in high yield to give products **31–33**. In the last case, the *exo*-addition product was formed exclusively. *N*-*tert*-butoxycarbonyl-2,5-dihydropyrrole (**34**) was cyclopropanated in 90% yield to generate **35**, which is a protected
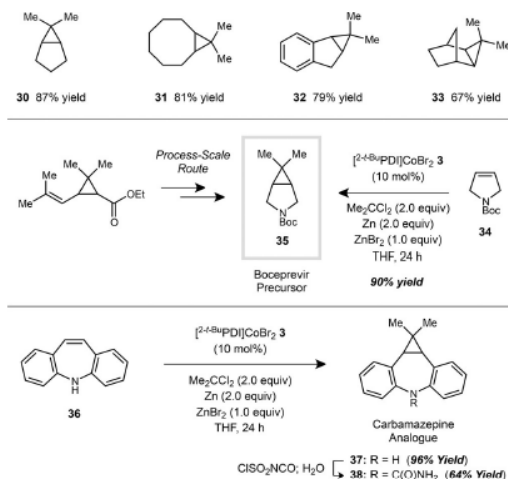
Scheme 4. Dimethylcyclopropanation of activated alkenes, including application to the synthesis of a boceprevir precursor and an analogue of carbamazepine. Standard dimethylcyclopropanation conditions: 1,3-diene (0.14 mmol, 1.0 equiv), Me_2CCl_2 (2.0 equiv), Zn (2.0 equiv), $ZnBr_2$ (1.0 equiv), [$^{2-t-Bu}$PDI]CoBr$_2$ (3; 10 mol%), THF (1 mL), 22°C, 24 h.

0.28 mmol, 2.0 equiv), $ZnBr_2$ (31 mg, 0.14 mmol, 1.0 equiv), THF (1.0 mL), and a magnetic stir bar. The reaction mixture was stirred at room temperature for approximately 15 min, during which time a deep violet color was observed corresponding to the reduced cobalt catalyst. Me_2CCl_2 (31.6 mg, 0.28 mmol, 2.0 equiv) was added, and the reaction mixture was stirred at room temperature. After 24 h, the reaction mixture was exposed to an ambient atmosphere and concentrated under reduced pressure. The crude residue was directly loaded onto a SiO_2 column for purification.

Acknowledgements

Conflict of interest

The authors declare no conflict of interest.

precursor to the HCV protease inhibitor boceprevir.[20] The process-scale route to this bicyclic amine consists of a multi-step sequence in which the *gem*-dimethylcyclopropane unit is ultimately derived from ethyl chrysanthemate.

Tricyclic antidepressants (TCAs) are a class of compounds that commonly contain a dibenzazepine.[21] Parent 5*H*-dibenz-[*b,f*]azepine (36), bearing an unprotected N−H group, could be directly dimethylcyclopropanated to provide 37 in 96% yield. Notably, previous attempts to cyclopropanate this substrate under Simmons–Smith conditions (CH_2I_2 + Zn/Cu) only yielded the product of methylene insertion into the N−H bond.[22] One-step derivatization of 37 using chlorosulfonyl isocyanate[23] yielded 38, a dimethylcyclopropane-containing analogue carbamazepine,[21b] which is used as a treatment for epilepsy and neuropathic pain.

In summary, cobalt catalysis enabled the synthesis of dimethylcyclopropanes that were not previously accessible in high yield using the Simmons–Smith reaction. In particular, the regioselective dimethylcyclopropanation of 1,3-dienes yielded polysubstituted vinyl cyclopropanes, which participate in strain-induced ring-opening reactions. Moderately activated monoalkenes were also cyclopropanated efficiently to generate building blocks for medicinal chemistry. These studies collectively highlight the unique properties of transition-metal carbenoids over their Zn counterparts as reactive species in cyclopropanation chemistry.

Experimental Section

General procedure: In an N_2-filled glovebox, a 2 dram vial was charged with [$^{2-t-Bu}$PDI]CoBr$_2$ (3; 9.0 mg, 0.014 mmol, 10 mol%), the 1,3-diene or alkene (0.14 mmol, 1.0 equiv), Zn powder (18 mg,

[1] a) T. J. Maimone, P. S. Baran, *Nat. Chem. Biol.* **2007**, *3*, 396; b) J. Gershenzon, N. Dudareva, *Nat. Chem. Biol.* **2007**, *3*, 408.
[2] T. T. Talele, *J. Med. Chem.* **2018**, *61*, 2166–2210.
[3] For examples of synthetic routes to *gem*-dimethyl groups in biologically active compounds, see: a) P. A. Glossop, C. A. L. Lane, D. A. Price, M. E. Bunnage, R. A. Lewthwaite, K. James, A. D. Brown, M. Yeadon, C. Perros-Huguet, M. A. Trevethick, N. P. Clarke, R. Webster, R. M. Jones, J. L. Burrows, N. Feeder, S. C. J. Taylor, F. J. Spence, *J. Med. Chem.* **2010**, *53*, 6640–6652; b) A. L. Gottumukkala, K. Matcha, M. Lutz, J. G. de Vries, A. J. Minnaard, *Chem. Eur. J.* **2012**, *18*, 6907–6914; c) J. Wang, R. Tong, *J. Org. Chem.* **2016**, *81*, 4325–4339; d) E. Kick, R. Martin, Y. Xie, B. Flatt, E. Schweiger, T.-L. Wang, B. Busch, M. Nyman, X.-H. Gu, G. Yan, B. Wagner, M. Nanao, L. Nguyen, T. Stout, A. Plonowski, I. Schulman, J. Ostrowski, T. Kirchgessner, R. Wexler, R. Mohan, *Bioorg. Med. Chem. Lett.* **2015**, *25*, 372–377.
[4] For recent studies on dimethylcyclopropane synthesis, see: a) L. Dian, D. S. Müller, I. Marek, *Angew. Chem. Int. Ed.* **2017**, *56*, 6783–6787; *Angew. Chem.* **2017**, *129*, 6887–6891; b) H. Cang, R. A. Moss, K. Krogh-Jespersen, *J. Am. Chem. Soc.* **2015**, *137*, 2730–2737.
[5] T. T. Talele, *J. Med. Chem.* **2016**, *59*, 8712–8756.
[6] a) M. Meazza, H. Guo, R. Rios, *Org. Biomol. Chem.* **2017**, *15*, 2479–2490; b) L. Souillart, N. Cramer, *Chem. Rev.* **2015**, *115*, 9410–9464; c) P.-h. Chen, B. A. Billett, T. Tsukamoto, G. Dong, *ACS Catal.* **2017**, *7*, 1340–1360.
[7] S. Sengmany, E. Léonel, J. P. Paugam, J.-Y. Nédélec, *Tetrahedron* **2002**, *58*, 271–277.
[8] K.-J. Stahl, W. Hertzsch, H. Musso, *Liebigs Ann. Chem.* **1985**, 1474–1484.
[9] A. B. Charette, N. Wilb, *Synlett* **2002**, 176–178.
[10] E. J. Corey, M. Jautelat, *J. Am. Chem. Soc.* **1967**, *89*, 3912–3914.
[11] P. J. Chirik, *Angew. Chem. Int. Ed.* **2017**, *56*, 5170–5181; *Angew. Chem.* **2017**, *129*, 5252–5265.
[12] H. Kanai, H. Matsuda, *J. Mol. Catal.* **1985**, *29*, 157–164.
[13] J. Werth, C. Uyeda, *Chem. Sci.* **2018**, *9*, 1604–1609.